UNIVERSIDAD DE GUANAJUATO

División de Ciencias e Ingenierías
Campus León

Higher-Order Dark Matter: From non-relativistic Proca Stars to Cosmological Spinor Production

Thesis submitted by

Mtr. Edgar Iván Preciado Govea

to obtain the degree of Ph.D. in Physics

Supervised by:
Dr. Alberto Diez Tejedor

Declaratory

I, Edgar Iván Preciado Govea, hereby declare that the work presented in this thesis is my own and is based on the research conducted during my PhD between the years 2021 and 2025. This thesis utilizes several books and article references on cosmology and gravitation as a guide for writing. In all cases, due credit is given to the authors, and relevant references are properly cited. Part of the content, presented in Chapter 2 and Chapter 4, is based on published and forthcoming papers product of my PhD: *Nonrelativistic Proca stars: Spherical stationary and multi-frequency states* [1], *Linear stability of nonrelativistic Proca stars* [2] and *Cosmic Spinors and the Weight of the Vacuum* [3]. I tried my best to summarize, re-phrase and re-write the content of this article to avoid self-plagiarism. Some figures presented in this thesis were already presented in the aforementioned articles.

I also acknowledge the use of Artificial Intelligence (AI) assistants such as Chat-GPT from OpenAI and Quillbot for providing information, for text suggestions and enhancements, and for proofreading.

Acknowledgements

I would like to express my sincere gratitude to my advisor, Dr. Alberto Diez Tejedor, for his guidance, patience, and unwavering support throughout this work. Likewise, I would like to thank Dr. Olivier Sarbach, Dr. Armando Roque, and Dr. Cristian Armendariz Picon for their guidance and advice. I also thank the thesis committee for their valuable observations and suggestions, which significantly contributed to improving this work. I extend my gratitude to the Consejo Nacional de Humanidades, Ciencias y Tecnologías (CONAHCYT) for the financial support provided during my PhD studies. Finally, I thank my family, friends, and colleagues.

Contents

Introduction

This thesis explores the possibilities of forming compact dark matter objects as solutions to the Einstein-Klein-Gordon and Einstein-Proca field equations, as well as accounting for the mechanism of dark matter production through gravitational particle production. According to quantum mechanics, particles are subdivided into two groups: those with integer spin (bosons) and those with half-integer spin (fermions). The former are capable of forming particle condensates in the ground state, while the latter, limited by Fermi-Dirac statistics, are forced to successively occupy higher energy levels. Here we will focus on describing the equilibrium configurations of compact objects of self-gravitating and self-interacting particles with spin $s = 0$ and $s = 1$, which share similar characteristics to their counterparts, the compact objects composed of fermions. On the other hand, one of the most notable results of the semiclassical treatment of quantum fields on curved spaces predicts the gravitational production of particles due to gravitational effects, in abundances that could account for the dark matter bounds imposed by current observations [4, 5]. Here we will focus on describing this phenomenon for quantum fields with spin $s = 0$ and spin $s = ½$ at different orders of approximation. In both objectives, we describe dark matter as a field that interacts only gravitationally with the rest of the matter. Both objectives aim to address particular issues (one intends to solve astrophysical and cosmological problems, while the other intends to explain the mechanism of production of these particles); however, they equally intend to account for the gravitational presence of dark matter in the observable universe. In both cases, we will explore different regimes of approximations for the bosonic or fermionic dark matter field according to each chapter.

In Chapters 1 and Chapter 2, we study stable compact objects composed of particles with spin $s = 0$ (boson stars) and $s = 1$ (Proca stars). In these chapters, we characterize these configurations as *equilibrium solutions* of the Einstein-Klein-Gordon systems (relativistic boson star), $s = 0$ Gross-Pitaevski-Poisson (non-relativistic boson star), and $s = 1$ Gross-Pitaevski-Poisson (non-relativistic Proca star), particularly for spherically symmetric configurations. In each case, dark matter is modeled through a massive self-interacting boson field that only interacts with the standard model of particles through gravitational interaction. In Chapter 3 and Chapter 4, we explore the mechanism by which non-interacting dark matter particles of spin $s = 0$ and $s = 1/2$, which only interact gravitationally with matter, can be produced, that is, the gravitational particle production mechanism. Throughout each chapter, we explore different orders of approximation (e.g. relativistic and non-relativistic) and analyze in which regimes a quantum field admits a classical field description. These concepts will be reviewed throughout this thesis.

Part I

Self-gravitating Objects

Un estudiante a quien le expusieron los sofismas de Zenon sobre la negación del movimiento juntamente con un ensayo de refutación y solución, dijo: "Veo la solución, pero no veo el problema." No seremos demasiado infelices, si no viendo completamente la solución, vemos al menos el problema.

Jean Wahl

Chapter 1

Boson Stars: Relativistic and Non-relativistic Configurations

1.1 Introduction

Compact objects like white dwarfs and neutron stars are part of the entities that populate the universe and play a role in astrophysical and cosmological observations. These are part of the family of compact objects made of fermions and are part of the catalog of entities that conform to the universe. Parallel to this family of objects are *boson* stars, which are hypothetical compact objects made of spin $s = 0$ bosons, and Proca stars, which are compact objects made of spin $s = 1$ bosons particles. These last ones, in their hypothetical nature, could account for the dark matter of the universe: massive self-gravitating (scalar or vector) fields can form stable astrophysical (or subatomic) objects supported by self-gravity and Heisenberg's uncertainty principle, and can populate the universe. Although the Cold Dark Matter model (CDM), within the framework of the standard cosmological model ΛCDM, has been surprisingly successful in explaining the large-scale structure of the universe, it has encountered problems on galactic or sub-galactic scales: CDM simulations lead to *cuspy* density profiles at galactic centers [6], while rotation curves signals a smooth core density [7]. Also, the predicted number of satellite galaxies around each galactic halo, is far beyond what we see around the Milky Way [8]. If dark matter is composed of boson particles in a Bose-Einstein condensate (like that of a boson compact object), these problems might be solved. Boson and Proca stars phenomenology could alleviate the small-scale problems of the CDM model, such as the *cusp* and the *missing satellite problem* [9].

A compact object is a collective arrangement of particles (that is, quantum excitations of a quantum field) that forms a stable macroscopic object. In the context of classical field theory, the seed idea of particles grouped together to form compact objects comes from John Wheeler in 1955 [10], who proposed stable solutions to the electromagnetic field within the framework of general relativity, that is, solutions to the Einstein-Maxwell system of equations. These objects called *geons* are unstable against linear perturbations. Conversely, Proca and boson stars turn out to be stable solutions to the Einstein-Klein-Gordon and the Einstein-Proca systems, respectively, for a complex massive scalar field and a complex massive vector field. Boson and Proca stars are

stable and massive compact objects susceptible to astrophysical studies and observations. These can be understood as a macroscopic arrangement in their minimum energy state, forming a condensate of integer spin particles characterized by a single macroscopic wave function $\Psi(t, \vec{x})$ (or $\vec{\Psi}(t, \vec{x})$). Boson and Proca stars may have masses comparable to the mass of neutron stars, or even larger. This makes them an interesting case for study like their counterparts, neutron and white dwarfs, and plausible candidates for dark matter.

In this chapter, we will describe the equilibrium solutions of the Einstein-Klein-Gordon system, the relativistic boson stars, and their non-relativistic limit, the solutions to the $s = 0$ Gross-Pitaevskii-Poisson system, i.e. the non-relativistic boson stars. Both solutions include the field's self-interaction term, parameterized in the action by a dimensionless coupling constant λ. When this coupling constant is negligible, the relativistic system reduces to the so-called *mini-boson* star solutions, and the non-relativistic system reduces to the Schrödinger-Poisson system. If the mass of the system is small, it will be possible to neglect relativistic effects and work with a Newtonian approximation, that is, with the $s = 0$ Gross-Pitaevsky-Poisson system. However, when the mass of the configuration approaches the Kaup mass $M_{\rm kaup} = 0.633 M_{\rm pl}^2/m$ (for non-interacting stars with field mass m), relativistic effects must be taken into account. Above this maximum mass, there will be no equilibrium configurations, similar to what happens for a fermion star [11]. As we shall observe, the mass profile for a relativistic boson star $M(\sigma_0)$ exhibits the same damped oscillation behavior as that of a fermion star [12]. However, stability, unlike a fermion star where collapse is prevented by the Pauli exclusion principle, for a boson star is prevented by the Heisenberg uncertainty principle. Also, as we will observe, a boson star is a system that does not exhibit a typical perfect fluid description, as its pressure is anisotropic. As we will see later, a self-interacting boson star has a maximum mass given by $M_{\rm max} \sim \sqrt{\lambda} M_{\rm pl}^3/m^2$, for strong coupling constant $\lambda \gg m^2/M_{\rm pl}^2$, that depends on the mass of the field m and the self-interaction parameter λ, which can become comparable to the maximum mass of a neutron star $M_{\rm max} \sim M_{\rm pl}^3/m^2$. This makes self-interacting boson stars particularly interesting compared to the free case where the mass of the configuration is much smaller than that of fermion stars. The phenomenology of a self-interacting boson star, relativistic and non-relativistic, will depend only on its self-interaction parameter and its mass.

Because of their mass range, extension, and stability, boson stars could be considered possible candidates to populate the universe in the form of dark matter. Advances in the detection of gravitational waves and gravitational lensing could help point towards considering boson stars and their growing phenomenology as explanations for the abundance of dark matter. As we mentioned above, the ΛCDM model has been incredibly successful in explaining the dynamics of the universe at cosmological scales ($\gg 10$ kpc). However, at galactic scales, this model presents challenges. To alleviate the tensions between physics at cosmological scales, described successfully in the ΛCDM model, and the physics of galactic scales, it is necessary to review the properties and nature of dark matter. Properties such as mass, spin, or the strength of self-interactions can be traced to astrophysical observables. For example, the phenomenology of a self-interacting bosonic field of *ultra-light mass* can

be traced to galactic scales [13] and the ground state solitonic solutions of the $s = 0$ Gross-Pitaevski-Poisson system can form the core of the galaxy halos [14]. In addition, given that the occupation numbers within galaxy halos are so high, the state of the boson field can be described as a classical non-relativistic boson condensate, and, since the velocities of visible matter in galaxies are non-relativistic and the mass range of a boson star (from 10^{-22}eV to $\sim M_{\rm pl}$) allows solutions with astrophysical scale of de Broglie lengths, the motivation to study the Newtonian limit is justified. Then, we can think of a non-relativistic boson star as a Bose-Einstein condensate with wave function $\psi(t, \vec{x})$, in which the excitations of the field represent identical particles that can occupy the same ground state. This system is described through the Gross-Pitaevskii equation for the wave function $\psi(t, \vec{x})$, and the Poisson equation for the Newtonian gravitational potential $\mathcal{U}(t, \vec{x})$. Equilibrium configurations correspond to a balance between the effects of pressure due to the self-interacting of the particles, the self-gravitational attraction of the fluid, and the repulsion due to quantum pressure.

The literature on boson stars is abundant. The works of Kaup [15], Ruffini and Bonazzola [11] are the pioneering works in the study of these solutions. Subsequently, works where the scalar field has self-interaction [16], non-minimal coupling to gravity [17], or electric charge [18] were considered, as well as the analysis of its stability [19, 20, 21, 22, 23]. We recommend to the reader the reviews of Visinelli [9], where the various properties of boson stars are studied, particularly for the free ($\lambda = 0$) and self-interacting ($\lambda \neq 0$) cases, and the work of Jetzer [24], where the non-relativistic limit of boson stars is reviewed as well as the analysis of their stability, and the work of Ruffini [25], Lee and Pang [26] and Liddle [27] where the mechanism of formation for boson stars is reviewed. In [28], the authors study the different possibilities of detecting boson stars (e.g. gravitational waves and lensing), of which they provide a detailed review. In [29], a special type of boson star, called ℓ-boson stars, is presented, formed by the collection of N non-interacting complex scalar fields parametrized by an angular momentum number $\ell = (N-1)/2$. Finally, we refer the reader to the work of Liebling and Palenzuela [30] where the different boson stars and their various astrophysical signals are reviewed.

In this chapter, we will focus on the study of relativistic [9, 24, 25, 26, 27, 28, 30] and non-relativistic [31, 32, 24, 33] boson stars, and we will postpone the study of non-relativistic Proca stars to the next chapter. We anticipate that, for these objects to be of astrophysical and cosmological interest, they must persist for at least the Hubble time, so we demand these configurations to be stable against small perturbations. Furthermore, if these configurations are to play the role of dark matter, they must be weakly (or null) interacting with the Standard Model, non-relativistic, and self-gravitating. Boson stars, being objects that remain bound only by the effect of their gravity and self-interaction, are candidates susceptible to study. In Section 1.2 we study relativistic boson star, their conserved charges 1.2.1 and the particular case of a relativistic spherically symmetric self-interacting configuration 1.2.3 and their numerical solutions 1.2.4. The analysis of the stability of the relativistic boson star is briefly introduced in the Section 1.2.5. In Section 1.3 we study non-relativistic boson stars and their numerical solutions for the spherically

symmetric system and, finally, a brief introduction to the analysis of its stability in Section 1.3.4. The mechanism of formation of these stars goes beyond the scope of this thesis, so it will not be addressed here.

1.2 Relativistic Boson Stars

We can define a non-topological soliton as a localized, and time-persistent object whose stability is guaranteed by a conserved charge[1], see Ref. [35, 9]. In this sense, a boson star is a non-topological soliton that is supported by gravity, and that is a stable and localized solution to the Einstein-Klein-Gordon equations, described by a classical complex scalar field $\phi(t, \vec{x})$. In the framework of general relativity, a classical complex scalar field $\phi(t, \vec{x})$ with mass m_0 and potential $V(|\phi|^2)$ is described by the Einstein-Klein-Gordon action of the form

$$S[g_{\mu\nu}, \phi] = \int d^4x\sqrt{-g}\left(\frac{1}{16\pi G}R + \mathcal{L}_M\right), \tag{1.1}$$

which consists of the Einstein-Hilbert action plus a matter term given by

$$\mathcal{L}_M = -\nabla_\mu\phi^*\nabla^\mu\phi - m_0^2|\phi|^2 - V(|\phi|^2), \tag{1.2}$$

where, as usual, g is the determinant of the spacetime metric $g_{\mu\nu}$, R is the Ricci scalar, $\phi^*(t, \vec{x})$ is the complex conjugate of $\phi(t, \vec{x})$, with $|\phi(t, \vec{x})|^2$ its modulus squared, and $V(|\phi|^2)$ the bosonic potential. This potential can consist of a self-interaction term of the form $\lambda|\phi|^4$ or higher-order terms. Similarly to a fermion star like a white dwarf, a boson star depends on the balance formed between the gravitational force that compacts the star and the pressure gradients that balance the self-gravity of the star. This self-gravity of the boson field is generated by the geometric aspects of the covariant derivatives in the action (1.1) and the dispersive nature of the Klein-Gordon equation provides the pressure gradients that balance the gravitational field generated by the boson field.

Variation of the action (1.1) with respect to the metric leads to the Einstein's equations,

$$R_{\mu\nu} - \frac{1}{2}g_{\mu\nu}R = 8\pi G T^\phi_{\mu\nu}, \tag{1.3}$$

where $R_{\mu\nu}$ is the Ricci tensor and $T^\phi_{\mu\nu}$ is the energy-momentum tensor of the scalar field given by

$$T^\phi_{\mu\nu} = -\frac{2}{\sqrt{-g}}\frac{\delta S_M}{\delta g^{\mu\nu}} = \nabla_\mu\phi^*\nabla_\nu\phi + \nabla_\nu\phi^*\nabla_\mu\phi - g_{\mu\nu}[\nabla^\gamma\phi^*\nabla_\gamma\phi + V(|\phi|^2)]. \tag{1.4}$$

Variation of the action (1.1) with respect to the scalar field $\phi(t, \vec{x})$ leads to the Klein-Gordon equation

$$\nabla^\mu\nabla_\mu\phi - m_0^2\phi = -\frac{dV(|\phi|^2)}{d|\phi|^2}\phi. \tag{1.5}$$

[1]Topological solitons do not require an additional conservation law, and boundary conditions at infinity are topologically different from the vacuum [9, 34].

The whole system is denominated the Einstein-Klein-Gordon system (EKG). Solutions to this system that conform a stable object, in which an equilibrium between self-gravity and pressure exists, similar to a fermion star, are denominated *boson star*.

1.2.1 Conserved Charges

Associated with the action (1.1) there are conserved charges. It is easy check that the action (1.1) possesses invariance under the global transformation $\phi \to e^{i\theta}\phi$, with θ a real constant. This invariance, according to the Noether theorem,[2] give rise a conserved current given by

$$J_\mu = i(\phi^* \nabla_\mu \phi - \phi \nabla_\mu \phi^*), \tag{1.6}$$

in such a manner that its covariant derivative vanishes, $\nabla_\mu J^\mu = 0$ (for scalar fields the covariant derivative coincides with the partial derivatives $\nabla_\mu \to \partial_\mu$). The conserved charge associated to the current J^μ is given by

$$N = \int d^3x \sqrt{-g} J^0, \tag{1.7}$$

where N can be identified with the number of boson particles present in the configuration. Note that if the field $\phi(t, \vec{x})$ were real, the conserved charge N would not exist. The requirement of a conserved charge N is essential to ensure the stability of the star. These configurations, whose condition at infinity is the vacuum, are what we have called above *non-topological soliton*. If the number of particles is not conserved, the stability is not ensured because of possible direct decays of the boson particles that constitute the star. In turn, if the condition at infinity were not the vacuum, the energy of the object would not be finite.

On the other hand, the mass of the star can be calculated using the Tolman mass formula [9, 28]

$$M = \int dx^3 \sqrt{-g} [2T_0{}^0 - T_\mu{}^\mu]. \tag{1.8}$$

1.2.2 Derrick Theorem

As we have already defined, a boson star is a compact object that is a solution to the Einstein-Klein-Gordon system and is stable over time. In this respect, Derrick's theorem states the following: for a wide class of nonlinear wave equations (e.g. the Klein-Gordon equation), there exist no stable time-independent solutions of finite energy, see Refs. [37, 38]. The mathematical

[2] If a continuous symmetry transformation $\phi \to \phi + D\phi$ only changes $\mathcal{L}$ by the addition of a four-divergence (i.e. $D\mathcal{L} = \partial_\mu W^\mu$) for arbitrary ϕ, then this implies the existence of a current $J^\mu_N = \Pi^\mu D\phi - W^\mu(x)$, where $\Pi^\mu = (\partial\mathcal{L}/\partial(\partial_\mu\phi))$ is the momentum density. If ϕ obeys the equations of motion then the current is conserved, i.e. $\partial_\mu J^\mu_N = 0$. Conserved currents are important because they give rise to conserved charges $Q_N = \int J^\mu_N d\mathcal{A}_\mu$. Here, if $\phi(x^\mu)$ changes under a symmetry transformation by an amount λ, then, an infinitesimal transformation on ϕ, induced by an infinitesimal $\delta\lambda$, can be written as $\delta\phi = D\phi\delta\lambda$ where $D\phi = (\partial\phi/\partial\lambda)|_{\lambda=0}$. In other words, if a system possesses some kind of invariance a quantity related to this invariance will be conserved, see Ref. [36] for a detailed explanation.

proof of Derrick's theorem goes beyond the scope of the present work. However, the Derrick theorem can be circumvented: it is possible to find stable and localized solutions of the Einstein-Klein-Gordon equation if we consider a field with periodic time dependence, allowing the gravitational field to remain time-independent. This allows us to write solutions of the form

$$\phi(t,\vec{x}) = e^{-i\omega t}\phi(\vec{x}), \tag{1.9}$$

where ω is a constant. It is important to note that the notion of a localized solution refers to a star that has finite energy, that is, the scalar field $\phi(t,\vec{x})$ vanishes at $r \to \infty$. For the spherical symmetric case, which we will analyze here, we need to replace $\phi(\vec{x}) = \phi(r)$.

1.2.3 Spherically Symmetric Relativistic Boson Stars

Now we will present solutions for case of a spherically symmetric configuration with self-interacting potential $V = \lambda|\phi|^4$ where ϕ is given by the harmonic ansatz (1.9) with $\phi(\vec{x}) = \phi(r)$ a real radial dependent function[3]. For spherically symmetric configurations the spacetime line element take the forms

$$ds^2 = -e^v dt^2 + e^u dr^2 + r^2 d\Omega^2, \tag{1.10}$$

where $v = v(r)$ and $u = u(r)$ are only radial dependent functions and $d\Omega^2 = d\theta^2 + \sin^2\theta d\phi^2$. Note that although the elements of the metric are time-independent, this does not guarantee that the field is time-independent, however, given that the energy-momentum tensor at Eq. (1.4) only presents combinations of $\phi^*(t,\vec{x})\phi(t,\vec{x})$ and its derivatives $\nabla_\mu\phi^*(t,\vec{x})\nabla_\nu\phi(t,\vec{x})$, the harmonic ansatz (1.9) guarantees that this is the case. These stationary spherically symmetric boson stars are the simplest configurations possible. However, configurations that include rotation (where the profile $\phi(\vec{x})$ is radial and angular dependent and the star has angular momentum) might be also of interest since in nature these configurations might rotate.

In order to solve the Einstein-Klein-Gordon system, Eqs. (1.3)-(1.5), we need to calculate the energy-momentum tensor $T_{\mu\nu}$, the Ricci tensor $R_{\mu\nu}$ and Ricci scalar R. Using the harmonic ansatz (1.9) and the spherical symmetric spacetime element (1.10), there are three non-trivial Einstein equations coming from the G_{tt}, G_{rr} and $G_{\theta\theta}$ components of the Einstein tensor, together with the conservation equation of the energy momentum tensor $\nabla_\mu T^\mu{}_\nu = 0$, giving us only a system of three independent equations. For the metric (1.10) the non-zero Ricci tensor components take the form

$$R_{tt} = \frac{1}{2}e^{v-u}\left[\partial_r^2 v + \frac{1}{2}(\partial_r v)^2 - \frac{1}{2}\partial_r v\partial_r u + \frac{1}{r}\partial_r v\right], \tag{1.11a}$$

$$R_{rr} = \frac{1}{2}\left[-\partial_r^2 v - \frac{1}{2}(\partial_r v)^2 + \frac{1}{2}\partial_r v\partial_r u + \frac{1}{r}\partial_r v\right], \tag{1.11b}$$

$$R_{\theta\theta} = e^{-u}\left[\frac{r}{2}(\partial_r u - \partial_r v) - 1)\right] + 1, \tag{1.11c}$$

$$R_{\phi\phi} = \sin^2\theta R_{\theta\theta}, \tag{1.11d}$$

[3]In principle, $\phi(r)$ is a complex scalar field dependent on the radius r, given by $\phi(r) = \phi_R(r) + i\phi_I(r)$ up to an arbitrary phase. However, the two components follow the same equation, so we can write $\phi(t,\vec{x}) = e^{-i\omega t}\phi_R(r) = e^{-i\omega t}\phi(r)$.

and the Ricci scalar is given by

$$R = e^{-u}\left[\partial_r^2 v + \frac{1}{2}(\partial_r v)^2 - \frac{1}{2}\partial_r v\partial_r u + \frac{2}{r}(\partial_r v - \partial_r u) + \frac{2}{r^2}(1-e^u)\right]. \quad (1.12)$$

Using these identities and the energy momentum tensor (1.4) into the $\{tt\}$ and $\{rr\}$ Einstein equations ($R_{\mu\nu} - \frac{1}{2}g_{\mu\nu}R = 8\pi T_{\mu\nu}$) we get

$$e^{-u}\left(\frac{u'}{r} - \frac{1}{r^2}\right) + \frac{1}{r^2} = 8\pi G\rho_\phi, \quad (1.13a)$$

$$e^{-u}\left(\frac{v'}{r} + \frac{1}{r^2}\right) - \frac{1}{r^2} = 8\pi G p_\phi, \quad (1.13b)$$

where the primes denote differentiation with respect to the radial coordinate r and the effective energy density and radial pressure are given respectively by

$$\rho_\phi = e^{-v}\omega^2\phi^2 + e^{-u}(\phi')^2 + \tilde{V}(\phi^2), \quad (1.14a)$$

$$p_r = e^{-v}\omega^2\phi^2 + e^{-u}(\phi')^2 - \tilde{V}(\phi^2), \quad (1.14b)$$

$$p_T = e^{-v}\omega^2\phi^2 - e^{-u}(\phi')^2 - \tilde{V}(\phi^2), \quad (1.14c)$$

where p_T is the tangential pressure and $\tilde{V} = m_0^2|\phi|^2 + V(\phi^2)$. Since the radial pressure and the tangential pressure differ by one sign in the second term, a perfect fluid (where pressure is isotropic) treatment will not in general be possible when we deal with a relativistic boson star. So, a boson star is an example of a configuration with an anisotropic fluid description.

Now, to calculate the Klein-Gordon equation (1.5) we need to obtain the d'Alembertian operator

$$\Box \equiv g^{\mu\nu}\nabla_\mu\nabla_\nu = \frac{1}{\sqrt{-g}}\frac{\partial}{\partial x^\mu}\left(\sqrt{-g}\,g^{\mu\nu}\frac{\partial}{\partial x^\nu}\right), \quad (1.15)$$

with $\sqrt{-g} = e^{(u+v)/2}r^2\sin^2\theta$ such that

$$\Box\phi = \Bigg[- e^{-v}\frac{\partial^2}{\partial t^2} + e^{-u}\left(\frac{\partial^2}{\partial r^2} + \frac{1}{2}\left(\frac{\partial v}{\partial r} - \frac{\partial u}{\partial r}\right)\frac{\partial}{\partial r} + \frac{2}{r}\frac{\partial}{\partial r}\right) + \frac{1}{r^2}\frac{\partial^2}{\partial\theta^2} + \frac{1}{r^2\sin^2\theta}\frac{\partial^2}{\partial\phi^2}\Bigg]\phi.$$

Finally, we can write the Klein-Gordon equation as

$$\phi''(r) + \left(\frac{2}{r} + \frac{v'-u'}{2}\right)\phi'(r) = e^u\left(\frac{\tilde{V}(\phi^2)}{d\phi^2} - e^{-v}\omega^2\right)\phi. \quad (1.16)$$

Together, equations (1.13) and (1.16) conform the relativistic spherical symmetric Einstein-Klein-Gordon system.

Now, if we define

$$g_{tt} \equiv -\left(1 - \frac{2M(r)}{r}\right) \quad (1.17)$$

and we use Eq. (1.13), we can recast this last as

$$\frac{dM(r)}{dr} = 4\pi r^2\rho_\phi, \quad (1.18)$$

with the finite-mass condition $M = \lim_{r\to\infty} M(r)$ where M is the total mass of the configuration, given by (1.8).

Now, let us consider the potential for self-interaction given by $\tilde{V} = m_0^2|\phi|^2 + \lambda|\phi|^4$. The simplest case in which $\lambda = 0$ is called *mini-boson* star configuration [39], and the case for $\lambda \neq 0$ is called a *massive-boson* star [40], with m_0 the mass of the boson particles (the reason for these names will soon become clear). In the particular case of a spherically symmetric configuration, and after rescaling the radial function $\phi(r)$ in units of the reduced Planck mass $M_{\rm pl}^2 = (8\pi G)^{-1}$ as $\tilde{\phi} = \phi/M_{\rm pl}$, and the radial coordinate as $x = m_0 r$, we can recast Eqs. (1.13) and (1.16) as

$$\frac{1}{x}\frac{du}{dx} = \frac{1-e^u}{x^2} + (1 + e^{-v}\tilde{\omega}^2 + \lambda'\tilde{\phi}^2)e^u\tilde{\phi}^2 + \left(\frac{d\tilde{\phi}}{dx}\right)^2, \tag{1.19a}$$

$$\frac{1}{x}\frac{dv}{dx} = \frac{e^u-1}{x^2} - (1 - e^{-v}\tilde{\omega}^2 + \lambda'\tilde{\phi}^2)e^u\tilde{\phi}^2 + \left(\frac{d\tilde{\phi}}{dx}\right)^2, \tag{1.19b}$$

$$\frac{d^2\tilde{\phi}}{dx^2} = -\left(1 + e^u - x^2 e^u(1+\lambda'\tilde{\phi}^2)\tilde{\phi}^2\right)\frac{1}{x}\frac{d\tilde{\phi}}{dx} + e^u(1 + 2\lambda'\tilde{\phi}^2 - e^{-v}\tilde{\omega}^2)\tilde{\phi}, \tag{1.19c}$$

where $\lambda' = \lambda M_{\rm pl}^2/m_0^2$ and $\tilde{\omega} = \omega/m_0$. With this change of variables, we have achieved that the mass of the boson m_0 does not appear explicitly in the equations and therefore the configurations have no dependence on the mass of the boson (it is absorbed in the numerical variables). In general, the value of λ plays a relevant role even for very small values of λ. When $\lambda < 0$ or $\lambda > 0$ we have the *attractive* and *repulsive* case, respectively.

To ensure that the solutions are regular, asymptotically flat and localized we need to impose the following boundary conditions

$$\tilde{\phi}(r=0) = \tilde{\phi}_0, \quad \lim_{r\to\infty}\tilde{\phi}(r) = 0, \tag{1.20a}$$

$$u(r=0) = 0, \quad \lim_{r\to\infty} u(r) = 0, \tag{1.20b}$$

$$v(r=0) = v_0, \quad \lim_{r\to\infty} v(r) = 0, \tag{1.20c}$$

$$M(r=0) = 0, \quad \lim_{r\to\infty} M(r) = M, \tag{1.20d}$$

where v_0 and $\tilde{\phi}_0$ are constants that we will call *central amplitudes*. We can see from Eq. (1.19c) that the first term inside the parentheses is singular at the origin unless $\frac{d\tilde{\phi}}{dx} = 0$. Similarly, if $e^u = 1$ the first term of Eqs. (1.19a) and (1.19b) is non-singular if $u(r=0) = 0$. To ensure the condition that the solutions are asymptotically flat we need that $e^u = e^v = 1$ at infinity $r \to \infty$. Additionally, given that the solutions must have finite mass, it is necessary to introduce the limit $\lim_{r\to\infty}\tilde{\phi} = 0$, as we can see from the mass expression (1.18). If we reduce the order of the differential equation (1.19c), we will have a total of four first-order differential equations and, therefore, to completely determine the system, we will require the boundary conditions for u, v, $\tilde{\phi}$, and $\tilde{\phi}'$, given by Eqs. (1.20), from which, the condition $\lim_{r\to\infty}\tilde{\phi}(r) = 0$ will allow us to determine the unique value of $\tilde{\omega}_n$ for $n = 0, 1, 2, 3, ...$ number of nodes in

$\tilde{\phi}(x)$ that satisfies all the conditions (1.20) given a specific value of the central amplitude $\tilde{\phi}_0$. The only parameters that remains free are the central amplitude ϕ_0, the scale determined through $x = m_0 r$ by the value of the mass m_0 and the self-interacting parameter λ, hence the boson star configurations will depend only on this values.

Now, if we analyze the asymptotic behavior of Eq. (1.19) considering the boundary conditions (1.20) and a weak coupling $\lambda \sim 0$, we can write the wave equation of the field ϕ as

$$\frac{d^2\tilde{\phi}}{dx^2} = (1-\tilde{\omega}^2)\tilde{\phi} \quad \rightarrow \quad \phi \sim \exp\left\{\left(-\sqrt{m_0^2-\omega^2}\right) r\right\}, \tag{1.21}$$

where if $\omega < m_0$ then the scalar field decays exponentially when $r \to \infty$ and if $m_0 < \omega$ then the profile will have an oscillatory behavior. Therefore, to obtain localized solutions, that is, configurations with finite energy, $\omega < m_0$ must be satisfied.

On another hand, using Eq. (1.7) we can calculate the conserved particle number

$$N = 4\pi \int_0^\infty dr r^2 \omega e^{\frac{v-u}{2}} \phi^2, \tag{1.22a}$$

and integrating Eq. (1.18) up to infinity we get the total mass of the star

$$M = 4\pi \int_0^\infty dr r^2 \rho_\phi = 4\pi \int_0^\infty dr r^2 [(e^{-v}\omega^2 + m_0^2 + \lambda\phi^2)\phi^2 + e^{-u}(\phi')^2]. \tag{1.23}$$

In terms of the variables x, $\tilde{\phi}$ and $\tilde{\omega}$ the mass and particle number scales as $M \sim (\lambda^{1/2} M_{\rm pl}^3/m_0^2)\tilde{M}$ (for large λ' [28, 40]) and $N = (M_{\rm pl}^2/m_0^2)\tilde{N}$, respectively.

Additionally, it is important to introduce the *binding energy* E_B of the star, defined as $E_B \equiv m_0 N - M$, that is the difference between the energy of the gravitationally bound configuration (M) and the energy that the same number of particles (N) would have if they were dispersed to infinity (see Refs. [24, 40, 41, 42]). We observe that if $E_B > 0$, the star is in a bound state, so it will not be possible for the constituent particles to disperse to infinity, the internal forces are sufficient to keep the system together. Stars with these characteristics will remain stable. On the contrary, if $E_B < 0$, then it will be possible for the star to disperse into its constituent particles to infinity. This star will be possibly unstable.

Another important quantity to define is the radius of the star. Although a boson star is certainly infinite in extension, an effective definition of his radius is given by the R_{99} radius. One can define implicitly the R_{99} radius as

$$0.99M = 4\pi \int_0^{R_{99}} dr r^2 \rho_\phi, \tag{1.24}$$

that is, the radius containing 99% of the mass of the boson star. Along with the radius of the star, another useful quantity is the relationship between the mass M and the radius R_{99} called compactness $C \equiv GM/R_{99}$. In this sense there is

a limit for the size of the radio, that is, the Schwarzschild radius $R_s = 2GM$, below which the solution no longer describes a boson star, since the system collapses into a black hole. Another quantity is the *kaup limit* associated to Kaup Mass M_{kaup}, which is the maximal mass determined numerically of a stable boson star, where $R_{\text{kaup}} > R_s$.

Given the value of the central amplitude ϕ_0 there are an infinite number of solutions associated with the system (1.19), one for each possible value of the frequency ω_n . However, if we characterize these solutions with the number of nodes n that the profile ϕ_n presents in the interval $0 < r < \infty$, it is possible to associate the state of minimum energy with the solution with $n = 0$ number of nodes and the states of higher energy with the solutions with $n = 1, 2, 3...$ number of nodes. This characterization is analogous to the excited states in an atom (see *Boson stars-Gravitational atom II*, in Ref. [43] or [44]). As we shall see, excited states have a maximum mass M_{max} greater than the ground state, with M_{max} increasing as n increases, with n the number of nodes.

Heisenberg Uncertainly Principle

In the semiclassical approach, gravity is sourced by the expectation value of the energy-momentum tensor $\langle N|\hat{T}_\mu{}^\nu|N\rangle$ in the Einstein equations. For a boson star, in their lowest energy state, the expectation value is given with respect to the state number $|N\rangle$ which represents the state of N bosons in the ground state $n = 0$. If the spacetime is asymptotically flat, the spherically symmetric and time-dependent scalar field $\phi(r, t)$ can be expanded in terms of the usual creation and annihilation operators $\hat{a}_n$ and $\hat{a}_n^\dagger$, which satisfy the commutation relations $[\hat{a}_m, \hat{a}_n^\dagger] = \delta_{mn}$, and the functions $\hat{\phi}_n$ which are orthonormal with respect to a defined inner product. For this configuration, a boson star with N bosons in its ground state $n = 0$ will be characterized by a unique value of the frequency ω_0 for the eigenvector $\hat{\phi}_0$. If we define a classical field ϕ_c with the form

$$\phi_c = (\omega_0)^{-1/2}\sqrt{N + \frac{1}{2}}\phi_0(r)e^{-i\omega_0 t}, \tag{1.25}$$

then the energy-momentum tensor of the classical configuration and the quantum configuration are exactly the same (a complete description of the previous treatment can be found in Ref. [45]). In this sense, it is justified to represent a boson star by a classical field. Another important consequence of the quantization of the field $\phi(t, r)$ is the appearance of the uncertainty principle, which provides the "quantum pressure" that balance the gravitational field and keeps the boson star in equilibrium. Heuristically, if we apply this principle to a macroscopic boson star, the Heisenberg uncertainly principle of quantum mechanics given by $\Delta p \Delta x \geq \hbar/2$ can be written as

$$4m_0 vR \geq \hbar, \tag{1.26}$$

where we have assumed that the boson star is confined within some radius $\Delta x = 2R$ with momentum $\Delta p = m_0 v$. We can write the particle velocity with a de Broglie wavelength $\lambda_{dB} \sim 2R = h/m_0 v$ as $v \sim h/(2m_0 R)$. With this, the total kinetic energy is $K \sim N\hbar^2/(8m_0 R^2)^{-1}$ (considering a free scalar field, $\lambda = 0$). If we neglect the binding energy E_B, we can make the approximation $m_0 N \approx M$, then the self-gravity potential energy is given by $U \sim$

$-(3/5)GM^2/R$, and the total energy $E = N\hbar^2/(8m_0R^2)^{-1} - (3/5)GM^2/R$ is minimized when $R_{bs} \sim (5/6)(2Gm_0^2M)$, where R_{bs} is the boson star radius. If the mass M increases, the radius R_{bs} decreases. The maximum value of the mass for which the radius R_{bs} reaches the Schwarzschild radius $R_S = 2GM$ is given by $M_{max} \propto m_{pl}^2/m_0$ where $m_{pl}^2 = 1/G$. As we will see in the next section, for a non-self-interacting boson star (a mini-boson star), the maximum mass (or Kaup mass) is given by $M_{max} \approx 0.63m_{pl}^2/m_0$ and for a self-interacting boson star (a massive-boson star), the maximum mass is given by $M_{max} \sim \sqrt{\lambda}m_{pl}^3/m_0^2$, which is still inversely proportional to the mass m_0, but it is larger in magnitude (compared with a mini-boson star) and depends on the coupling constant λ. It is for this reason that configurations with $\lambda = 0$ are called *mini*-boson stars and configurations with $\lambda \neq 0$ are called *massive*-boson stars. Note that the maximum mass M_{max} of the boson star is inversely related to the mass of the constituent scalar field m_0 (and in the case of a self-interactive boson star depends also on the coupling constant λ) in such a way that the size and mass of a boson star can reach from astrophysical scales to atomic scales.

1.2.4 Numerical Solutions

Mini-boson Stars

In the free case, $\lambda = 0$, we can set the change of variables $du/dx = (1/A)(dA/dx)$, $dv/dx = (1/B)(dB/dx)$, $e^u = A(x)$, $e^v = B(x)$, $\tilde{\phi}(x) = \sigma(x)$, and recast the differential equations (1.19) in the form

$$\frac{dA}{dx} = xA^2\left[\left(\frac{\tilde{\omega}^2}{B}+1\right)\sigma^2 + \frac{1}{A}\left(\frac{d\sigma}{dx}\right)^2\right] - \frac{A}{x}(A-1), \tag{1.27a}$$

$$\frac{dB}{dx} = xBA\left[\left(\frac{\tilde{\omega}^2}{B}-1\right)\sigma^2 + \frac{1}{A}\left(\frac{d\sigma}{dx}\right)^2\right] + \frac{B}{x}(A-1), \tag{1.27b}$$

$$\frac{d^2\sigma}{dx^2} = -\left(\frac{2}{x} + \frac{1}{2B}\frac{dB}{dx} - \frac{1}{2A}\frac{dA}{dx}\right)\frac{d\sigma}{dx} - A\left(\frac{\omega^2}{B}-1\right)\sigma. \tag{1.27c}$$

In order to solve numerically the system of equations (1.27) we reduce the wave equation (1.27c) to a pair first order differential equations. The resulting system of four first-order differential equations must satisfy the boundary conditions (1.20) with the condition $\sigma'(r=0) = 0$. We can write the boundary conditions as

$$\sigma(r=0) = \sigma_0, \quad \lim_{r\to\infty}\sigma(r) = 0, \tag{1.28a}$$

$$A(r=0) = 1, \quad B(r=0) = B_0, \tag{1.28b}$$

$$M(r=0) = 0, \quad \lim_{r\to\infty} M(r) = M. \tag{1.28c}$$

The central amplitude σ_0 and B_0 are free parameters. However, we can observe from Eq. (1.27) that if we choose $B \to cB$ and $\tilde{\omega} \to \sqrt{c}\tilde{\omega}$, the system of equations does not change. Therefore the equations are linear in B and the structure of the configuration will be independent of B_0. Furthermore, the condition at infinity for the field $\sigma(r \to \infty) = 0$ ensures that the star is

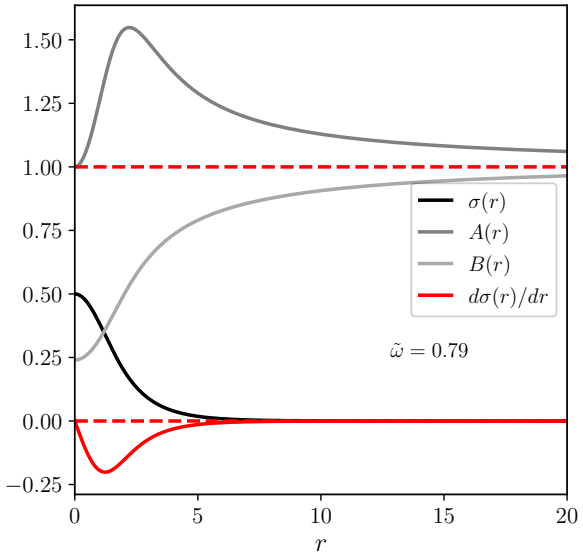

Figure 1.1: **Mini-boson star configuration ($\lambda = 0$).** A, B, σ and σ' as functions of r for the case $A_0 = 1, B_0 = 0.2$, $\sigma_0 = 0.5$ and $\sigma_0' = 0$ with $\tilde{\omega} = 0.7$ and $n = 0$. As we can observe $A(r \to \infty)$ and $B(r \to \infty) = 1$ (remember that it is always possible to rescale the value of $B \to \alpha B$ and $\tilde{\omega} \to \sqrt{\alpha}\tilde{\omega}$ to ensure the boundary condition $B(r \to \infty) = 1$). Also $\sigma(r \to \infty) = 0$ and $\sigma'(r = 0) = 0$.

localized and has finite energy. This condition determines the value for $\tilde{\omega}_n$ for each $n = 1, 2, 3...$ number of nodes in the solution $\sigma_n(r)$. As we mentioned previously, there are an infinite number of discrete values of $\tilde{\omega}_n$ that satisfy this system of equations. The state that minimizes the energy will be characterized by the solution $\sigma_{n=0}(r)$ with $n = 0$ nodes. Solutions with a larger number of nodes represent solutions with increasing higher energy and satisfies $\tilde{\omega}_0 < \tilde{\omega}_1 < \tilde{\omega}_2 ... < \tilde{\omega}_n$. Let us also remember that the condition $\omega_n < m_0$ must be satisfied for all n to ensure solutions with finite energy.

To determine the value of $\tilde{\omega}_n$ that satisfies the boundary conditions (1.28) we use the numerical shooting method, reducing the boundary value problem to finding the initial conditions that give a root. Given the value of the central amplitude σ_0, we choose a seed value for $\tilde{\omega}_n$ and solve the system accordingly. For example, in the case of $n = 0$ number of nodes, if we have chosen $\tilde{\omega}_0$ very large, then $\sigma'(x)$ will become negative at a finite value of the radius $x = m_0 r$ going through a inflection point, and if we have chosen $\tilde{\omega}$ too small then $\sigma'(x)$ becomes positive at a finite value of the radius. We can observe this behavior for a central amplitude of $\sigma_0 = 0.1$ in Figure 1.3 left and right panels, in both cases, the limit $\lim_{r\to\infty} \sigma(r) = 0$ is broken. We must then choose a more appropriate value for $\tilde{\omega}_0$. We can do this by bisecting $\tilde{\omega}_{avg} = (\tilde{\omega}_{max} + \tilde{\omega}_{min})/2$ in a range $[\tilde{\omega}_{min}, \tilde{\omega}_{max}]$ for a sufficient number of iterations until we have reach the desired precision. In Appendix B.1, we analyze a detailed example of this numerical method applied to a non-relativistic stationary Proca star.

Figure 1.1 shows a sample configuration illustrating the functions A, B, σ and $d\sigma/dr$ as functions of $r = x/m$ for the case $A_0 = 1, B_0 = 0.25$ and $\sigma_0 = 0.5$

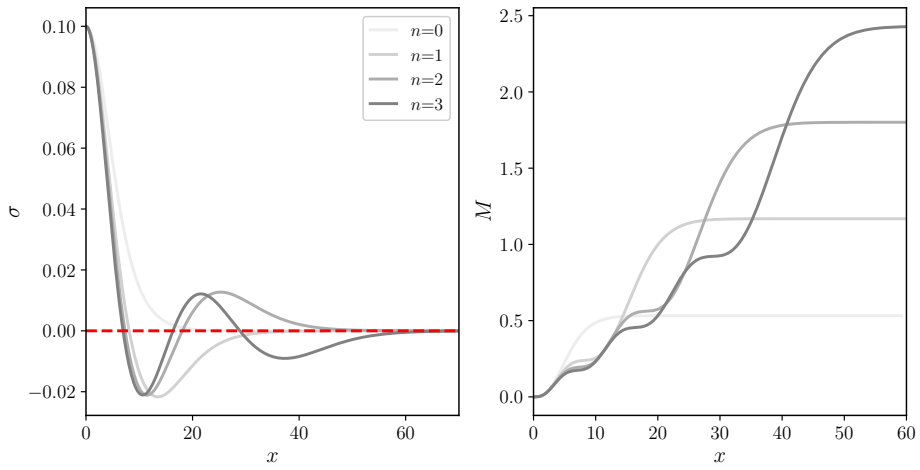

Figure 1.2: **Excited mini-boson star configurations**. Mini-boson star configurations ($\lambda = 0$) for different excited solutions ($n = 0, 1, 2, 3$). *Left panel*: radial profile σ_n for $n = 0, 1, 2, 3$ number of nodes. *Right panel*: mass profile M as a function of $x = m_0 r$ for each one of the configurations on the right. Here $M \sim (M_{\rm pl}^2/m_0)\tilde{M}$ and $\sigma = M_{\rm pl}\tilde{\phi}$.

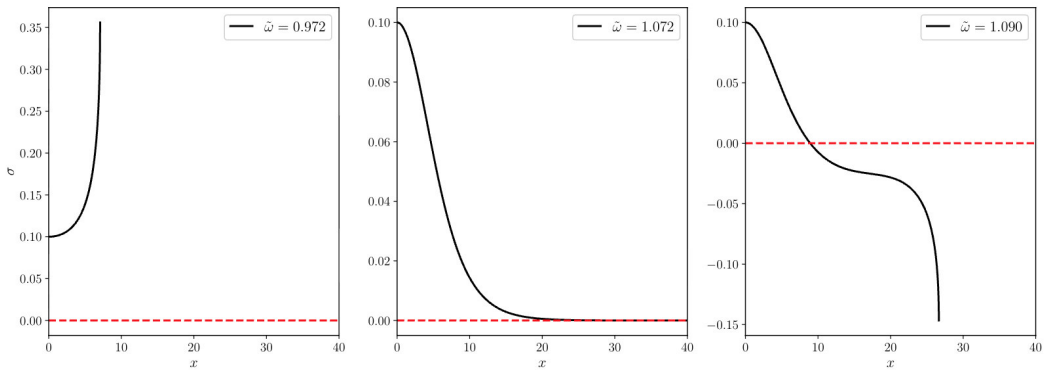

Figure 1.3: **Shooting method for a mini-boson star ($\lambda = 0$)**. We need to find the value for ω_0 that satisfies the appropriate boundary conditions (1.28) given the values for $\sigma(r = 0) = \sigma_0$ and $B(r = 0) = B_0$. *Left panel*: if we choose a value too small for ω, then σ' becomes positive at a finite value of $x = m_0 r$. *Right panel*: if we choose a value too large for ω, the radial profile σ becomes negative at a finite value of the radius going through a inflection point. In both cases, the boundary condition $\lim_{r\to\infty} \sigma(r) = 0$ is broken. *In the central panel* we have chosen an appropriate value for ω_0 in the range $[\omega_{min}, \omega_{max}]$ to a certain degree of precision for the approximate solution $\sigma(r)$. In this case the boundary condition $\lim_{r\to\infty} \sigma(r) = 0$ is satisfied. Also, given the invariance of the system (1.27c) under the rescaling $B \to \alpha B$ and $\tilde{\omega} \to \sqrt{\alpha}\tilde{\omega}$, for $B_0 = 1$, in order to get $B(r \to \infty) = 1$ we need to rescale $\tilde{\omega} \to \sqrt{1/4.1}\tilde{\omega}$ (note that this ensure the condition $\omega < m_0$).

with $\tilde{\omega} = 0.7$. We can observe that A, B and σ reach asymptotic values as $r \to \infty$ according to the boundary conditions (1.20). In Figure (1.4) we show M and $m_0 N$ as functions of the central amplitude σ_0. Let's remember that if the binding energy, defined as $E_B = m_0 N - M$, is positive $E_B > 0$, the configuration is possible to be stable, otherwise it will be possible for the star to disperse into its constituent particles to infinity (or more likely, the radiation of some of the particles until the system reaches a stable state). In Figure 1.4 the second vertical line signals when the binding energy vanishes. When the total mass of the configuration reaches its maximum value, the binding energy is positive, but this is only a small fraction of the total mass M. Finally, Figure 1.2 shows the solutions to the system (1.27) with a central amplitude value of $\sigma = 0.1$ for $n = 0, 1, 2, 3$ number of nodes. We plot the radial profile σ and the mass M of the star as functions of radius $x = m_0 r$ in the first and second panel, respectively. We can observe that the value of the total mass $M = M(r \to \infty)$ grows as n increases. As we mentioned before, excited states have a higher value of M with respect to the ground state $n = 0$. Actually, we can observe that M is linear with respect to n.

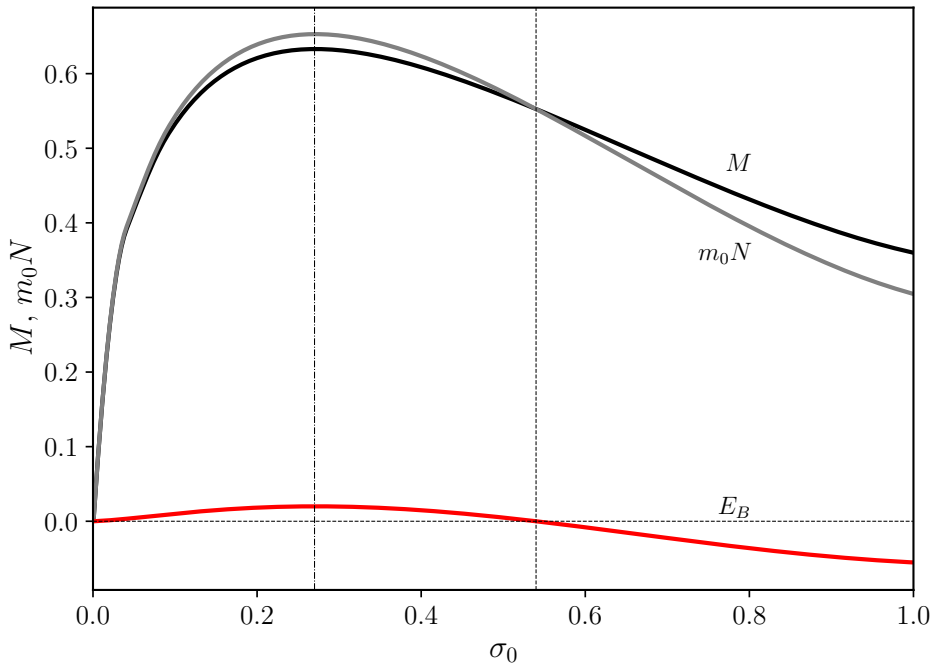

Figure 1.4: **Total mass and particle number.** The total mass M and the particle number $m_0 N$ as functions of central amplitude σ_0. The first dotted vertical line marks the point of maximum mass M_{max}. The second vertical line marks the point where the binding energy E_B vanishes. When E_B is positive, it represents only a small fraction of the total mass M.

Self-interacting Boson Stars

In the case in which the self-interaction term λ is different from zero, we can solve the system of equations in a similar way to the free case $\lambda = 0$. To do

this, let us write equations (1.19) in terms of the variables A, B, $\tilde{\omega}$ and σ, such that

$$\frac{dA}{dx} = xA^2\left[\left(\frac{\tilde{\omega}^2}{B}+1\right)\sigma^2+\lambda'\sigma^4+\frac{1}{A}\left(\frac{d\sigma}{dx}\right)^2\right]-\frac{A}{x}(A-1), \quad (1.29a)$$

$$\frac{dB}{dx} = xBA\left[\left(\frac{\tilde{\omega}^2}{B}-1\right)\sigma^2-\lambda'\sigma^4+\frac{1}{A}\left(\frac{d\sigma}{dx}\right)^2\right]+\frac{B}{x}(A-1), \quad (1.29b)$$

$$\frac{d^2\sigma}{dx^2} = -\left(\frac{2}{x}+\frac{1}{2B}\frac{dB}{dx}-\frac{1}{2A}\frac{dA}{dx}\right)\frac{d\sigma}{dx}-A\left[\left(\frac{\omega^2}{B}-1\right)-2\lambda'\sigma^3\right]\sigma, \quad (1.29c)$$

and from Eq. (1.18), the differential mass equation take the form

$$\frac{dM(r)}{dx} = \frac{1}{2}x^2\left[\left(\frac{\tilde{\omega}^2}{B}+1\right)\sigma^2+\lambda'\sigma^4+\frac{1}{A}\left(\frac{d\sigma}{dx}\right)^2\right]. \quad (1.30)$$

Let's remember that $\lambda' = \lambda\frac{M_{\rm pl}^2}{m_0^2}$. This self-coupling term may be important even for small values of λ. For the case of mini-boson star, Figure 1.4 shows that the maximum mass M_{max} is reached for an approximate value of central amplitude $\sigma_0 = 0.3$, which in physical terms is given by $\phi_0 \sim (0.3)M_{\rm pl}$. If we take the ratio between the mass term $m_0^2\phi_0^2$ and the self-interaction term $\lambda\phi_0^4$ for this value of the central amplitude, we have $\lambda\phi_0^4/m_0^2\phi_0^2 = \lambda(0.3)^2M_{\rm pl}^2/m_0^2$, so it will be relevant even for values on the order of $\lambda > m_0^2/(0.3M_{\rm pl})^2$ typically small. For example, if we consider a boson mass m_0 of the order of the neutron mass, we need that $|\lambda| > 10^{-39}$. This implies that in general, the value of λ plays a relevant role even for very small values of λ. Therefore, we can consider that the coupling term plays a significant role in the configuration. The system of equations (1.29) represents a family of configurations characterized by each of the values that λ can take.

The method to solve Eqs.(1.29), is the same described above for a mini-boson star. Given the boundary conditions A_0, B_0, σ_0 and $\lim_{r\to\infty}\sigma(r) = 0$, we use the shooting method based on bisection method to determine the value of $\tilde{\omega}_n$. This value of $\tilde{\omega}_n$ characterizes the solution $\sigma_n(r)$ with n number of nodes that satisfies $\lim_{r\to\infty}\sigma(r) = 0$. It is important to note that to solve Eqs. (1.29) we need to choose values of λ' that are sufficiently small. For large values of λ', the relative size of the terms in Eqs. (1.29) differs by several orders of magnitude and also their ratio varies with respect to the radius. Therefore, it is not possible to systematically neglect specific terms in the equations. However, it is possible to consider an approximate solution in the weak and strong coupling limit (see the approximations to the strong limit in Ref. [40]). In Figure 1.5 we present the profiles σ with zero nodes, considering different values of λ', including the case of a mini-boson star $\lambda' = 0$. Also, we can see that the value of the mass M increases as the value of the coupling constant does.[4] Figure 1.6 shows the total mass as a function of the central amplitude

[4]Now it is clear that a self-interacting boson star is more massive than its non-self-interacting counterpart, from which we derive the names *mini-* and *massive-* boson star.

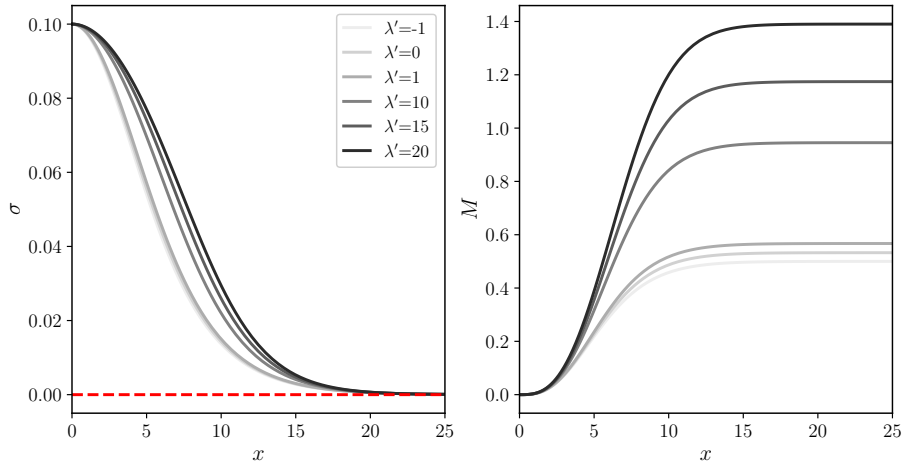

Figure 1.5: **Self-interacting relativistic massive-boson star**. Self-interactive relativistic boson star for different values of the constant coupling $\lambda' = -1, 0, 10, 15, 20$ and $n = 0$ nodes. *Left panel*: radial profile σ for each λ'. The profile widens as the coupling constant increases. *Right panel*: the mass profile M for each configuration on the left. The total mass increases as the value of the coupling constant increases.

σ_0 for the cases $\lambda' = 0, 10, 15$ and 20. For each case, the total mass increases successively. The maximum mass increases as a function of λ'.

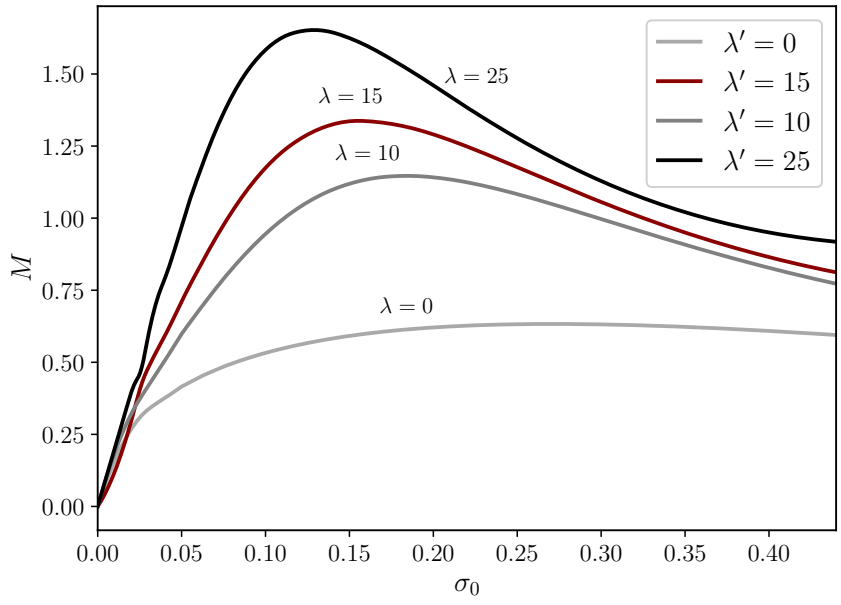

Figure 1.6: **Total mass M as function of central amplitude σ_0 for a massive- and mini-boson star.** The mass increases as a function of the value of the coupling constant λ'. Particularly, let us note that the value of the maximum mass M_{max} increases as we increase the value of λ'.

1.2.5 Dynamical Stability of Relativistic Boson Stars

The configurations we have studied so far, mini- and massive- boson stars, are susceptible of instability against small perturbations. As we have already mentioned, if $E_B < 0$, then there exists the possibility that the entire star could be unstable and disperse to infinity. Otherwise, those configurations for which their binding energy E_B is positive cannot disperse completely to infinity, therefore, these configurations could form stable stars over time. As we shall see, there is a limit, within the range of configurations with $E_B > 0$, beyond which stable stars cannot be formed in the presence of linear perturbations. Certainly, configurations for which the value of the central amplitude σ_0 exceeds the point of the maximum mass of the configuration M_{max} (including a region where $E_B > 0$) will be unstable, thereby either evolving into a black hole or transitioning from an unstable state to a stable configuration.

A way to analyze the dynamical stability of boson stars is to study the time evolution of infinitesimal perturbations around an equilibrium configuration, while considering that the number of particles is conserved (see Refs. [20, 22, 40]). We can obtain the perturbed equations if we decompose the scalar $\phi(t,x)$ and the metric field $g_{\mu\nu}(t,x)$ into an equilibrium configuration $\phi^{(0)}(x)$ and $g^{(0)}_{\mu\nu}(x)$ and a small perturbation $\delta\phi(t,x)$ and $\delta g_{\mu\nu}(t,x)$, which are generally dependent on r, φ and θ. Here we restrict ourselves to the case of spherically symmetric perturbations that depend only on r. In this case the functions $\phi(r,t)$ and $u(r,t)$ and $v(r,t)$ can be written as

$$u(r,t) = u^{(0)}(r) + \delta u(r,t), \quad v(r,t) = v^{(0)}(r) + \delta v(r,t), \tag{1.31a}$$

$$\phi(r,t) = \phi^{(0)}[1 + \delta\phi_R(r,t) + i\delta\phi_I(r,t)]e^{-i\omega t}, \tag{1.31b}$$

where $\delta u(r,t)$, $\delta v(r,t)$, $\delta\phi_R(r,t)$ and $\delta\phi_I(r,t)$ are small time-dependent perturbations. Here $\phi(t,r)$ is a generalization of the ansatz (1.9). By introducing the perturbations (1.31) into Einstein's equations (1.3), we obtain a set of independent linearized perturbation equations. If we also consider that perturbations conserve the number of particles N, we can add an additional constraint equation, counting a total of two second-order differential equations and one constraint. Although obtaining these equations is a challenging task, they can be consulted in Ref. [40]. However, the spirit of this section is to show the general process that we need to apply in the relativistic and non-relativistic limit.

The next step is to assume that all perturbations have a harmonic dependence on time (see Refs. [40, 41, 46, 47]) as

$$\delta q_i(t,\vec{x}) = \delta q_i(r)e^{i\lambda t}, \quad \text{with} \quad q_i \in \{u, v, \phi_R, \phi_I\}, \tag{1.32}$$

where λ is the characteristic frequency of the system to be determined and $\delta q_i(r)$ is a radial-dependent function. Once the ansatz (1.32) has been introduced, the system of coupled equations, along with the condition $dN/dt = 0$, defines an eigenvalue value problem for λ and the eigen-functions $\delta q_i(r)$. These system of equations can be written as

$$L_{ij}\delta q_{i,n} = \lambda_n^2 M_{ij}\delta q_{i,n}, \tag{1.33}$$

with L_{ij} a differential operator and M_{ij} a matrix depending on the background fields $q_i^{(0)}$, with $q_i^{(0)} \in \{u^{(0)}, v^{(0)}, \phi^{(0)}\}$, see Ref. [40, 41, 46] for a detailed derivation. The eigen-equation (1.33) yields a spectrum of solutions $\delta q_{i,n}(r)$ with their respective eigenvalues λ_n. As we will see, the sing of the eigenvalue λ_n^2 is crucial to determine the stability of the star. If λ_n^2 is negative, then λ_n is imaginary and the eigenfunction $\delta q_{i,n}(r)$ grows exponentially with time and the star will be unstable. Otherwise, if λ_n^2 is positive, λ_n is real and the star has no unstable modes, so will be stable. Actually, the system (1.33) is self-adjoint with real eigenvalues λ_n^2. Since λ_n^2 acquires a family of values given by $\lambda_0^2 < \lambda_1^2 < \lambda_2^2 < ...$, it is only necessary to determine the sign of λ_0^2 to establish the existence or absence of growing modes. Therefore, the critical value of λ_c at which the star becomes unstable is given by $\lambda_c = 0$. The case $\lambda_c = 0$, corresponds to a static perturbation according to Eq. (1.32). In particular, in the case of static perturbations the perturbed functions defined in Eq. (1.32) satisfy the same equations as the equilibrium solutions $u^{(0)}, v^{(0)}, \phi^{(0)}$ · Thus if we have an equilibrium configuration with $\sigma_0^{(0)}$, the perturbed fields will describe another equilibrium configuration with $\sigma_0^{(0)} + \delta\sigma_0$, for some infinitesimal $\delta\sigma_0$. We already know that the equilibrium *mini*-boson and *massive*-boson stars configurations are parameterized with the only parameter σ_0, cf. Figures 1.4 and 1.6, that is, the central amplitude of the scalar field, as

$$M = M(\sigma_0), \quad N = N(\sigma_0), \tag{1.34}$$

with M the total mass and N the number of particles. Hence, in the static case perturbed configurations must correspond to some central density $\sigma_0+\delta\sigma_0$, and, since the perturbations conserve the particle number δN, we can establish that only static perturbations exist when

$$\frac{dM(\sigma_0)}{d\sigma_0} = 0, \quad \frac{dN(\sigma_0)}{d\sigma_0} = 0. \tag{1.35}$$

In conclusion, the stable modes present in Eq. (1.33) correspond to real and positive eigenvalues λ_n^2 with $\lambda_c = 0$ the minimum value below which the modes become unstable. When $\lambda_c = 0$, there exists an extreme value of the mass $M(\sigma_0)$, beyond which the star becomes unstable. The maximum value of this mass corresponds to the value of the mass M_{max}. In the left panel of Figure 1.7, we plot the relation between the total mass of the star M for the relativistic case versus the value of the central profile σ_0. We can see that there exists a value of σ_0 for which M is maximized which is a critical point of Eq. (1.35). The gray band indicates a sector of configurations whose total mass is below the Kaup mass value and positive binding energy $E_B > 0$. Configurations within this range could be stable against linear perturbations. Therefore, M_{kaup} signs the transition limit between stability and instability.

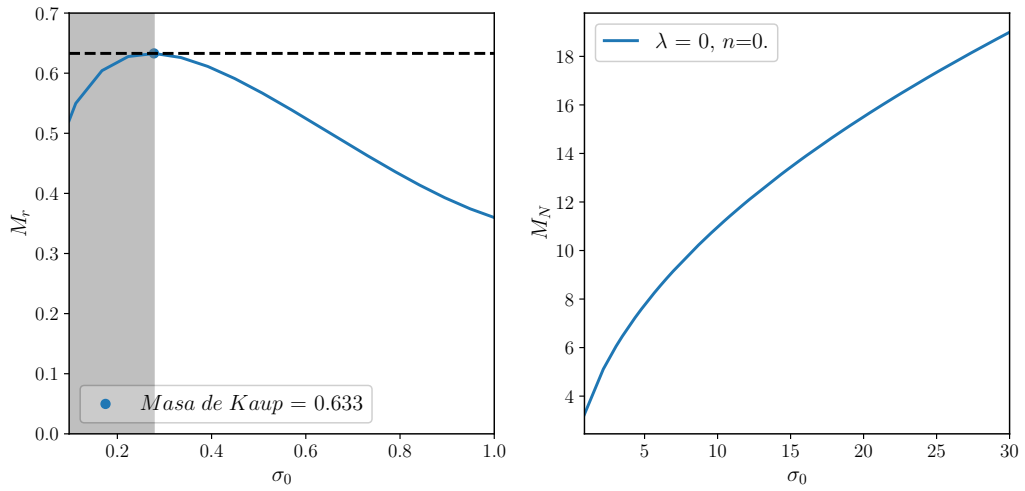

Figure 1.7: **Relativistic and non-relativistic mini-boson stars ($\lambda = 0$) for $n = 0$.** *Right panel*: mass profile M_r for a relativistic mini-boson star. There is a region (gray zone) beyond which the star is unstable. The critical mass value at this point is given by the Kaup mass ($M_{\text{kaup}} = 0.629$). *Left panel*: mass profile M_N for a non-relativistic mini-boson star. In this case, there is no critical mass value since relativistic effects are not present.

1.3 Non-relativistic Boson Stars

1.3.1 Gross-Pitaevskii-Poisson System

In the non-relativistic limit, the action (1.1) takes the form

$$S[\mathcal{U},\psi] = \int dt \int d^3x \left[\frac{1}{8\pi G}\mathcal{U}\Delta\mathcal{U} + \psi^*\left(i\frac{\partial}{\partial t} + \frac{1}{2m_0}\Delta\right)\psi - \frac{\lambda}{4m_0^2}|\psi|^4 - m_0\mathcal{U}|\psi|^2\right] \quad (1.36)$$

where we have introduced the scalar field as $\phi(t,\vec{x}) = \frac{1}{\sqrt{2m_0}}e^{-im_0t}\psi(t,\vec{x})$ and $\mathcal{U}(t,\vec{x})$ is the Newtonian potential. The first term describes the gravitational field, the second and third terms describes the sector of matter, and the last term describes the interaction of the matter field with the gravitational potential. In particular, we will consider a self-interacting potential $V = \lambda|\psi|^4/(4m_0^2)$ with λ a dimensionless coupling constant, which can take the values $\lambda > 0$ if the self-interaction is repulsive or $\lambda < 0$ if the self-interaction is attractive. When $\lambda = 0$ we recover the case with no self-interaction, in such a case the scalar field is only coupled to gravity. In Appendix A.1, we analyze in detail how to proceed to take the non-relativistic limit of the action (1.1).

Now, varying the action (1.36) with respect to the field ψ, we obtain the Gross-Pitaevskii equation

$$i\frac{\partial\psi}{\partial t} = -\frac{1}{2m_0}\Delta\psi \pm \frac{|\lambda|}{2m_0^2}|\psi|^2\psi + m_0\mathcal{U}\psi \quad (1.37a)$$

where the signs $\pm$ refer to the repulsive ($\lambda > 0$) and attractive case ($\lambda < 0$), and varying with respect to the Newtonian potential we obtain the familiar

Poisson equation as

$$\Delta\mathcal{U} = 4\pi G m_0 |\psi|^2. \tag{1.37b}$$

The whole system (1.37a) and (1.37b) conform the $s = 0$ Gross-Pitaevskii-Poisson system. If we restrict to the case $\lambda = 0$, we recover the Schrödinger-Poisson system. So, we can think of this system as a self-gravitating Bose-Einstein condensate with wave function $\psi(t, \vec{x})$. As we expected, the system does not contain temporal derivatives of the gravitational potential. In contrast to the self-interacting relativistic system (1.29), which depends on the gravitational fields $A(t, \vec{x})$ and $B(t, \vec{x})$, and the scalar field $\phi(t, \vec{x})$, the non-relativistic Gross-Pitaevskii-Poisson system (1.37) only depends on the gravitational field $\mathcal{U}$ and the scalar wave function $\psi(t, \vec{x})$. Beyond this simplification, to solve the system (1.37), we follow a process that is entirely analogous to the relativistic case.

We can recast the Gross-Pitaevskii-Poisson system (1.37a)-(1.37b) as an integro-defferential nonlinear equation in the form

$$i\frac{\partial\psi}{\partial t} = \hat{\mathcal{H}}(\psi)\psi \tag{1.38}$$

with the Hamiltonian operator

$$\hat{\mathcal{H}}(\psi) = -\frac{1}{2m_0}\Delta \pm \frac{|\lambda|}{2m_0^2}|\psi|^2 + 4\pi G m_0^2 \Delta^{-1}(|\psi|^2), \tag{1.39}$$

where

$$\Delta^{-1}(|\psi|^2)(\vec{x}) = -\frac{1}{4\pi}\int \frac{|\psi(\vec{y})|^2}{|\vec{x} - \vec{y}|} d^3y. \tag{1.40}$$

Note that the Hamiltonian operator $\hat{\mathcal{H}}[\psi]$ is hermitian, i.e. $(\psi_1, \hat{\mathcal{H}}[\psi]\psi_2) = (\hat{\mathcal{H}}[\psi]\psi_1, \psi_2))$ and nonlinear in ψ. Solutions to the system (1.38) that minimize the energy functional and conserve the number of particles are given by the harmonic ansatz of the form Eq. (1.9) and are called *stationary states*. Here, we are interested in characterizing these configurations, particularly configurations spherically symmetric. In what follows, we will make an effort to describe these solutions, and a brief review of the methodology for studying their stability.

1.3.2 Conserved Quantities

Particle Number

The invariance of the Lagrangian in the non-relativistic action (1.36) under continuous shifts in the phase of the wave function $\psi(t, \vec{x}) = e^{-i\alpha}\psi(t, \vec{x})$, with α a real constant, leads to the conservation of the "*particle number*", $N = \int d^3x n$, where the number density n is given by $n = |\psi(t, \vec{x})|^2$. In the non-relativistic case we have that the total mass of the configurations is given by $M = m_0 N$, where the energy density is given by $\rho = m_0|\psi|^2$.

Note: Given the Lagrangian density

$$\mathcal{L} = \left[\psi^*\left(i\frac{\partial}{\partial_t} + \frac{1}{2m_0}\Delta\right)\psi - V - m_0\mathcal{U}|\psi|^2\right], \tag{1.41}$$

the complex scalar field ψ has internal $U(1)$ symmetry. This means that global transformations of the fields $\psi \to e^{i\alpha}$ and $\psi^* \to e^{-i\alpha}\psi^*$ have no effect on the Lagrangian. According to the Noether theorem (see footnote (2)), every symmetry yields a conserved current. To get the conserved current associated to the U(1) symmetry, we write the transformation for an infinitesimal change in the phase α:

$$\psi \to \psi + \delta\psi = \psi + D\psi\delta\alpha = \psi + i\psi\delta\alpha, \quad D\psi = \left.\frac{\partial\psi}{\partial\alpha}\right|_{\alpha=0} = i\psi,$$
$$\psi^* \to \psi^* + \delta\psi^* = \psi^* + D\psi^*\delta\alpha = \psi - i\psi\delta\alpha, \quad D\psi^* = \left.\frac{\partial\psi^*}{\partial\alpha}\right|_{\alpha=0} = -i\psi^*,$$

with $D\mathcal{L} = \frac{\partial\mathcal{L}}{\partial x^\mu}\frac{\partial\psi}{\partial\alpha}|_{\alpha=0} = 0$. Given that the conserved current is given by the expression $J^\mu_N = \Pi^\mu(x)D\psi - W^\mu(x)$ with $D\mathcal{L} = \partial_\mu W^\mu = 0$, we have $W^\mu = 0$ and $J^\mu_N = \sum_\sigma \Pi^\mu_\sigma D\sigma$ where the sum is over the fields ψ and ψ^*. So, the conserved current is given by

$$J^\mu_N = \sum_\sigma \Pi^\mu_\sigma D\sigma = \Pi^\mu_\psi D\psi + \Pi^\mu_{\psi^*} D\psi^* \tag{1.42}$$

with the conserved charge

$$N = \int d^3x J^0_N = \int d^3x|\psi|^2. \tag{1.43}$$

See Ref. [36] for a comprehensive exposition of Noether's theorem and conserved charges.

Energy Functional

Analogous to the relativistic case, we can write the total energy of the system for the non-relativistic action (1.36) as

$$E = \int d^3x \left[\frac{\partial\mathcal{L}}{\partial(\dot\psi^*)}\dot\psi^* + \frac{\partial\mathcal{L}}{\partial(\dot\psi)}\dot\psi + \frac{\partial\mathcal{L}}{\partial(\dot{\mathcal{U}})}\dot{\mathcal{U}} - \mathcal{L}\right], \tag{1.44}$$

where dots indicates time-derivatives. Using the relations $\nabla(\mathcal{U}\nabla\mathcal{U}) = \nabla\mathcal{U}\nabla\mathcal{U} + \mathcal{U}\Delta\mathcal{U}$, $\psi^*\Delta\psi = \nabla(\psi^*\nabla\psi) - \nabla\psi^*\nabla\psi$, the Poisson equation (1.37b) and discarding the boundary terms, we can recast this as

$$\mathcal{E}[\psi] \equiv \int d^3x \left(\frac{1}{2m_0}|\nabla\psi|^2 \pm \frac{|\lambda|}{4m_0^2}|\psi|^4 + \frac{1}{2}m_0\mathcal{U}|\psi|^2\right), \tag{1.45}$$

which, due to the invariance of the Lagrangian under time translations $\psi(t,\vec{x}) \to \psi(t - t_0, \vec{x})$, with t_0 a real constant, is conserved whereas the system evolves.

Properties of the Energy Functional

We are interested in characterizing equilibrium configurations that represent perdurable solutions over time, that is, that are susceptible to stability against perturbations. Equilibrium configurations correspond to critical points of the

energy functional $\mathcal{E}[\psi]$ that conserves the number of particles N.[5] Given the constriction $N =$ constant, we need to perform the variation of the functional $\mathcal{E}_E[\psi] = \mathcal{E}[\psi] - \frac{E}{2}(N - \int \psi^* \psi dV)$ with E a Lagrange multiplier associated with the constraint that guarantees that the particle number remains fixed in the variation. After the first variation of $\mathcal{E}[\psi]$ we have $\delta\mathcal{E}_E = \mathrm{Re}(\hat{\mathcal{H}}[\psi]\psi - E\psi, \delta\psi)$. A critical point is characterized by the criteria $\delta\mathcal{E}_E = 0$ for the field $\delta\psi$; Then, equilibrium configurations satisfies the eigenvalue equation $E\psi = \hat{\mathcal{H}}\psi$. These configurations are called stationary configurations, and they are given by the solutions of the form

$$\psi(t, \vec{x}) = e^{-iEt}\sigma^{(0)}(\vec{x}). \tag{1.49}$$

For these solutions, the energy functional allows us to shed light on the stability of stationary configurations. In order to see this, we can recast the energy functional (1.45) in the form

$$\mathcal{E}[\psi] = T[\psi] \pm F[n] - D[n, n], \tag{1.50}$$

with $n = |\psi|^2$, and

$$T[\psi] \equiv \frac{1}{2m_0}\int |\nabla\psi(\vec{x})|^2 d^3x, \tag{1.51a}$$

$$F[n] \equiv \frac{|\lambda|}{4m_0^2}\int n(\vec{x})^2 d^3x, \tag{1.51b}$$

$$D[n, n] \equiv 2\pi G m_0^2 \int\int \frac{n(\vec{x})n(\vec{x})}{|\vec{x} - \vec{y}|} d^3y d^3x. \tag{1.51c}$$

Invariance of the particle number N with respect to the rescaled wave function $\psi_\nu(t, \vec{x}) = \nu^{3/2}\psi(t, \nu\vec{x})$ allows us to establish some properties of the energy functional for stationary states (states that minimize $\mathcal{E}[\psi]$):

1. The first variation of $\mathcal{E}[\psi_\nu]$ allows us to write the energy functional for stationary states as $\mathcal{E}[\psi] = -T[\psi] \mp 2F[\psi]$.

2. The energy of a stationary state is always negative in the repulsive case.

3. In the attractive case, stationary states cannot be a minimum of the energy function if the self-interaction term dominates over the kinetic term $T < 3F$.

[5] To perform the variation of the functional $\mathcal{E}[\psi]$, we expand the wave function as

$$\psi(t, \vec{t}) = \psi^{(0)} + \epsilon\delta\psi(t, \vec{x}) + \frac{\epsilon^2}{2}\delta^2\psi(t, \vec{x}) + \mathcal{O}(\epsilon^2) \tag{1.46}$$

where $\psi^{(0)}$ denote the background field and $\delta\psi(t, \vec{x})$, $\delta^2\psi(t, \vec{x})$ denote the first and second order perturbations, respectively. So, the n-th variation is defined as

$$\delta^n\varepsilon = \frac{d^n}{d\epsilon^n}\varepsilon[\psi]\bigg|_{\epsilon=0}. \tag{1.47}$$

With this, integrating by parts and discarding the boundary terms, the first variation on the energy functional $\varepsilon[\psi]$ take the form

$$\delta\epsilon = \mathrm{Re}(\mathcal{H}(\psi), \delta\psi), \tag{1.48}$$

where we have used the $\hat{\mathcal{H}}$ definition (1.39) and we have defined the L^2-scalar product $(\psi, \phi) = \int \psi^*\phi d^3x$ between ψ and ϕ.

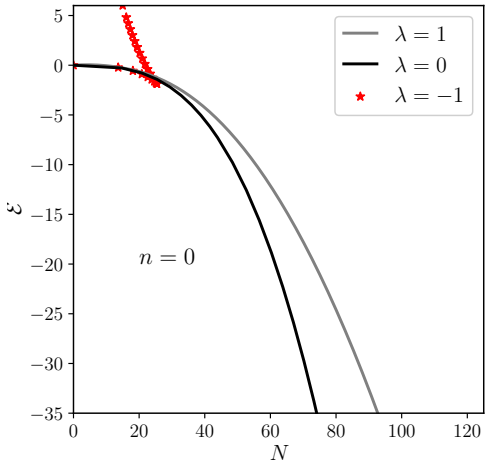

Figure 1.8: **Energy functional $\mathcal{E}$ for stationary states as function of the number of particles.** Energy for a stationary state with $n = 0$ nodes in the the free ($\lambda = 0$), repulsive ($\lambda = 1$) and attractive ($\lambda = -1$) cases.

The first point allows us to write the energy functional for stationary states without the need to calculate D. The second point indicates that excluding the attractive case, the energy functional will always be negative and increasing. The third point provides us with important information about the stability of stationary configurations for the attractive case $\lambda = -1$. The point at which the quantity $T - 3F$ transitions from positive to negative values, that is, when $T[\sigma_0] - 3F[\sigma_0] = 0$, marks the transition point from the stable band of configurations to the unstable band. Particularly, the value at which this transition occurs coincides with the point of maximum mass in the Figure 1.9, right panel. We will replicate these demonstrations in more detail in the next chapter for non-relativistic Proca stars.

1.3.3 Numerical System and Results

In order to numerically solve the system of equations (1.37a)-(1.37b), we can make a change of variable to obtain a dimensionless system. If we define the new dimensionless quantities

$$\Lambda := \frac{|\lambda| M_{pl}^2}{2\pi m_0^2}, \quad t := \frac{2m_0}{\Lambda} t^{phys}, \quad x := \frac{2m_0}{\Lambda^{1/2}} x^{phys}, \tag{1.52a}$$

$$\mathcal{U}^{phys} := \frac{\Lambda}{2}\mathcal{U}, \quad \psi := \left(\frac{\pi\Lambda^2}{2M_{\rm pl}^2 m_0}\right)^{1/2} \psi^{phys}. \tag{1.52b}$$

where *phys* makes reference to physical quantities. In terms of these variables we can write a dimensionless Gross-Pitaevski-Poisson system as

$$i\frac{\partial\psi}{\partial t} = (-\Delta \pm |\psi|^2 + \mathcal{U})\psi, \tag{1.53a}$$

$$\Delta\mathcal{U} = |\psi|^2, \tag{1.53b}$$

where the coupling constant λ is present in the dimensionless variables. Beyond the relative simplification of the relativistic system (1.29c), it is noteworthy to observe that the Gross-Pitaevskii-Poisson system (1.54) does not depend on the strength of the coupling constant λ. Therefore, the solutions will not depend on how strong λ is, but only on the repulsive or attractive nature of the self-interaction. In the relativistic case, a similar situation arises when $\lambda \gg 1$, (see Ref. [40]). As in the relativistic case with strong coupling constant, λ plays only a role through the dimensionless variables (1.52) and we have only two differential equations to solve, however, in the non-relativistic case, these are second order differential equations. The mass, similar to the relativistic case, will scale as $M = 4\pi\Lambda^{1/2} m_0/M_{\rm pl}^2 M^{phys}$ and the particle number scales like $N = 4\pi\Lambda^{1/2} m_0^2/M_{\rm pl}^2 N^{phys}$.

Spherically Symmetric Configurations

Now, let us study the case of a spherically symmetric stationary state with a spherically symmetric gravitational potential $U(r)$. Note that the spherical symmetry in $\psi(t,r)$ guarantees the symmetry of $T^{\mu}_{\ \nu}(t,r)$ and therefore the symmetry of $\mathcal{U}(r)$ through the Poisson equation ($\mathcal{U}$ is time independent, since it is not dynamic in the non-relativistic limit). Given the stationary ansatz $\psi(t,x) = e^{-iEt}\sigma(r)$ and defining the shifted potential $u(r) \equiv E - \mathcal{U}(r)$, the dimensionless Gross-Pitaevskii-Poisson system (1.53) is given by

$$\frac{d^2\sigma}{dr^2} = -\frac{2}{r}\frac{d\sigma}{dr} \pm \sigma^3 - u\sigma, \tag{1.54a}$$

$$\frac{d^2u}{dr^2} = -\frac{2}{r}\frac{du}{dr} - \sigma^2. \tag{1.54b}$$

In order to ensure regularity at the origin, we must impose the following boundary conditions: $\sigma'(r=0) = u'(r=0) = 0$, $\sigma(r=0) = \sigma_0$ and $u(r=0) = u_0$. And to guarantees finite energy solutions we need impose $\lim_{r\to\infty}\sigma(r) = 0$. To solve the system of equations (1.54), we must reduce the equations to four first-order differential equations[6] and proceed in a similar manner as we did in the relativistic case. Then, we can solve the system for σ_0 and u_0 through the shooting-bisection method before described (in Appendix B, we review in detail this method applied to a non-relativistic Proca star), and determine the u_0 value that yields a solution with $n = 0, 1, 2, ...$ nodes and satisfies the condition of finite energy $\lim_{r\to\infty}\sigma(r) = 0$. For a given value of the central amplitude σ_0 we get a discrete set of infinite values of u_n that satisfies the boundary conditions whit successive solutions representing higher energy regular solutions $u_0 < u_1 < u_2 < ... < u_n$.

Additionally, we need to connect the numerical solution obtained for a finite value of r (this value depends on the maximum precision achieved by

[6]System of equations (1.54) reduced to four first-order differential equations for $r > 0$:

$$\frac{d\sigma}{dr} = y, \quad \frac{dy}{dr} = -\frac{2y}{r} \pm \sigma^3 - u\sigma, \tag{1.55a}$$

$$\frac{du}{dr} = x, \quad \frac{dx}{dr} = -\frac{2x}{r} - \sigma^2. \tag{1.55b}$$

When $\lim r \to 0$ (using L'Hôpital's rule) we can write $dy/dr = -\sigma_0 u_0/3$ and $dx/dr = -\sigma_0^3/3$.

the shooting method) with the asymptotic solution of $\sigma(r)$ and $u(r)$ as $r \to \infty$. At this limit, the equation (1.54a) takes the form $\frac{d^2}{dr^2}(r\sigma(r)) - |E|r\sigma(r) \approx 0$ from which the radial profile take the form

$$\sigma(r) \approx \frac{C}{r} e^{-\sqrt{|E|}r}, \tag{1.56}$$

where C is a constant of integration. To obtain Eq. (1.56) we have used the fact that $\lim_{r\to\infty} \sigma(r) = 0$ and $\lim_{r\to\infty} \mathcal{U}(r) = 0$. Since the gravitational potential vanishes at infinity, the shifted potential is given by $\lim_{r\to\infty} u(r) = E - \mathcal{U}(r) = E$. On the other hand, it is also possible to demonstrate, see Appendix C in Ref. [48], that the asymptotic behavior of $u(r)$ takes the form

$$E = u_0 - \frac{M}{r} \tag{1.57}$$

with M the total mass given by $M = m_0 N = m_0 \int r^2 \sigma(r)^2 dr$.

Figure 1.9, left panel, shows the radial profile with $n = 0$ nodes for the attractive, free, and repulsive cases, and a central amplitude $\sigma_0 = 1.0$. For these configurations, the shooting method produces a value for the shifted potential $u_0 = 0.56$ ($\lambda = -1$), $u_0 = 0.91$ ($\lambda = 0$) and $u_0 = 1.47$ ($\lambda = 1$). From this value, it is possible to obtain the eigenvalue E_0 through the expression (1.57). Let's note that, as in the relativistic case (cf. Figure 1.5), the profile shrinks or expands depending on the value of the self-interaction. When $r \to \infty$, the value of the profile approaches zero numerically, as we expect.

Finally, it is important to note that the numerical system (1.54) is identical to the system $s = 1$ Gross-Pitaevskii-Poisson for the case of a self-interacting non-relativistic Proca star with linear(circular) polarization (2.87) that evolves harmonically with only one frequency E. We will solve these equations in the next chapter.

Mass and Radius

The mass of a non-relativistic boson star can be computed as the product of m_0 with the particle number defined in Eq. (1.43), which yields $M^{phys} = m_0 N^{phys}$ where $N^{phys} = M_{\rm pl}^2/(4\pi\Lambda^{1/2} m_0^2) N$, and N represent the number of particles in the dimensionless variables (1.52), that in the spherically symmetric case is given by

$$N = 4\pi \int_0^\infty |\sigma(r)|^2 r^2 dr. \tag{1.58}$$

Let's remember that to calculate the total mass of the configuration $\sigma(r)$ we need to make the integral in $4\pi \int_0^\infty dr r^2 \rho$ with $\rho = m_0 |\sigma(r)|^2$ and to calculate the radius of the star R_{99} we have to calculate the integral $0.99M = 4\pi \int_0^{R_{99}} dr r^2 \rho$ with $R_{99} = 2\sqrt{2\pi} m_0^2/(|\lambda|^{1/2} M_{\rm pl}) R_{99}^{phys}$. In Figure 1.9, we plot $\sigma(r)$ vs r for $\lambda = 1, 0, -1$, that is the systems Gross-Pitaevskii-Poisson (GPP) in the repulsive ($\lambda = 1$), free (SP, $\lambda = 0$), and attractive ($\lambda = -1$) case, respectively, for a central amplitude $\sigma_0 = 1$. We can see that, if we compare with respect to the Schrödinger-Poisson (SP) profile $\lambda = 0$, the profile of the configuration expands if the self-interaction is repulsive $\lambda = 1$ and shrinks if it is attractive $\lambda = -1$. Also, in the right panel of Figure 1.9, we have plotted

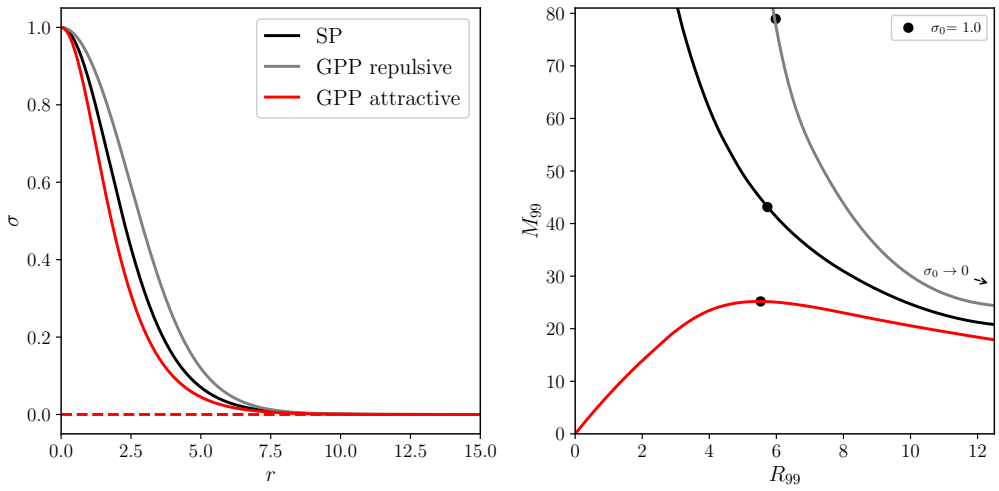

Figure 1.9: **Self-interactive non-relativistic boson star** $n = 0$**.** Radial profile $\sigma(r)$ for a non-relativistic boson star for different values of the coupling constant $\lambda = 0, 1, -1$. We can observe that the profile becomes wider as the value of the self-interaction increases. M_{99}vsR_{99} for a non-relativistic self interactive boson star for the attractive ($\lambda = -1$), free ($\lambda = 0$) y repulsive ($\lambda = 1$) case. M_{99} is 99% of the value of the star's mass contained within 99% of the star's radius. For the attractive case ($\lambda = -1$), we observe that there is a critical mass value similar to the one that appears in the relativistic case.

M_{99} vs R_{99}, that is, the relation between $0.99M$ of the total mass and R_{99}, the radius of the $0.99M$ mass. In the free and repulsive case, the configurations become more compacts as we increase the value of the central amplitude σ_0, whereas in the attractive case, the configuration reaches a maximum mass M_{99} corresponding to a central amplitude $\sigma_0^{\max}$. In the case of $\sigma_0 \to 0$, we can see from Eq. (1.37a) that the self-interactive term is negligible with respect to all the other terms. In Figure 1.9 it is clear when $\sigma \to 0$ and the profiles approximate the Schrödinger-Poisson solution.

Energy Functional

As we have seen, the energy functional $\mathcal{E}[\psi]$ plays an important role in determining equilibrium configurations, and for this reason, we analyze it separately. From Eq.(1.45) the total energy is given by $\mathcal{E}^{phys} = m_0^4(2\pi)^{5/2}/(2\pi^2|\lambda|^{5/2}M_{\rm pl})\mathcal{E}$ with

$$\mathcal{E} = -2\pi \int \left[\frac{d^2\sigma(r)}{dr^2} \pm \sigma(r)^4\right] r^2 dr \tag{1.59}$$

where we have used the relation, $\mathcal{E}[\psi] = -T[\psi] \mp 2F[\psi]$. In Figure 1.8 we show the energy functional $\mathcal{E}[\psi]$ as function of the number of particles of the configuration N for the attractive ($\lambda = -1$), free ($\lambda = 0$) and repulsive ($\lambda = 1$) case. Note that for the free and repulsive case the energy is always negative (in agreement with the point two above), contrary to the attractive case for which the energy takes positive values at a finite value of N. For the repulsive and free case the energy increases with the number of particles. Remember that in the attractive case, stationary states cannot be a minimum of the

energy function if the self-interaction term dominates over the kinetic term $T < 3F$, that is, when $T - 3F = 0$ marks the point in which stationary states with attractive self-interaction becomes instable. In Figure 1.8, the point at which the energy reaches its minimum coincides with the state at which the configuration reaches its maximum mass. We can also observe that stationary states without self-interaction represent a state of lower energy compared to those for which the self-interaction is $\lambda = 1$. Naturally, the energy will increase in value as we increase the value of n. The ground state configuration (i.e. the lowest possible energy state that exists for a given particle number) is given by nodeless ($n = 0$) spherically symmetric stationary states in the absence of self-interactions. As we shall demonstrate in the following chapter, the $s = 0$ Gross-Pitaevskii-Poisson system (1.54) is equivalent to the $s = 1$ Gross-Pitaevskii-Poisson system with linear (circular) polarization. For stationary solutions with $\lambda \geq 0$, we find that the energy functional is bounded from below and that, moreover, for spherically symmetric configurations, the system reaches its minimum energy state. That is, stationary configurations with spherical symmetry and $\lambda \geq 0$ constitute the ground state.

Excited stationary configurations

With an harmonic ansatz of the form $\psi(t, x) = e^{-iEt}\sigma(\vec{x})$, we can write the integro-differential equation (1.38) in the form of an eigen-value problem as

$$E\sigma = \hat{\mathcal{H}}(\sigma)\sigma(\vec{x}). \tag{1.60}$$

Given a value for the central amplitude σ_0, there are an infinite number of possible eigenvalue solutions E_n for $n = 0, 1, 2, 3...$ that satisfy the integro-differential equation (1.60) for the regular and finite boundary conditions. If we characterize the solutions to Eq. (1.60) in terms of the number of nodes n present in the profile $\sigma(\vec{x})$, it is possible to associate the ground state (that is, the state with minimum energy) to the solution with the $n = 0$ number of nodes and the states with higher energy to solutions with $n = 1, 2, 3...$ number of nodes. With this, the association of the value of the constant ω in Eq. (1.9) with the value of the frequency (energy) of the boson field is clear.

In Figure 1.10 we can see the $\sigma(r)$ profile (right panel) in the attractive, free (SP, $\lambda = 0$) and repulsive case for the Gross-Pitaevskii-Poisson system with $n = 1$ number of nodes and the 99% of the total mass M_{99} as function of R_{99} the value of the radius containing 99% of the mass (left panel). Solutions to the eigenvalue problem with $n = 1$ number of nodes correspond to a value $E_{n=1}$ given by Eq. (1.57). For this case, the shooting method produces the values for the shifted potential given by $u_0 = 0.91$ ($\lambda = -1$), $u_0 = 1.2$ ($\lambda = 0$), and $u_0 = 1.66$ ($\lambda = -1$). Note that for a fixed value of R_{99}, solutions with $n = 1$ represent more massive solutions compared to the solutions without nodes. Also, as we observed for the stationary solutions with $n = 0$ (see Figure 1.9), the attractive case ($\lambda = -1$) reaches a maximum value of the mass M_{99} for a unique value of R_{99} (or σ_0). For $\sigma_0 \to 0$ the effects of the self-interactions becomes negligible and we recover the non-interacting Schrödinger-Poisson system. Figure 1.12 shows these systems for $n = 1$ and $n = 2$ solutions for $\lambda = -1, 0, 1$, in the first and second panels, and the value

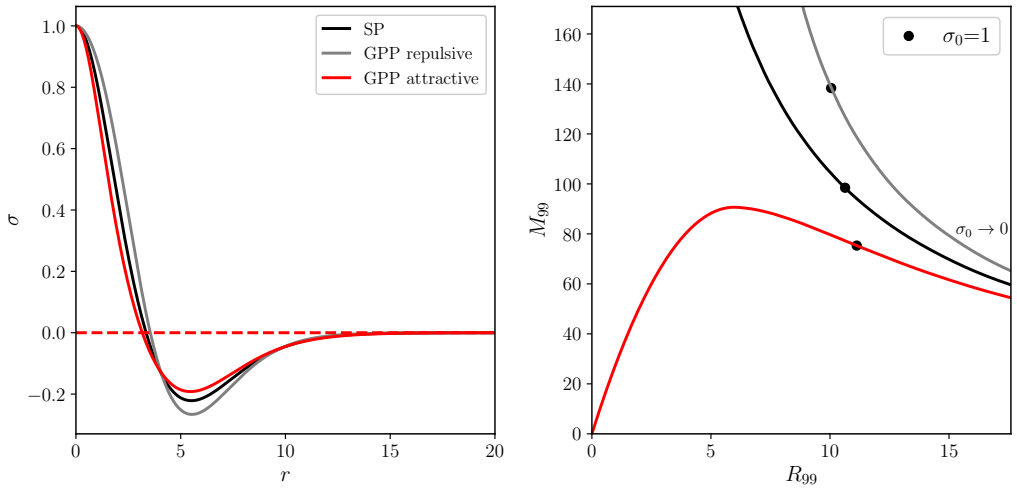

Figure 1.10: **Self-interactive boson star** $n = 1$.*Left panel*: radial profile $\sigma(r)$ for a non-relativistic Boson star for $n = 1$ number of nodes and central amplitude $\sigma_0 = 1$. In each case, these profiles represent excited states with $\lambda = -1, 0, 1$. *In the right panel*: M_{99}vsR_{99} for each case in the left panel. Again, we can see that the attractive case ($\lambda = -1$) has a maximum mass value similar to the relativistic case.

of the total mass M for each case, in the third panel. Note that the total mass M increases with the values of λ and n. This is expected since configurations with a greater number of nodes have greater energy. In each case, the solutions are regular at the origin, localized (that is, $\lim_{r\to\infty} \sigma(r) = 0$) and energy finite. Finally, Figure 1.11 shows the energy functional $\mathcal{E}$ as a function of the number of particles N for the first excited state $n = 1$. For a fixed N, the energy is greater than that corresponding to the state with $n = 0$, for each $\lambda = -1, 0, 1$.

1.3.4 Linear Stability

To study the stability of the Gross-Piaevskii-Poisson system (1.37a)-(1.37b) against small perturbations to the stationary solutions $\psi(t, \vec{x}) = e^{-iEt}\sigma(\vec{x})$ that we have studied so far, we propose the ansatz (see Ref. [49] for an exhaustive analysis of the methodology described in this section) of the form

$$\psi(t, \vec{x}) = e^{-iEt}\left[\sigma^{(0)} + \epsilon\sigma(t, \vec{x}) + \mathcal{O}(\epsilon^2)\right] \tag{1.61}$$

where ϵ is a small positive parameter, $\sigma^{(0)}$ is the background solution to eigenvalue problem (1.60) and $\sigma(t, \vec{x})$ is a complex function that describes the linear perturbation. Note that in the relativistic case we have written the perturbation with spherical symmetry as $\phi(t, r) = \phi^{(0)}\delta\phi_R(r, t) + \phi^{(0)}\delta\phi_I(r, t)$, which is an analogous construction to the ansatz (1.61). In Ref. [40] they write the decomposition for the relativistic case with spherical symmetry in the form $\phi(r, t) = e^{-iEt}[\phi(r, t)^{(0)} + \phi(t, r)^{(1)}]$ in accordance with Eq. (1.61).

Following the same procedure described in Section 1.2.5, we insert the ansatz (1.61) into the integro-differential Gross-Pitaevski-Poisson system, and

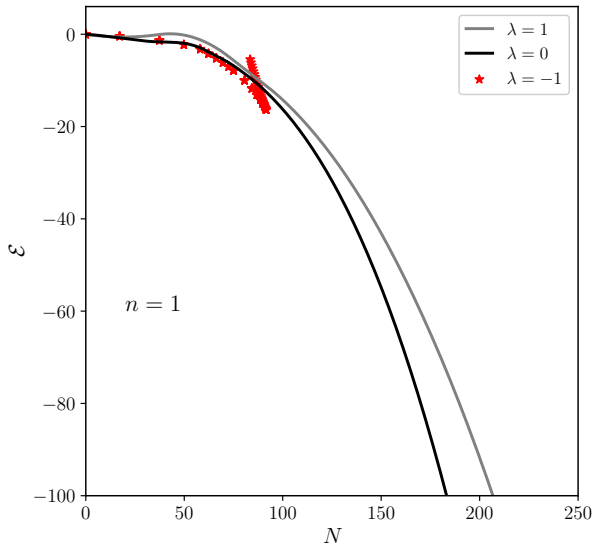

Figure 1.11: **Energy functional $\mathcal{E}$ as function of the number of particles N for $n = 1$.** Energy functional $\mathcal{E}$ as a function of the number of particles N for the first excited state $n = 1$. For a fixed N , the energy is greater than that corresponding to the state with $n = 0$, for each $\lambda = -1, 0, 1$.

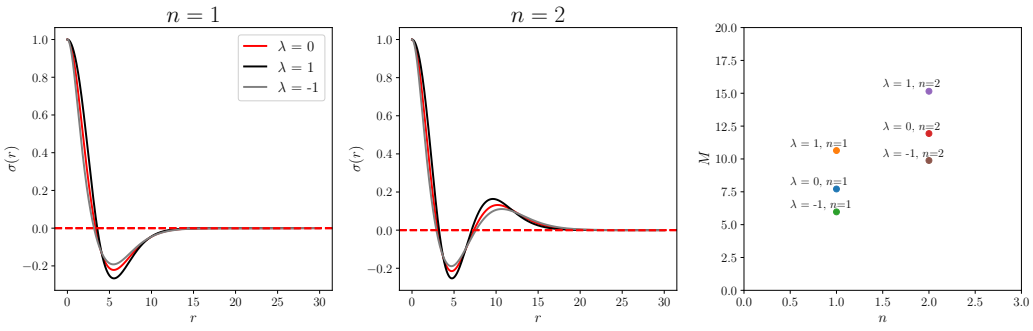

Figure 1.12: **First two excited state for a self-interactive boson star $n = 1, 2$.** *Left and center panel*: radial profile $\sigma(r)$ for the two first excited states ($n = 1, 2$ number of nodes) of a non-relativistic boson star for the attractive ($\lambda = -1$), free ($\lambda = 0$), and repulsive ($\lambda = 1$) cases. *Left panel*: the total mass M for each one of the profiles on the left.

up to linear order in ϵ, we get

$$i\frac{\partial\sigma}{\partial t} = \left(\hat{\mathcal{H}}^{(0)} - E\right)\sigma(t,\vec{x}) + 2\sigma^{(0)}\hat{K}\left[\sigma^{(0)}\mathrm{Re}(\sigma(t,\vec{x})\right], \tag{1.62}$$

where

$$\hat{\mathcal{H}}^{(0)} := -\Delta \pm \sigma^{(0)2} + \Delta^{-1}(\sigma^{(0)2}) \quad \text{and} \quad \hat{K} = \pm 1 + \Delta^{-1}. \tag{1.63}$$

Now, similar to the harmonic decomposition of the perturbation (1.32) in the relativistic case, we can write $\sigma(t,\vec{x})$ as $\sigma(t,\vec{x}) = \sigma_{\mathrm{R}}(t,\vec{x}) + \sigma_{\mathrm{I}}(t,\vec{x}) = 2\mathrm{Im}\left(B(\vec{x})e^{\lambda t}\right) + 2\mathrm{Re}\left(A(\vec{x})e^{\lambda t}\right)$ or

$$\sigma(t,\vec{x}) = \left[A(\vec{x}) + B(\vec{x})\right]e^{\lambda t} + \left[A^*(\vec{x}) - B^*(\vec{x})\right]e^{\lambda^* t} \tag{1.64}$$

where $A(\vec{x})$ and $B(\vec{x})$ are complex-valued functions and λ (do not confuse λ with the self-coupling constant and $A(\vec{x})$ and $B(\vec{x})$ with the relativistic gravitational potentials) is the characteristic frequency of the perturbation. Here Eq. (1.64) is equivalent to the system (1.32) for the relativistic case, in this case the only field to be perturbed is given by $\psi(t,\vec{x})$ through the fields $A(\vec{x})$ and $B(\vec{x})$ in a way similar to that of $\delta\phi_I$ and $\delta\phi_R$. Putting Eq. (1.64) into Eq. (1.62), and setting the coefficients in front of $e^{\lambda t}$ and $e^{\lambda^* t}$ to zero, we get

$$L_{ij}X_j = i\lambda X_i \quad \text{with} \quad \vec{X} = (A(\vec{x}), B(\vec{x}))^T \tag{1.65a}$$

where

$$\hat{L} = \begin{bmatrix} 0 & \left(\hat{\mathcal{H}}^{(0)} - E\right) \\ \left(\hat{\mathcal{H}}^{(0)} - E\right) + 2\sigma^{(0)}\hat{K}\left[\sigma^{(0)}\right] & 0 \end{bmatrix}. \tag{1.65b}$$

and $\hat{K}[\sigma^{(0)}]A$ acts as $\hat{K}\left[\sigma^{(0)}A\right]$. Note the similitude and simplification in form with Eq. (1.33) now with $\hat{L}$ containing both partial derivatives and background equilibrium solution $\sigma^{(0)}$. The system (1.65) is a linear eigenvalue problem for the constant λ, such that, if $\hat{L}$ is a self-adjoint matrix, then λ will be real. In this last case $\sigma(t,\vec{x}) = [\mathrm{Re}\{A(\vec{x})\} + \mathrm{Im}\{B(\vec{x})\}]e^{\lambda t} \sim e^{\lambda t}$, and the perturbations grow exponentially with t. So, linear instability is determined by the existence of solutions with positive real part of λ. In Ref. [49], the authors demonstrate that stationary ground state configurations can have only real or purely imaginary λ and that real eigenvalues are excluded if these configurations are a local minimum of the energy functional $\mathcal{E}[\psi]$.

Spherical and Non-spherical perturbations

The background solutions $\sigma^{(0)}(r)$ that we have calculated are spherically symmetric, so the linearized equations (1.65) can be decoupled into a family of purely radial systems by expanding the perturbation functions $A(\vec{x})$ and $B(\vec{x})$ in terms of spherical harmonics Y^{lm} as

$$A(\vec{x}) = \sum_{lm} A_{lm}(r)Y^{lm}(\theta,\varphi), \tag{1.66a}$$

$$B(\vec{x}) = \sum_{lm} B_{lm}(r)Y^{lm}(\theta,\varphi). \tag{1.66b}$$

For radial perturbations we need to consider $l, m = 0$. With these functions, the eigen-value system (1.65) can be written in terms of

$$X_i = (A_{lm}, B_{lm}) \quad \text{with} \quad \hat{L} = \begin{bmatrix} 0 & \left(\hat{\mathcal{H}}_l^{(0)} - E\right) \\ \left(\hat{\mathcal{H}}_l^{(0)} - E\right) + 2\sigma^{(0)}\hat{K}_l\left[\sigma^{(0)}\right] & 0 \end{bmatrix}, \tag{1.67}$$

where the operators $\hat{\mathcal{H}}^{(0)}$ and $\hat{K}_l$ are defined as

$$\hat{\mathcal{H}}^{(0)} := -\Delta_l \pm \sigma^{(0)2} + \Delta_s^{-1}(\sigma^{(0)2}) \quad \text{and} \quad \hat{K}_l := \pm 1 + \Delta_l^{-1}, \tag{1.68}$$

with $\Delta_l := (\frac{1}{r}\frac{d^2}{dr^2}r) - l(l+1)/r^2$ and

$$\Delta_l^{-1}(f)(r) := -\frac{1}{2l+1}\int_0^\infty \frac{r_<^l}{r_>^{l+1}} f(\tilde{r})\tilde{r}^2 d\tilde{r}, \tag{1.69}$$

where $r_< := \min\{r, \tilde{r}\}$ and $r_> := \max\{r, \tilde{r}\}$.

We need to solve the system (1.65), with $\hat{L}$ and $\vec{X}$ given by Eq. (1.67), to find the eigenvalues λ and the eigen-functions $A(\vec{x})$ and $B(\vec{x})$ that satisfies a set of appropriate boundary conditions. For this, we recast the system defining the new rescaled functions $a_{lm}(r) = rA_{lm}(r)$ and $b_{lm}(r) = rB_{lm}(r)$ which reduce the perturbed system to

$$-i\lambda a_{lm} = b''_{lm} \pm \sigma^{(0)2} + U_l^{\text{eff}} b_{lm}, \tag{1.70a}$$

$$-i\lambda b_{lm} = a''_{lm} + U_l^{\text{eff}} a_l \pm 3\sigma^{(0)2} a_{lm} - 2\sigma^{(0)}\left(\frac{d^2}{dr^2} - \frac{l(l+1)}{r^2}\right)^{-1}\left[\sigma^{(0)} a_{lm}\right], \tag{1.70b}$$

where $U_l^{\text{eff}} = u^{(0)} - l(l+1)/r^2$, and the operator $(d^2/dr^2 - l(l+1)/r^2)^{-1} = r\Delta_l^{-1}r^{-1}$ denotes the inverse of $r\Delta_l(r^{-1})$ with homogeneous Dirichlet boundary conditions at $r = 0$ and $r \to \infty$. To determine the boundary conditions that ensure regular and finite solutions, we need to analyze the asymptotic behavior of the system (1.70) and their behavior near the origin. We know that near the origin $r \approx 0$, $\sigma^{(0)} \approx \sigma_0$, $u^{(0)} \approx u_0$, so the dominant term in Eq. (1.70) is the centrifugal U_l^{eff} term, and the system takes the form

$$b''_{lm} - \frac{l(l+l)}{r^2} b_{lm} \approx 0 \quad a''_{lm} - \frac{l(l+l)}{r^2} a_{lm} \approx 0, \tag{1.71}$$

whose solutions are $b_{lm}, a_{lm} \sim r^{1/2+1/2\sqrt{4(l(l+1))+1}}$ regular at the origin. On the other hand, when $r \to \infty$, we know that $\lim_{r\to\infty} \sigma(r)^{(0)} = 0$, and $\lim_{r\to\infty} u(r)^{(0)} = E$, so the system (1.70) take the form

$$b''_{lm} + Eb_{lm} \approx 0 \quad a''_{lm} + Ea_{lm} \approx 0. \tag{1.72}$$

In order to have $\lim_{r\to\infty}(a_{lm}, b_{lm}) = 0$ we must choose the solution that vanishes at infinity, that is, when $E < 0$. This implies the following boundary conditions

$$a_{lm}(r=0) = 0, \quad b_{lm}(r=0) = 0, \tag{1.73a}$$

$$\lim_{r\to\infty} a_{lm}(r) = 0, \quad \lim_{r\to\infty} b_{lm}(r) = 0, \tag{1.73b}$$

which means that the solutions are regular at the center and have finite total energy. Also, note that Eq. (1.70) do not depend on the quantum number m. Particularly, in Ref. [49], the authors demonstrated that for large values of l, there are no unstable modes.

Given the system of second order differential equations (1.70) and the set of boundary conditions (1.73), it is possible to find solutions to a_{lm} and b_{lm} that will be regular at the origin and will have finite energy. The procedure to obtain these solutions goes beyond the scope of this thesis work, however, we summarize it as follows: first, 1) we need to extend the range in r of the numerical solutions to $\sigma^{(0)}(r)$ and $u^{(0)}(r)$ obtained through the shooting method using the asymptotic solutions (1.57) and (1.56), second, 2) the extended versions of the stationary solutions $\sigma^{(0)}_{\rm ext}(r)$ and $u^{(0)}_{\rm ext}(r)$, the perturbed fields a_{lm} and b_{lm}, and the differential operators $r\Delta_l^{-1}r^{-1}$, Δ_s^{-1}, Δ_s and Δ^{-1} are discretized in terms of Chebyshev polynomials using a standard *spectral method*, which leads to a finite-dimensional eigenvalue problem.

It is important to mention the results obtained with the methodology described above applied to the Gross-Pitaevskii-Poisson system developed by Nambo et al. in Ref. [49]. First, for radial perturbations ($l = 0$) regarding the ground state $n = 0$, the authors found that the configurations will be stable if the self-interaction is repulsive, that is, $\lambda > 0$. Furthermore, in the case of attractive self-interaction, that is $\lambda < 0$, there exists a maximum value for the mass M_{max} beyond which the configurations transition to unstable states under radial perturbations ($l = 0$). In Figure 1.9, we can verify that there is a maximum value for the mass M_{99} when $\lambda < 0$. This behavior is analogous to the relativistic case where the transition to unstable states is determined by the value of the kaup mass M_{kaup}, as we can see in the Figure 1.7. The difference with respect to the relativistic case is due to the fact that this maximum mass arises from relativistic effects, while in the non-relativistic case, this limit is caused by the effect of attractive self-interaction. Second, regarding excited states under spherical perturbations ($l = 0$), Nambo et al. Ref. [49] found that, if in general these are unstable, there exist configurations belonging to the first excited states that remain stable under spherical linear perturbations for repulsive case ($\lambda > 0$). In particular, they found that, in the free and attractive case, spherically symmetric excited boson stars are unstable under radial perturbations. In Table 1.1 we summarize these results for $n = 0, 1, 2$.

For non-spherical perturbations ($l > 0$), regarding the ground state $n = 0$, the authors found that the configurations will be stable if the self-interaction is repulsive ($\lambda > 0$). Furthermore, in the case of attractive self-interaction ($\lambda < 0$), there exists a common stability band (at least for $l \leq 6$) for the configurations in the range $\sigma_0 \leq 1$. Second, with respect to excited states, under non-spherical perturbations ($l > 0$), Nambo et al. Ref. [49] found that, if in general these are unstable, there exist configurations belonging to the first excited states that remain stable under generic linear perturbations in the repulsive case ($\lambda > 0$). They found that, in the free ($\lambda = 0$) and attractive case, spherically symmetric excited boson stars are unstable under generic perturbations. In Table 1.2 we summarize these results for $n = 0, 1, 2$. Although in this thesis we only present a general outline of this methodology applied to Boson stars and non-relativistic Proca stars, detailed future works on the

stability analysis of non-relativistic Proca stars are in progress [2].

Spherical perturbations $l = 0$			
	GPP Attractive	SP ($\lambda = 0$)	GPP Repulsive
$n = 0$ ground state	there exist a maximum mass $M_{\max}$ beyond which the configurations are unstable	stable	stable
$n = 1, 2, ..$ excite states	unstable	unstable	there exist configurations that remain stables

Table 1.1: **Stability for a non-relativistic self-interacting boson star ($l = 0$).** For ground state configurations ($n = 0$) the repulsive ($\lambda = 1$) and free ($\lambda = 0$) case are always stable under radial perturbations ($l = 0$). For the attractive case ($\lambda = -1$), there exists a maximum mass $M_{\max}$ beyond which the configurations transition to unstable states (for $\sigma_0 \geq \sigma_0^{\max}$). For excited configurations ($n = 1, 2$), the attractive and free self-interacting configurations are unstable under radial perturbations, whereas the in the repulsive case there exists values of σ_0 for which the configurations are stable.

Non-spherical perturbations $l > 0$			
	GPP attractive	SP ($\lambda = 0$)	GPP repulsive
$n = 0$ ground state	there exist an stability band for $\sigma_0 \leq 1$	stable	stable
$n = 1, 2, ..$ excite states	unstable	unstable	there exist configurations that remain stables

Table 1.2: **Stability of non-relativistic self-interacting boson star ($l > 0$).** Only configurations lying in the intersection of the stability bands for all $l > 0$ are stable with respect to generic linear perturbation. For ground state configurations ($n = 0$) the repulsive ($\lambda = 1$) and free ($\lambda = 0$) cases are always stable under non-spherical perturbations (do not exhibit unstable modes (at least for $l \leq 12$). For the attractive case ($\lambda = -1$), there exists an common stability band (at least for $l \leq 6$)) for the configurations in the range $\sigma_0 \leq 1$. For excited configurations ($n = 1, 2$), the attractive and free cases are unstable under non-spherical perturbations, whereas the in the repulsive case for ($n = 1$) there exists a very narrow band of stability for $1.55 \leq \sigma_0 \leq 2.07$ for which the configurations are stable.

Chapter 2

Non-relativistic Proca Stars: Spherical Stationary and Multi-frequency States

2.1 Introduction

As we have already seen in the previous chapter, boson stars are regular, finite energy configurations that do not disperse in time and are encountered in massive, self-gravitating scalar field theories [15, 11, 46, 40, 43, 50, 51, 52]. In this chapter, we will review similar solutions that arise when dealing with self-gravitating massive spin-1 fields, known as *Proca stars*. Particularly, we will study the non-relativistic effective theory of a self-interacting massive vector field minimally coupled to gravity, and we pay particular attention to spherically symmetric states and *equilibrium configurations*. This chapter is the result of the research work *Non-relativistic Proca stars: Spherical stationary and multi-frequency states* [1] from which the description below is derived. On small scales, weakly interacting dark matter models, like the WIMP model, have problems like the "missing satellite" and "cuspy core" problems discussed in the previous chapter. By nature, boson stars might be able to mitigate these problems in this way [53, 54]. Further, massive vector fields may be especially relevant to ultralight dark matter models [55, 56, 57, 58], exhibiting a richer phenomenology compared to spin $s = 0$ axion-like particles [59]. In galaxies, these particles could form dark matter halos, whose global structure is inherently Newtonian, and this motivates our focus on the non-relativistic theory in this thesis report.

Proca stars were first introduced by Brito, Cardoso, Herdeiro, and Radu in Ref. [60], where they constructed solutions of the Einstein-Proca equations with both static spherically symmetric and stationary axially symmetric spacetime. This pioneering work triggered a surge in research on such stars that includes theoretical investigations [61, 62, 63, 64, 65, 66, 67], numerical simulations [68, 69, 70], and astrophysical applications [71, 72, 73, 74, 75]. In the non-relativistic regime, Proca stars have been explored by Amin, Jain, and collaborators in [76, 77, 78, 79, 80] (see also Refs. [81, 82, 83, 84, 85]).

We can think of *non-relativistic Proca star* as self-gravitating condensates of spin $s = 1$ particles, where matter is described in terms of a vector-valued wave function $\vec{\psi}(t, \vec{x})$ satisfying the Schrödinger wave equation and obeying Poisson's equation in terms of the Newtonian gravitational potential $\mathcal{U}(t, \vec{x})$.

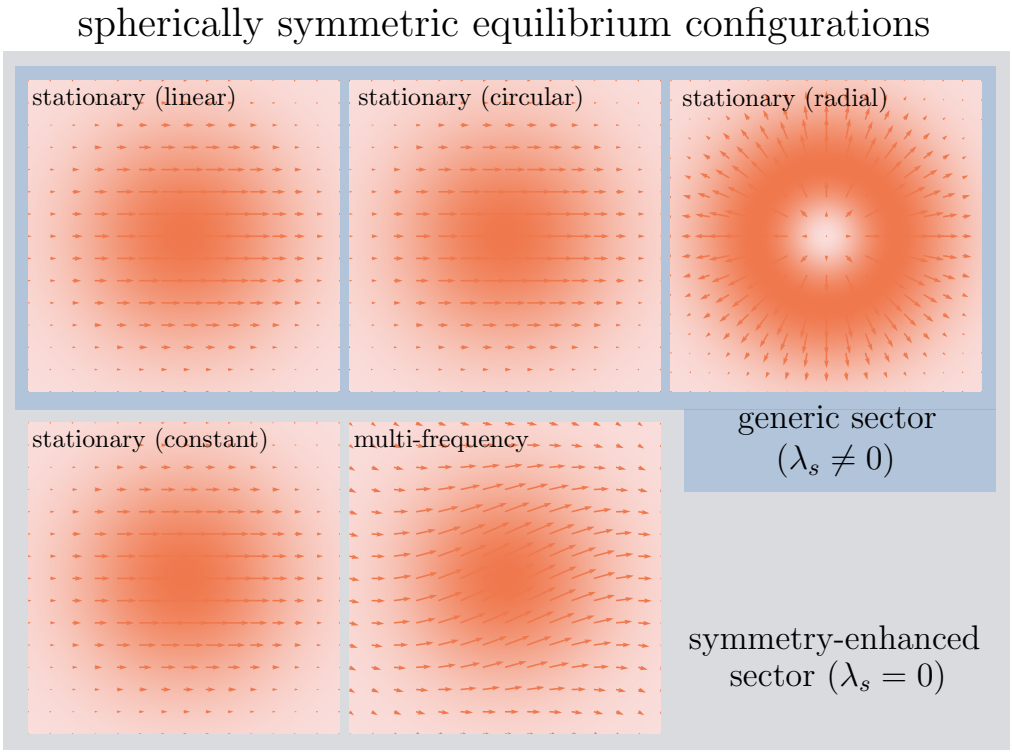

Figure 2.1: **Spherical Proca stars' inventory:** The normalized real part of the vector field, $\vec{\psi}_R(t, \vec{x})$, and the normalized particle number density, $n(t, \vec{x})$, in color gradient, of some representative equilibrium configurations at time $t = 0$. When $\lambda_s \neq 0$, all equilibrium configurations are stationary states, with only linear, circular, and radial polarizations allowed in spherical symmetry. When $\lambda_s = 0$, in addition to the aforementioned stationary states, spherical symmetry permits general constantly polarized stationary states and multi-frequency states. At $t = 0$, all constant polarization states look the same, although they differ in their time evolution (see Figure 2.2 for details).

When self-interactions are included, the Schrödinger wave equation needs to be replaced by a Gross-Pitaevskii type equation with two coupling constants λ_n and λ_s. We refer to these equations as the $s = 1$ *Schrödinger-Poisson system* when $\lambda_n = \lambda_s = 0$, and as the $s = 1$ *Gross-Pitaevskii-Poisson system* otherwise, and to the resulting finite energy equilibrium configurations as *non-relativistic Proca stars*. Let's remember that a non-relativistic boson star could also be interpreted as a non-relativistic condensate of self-gravitating and self-interacting $s = 0$ particles, with scalar wave function $\phi(t, \vec{x})$, depending only on the self-interaction parameters λ_n and the mass of the particle m_0. In this sense, Proca stars exhibit a more extensive phenomenology.

The spectrum of Proca star solutions depends on the spin-spin self-interaction parameter λ_s. When $\lambda_s \neq 0$, which we henceforth call the *generic sector* of the theory, the Proca star's wave function evolves in time harmonically. As in standard quantum mechanics, we shall refer to these equilibrium configurations as *stationary* (or single-frequency) states. However, when $\lambda_s = 0$, the effective theory acquires an additional (accidental) symmetry, resulting in the *symmetry-enhanced sector*. In this sector, new types of equilibrium configurations appear besides the stationary states in which the wave function oscillates with two or three distinct frequencies. We shall call these configurations *multi-frequency* states. This spectrum of configurations differs from that of a boson star, where we only find stationary configurations that evolve harmonically with a frequency. The spin term introduces this difference here. In this sense, single-field boson Stars only constitute stationary (single-frequency) equilibrium configurations.

By definition, *equilibrium configurations* are critical points of the total energy functional keeping fixed suitable constants of motion. It is relevant to determine whether these points correspond to local or global minima or maxima, or to saddle points, since this provides information regarding their stability. We prove that, under certain conditions on the parameters λ_n and λ_s, ground state configurations (i.e. lowest energy solutions for fixed particle number) exist. Moreover, when these conditions are satisfied, there exits a spherically symmetric stationary state of constant polarization which has lowest possible energy, regardless what sector of the theory we are exploring. In the free theory, defined by $\lambda_n = \lambda_s = 0$, we show that the ground state is unique (up to translations and rigid unitary transformations). Otherwise, even if there could in principle exist additional states which minimize the energy, they must also be stationary, spherically symmetric, and exhibit constant polarization.

In this chapter, we further concentrate on spherical configurations. In this case, stationary Proca stars can be classified according to the node number of their radial profile and their polarization vector, which can be constant or radial, although in the former case the polarization has to be linear or circular when $\lambda_s \neq 0$. In contrast, multi-frequency Proca stars are classified according to the node number of each component of the wave function $\vec{\psi}(t, \vec{x})$. Figure 2.1 illustrates the classification of spherical equilibrium configurations that appear in the different sectors of our effective theory, whereas in Figure 2.2 we show some features of their time evolution which will be discussed later.

It is worth noting that the equilibrium, spherically symmetric $s = 1$ Gross-Pitaevskii-Poisson system is equivalent to other systems studied in the frame-

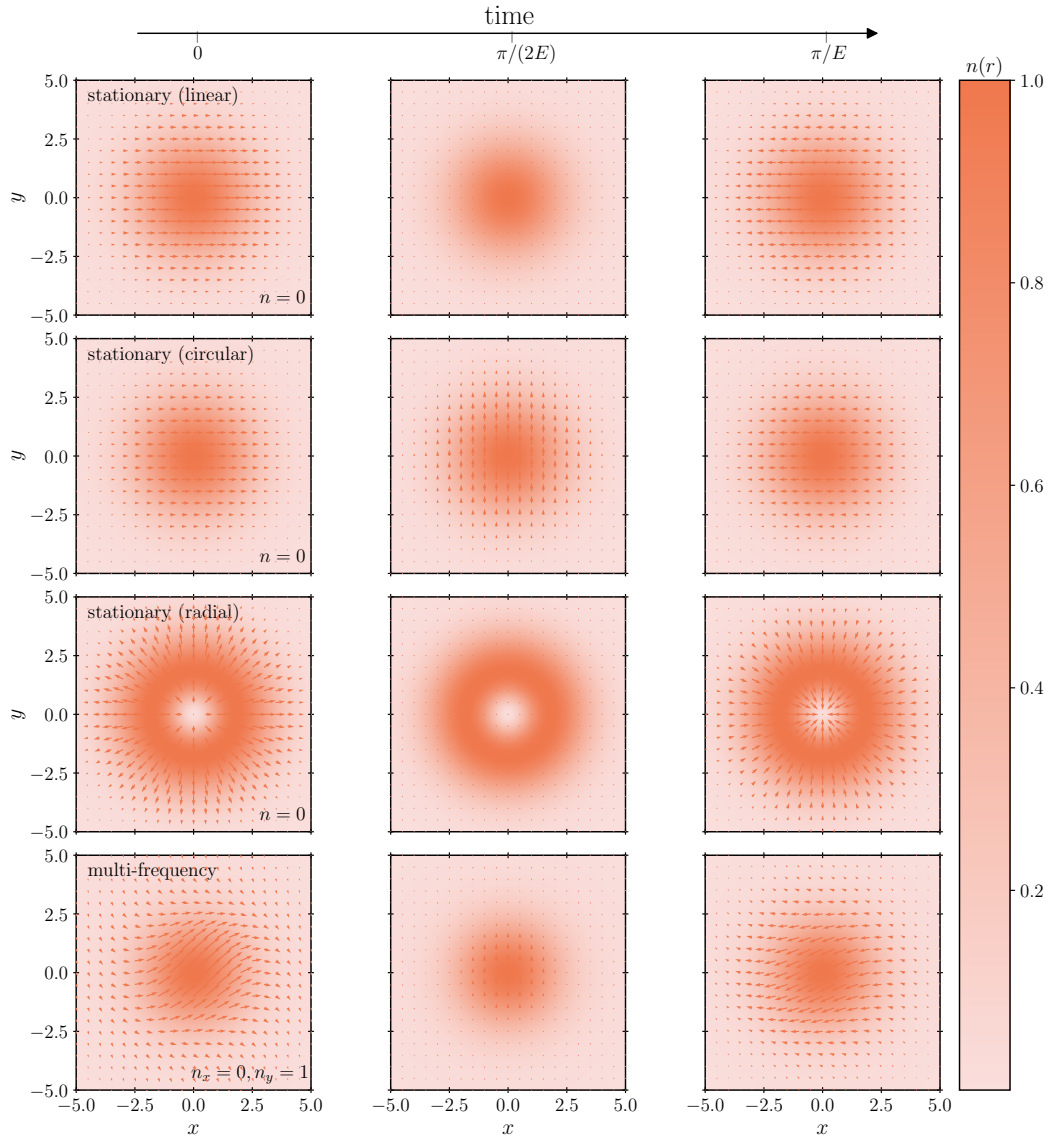

Figure 2.2: **Time evolution of spherical Proca stars:** The normalized real part of the vector field, $\vec{\psi}_R(t,\vec{x})$, and the normalized particle number density, $n(t,\vec{x})$, of some representative equilibrium configurations at different moments of time. In the first three rows, we consider stationary Proca stars of unit central "amplitude", $\sigma_0 = 1$, no nodes, $n = 0$, and different polarization vectors $\hat{\epsilon}$ at times $t_1 = 0$, $t_2 = \frac{\pi}{2E}$ and $t_3 = \frac{\pi}{E}$. *First row:* Linear polarization along the x axis, $\hat{\epsilon} = \hat{e}_x$. *Second row:* Circular polarization along the z axis, $\hat{\epsilon} = \hat{\epsilon}_z^{(+)} := \frac{1}{\sqrt{2}}(\hat{e}_x + i\hat{e}_y)$. *Third row:* Radial polarization, $\hat{\epsilon} = \hat{e}_r$. *Fourth row:* A multi-frequency Proca star of central amplitude $(\sigma_{x0}, \sigma_{y0}, \sigma_{z0}) = (1,1,0)$ and nodes $(n_x, n_y, n_z) = (0,1,0)$ at times $t_1 = 0$, $t_2 = \frac{\pi}{2E_x}$ and $t_3 = \frac{\pi}{E_x}$. Apart from radially polarized states, the spherical symmetry is only manifest in the gravitational field trough $n(t,\vec{x})$, since in other cases the wave function selects a preferred direction in space. This occurs because, in these cases, the field transforms under a non-standard representation of the $SO(3)$ group. Radially polarized Proca stars are characterized by a "hole" in their center, which is due to the regularity conditions at the origin. In all these cases we have assumed repulsive self-interactions. To better visualize the time evolution of these objects, we refer the reader to the movies provided in [86].

work of multi-scalar field theories. The free theory possesses an internal global $U(3)$ symmetry and is identical to the N-particle $s = 0$ Schrödinger-Poisson system studied in Refs. [87], specifically in the case where no more than three orthogonal states are occupied. This system admits non-relativistic $\ell = 0$ and $\ell = 1$ boson star solutions [87, 88], which in the context of Proca stars lead to stationary states of constant and radial polarization, respectively, and multi-state boson stars solutions [89], which in the present context correspond to multi-frequency states.

When $\lambda_n \neq 0$ and $\lambda_s = 0$, the theory retains the $U(3)$ symmetry and generalizes the theories discussed in Refs. [87] and [49] in several ways. On the one hand, in the present work we include self-interactions, which were not considered in Ref. [87]. On the other hand, the internal structure of the vector field allows new configurations, such as the stationary states of radial polarization and the multi-frequency solutions, which do not exist in the theory with a single scalar field considered in Ref. [49]. In contrast, when $\lambda_s \neq 0$, the spin-spin self-interaction term breaks the $U(3)$ symmetry which forbids the existence of multi-frequency states and removes the degeneracy of the constant polarization equilibrium configurations.

Conversely, in the framework of relativistic vector field theories, the static and spherically symmetric solutions reported in Ref. [60] correspond to stationary configurations of radial polarization in our classification of the equilibrium solutions. These configurations were subsequently recognized as excited states of the Einstein-Proca theory [66], indicating the potential existence of lower-energy solutions. In the non-relativistic regime, the works [76, 77] discuss the linearly and circularly polarized states. These studies were further extended in Ref. [70], where the stability of linearly, circularly, as well as radially polarized Proca stars was investigated by means of $3 + 1$ dimensional numerical simulations in general relativity, and in Ref. [81], where stationary non-spherical solutions were also considered. However, as far as we are aware, multi-frequency states have not been reported in previous studies.

In Section 2.2 we review the general scheme of relativistic Proca stars. This scheme generalizes to a vector field that we have previously discussed for a relativistic boson star. In Section 2.3, we study the main topic of this chapter, the non-relativistic Proca stars. In Section 2.3.1 we review the $s = 1$ Gross-Pitaevskii-Poisson system, in Section 2.3.2 the symmetries and conserved quantities of the system, and in Section 2.3.3 we study the equilibrium configurations and their general properties. In Section 2.3.4 we write the $s = 1$ Gross-Pitaevskii-Poisson system for an spherically symmetric equilibrium configurations and finally, in Section 2.3.5 we present the numerical results for this system. Again, here we work in natural units, for which $c = \hbar = 1$.

2.2 Relativistic Proca Stars: a concise summary

As we already mentioned, relativistic Proca stars were first introduced by Brito, Cardoso, Herdeiro, and Radu in Ref. [60]. These consist of one complex Proca field, with mass m_0, that is described by the potential $A^\mu(t, \vec{x})$ and the

"electromagnetic tensor" $F \equiv \nabla_\mu A_\nu - \nabla_\nu A_\mu$. The Einstein-Proca model is described by the action

$$S[g_{\mu\nu}, A_\mu] = \int d^4x\sqrt{-g}\left(\frac{1}{16\pi}R + \mathcal{L}_M\right) \tag{2.1}$$

where R is the Ricci scalar, $g = det(g_{\mu\nu})$ is the determinant of the metric tensor and the matter sector term is given by

$$\mathcal{L}_M = -\frac{1}{2}F^*_{\mu\nu}F^{\mu\nu} - m_0^2 A^*_\mu A^\mu. \tag{2.2}$$

Variations with respect to the metric $g_{\mu\nu}$ and with respect to the Proca field $A^\mu(t, \vec{x})$, yields the Einsten and Proca field equations, respectively

$$G_{\mu\nu} = 8\pi G T_{\mu\nu} \quad \text{and} \quad \nabla_\mu F^{\mu\nu} = m_0^2 A^\nu, \tag{2.3}$$

where the energy-momentum tensor takes the form

$$\begin{aligned} T_{\mu\nu} = \frac{1}{2}\left(F_{\mu\rho}F^*{}_\nu{}^\rho + F^*{}_{\mu\rho}F_\nu{}^\rho\right) - \frac{1}{4}F_{\rho\gamma}F^{*\rho\gamma}g_{\mu\nu} \\ + \frac{m_0^2}{2}\left(A_\mu A^*_\nu + A^*_\mu A_\nu - g_{\mu\nu}A^{*\rho}A_\rho\right). \end{aligned} \tag{2.4}$$

If $m_0 \neq 0$ in the above system equations, and $F^{\mu\nu}$ is an antisymmetric tensor, then the Proca equation must satisfy the Lorentz constriction $\nabla_\nu A^\nu = 0$. Additionally, global $U(1)$ invariance of the action (2.1), that is, invariance with respect to transformations $A_\mu \to e^{i\alpha}A_\mu$ with α a constant, implies the existence of a conserved current

$$J^\mu = \frac{i}{2}\left(F^{*\mu\alpha}A_\alpha - F^{\mu\alpha}A^*_\alpha\right) \tag{2.5}$$

with an associated Noether charge Q given by

$$Q = \int d^3x\sqrt{-g}J^0. \tag{2.6}$$

Similar to the treatment we performed for a relativistic boson star, the simplest case is to first study a spherically symmetric configuration for a Proca massive field. Let's remember that a line element with spherical symmetry is given by (1.10), and using a harmonic ansatz for the potentials $A^0 = e^{-i\omega t}f(r)$ and $A^i = e^{-i\omega t}g(r)\hat{r}$, it is possible to write the Proca and Einstein equations in terms of the four functions $u(r), v(r), f(r), g(r)$ that depend only on the radial coordinate r. Similar to boson star case, the solutions $u(r), v(r), f(r), g(r)$ to these equations for each discrete value of the frequency ω_n must satisfy regularity conditions at the origin $r = 0$ and finitude to $r \to \infty$ in order to ensure localized configurations with finite energy. Delve into this procedure goes beyond the purpose of this thesis report; however, we note that the procedure to follow in order to determine the solutions is very similar to the one we already developed for relativistic boson stars. In Ref. [60], the authors have found self-gravitating solitonic solutions to these spherically symmetric configurations. These solutions are stationary, regular, and asymptotically flat, forming

a family of solutions labeled by the integer n for each frequency ω_n, similar to the configurations we have studied for scalar fields. The stationary relativistic Proca star share with boson stars the existence of a maximum value M_{max} for the mass beyond which the solutions are possibly unstable. In Ref. [60], the authors have calculated, for spherically symmetric and axially symmetric configurations, the maxima mass value given by $M_{\rm max} \simeq 1.058 M_{\rm pl}^2/m_0$ (for spherically symmetric configurations) and $M_{\rm max} \simeq 1.568, 2.337, 3.297 M_{\rm pl}^2/m_0$ (for axially symmetric configurations with $m = 1, 2, 3$), which are slightly larger values than those for mini-boson star $M_{\rm max} \simeq 0.6 M_{\rm pl}^2/m_0$. Regarding the stability of these free spherically symmetric configurations, a stability analysis like that we presented in the previous Chapter 1 for boson stars, Ref. [60] has found that $M_{\rm max}$ corresponds to a transition point beyond which the configurations become unstable, similar to the case of a relativistic boson star. Unstable configurations could collapse into black holes or migrate to stable configurations of lower energy.

In Ref. [70], Wang and collaborators investigate relativistic Proca stars, considering, in addition to the aforementioned radially polarized spherically configurations, the cases of a linearly and circularly polarized vector field, and numerically analyze the stability of these compact objects. They found that the initial values of compactness ($C = M/R_{95}$) that lead to the formation of black holes are larger for circularly polarized configurations (which carry macroscopic spin angular momentum) compared to the compactness of linearly polarized configurations, which in turn have a greater compactness than configurations with radial polarization (values in range $C \ll 1$, the object is non-relativistic, $C \sim 0.1$ indicates a compact object like a white dwarf or neutron star and $C \to 0.5$ indicate the limit of black hole formation).

Relativistic Proca stars with quartic order self-interaction term $\lambda(A^\mu A^*_\mu)^2$ are considered in Ref. [63]. There, the authors show that in comparison with the case without self-interaction $\lambda = 0$, the maximal mass $M_{\rm max}$ and the Noether charge increase for $\lambda > 0$ and decrease for $\lambda < 0$, considering only radially polarized configurations. For a sufficiently large positive coupling constant $\lambda \gg 1$, the maximal mass and Noether charge for Proca stars is of order $\mathcal{O}[\sqrt{\lambda} M_{pl}^3/m_0^2 \ln(\lambda M_{pl}^2/m_0^2)]$ which is different from that of a boson star $\mathcal{O}[\sqrt{\lambda} M_{pl}^3/m_0^2]$. In Ref. [90], Herdeiro and Radu introduces self-interaction terms up to sixth order, and, spherically symmetric self-interacting configurations with radial polarization and charge (charged Proca stars) are considered in Ref. [91]. There, the authors calculate the values of the maximum mass $M_{\rm max}$ for Proca stars, charged Proca stars, Proca Q-stars, and charged Proca Q-stars.

Finally, in Ref [68], Herdeiro, Radu, and collaborators report fully-non linear numerical evolutions of spherically symmetric relativistic Proca stars for $\lambda = 0$, with the aim of exploring linear stability and the critical point beyond which these configurations become unstable. Their results confirm the value of the maximum mass $M_{\rm max}$ as the point from which the configurations become unstable and divides the configurations into bands of stability and instability. Depending on the sign of the binding energy of the solutions, they find that unstable configurations can either i) migrate to stable bands, ii) completely disperse, or iii) collapse into a black hole. These results are similar to those

we have reviewed for a relativistic boson star in Chapter 1.

2.3 Non-relativistic Proca Stars

We have postponed much of the details concerning to the numerical methods that we have described in the study of boson stars, both relativistic and non-relativistic, to the analysis of non-relativistic Proca stars. This section will describe the numerical and analytical methodology that we have followed to find the solutions to the stationary and multi-frequency configurations and the system of equations for the perturbations. In Appendix B will delve into the shooting method that we have used to find the stationary solutions for the boson Stars, now applied to non-relativistic Proca stars.

Numerical studies for the case of relativistic Proca stars can be found in Ref. [60, 78] for the three types of polarization that we present here. In the present study, we address these results now for the non-relativistic case and report results analogous to these works along with other novel aspects. The analysis of non-relativistic Proca stars allows a general understanding of the methods we have already presented for boson stars. Thus, details in describing these methods allow us to better understand both cases, as we will soon see.

We can anticipate that since the treatment is now for a vector field $\vec{\psi}(t,\vec{x})$ with mass m_0, the $s=1$ Gross-Pitaevskii-Poisson system analogous to the $s=0$ Gross-Pitaevskii-Poisson system for boson stars will depend on the parameters that define the polarization of the vector field and the self-interacting coupling constants, λ_n and λ_s, related to the self-coupling number density $n=\vec{\psi}^*\cdot\vec{\psi}$ and the self-coupling of the spin density term $\vec{s}=-i\vec{\psi}^*\times\vec{\psi}$. With this in mind, the level of complexity will be greater than that before reported for boson stars, and the phenomenology of these Proca stars will be more richer.

2.3.1 The $s=1$ Gross-Pitaevskii-Poisson System

Here, we present the effective construction of the non-relativistic action compatible with the symmetries of Galileo, from which we aim to recover the physics related to galactic speeds and Newtonian scales. Constructed from operators depending up to fourth order on the field $\vec{\psi}(t,\vec{x})$, this action should naturally lead to the Poisson gravitational equation for the Newtonian potential $\mathcal{U}(t,\vec{x})$, and to the Gross-Pitevski equations for a self-interacting and self-gravitating vector field. We shall also observe, how it is possible to obtain this effective action from the non-relativistic limit of the Einstein-Proca action for the potential $V(A^\mu)$ that includes the self-interaction terms $\lambda_1(A^*_\mu A^\mu)^2+\lambda_2(A_\mu A^\mu)(A^*_\nu A^{\nu *})$. Also, writing the $s=1$ Gross-Pitaevskii-Poisson system in the compact form of the Schrödinger eigen-equation $i\partial\vec{\psi}/\partial t=\hat{H}[\vec{\psi},\mathcal{U}]\vec{\psi}$ will allow us to talk about $\vec{\psi}$ in terms of a "wave function".

Non-relativistic Effective Action

Our purpose is the construction of a non-relativistic, low energy effective theory that describes a self-interacting vector field $\vec{\psi}(t,\vec{x})$ coupled to the Newtonian

gravitational potential $\mathcal{U}(t,\vec{x})$. This theory is expressed in terms of the action

$$\begin{aligned} S[\mathcal{U},\vec{\psi}] &= \int dt \int dV \Bigg[\frac{1}{8\pi G}\mathcal{U}\Delta\mathcal{U} - m_0\mathcal{U}n \\ &+\vec{\psi}^* \cdot \left(i\frac{\partial}{\partial t} + \frac{1}{2m_0}\Delta \right)\vec{\psi} - \frac{\lambda_n}{4m_0^2}n^2 - \frac{\lambda_s}{4m_0^2}\vec{s}^2 \Bigg], \end{aligned} \tag{2.7}$$

which consists of all operators of mass dimension 6 or lower that can be constructed from the field $\vec{\psi}(t,\vec{x})$ and are scalars under the Galilei group. In this expression, $i=\sqrt{-1}$ is the unit imaginary number, G is Newton's constant, the star denotes complex conjugation, and dV and Δ refer to the volume element and Laplace operator, respectively, associated with three-dimensional Euclidean space. As we mentioned, the variation with respect to the Newtonian gravitational field $\mathcal{U}(t,\vec{x})$ leads to the Poisson equation and the variation with respect to the vector field $\vec{\psi}(t,\vec{x})$ leads to the Gross-Pitaevskii equation.

We start with the Newtonian gravity in order to build the effective theory shown by Eq. (2.7). This is expressed in terms of the action

$$S = \int dt \int dV \left[\frac{1}{8\pi G}\mathcal{U}\Delta\mathcal{U} - m_0\mathcal{U}n + \mathcal{L}_m \right]. \tag{2.8}$$

The first two terms of this equation correspond to the "kinetic" term of the gravitational field $\mathcal{U}(t,\vec{x})$ and its coupling with the mass density $m_0 n(t,\vec{x})$, respectively. Conversely, the last term of Eq. (2.8) comprises the matter sector, that for the purposes of this thesis consists of a vector field $\vec{\psi}(t,\vec{x})$ of mass dimension 3/2, i.e. $[\vec{\psi}] = E^{3/2}$, where E denotes dimensions of energy. Following an effective theory approach, we write down the most general expression for $\mathcal{L}_m$ that is compatible with the allowed symmetries of the theory, that we assume to consist of locality (i.e. all fields are evaluated at the same spacetime point) and Galilean transformations [92]:

$$\vec{\psi}(t,\vec{x}) \mapsto e^{-i(m_0\vec{v}\cdot\vec{x}+\frac{1}{2}m_0\vec{v}^2 t)} R\vec{\psi}(t-t_0, R^{-1}\vec{x}+\vec{v}t-\vec{x}_0). \tag{2.9}$$

In this equation t_0, $\vec{x}_0$, $\vec{v}$, and R are constant, with R an element of the orthogonal group. With these assumptions, there is an infinite number of terms that can contribute to the effective action, with higher-dimensional operators being suppressed at low energies. For concreteness, in this thesis, we will restrict ourselves to operators of mass dimension 6 or lower.[1]

The vector field transforms non-trivially under the Galilei group, Eq. (2.9), which implies that derivative terms must appear in combinations of the form:

$$\int dt \int dV \vec{\psi}^* \cdot m_0^{1-n} \left(i\frac{\partial}{\partial t} + \frac{1}{2m_0}\Delta \right)^n \vec{\psi}. \tag{2.10}$$

When $n=1$, this leads to the standard Schrödinger operator appearing in Eq. (2.7). At this point one might be tempted to include terms with $n=$

[1] In natural units $\hbar = c = 1$ these operators have dimensions of $[E^6] \sim [m_0^6]$ or less. For example, for the self-interactive term we have $[S] = [E][T] \sim [T][L^3][n^2]/[m_0^2]$, and since $[m_0^2] \sim [E^2]$, $[L] \sim [T]$ and $[E] \sim [T^{-1}]$, then $[n^2] \sim [E^6] \sim [m_0^6]$.

$2, 3, 4, \ldots$ However, they involve operators of mass dimension 7 or higher, and this is why we have excluded them from our effective theory.

Moreover, non-derivative terms must appear in combinations of the form: $\delta^{ij}\psi_i^*\psi_j$, $\delta^{i\ell}\delta^{jk}\psi_i^*\psi_j\psi_k^*\psi_\ell$, $\delta^{ik}\delta^{j\ell}\psi_i^*\psi_j\psi_k^*\psi_\ell$, $\delta^{i\ell}\delta^{jm}\delta^{kn}\psi_i^*\psi_j\psi_k^*\psi_\ell\psi_m^*\psi_n$, ..., although only the first three of this series are of mass dimension 6 or lower. The first term in this list is equal to the particle number density, $\delta^{ij}\psi_i^*\psi_j = n$, and is already included in the first line of Eq. (2.7).[2] The second term of the list gives rise to a self-interaction operator that depends on the number density squared, $\delta^{i\ell}\delta^{jk}\psi_i^*\psi_j\psi_k^*\psi_\ell = (\psi_i^*\psi^i)(\psi_j^*\psi^j) = n^2$, and it is also present in our effective theory. Apparently, the third term is absent from Eq. (2.7), however, using the identity $\varepsilon^{mij}\varepsilon_m{}^{k\ell} = \delta^{ik}\delta^{j\ell} - \delta^{i\ell}\delta^{jk}$, we can express this operator as $\delta^{ik}\delta^{j\ell}\psi_i^*\psi_j\psi_k^*\psi_\ell = (\varepsilon^{mij}\varepsilon_m{}^{k\ell} + \delta^{i\ell}\delta^{jk})\psi_i^*\psi_j\psi_k^*\psi_\ell = -s_i s^i + n^2$, where $s^m = -i\varepsilon^{mk\ell}\psi_k^*\psi_\ell$ represents the spin density. Thus, in general, our theory includes two self-interaction terms of mass dimension 6: one depending on the square of the number density, n^2, and the other on the square of the spin density, $\vec{s}^{\,2} = \vec{s}\cdot\vec{s}$.

Non-relativistic Limit of a Self-interacting Einstein-Proca Theory

Now, we compute the non-relativistic limit of a massive vector field theory. Our starting point is the Einstein-Proca theory for a complex-valued[3] vector field $A^\mu(t, \vec{x})$ of mass m_0 and quartic self-interaction $\lambda_1(A_\mu^* A^\mu)^2 + \lambda_2(A_\mu A^\mu)(A_\nu^* A^{\nu *})$.[4] In natural units, this theory is described by the action (2.1) which consists of the Einstein-Hilbert term with matter sector

$$\begin{aligned}\mathcal{L}_M &= -\frac{1}{2}F_{\mu\nu}^* F^{\mu\nu} - m_0^2 A_\mu^* A^\mu \\ &\quad -\lambda_1(A_\mu^* A^\mu)^2 - \lambda_2(A_\mu A^\mu)(A_\nu^* A^{\nu *}),\end{aligned} \tag{2.11}$$

where $F_{\mu\nu} \equiv \nabla_\mu A_\nu - \nabla_\nu A_\mu$ is the "electromagnetic" tensor.

To proceed, we will explore the non-relativistic limit of this theory at increasing levels of complexity. First, we will focus on the free theory, which excludes the effects of self-interactions and gravity. Subsequently, we will incorporate the self-interaction terms, and finally, we will consider the influence of gravity. At the end of the presentation, we will arrive at an expression that coincides with the effective action that we introduced in Eq. (2.7). Here, we employ the $(-,+,+,+)$ signature convention for the spacetime metric, and for convenience we occasionally represent Newton's constant G in terms of the Planck mass, denoted as $M_{\rm Pl} \equiv 1/\sqrt{G}$. We have followed this same procedure in Appendix A.1 to obtain the non-relativistic limit of a boson star.

[2] An operator of the form $\lambda_0 m_0 n$ (where λ_0 is a dimensionless coupling constant) can be absorbed into the second term of Eq. (2.7) by redefining the gravitational potential as $\mathcal{U}' = \mathcal{U} + \lambda_0$.

[3] For the non-relativistic limit of a real-valued vector field theory, see e.g. Ref. [77].

[4] Recent works [93, 94, 95] have pointed out to a fundamental problem with relativistic self-interacting vector fields due to the appearance of unstable modes that could render these theories unphysical. However, the authors of Refs. [96, 97, 98] have argued that these instabilities are not indicative of ghosts and/or tachyons, but rather of the breakdown of the well-posedness of the Cauchy problem and the regime of validity of the effective theory.

A. Free Theory

In absence of gravity, a non-selfinteracting complex-valued vector field $A^\mu(t,\vec{x})$ of mass m_0 is described in terms of the action

$$S = \int d^4x \left[-\frac{1}{2} F^*_{\mu\nu} F^{\mu\nu} - m_0^2 A^*_\mu A^\mu \right]. \tag{2.12}$$

If we perform a $1+3$ decomposition of the vector field $A^\mu = (A^0, A^i)$ we can write this expression in the form:

$$\begin{aligned} S = \int d^4x \Big(& \dot{A}^*_i \dot{A}^i + \partial_i A^*_0 \partial^i A_0 - \partial_i A^*_j \partial^i A^j - \dot{A}^*_i \partial^i A_0 \\ & - \partial_i A^*_0 \dot{A}^i + \partial_i A^*_j \partial^j A^i + m_0^2 A^*_0 A_0 - m_0^2 A^*_i A^i \Big), \end{aligned} \tag{2.13}$$

where the overdot indicates time derivative and indices are raised and lowered with the flat spacetime metric.

Now, we express the time $A_0(t,\vec{x})$ and spatial $A_i(t,\vec{x})$ components of $A_\mu(t,\vec{x})$ in the form

$$A_0(t,\vec{x}) = \frac{1}{\sqrt{2m_0}} e^{-im_0 t} a_0(t,\vec{x}), \tag{2.14a}$$

$$A_i(t,\vec{x}) = \frac{1}{\sqrt{2m_0}} e^{-im_0 t} \psi_i(t,\vec{x}). \tag{2.14b}$$

This allows us to write Eq. (2.13) as

$$\begin{aligned} S = \int d^4x \Big(& \frac{i}{2}\psi^*_i \dot{\psi}^i - \frac{i}{2}\dot{\psi}^*_i \psi^i + \frac{1}{2m_0}\dot{\psi}^*_i \dot{\psi}^i + \frac{1}{2m_0}\partial_i a^*_0 \partial^i a_0 \\ & - \frac{1}{2m_0}\partial_i \psi^*_j \partial^i \psi^j - \frac{i}{2}\psi^*_i \partial^i a_0 - \frac{1}{2m_0}\dot{\psi}^*_i \partial^i a_0 + \frac{i}{2}\partial_i a^*_0 \psi^i \\ & - \frac{1}{2m_0}\partial_i a^*_0 \dot{\psi}^i + \frac{1}{2m_0}\partial_i \psi^*_j \partial^j \psi^i + \frac{m_0}{2} a^*_0 a_0 \Big). \end{aligned} \tag{2.15}$$

In the non-relativistic limit, the different quantities scale as $\partial_t \sim \epsilon m_0$, $\partial_i \sim \epsilon^{1/2} m_0$, and $a_0 \sim \epsilon^{1/2}|\psi_i|$, with ϵ a small positive number, so to leading order in ϵ we can approximate:

$$\begin{aligned} S = \int d^4x \Big(& \frac{i}{2}\psi^*_i \dot{\psi}^i - \frac{i}{2}\dot{\psi}^*_i \psi^i - \frac{1}{2m_0}\partial_i \psi^*_j \partial^i \psi^j - \frac{i}{2}\psi^*_i \partial^i a_0 \\ & + \frac{i}{2}\partial_i a^*_0 \psi^i + \frac{1}{2m_0}\partial_i \psi^*_j \partial^j \psi^i + \frac{m_0}{2} a^*_0 a_0 \Big). \end{aligned} \tag{2.16}$$

Note that there are no time derivatives of a_0 in this expression, indicating that this component is not dynamical and can be integrated out from the action. In order to do that, we vary Eq. (2.16) with respect to a_0, and obtain

$$a_0 = \frac{i}{m_0}\partial_j \psi^j, \tag{2.17}$$

which is a condition that must be satisfied by a_0. Introducing the constraint (2.17) back into Eq. (2.16), integrating by parts, and neglecting surface terms, yields

$$S = \int d^4x \left[\psi_i^* \left(i\frac{\partial}{\partial t} + \frac{1}{2m_0}\Delta \right) \psi^i \right]. \tag{2.18}$$

This is just the Schrödinger action for a vector wave function $\psi_i(t, \vec{x})$ that describes free particles of spin $s = 1$.

B. self-interactions

In presence of self-interactions, Eq. (2.15) requires the addition of the new terms:

$$\int d^4x \left\{ \frac{\lambda_1}{4m_0^2} \left[-(a_0^* a_0)^2 + 2a_0^* a_0 \psi_i^* \psi^i - (\psi_i^* \psi^i)^2 \right] \right. \tag{2.19}$$
$$\left. + \frac{\lambda_2}{4m_0^2} \left[-(a_0^* a_0)^2 + a_0^2 \psi_i^* \psi^{i*} + a_0^{*2} \psi_i \psi^i - \psi_i \psi^i \psi_j^* \psi^{j*} \right] \right\}.$$

In the non-relativistic limit, the third and seventh terms dominate over the other five, and hence the constraint in Eq. (2.17) is unaffected. If again we integrate out the field a_0, we obtain

$$S = \int d^4x \left[\psi_j^* \left(i\frac{\partial}{\partial t} + \frac{1}{2m_0}\Delta \right) \psi^j - \frac{\lambda_n}{4m_0^2} n^2 - \frac{\lambda_s}{4m_0^2} s_j s^j \right], \tag{2.20}$$

where $n = \psi_i^* \psi^i$ is the number density, $s^m = -i\varepsilon^{mij} \psi_i^* \psi_j$ is the spin density and we have defined $\lambda_n := \lambda_1 + \lambda_2$ and $\lambda_s := -\lambda_2$. In order to obtain Eq. (2.20), we have used some properties of the Levi-Civita symbol that we have previously introduced. Note that the only difference with respect to the free theory, Eq. (2.18), is the appearance of two self-interaction terms.

C. Gravity

Finally, we include the effects of gravity, which are codified in the spacetime metric $g_{\mu\nu}(t, \vec{x})$. For that purpose, it is convenient to decompose the spacetime line element in the form [49]

$$ds^2 = -\left[1 + 2\Phi(t, \vec{x})\right] dt^2 + \left[1 - 2\Psi(t, \vec{x})\right] \delta_{jk} dx^j dx^k, \tag{2.21}$$

which has been expressed in the Newtonian gauge and codifies only the scalar degrees of freedom of the gravitational field (vector and tensor modes do not couple to non-relativistic matter and we have omitted them here). The functions $\Phi(t, \vec{x})$ and $\Psi(t, \vec{x})$ transform as scalars under spatial rotations and constitute the gravitational potentials.

This introduces the additional terms

$$\int d^4x \left[\frac{1}{8\pi G} \Psi \Delta \left(2\Phi - \Psi \right) - m_0 \Phi n \right] \tag{2.22}$$

into the action (2.20), where we have taken into account that, in the non-relativistic limit, $\Phi \sim \Psi \sim \epsilon$ and $|\psi_i| \sim \sqrt{M_{\rm Pl}^2 m_0}\epsilon$. Here, the first term of

Eq. (2.22) originates from the Einstein-Hilbert action, whereas the second one from the kinetic term of the vector field. Note that the field a_0 is absent from Eq. (2.22), and hence the constraint (2.17) is not affected.

Combining Eqs. (2.20) and (2.22), we obtain

$$S[\Phi,\Psi,\psi_j] = \int dt \int d^3x \Bigg[\frac{1}{8\pi G}\Psi\Delta\left(2\Phi-\Psi\right) - m_0\Phi n \\ +\psi_j^*\left(i\frac{\partial}{\partial t}+\frac{1}{2m_0}\Delta\right)\psi^j - \frac{\lambda_n}{4m_0^2}n^2 - \frac{\lambda_s}{4m_0^2}s_j s^j\Bigg]. \tag{2.23}$$

Varying this expression with respect to Ψ yields $\Delta(\Phi-\Psi)=0$, and assuming that Φ and Ψ vanish at infinity this implies that $\Phi=\Psi$. Introducing this result back into Eq. (2.23), we arrive at Eq. (2.7), where we have defined $\Phi=\Psi:=\mathcal{U}$ as the Newtonian gravitational potential. The action (2.23) has the same form as that of a non-relativistic self-interacting boson star, Eq. (1.36), with the difference that the action (2.23) now considers the phenomenology of the polarization of the vector field $\vec{\psi}$ encoded in the parameter λ_s.

The $s=1$ Gross-Pitaevskii-Poisson System

The theory described by the action $S[\mathcal{U},\vec{\psi}]$, Eq. (2.7), is characterized in terms of three parameters: the positive and non-vanishing field's mass m_0 and the dimensionless coupling constants λ_n and λ_s.[5] The first term in the first line of Eq. (2.7) describes Newtonian gravity, the second line the matter sector and the last term in the first line the interaction between gravity and matter. The matter sector consists of the free Schrödinger action plus two short-range self-interaction terms, one that depends on the particle number density, $n:=\vec{\psi}^*\cdot\vec{\psi}$, and the other on the spin density, $\vec{s}:=-i\vec{\psi}^*\times\vec{\psi}$, which by definition are real-valued.

Varying Eq. (2.7) with respect to $\vec{\psi}$ we obtain a Gross-Pitaevskii type equation of the form

$$i\frac{\partial\vec{\psi}}{\partial t} = -\frac{1}{2m_0}\Delta\vec{\psi} + \frac{\lambda_n}{2m_0^2}n\vec{\psi} + i\frac{\lambda_s}{2m_0^2}\vec{s}\times\vec{\psi} + m_0\mathcal{U}\vec{\psi}, \tag{2.24a}$$

whereas varying it with respect to $\mathcal{U}(t,\vec{x})$ leads to the Poisson equation,

$$\Delta\mathcal{U} = 4\pi G m_0 n. \tag{2.24b}$$

We will refer to Eqs. (2.24) as the $s=1$ Gross-Pitaevskii-Poisson system. Setting $\lambda_n=\lambda_s=0$ the self-interactions vanish and Eqs. (2.24) reduce to the $s=1$ Schrödinger-Poisson system.

Reformulation of the Dynamical Equations

In this section we reformulate the system (2.24) in terms of a non-linear Hamilton operator, which will bring more transparency for several of the discussions.

[5] In the effective theory, the parameters λ_n and λ_s are in principle arbitrary and unrelated. Compare this with e.g. Ref. [77], where taking the non-relativistic limit of a generic massive real-valued vector field the authors obtain $\lambda_s=-\frac{1}{3}\lambda_n$.

The $s = 1$ Gross-Pitaevskii (2.24a) and Poisson (2.24b) equations can be expressed more compactly as:

$$i\frac{\partial\vec{\psi}}{\partial t} = \hat{\mathcal{H}}[\vec{\psi},\mathcal{U}]\vec{\psi}, \tag{2.25a}$$

$$\Delta\mathcal{U} = 4\pi G m_0 n, \tag{2.25b}$$

where, for fixed $\vec{\psi}$ and $\mathcal{U}$, we have defined the Hamilton operator

$$\hat{\mathcal{H}}[\vec{\psi},\mathcal{U}] := -\frac{1}{2m_0}\Delta + \frac{\lambda_n}{2m_0^2}n + i\frac{\lambda_s}{2m_0^2}\vec{s}\times + m_0\mathcal{U}. \tag{2.26}$$

In this equation, $\vec{s}\times$ represents the cross product of the spin density with the vector-valued function that the operator $\hat{\mathcal{H}}[\vec{\psi},\mathcal{U}]$ is acting on. Furthermore, by inverting the Laplacian in Eq. (2.25b), one can eliminate the gravitational potential $\mathcal{U}$ from Eq. (2.25a), which yields a nonlinear integro-differential equation for the wave function $\vec{\psi}$,[6]

$$i\frac{\partial\vec{\psi}}{\partial t} = \hat{\mathcal{H}}[\vec{\psi}]\vec{\psi}, \tag{2.27}$$

with

$$\begin{aligned}\hat{\mathcal{H}}[\vec{\psi}] &:= \hat{\mathcal{H}}[\vec{\psi},\mathcal{U} = \Delta^{-1}(n)] \\ &= -\frac{1}{2m_0}\Delta + \frac{\lambda_n}{2m_0^2}n + i\frac{\lambda_s}{2m_0^2}\vec{s}\times + 4\pi G m_0^2\Delta^{-1}(n),\end{aligned} \tag{2.28}$$

and where for a generic function $f(\vec{x})$ we have introduced the inverse Laplacian as

$$\Delta^{-1}(f)(\vec{x}) := -\frac{1}{4\pi}\int\frac{f(\vec{x}')}{|\vec{x}-\vec{x}'|}dV'. \tag{2.29}$$

It is worth noting that, for fixed $\vec{\psi}$, the Hamilton operator $\hat{\mathcal{H}}[\vec{\psi}]$ is Hermitian, i.e. $(\vec{\psi}_1, \hat{\mathcal{H}}[\vec{\psi}]\vec{\psi}_2) = (\hat{\mathcal{H}}[\vec{\psi}]\vec{\psi}_1, \vec{\psi}_2)$, where $(\vec{\psi}_1, \vec{\psi}_2) = \int(\vec{\psi}_1^* \cdot \vec{\psi}_2)dV$ denotes the standard L^2-scalar product between $\vec{\psi}_1$ and $\vec{\psi}_2$. However, despite the apparent simplicity of Eq.(2.27), the operator $\hat{\mathcal{H}}[\vec{\psi}]$ is non-linear, as all terms beyond the first one in Eq.(2.28) are quadratic in the field $\vec{\psi}$.

2.3.2 Symmetries and Conserved Quantities

In this section, we will study some conserved quantities in the temporal evolution of the $s = 1$ Gross-Pitaevskii-Poisson system, which will be relevant in the characterization of equilibrium solutions and the study of stability. These quantities are associated with the different global symmetries present in the action (2.7). As we have done for boson stars, we will observe that for Proca stars the number of particles and energy are also conserved. Additionally, for Proca stars, we will observe that the spin contribution will imply the conservation of total angular momentum.

[6] While we refer to $\vec{\psi}(t,\vec{x})$ as the *wave function*, it should be noted that this is a classical field. In particular, $n = \vec{\psi}^* \cdot \vec{\psi}$ describes the particle and not the probability density.

Note: Given that the action (2.7) does not contain the time and the spatial coordinates explicitly, the (canonical) energy-momentum tensor $T_{\mu}{}^{\nu}$ must be conserved, that is $\partial_{\nu}T_{\mu}{}^{\nu}=0$, where

$$T_{\mu}{}^{\nu}=\frac{\partial\mathcal{L}}{\partial(\partial_{\nu}\psi_{i}^{*})}\partial_{\mu}\psi_{i}^{*}+\frac{\partial\mathcal{L}}{\partial(\partial_{\nu}\psi_{i})}\partial_{\mu}\psi_{i}+\frac{\partial\mathcal{L}}{\partial(\partial_{\nu}\mathcal{U})}\partial_{\mu}\mathcal{U}+-\mathcal{L}\delta_{\mu}{}^{\nu} \tag{2.30}$$

with $\mathcal{L}$ given by

$$\mathcal{L}=\frac{1}{8\pi G}\mathcal{U}\Delta\mathcal{U}-m_{0}\mathcal{U}n+\vec{\psi}^{*}\cdot\left(i\frac{\partial}{\partial t}+\frac{1}{2m_{0}}\Delta\right)\vec{\psi}-\frac{\lambda_{n}}{4m_{0}^{2}}n^{2}-\frac{\lambda_{s}}{4m_{0}^{2}}\vec{s}^{2}. \tag{2.31}$$

Here $T_{0}{}^{0}$ is the energy density, $T_{0}{}^{j}$ is the j-component of the energy current density, $T_{i}{}^{0}$ is (minus) the linear momentum density along the i-th direction, and $T_{i}{}^{j}$ is (minus) the j-component of the linear momentum current density along the i-th direction.

The non-relativistic action (2.7) is invariant under time translations, which means that Eq. (2.31) is not affected by shifts in the time parameter, $\vec{\psi}(t,\vec{x})\mapsto\vec{\psi}(t-t_{0},\vec{x})$, with t_{0} a real constant. Associated to this symmetry is the conserved total energy (the spatial integral of the 00 component of the energy-momentum tensor) given by

$$\mathcal{E}\;=\;\int dV\left[\frac{1}{8\pi G}\partial_{i}\mathcal{U}\partial^{i}\mathcal{U}+\frac{1}{2m_{0}}\partial_{i}\psi_{j}^{*}\partial^{i}\psi^{j}+\frac{\lambda_{n}}{4m_{0}^{2}}n^{2}+\frac{\lambda_{s}}{4m_{0}^{2}}s_{i}s^{i}+m_{0}\mathcal{U}n\right]. \tag{2.32}$$

Using the Poisson equation (2.24b) and discarding the boundary terms, we can express Eq. (2.32) as

$$\mathcal{E}=\int\left[\frac{1}{2m_{0}}|\nabla\vec{\psi}|^{2}+\frac{\lambda_{n}}{4m_{0}^{2}}n^{2}+\frac{\lambda_{s}}{4m_{0}^{2}}\vec{s}^{2}+\frac{m_{0}}{2}n\mathcal{U}\right]dV. \tag{2.33}$$

In addition, one can also prove that the action (2.7) remains invariant under rotations, $\vec{\psi}(t,\vec{x})\mapsto U(R)\vec{\psi}(t,R^{-1}\vec{x})$, with $U(R)=R$ a rotation matrix or $U(R)=I$ the identity matrix. Consequently, one has conservation of the total angular momentum

$$\vec{J}=-i\int(\vec{\psi}^{*}\times\vec{\psi})dV-i\int[\vec{x}\times(\vec{\psi}^{*}\cdot\nabla\vec{\psi})]dV, \tag{2.34}$$

where $\vec{S}=-i\int(\vec{\psi}^{*}\times\vec{\psi})dV$ is the internal (or spin) angular momentum and $\vec{L}=-i\int[\vec{x}\times(\vec{\psi}^{*}\cdot\nabla\vec{\psi})]dV$ is the orbital angular momentum. Both, $\vec{S}$ and $\vec{L}$ are conserved individually.

Note: Given that the Lagrangian density (2.31) is symmetric respect to the transformation $\psi^{i}\rightarrow\psi^{i}+\epsilon^{i}{}_{jk}\theta^{j}\psi^{k}$, there exist a conserved quantity associated to this symmetry. For example, a rotation about the ψ_{3}-axis gives $\psi^{i}\rightarrow\psi^{i}+\epsilon^{i}{}_{3k}\theta^{3}\psi^{k}$ and $D^{3}\psi^{1}=-\psi^{2}$, $D^{3}\psi^{2}=\psi^{1}$ where the symmetry from rotation around the b-axis is $D^{b}\psi^{a}$. Also, we have that $D\mathcal{L}=(\partial\mathcal{L}/\partial x^{\mu})(\partial x^{\mu}/\partial\theta)$=0 and $W^{\mu}=0$. So, the conserved current is

given by

$$J_N^{3\mu} = \sum_a \Pi^{a\mu} D^3\psi^a - W^\mu \to S^{(3)} = -i\int d^3x\big(\psi^{1*}\psi^2 - \psi^{2*}\psi^1\big). \quad (2.35)$$

Finally, generalizing we have

$$S^i = -i\int \epsilon^i{}_{jk}\psi^{*j}\psi^k d^3x. \quad (2.36)$$

Note: Given that the Lagrangian density is invariant under infinitesimal Lorentz (Galilei) transformation

$$\Lambda^\mu{}_\nu = \delta^\mu{}_\nu + \omega^\mu{}_\nu, \quad x^\mu \to x^\mu + \delta x^\mu = x^\mu + \omega^{\mu\nu}x_\nu\delta\lambda, \quad (2.37)$$

where $\omega^{\mu\nu}$ is an antisymmetric tensor, we have a conserved current associated to this symmetry. Hence $\delta\psi^i = \partial_\mu\psi^i[\omega^{\mu\nu}x_\nu\delta\lambda]$ and $D\psi^i = (\partial\psi^i/\partial\lambda)|_{\lambda=0} = \omega^{\mu\nu}x_\nu\partial_\mu\psi^i = \omega_{\mu\nu}x^\nu\partial^\mu\psi^i$. So, we have that $\sum_{i=1}^{n} i^2 D\mathcal{L} = \omega_{\mu\nu}x^\mu\partial^\nu\mathcal{L} = \partial_\mu[g^{\mu\rho}\omega_{\rho\sigma}x^\sigma\mathcal{L}] = \partial_\mu W^\mu$ and $W^\mu = g^{\mu\rho}\omega_{\rho\sigma}x^\sigma\mathcal{L}$. Thus, we can write

$$J_N^\mu = \sum_a \Pi^{a\mu}D\psi^a - W^\mu = \omega_{\rho\sigma}\big[\sum_a \Pi^{a\mu}x^\sigma\partial^\rho\psi^a - g^{\mu\rho}x^\sigma\mathcal{L}\big]$$
$$= \omega_{\rho\sigma}x^\sigma T^{\rho\mu} = \omega_{\rho\sigma}(\tilde{J}^\mu)^{\rho\sigma}, \quad (2.38)$$

where $(\tilde{J}^\mu)^{\rho\sigma} = x^\sigma T^{\rho\mu}$. There are six parameters in $\omega^{\rho\sigma}$ and so there are six conserved currents. Now, if we write $(J^\mu)^{\rho\sigma} = x^\rho T^{\mu\sigma} - x^\sigma T^{\mu\rho}$ where $(J^\mu)^{\rho\sigma} = (\tilde{J}^\mu)^{\rho\sigma} - (\tilde{J}^\mu)^{\sigma\rho}$ and $\partial_\mu(J^\mu)^{\rho\sigma} = 0$, we obtain the conserved charge

$$Q^{\lambda\rho} = \int d^3x(\tilde{J}^\mu)^{\sigma\rho} \quad \text{where} \to Q^{ij} = \int d^x x\big(x^iT^{j0} - x^jT^{0i}\big) \quad (2.39)$$

are the angular momentum components. Finally, using the expression $T^{i0} = i\psi_j^*\partial^i\psi^j$ we get

$$J^i = i\int d^3x\big[\epsilon^i{}_{jk}x^j\psi_l^*\partial^k\psi^l\big]. \quad (2.40)$$

Other conserved quantities associated with the Galilei group lead to the fact that the center of mass follows a free-particle trajectory. However, we will mostly limit ourselves to the study of spherically symmetric equilibrium configurations which are centered at the origin, where these quantities do not play a significant role.

Also, we know that the Eq. (2.7) is invariant under continuous shifts in the phase of the wave function, $\vec{\psi}(t,\vec{x}) \mapsto e^{i\alpha}\vec{\psi}(t,\vec{x})$, with α a real constant, leading to the conservation of the "particle number" given by

$$N = \int(\vec{\psi^*}\cdot\vec{\psi})dV. \quad (2.41)$$

where, in contrast with the relativistic expression (2.6), there not are time and spatial derivates of the field.

Moreover, our theory features an "accidental" symmetry: in absence of spin-spin self-interactions ($\lambda_s = 0$), the action (2.7) is also invariant under global unitary transformations, $\vec{\psi}(t,\vec{x}) \mapsto \hat{U}\vec{\psi}(t,\vec{x})$, where $\hat{U}$ is a constant unitary 3×3 matrix.[7] This symmetry induces the conserved, self-adjoint, second-rank tensor[8]

$$\hat{Q} = \int (\vec{\psi}^* \otimes \vec{\psi}) dV, \tag{2.43}$$

with the following properties: $N = \mathrm{Tr}(\hat{Q}) = N_1 + N_2 + N_3$ where for example $N_1 = \int d^3x \psi_1^* \psi_1$ and $\vec{S} = -i\mathrm{Tr}(\hat{\varepsilon}\hat{Q})$, where $\hat{\varepsilon}$ is the third-rank Levi-Civita tensor and in the last expression the trace denotes the contraction of the last two indices of $\hat{\varepsilon}$ with the two indices of $\hat{Q}$. The reason why the particle number N and the spin angular momentum $\vec{S}$ are codified in the tensor $\hat{Q}$ is because rotations and global phase factors are elements of the $U(3)$ group. On the other hand, the other components of $\hat{Q}$ are only conserved when $\lambda_s = 0$.[9]

In the following, we will distinguish between two scenarios: the *symmetry-enhanced sector* of the effective theory, where $\lambda_s = 0$ and the accidental $U(3)$ symmetry is manifest, and the *generic sector* of the effective theory, where the two coupling constants λ_n and λ_s can take arbitrary values, except $\lambda_s = 0$. In addition, we will consider two configurations, $\psi_1(t,\vec{x})$ and $\psi_2(t,\vec{x})$, as "equivalent" if they are related by a symmetry transformation (note that the notion of equivalent configurations depends on the specific sector of the theory that we are exploring). In this thesis, we will not distinguish between equivalent configurations and will always use symmetry transformations for our convenience. In particular, if $\lambda_s = 0$, we can use the $U(3)$ symmetry to diagonalize the operator $\hat{Q}$, leaving only the diagonal elements non-zero.

G. Constant Polarization States

Now, we introduce some simple properties of constant polarization states, which will be of interest later. Constant polarization states are defined as

$$\vec{\psi}(t,\vec{x}) = f(t,\vec{x})\hat{\epsilon}, \tag{2.45}$$

[7] We can see, for example, that under the transformation $\hat{U}$ with $\hat{U}^\dagger\hat{U} = \mathbf{1}$, the term $n = \vec{\psi}^* \cdot \vec{\psi}$ is invariant since $n' = \vec{\psi}'^* \cdot \vec{\psi}' = (\hat{U}\vec{\psi})^\dagger \cdot \hat{U}\vec{\psi} = U^*_{lk}U_{kj}\psi^{l*}\psi_j = \psi^* \cdot \psi = n$. However, the term $\vec{s} = -i\vec{\psi}^* \times \vec{\psi}$ is not invariant since $s'^i = -i\epsilon^{ijk}U^*_{jm}U_{kl}\psi^*_m\psi_l \neq -i\epsilon^{ijk}\psi^*_j\psi_k = s^i$.

[8] Since the Lagrangian (2.31) is invariant to unitary infinitesimal transformations $\hat{U}(\alpha) = \mathbf{1} + i\alpha\hat{D}$ we have an induced a conserved current of the form

$$J^\mu_N = \sum_a \Pi^{a\mu} D\psi^a \to Q_{ij} = \int d^3x \psi^*_i \psi_j. \tag{2.42}$$

[9] The tensor $\hat{Q}$ evolves in time according to

$$\frac{d\hat{Q}}{dt} = \frac{\lambda_s}{m_0^2}\,\mathrm{Im}\int (\vec{\psi}\cdot\vec{\psi})^*(\vec{\psi}\otimes\vec{\psi})dV. \tag{2.44}$$

If $\lambda_s = 0$, this tensor is conserved. If $\lambda_s \neq 0$, however, only the anti-symmetric part of this tensor and its trace are conserved.

where $f(t,\vec{x})$ is an arbitrary complex-valued function and $\hat{\epsilon}$ is a polarization vector that is independent of the space-time coordinates and that, for convenience, we have normalized to one, $\hat{\epsilon}^* \cdot \hat{\epsilon} = 1$.

Given that the wave function $\vec{\psi}(t,\vec{x})$ contains an arbitrary global phase, we can parametrize a constant polarization vector in the form:

$$\hat{\epsilon} = \sin\theta\cos\phi\hat{e}_x + e^{i\gamma_1}\sin\theta\sin\phi\hat{e}_y + e^{i\gamma_2}\cos\theta\hat{e}_z, \tag{2.46}$$

where θ, ϕ, γ_1 and γ_2 are 4 real constants and $\hat{e}_x$, $\hat{e}_y$, and $\hat{e}_z$ are the Cartesian unit vectors. Furthermore, given the symmetries of our effective theory, one can always perform a rotation such that the polarization vector is contained in the xy plane, and obtain

$$\hat{\epsilon} = \cos\phi\hat{e}_x + e^{i\gamma_1}\sin\phi\hat{e}_y, \tag{2.47}$$

which is the expression for a general elliptical polarization vector.[10]

On the other hand, from the definition of the spin density $\vec{s} = -i\vec{\psi}^*(t,\vec{x}) \times \vec{\psi}(t,\vec{x})$, one has $\vec{s} = 2|f|^2\cos\phi\sin\phi\sin\gamma_1$ such that using the identity $\sin^2(2\phi) = 4\cos^2(\phi)\sin^2(\phi)$, we have

$$\vec{s}^{\,2} = |f|^4\sin^2(2\phi)\sin^2\gamma_1, \tag{2.48}$$

which implies that $|\vec{s}| \leq |f|^2 = n$.[11] Configurations with zero spin density ($\gamma_1 = 0$) are (up to a global phase factor) of the form $\hat{\epsilon} = \cos\phi\hat{e}_x \pm \sin\phi\hat{e}_y$, which after a rotation can be further reduced to

$$\hat{\epsilon} = \hat{\epsilon}_x := \hat{e}_x. \tag{2.49a}$$

In contrast, configurations which saturate the spin density ($\phi = \pi/4$ and $\gamma_1 = \pi/2$), $|\vec{s}| = n$, are of the form $\hat{\epsilon} = \frac{1}{\sqrt{2}}(\hat{e}_x \pm i\hat{e}_y)$, which using a rotation can be reduced to

$$\hat{\epsilon} = \hat{\epsilon}^{(+)}_z := \frac{1}{\sqrt{2}}(\hat{e}_x + i\hat{e}_y)\,. \tag{2.49b}$$

We call constant polarization states having $\hat{\epsilon}$ as in Eq. (2.49a) *linearly polarized*, and states as in (2.49b) *circularly polarized*.

When the spin-spin self-interaction is absent ($\lambda_s = 0$) the theory is $U(3)$ invariant and all states with constant polarization are equivalent to each other.[12] In particular, this means that when exploring constant polarization states in the symmetry enhanced sector of the effective theory we can restrict ourselves

[10] This name takes on particular significance when the state is stationary, i.e. $f(t,\vec{x}) = e^{-iEt}\bar{f}(\vec{x})$, and the real $\vec{\psi}_R$ and the imaginary $\vec{\psi}_I$ parts of the vector $\vec{\psi}$ evaluated at a fixed point $\vec{x}$ describe an ellipse as time progresses.

[11] Note that, in general, $\vec{s}^{\,2} = n^2 - |\vec{\psi}\cdot\vec{\psi}|^2$, so the inequality $|\vec{s}| \leq n$ holds true for any wave vector $\vec{\psi}(t,\vec{x})$

[12] Any elliptical polarization vector (2.47) can be expressed in the form $\hat{\epsilon} = \hat{U}\hat{e}_x$, where

$$\hat{U} = \begin{pmatrix} \cos\phi & -e^{-i\gamma_1}\sin\phi & 0 \\ e^{i\gamma_1}\sin\phi & \cos\phi & 0 \\ 0 & 0 & 1 \end{pmatrix} \tag{2.50}$$

is a unitary matrix.

to the simplest case in which $\hat{\epsilon} = \hat{\epsilon}_x$. In contrast, when $\lambda_s \neq 0$, one can prove that any solution of Eq. (2.24a) with constant polarization has either linear ($\vec{s}^2 = 0$) or circular ($\vec{s}^2 = n^2$) polarization, which in this case are different to each other. To summarize, if we restrict ourselves to constant polarization states, it is sufficient to consider the linear and circular ones, which degenerate when $\lambda_s = 0$.

Note: We can prove that when $\lambda_s \neq 0$, constant polarization states satisfying the field equations are necessarily linear or circular. To do so, we substitute the definition (2.45) into Eq. (2.24) and obtain

$$i\frac{\partial f}{\partial t}\hat{\epsilon} = -(\Delta f)\hat{\epsilon} + \lambda_n|f|^2 f\hat{\epsilon} + \lambda_s|f|^2 f(\hat{\epsilon}^* \times \hat{\epsilon}) \times \hat{\epsilon} + \Delta^{-1}(|f|^2)f\hat{\epsilon}. \quad (2.51)$$

where the condition $(\hat{\epsilon}^* \times \hat{\epsilon}) \times \hat{\epsilon} = \hat{\epsilon} - (\hat{\epsilon} \cdot \hat{\epsilon})\hat{\epsilon}^* = C\hat{\epsilon}$ must be satisfied, with C a complex constant. Taking the dot product with $\hat{\epsilon}$ on both sides yields $C(\hat{\epsilon} \cdot \hat{\epsilon}) = 0$. There are two solution to this equation: $C = 0$ and $\hat{\epsilon} \cdot \hat{\epsilon} = 0$. In the first case, the above condition leads to $\hat{\epsilon} = (\hat{\epsilon} \cdot \hat{\epsilon})\hat{\epsilon}^*$, which, together with the normalization condition $\hat{\epsilon}^* \cdot \hat{\epsilon} = 1$, implies that $\hat{\epsilon}$ is real-valued up to a global phase factor. This is the condition for linear polarization. In the second case, if one writes $\hat{\epsilon} = \hat{\epsilon}_R + i\hat{\epsilon}_I$ (with $\hat{\epsilon}_R$ and $\hat{\epsilon}_I$ denoting the real and imaginary parts of $\hat{\epsilon}$, respectively) then the equation $\hat{\epsilon} \cdot \hat{\epsilon} = 0$ implies that $|\hat{\epsilon}_R| = |\hat{\epsilon}_I| = \frac{1}{\sqrt{2}}, \hat{\epsilon}_R \cdot \hat{\epsilon}_I = 0$, which is the condition for circular polarization in the direction $\hat{\epsilon}_R \times \hat{\epsilon}_I$.

2.3.3 Equilibrium Configurations

Now, we identify the different types of equilibrium configurations that can exist in our effective theory. For that purpose, we define an equilibrium configuration as a critical point of the energy functional $\mathcal{E}[\vec{\psi}]$. In practice, we restrict ourselves to variations that keep conserved quantities fixed. As we will demonstrate, the choice of which quantities are fixed might affect the location of the critical points, and, ultimately, the equilibrium states that can exist in the different sectors of the theory.

To proceed, let us first concentrate on the generic sector, where the two coupling constants λ_n and λ_s can take arbitrary values (except $\lambda_s = 0$) and the particle number N is conserved. In this case, the relevant critical points are obtained from varying the modified energy functional

$$\mathcal{E}_E[\vec{\psi}] := \mathcal{E}[\vec{\psi}] + \frac{1}{2}E\left(N - \int(\vec{\psi}^* \cdot \vec{\psi})dV\right), \quad (2.52)$$

where E is a Lagrange multiplier associated with the constraint that guarantees that the particle number remains fixed in the variations.[13] Remember that the functionals $\mathcal{E}[\vec{\psi}]$ and $N[\vec{\psi}]$ defined in Eqs. (2.33) and (2.41) depend on

[13]Let's remember that when varying a functional subject to a constraint, we must use the method of *Lagrange multipliers*. This method reduces the problem with n variables and k constraints to one with $n + k$ variables without constraints. In our case, the constraint is given by $g[\vec{\psi}] = \int(\vec{\psi}^* \cdot \vec{\psi})dV = N$, so the function for which we need to find the extrema is given by $h[\vec{\psi}] = \mathcal{E}[\vec{\psi}] - \lambda(N - g[\vec{\psi}])$.

the field $\vec{\psi}$ and its spatial gradients, but not on its time derivatives, and for that reason we will treat $\mathcal{E}_E[\vec{\psi}]$ as a functional of $\vec{\psi}(\vec{x})$ alone, ignoring any time evolution. Correspondingly, we assume that the Lagrange multiplier E is time-independent.

The first variation of $\mathcal{E}_E[\vec{\psi}]$ with respect to $\vec{\psi}$ yields[14]

$$\delta\mathcal{E}_E = \mathrm{Re}(\hat{\mathcal{H}}[\vec{\psi}]\vec{\psi} - E\vec{\psi}, \delta\vec{\psi}). \tag{2.54}$$

A critical point is characterized by the condition that $\delta\mathcal{E}_E = 0$ for all $\delta\vec{\psi}$; hence, equilibrium configurations $\vec{\psi}(\vec{x})$ must fulfill the nonlinear equation

$$E\vec{\psi} = \hat{\mathcal{H}}[\vec{\psi}]\vec{\psi}, \tag{2.55}$$

which must be solved subject to appropriate boundary conditions. Note that if $\vec{\psi}(\vec{x})$ satisfies Eq. (2.55), then $e^{i\alpha}\vec{\psi}(\vec{x})$, where α is an arbitrary phase independent of $\vec{x}$, is also a solution to this equation. If we make this phase time-dependent and introduce this expression into the dynamical Eq. (2.27), we obtain

$$\vec{\psi}(t, \vec{x}) = e^{-iEt}\vec{\psi}(t = 0, \vec{x}), \tag{2.56}$$

with $\vec{\psi}(t = 0, \vec{x}) = \vec{\psi}(\vec{x})$. In the context of quantum mechanics, these solutions are usually referred to as *stationary states*. They have time-independent particle $n(t, \vec{x})$ and spin $\vec{s}(t, \vec{x})$ densities, and, consequently, the Hamiltonian (2.28) remains constant in the evolution. Furthermore, stationary states are eigenfunctions of the Hamilton operator.

Next, we extend the study of the equilibrium configurations to the symmetry-enhanced sector, where $\lambda_s = 0$ and in addition to the particle number N the charges $\hat{Q}$ associated with the accidental symmetry are conserved. In analogy with the previous case, we define the energy functional

$$\mathcal{E}_{\hat{E}}[\vec{\psi}] := \mathcal{E}[\vec{\psi}] + \frac{1}{2}\mathrm{Tr}\left[\hat{E}\left(\hat{Q} - \int(\vec{\psi}^* \otimes \vec{\psi})dV\right)\right], \tag{2.57}$$

with $\hat{E}$ a constant Hermitian transformation that plays the role of the Lagrange multiplier associated with $\hat{Q}$. In this case, the first variation of Eq. (2.57) can be expressed in the form

$$\delta\mathcal{E}_{\hat{E}} = \mathrm{Re}(\hat{\mathcal{H}}[\vec{\psi}]\vec{\psi} - \hat{E}\vec{\psi}, \delta\vec{\psi}), \tag{2.58}$$

and, therefore, imposing $\delta\mathcal{E}_{\hat{E}} = 0$ for all $\delta\vec{\psi}$, yields

$$\hat{E}\vec{\psi} = \hat{\mathcal{H}}[\vec{\psi}]\vec{\psi}. \tag{2.59}$$

[14]To perform the variation, we expand the wave function $\vec{\psi}$ as

$$\vec{\psi}(t, \vec{x}) = \vec{\psi}^{(0)}(t, \vec{x}) + \epsilon\delta\vec{\psi}(t, \vec{x}) + \frac{\epsilon^2}{2}\delta^2\vec{\psi}(t, \vec{x}) + \mathcal{O}(\epsilon^3) \tag{2.53a}$$

where $\vec{\psi}^{(0)}(t, \vec{x})$ denote the background field and $\delta\vec{\psi}(t, \vec{x})$, $\delta^2\vec{\psi}(t, \vec{x})$ are the first and second order perturbations. The n-th variation of $\mathcal{E}[\vec{\psi}]$ is given by $\delta^n\mathcal{E}[\vec{\psi}] = \frac{d^n}{d\epsilon^n}\mathcal{E}[\vec{\psi}]|_{\epsilon=0}$. Using (2.53a) and (2.33) we have

$$\delta\mathcal{E}[\vec{\psi}] = Re(\hat{H}\vec{\psi}^{(0)}, \delta\vec{\psi}). \tag{2.53b}$$

where $(\vec{\psi}_1, \vec{\psi}_2) = \int(\vec{\psi}_1^* \cdot \vec{\psi}_2)dV$ denotes the standard L^2-scalar product between $\vec{\psi}_1$ and $\vec{\psi}_2$.

Now, if $\vec{\psi}(\vec{x})$ is a solution of Eq. (2.59), then $\hat{U}\vec{\psi}(\vec{x})$ also satisfies this equation, where $\hat{U} = e^{i\hat{A}}$ is a constant unitary transformation with $\hat{A}$ Hermitian and commuting with $\hat{E}$. However, if we allow $\hat{A}$ to depend on time, and substitute this expression into the dynamical Eq. (2.27), we obtain

$$\vec{\psi}(t, \vec{x}) = e^{-i\hat{E}t}\vec{\psi}(t = 0, \vec{x}), \tag{2.60}$$

where again $\vec{\psi}(t = 0, \vec{x}) = \vec{\psi}(\vec{x})$. We will refer to these configurations as *multi-frequency states*, given that they involve more than one frequency of oscillation. These states maintain the particle number density $n(t, \vec{x})$ time-independent, although, in general, the spin density $s(t, \vec{x})$ depends on time. Nonetheless, this does not affect the Hamiltonian $\hat{\mathcal{H}}[\vec{\psi}]$, which is independent of the spin density when $\lambda_s = 0$. Stationary states arise for the particular case in which $\hat{E}$ is proportional to the identity matrix; however, in the following, we will exclude this case when referring to multi-frequency states. Under this assumption, we can conclude that multi-frequency states are not eigenfunctions of the Hamilton operator.

To summarize, the equilibrium configurations of the generic sector of the effective theory (where λ_n is arbitrary and $\lambda_s \neq 0$), consist only of stationary states (2.56). In the symmetry-enhanced sector (where λ_n is arbitrary and $\lambda_s = 0$), in addition to the stationary (i.e. single-frequency) states, one must also consider the multi-frequency solutions (2.60).

General Properties of the Energy Functional and the Equilibrium Configurations

Following Ref. [49], we discuss some interesting properties of the energy functional and the equilibrium configurations that to a large extent can be deduced from a simple scaling argument. To this purpose, it is convenient to express Eq. (2.33) in the form

$$\mathcal{E}[\vec{\psi}] = T[\vec{\psi}] + \lambda_n F_n[n] + \lambda_s F_s[\vec{s}] - D[n, n], \tag{2.61}$$

where the functionals T, F_n, F_s and D are defined by

$$T[\vec{\psi}] := \frac{1}{2m_0}\int |\nabla\vec{\psi}(\vec{x})|^2 dV, \tag{2.62a}$$

$$F_n[n] := \frac{1}{4m_0^2}\int n(\vec{x})^2 dV, \tag{2.62b}$$

$$F_s[\vec{s}] := \frac{1}{4m_0^2}\int \vec{s}(\vec{x})^2 dV, \tag{2.62c}$$

$$D[n, n] := \frac{Gm_0^2}{2}\int\int \frac{n(\vec{x})n(\vec{x}')}{|\vec{x} - \vec{x}'|} dV' dV, \tag{2.62d}$$

and are positive definite.

Next, let $\nu > 0$ be an arbitrary real and positive parameter, and $\vec{\psi}(\vec{x})$ a given wave function which does not vanish identically. Consider the rescaled function

$$\vec{\psi}_\nu(\vec{x}) := \nu^{3/2}\vec{\psi}(\nu\vec{x}), \tag{2.63}$$

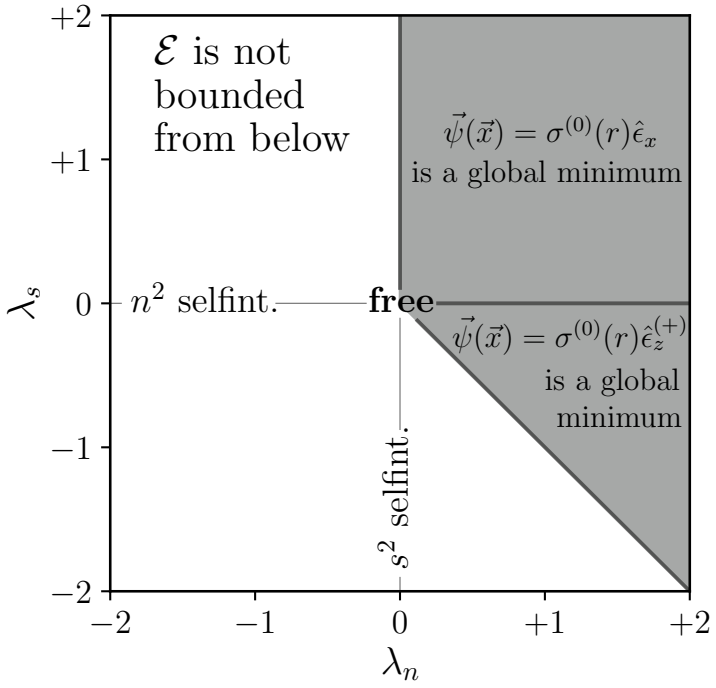

Figure 2.3: **Parameter space of the theory:** The shadow region ($\lambda_0 \geq 0$) represents the parameter space of our effective theory for which, when N is fixed, the energy functional is bounded from below. Furthermore, in this region there exists a global minimum of the energy functional, which is attained for a stationary and spherically symmetric state of constant polarization (linear if $\lambda_s > 0$ and circular if $\lambda_s < 0$) and negative energy. In general, we cannot guarantee the uniqueness of the ground state, unless $\lambda_n = \lambda_s = 0$, in which case the ground state is unique up to translations and rigid unitary transformations.

which leaves the particle number and the global $U(3)$ charges invariant, i.e. $N[\vec{\psi}_\nu] = N[\vec{\psi}]$ and $\hat{Q}[\vec{\psi}_\nu] = \hat{Q}[\vec{\psi}]$ for all $\nu > 0$. Under the rescaling (2.63), the energy functional (2.61) transforms according to

$$\mathcal{E}[\vec{\psi}_\nu] = \nu^2 T[\vec{\psi}] + \nu^3 \lambda_n F_n[n] + \nu^3 \lambda_s F_s[\vec{s}] - \nu D[n,n]. \tag{2.64}$$

Furthermore, the first and second variations of $\mathcal{E}[\vec{\psi}_\nu]$ at $\vec{\psi}_{\nu=1} = \vec{\psi}$ are given by

$$\left.\frac{d}{d\nu}\mathcal{E}[\vec{\psi}_\nu]\right|_{\nu=1} = 2T[\vec{\psi}] + 3\lambda_n F_n[n] + 3\lambda_s F_s[\vec{s}] - D[n,n], \tag{2.65a}$$

$$\left.\frac{d^2}{d\nu^2}\mathcal{E}[\vec{\psi}_\nu]\right|_{\nu=1} = 2T[\vec{\psi}] + 6\lambda_n F_n[n] + 6\lambda_s F_s[\vec{s}]. \tag{2.65b}$$

A number of interesting conclusions can be drawn from these results.

A. ***Lower Bound of the Energy Functional***

First, we claim that, for fixed N, the energy functional (2.61) is bounded from below if and only if $\lambda_0 \geq 0$, where

$$\lambda_0 := \begin{cases} \lambda_n, & \text{if } \lambda_s \geq 0, \\ \lambda_n - |\lambda_s|, & \text{if } \lambda_s < 0, \end{cases} \tag{2.66}$$

see Figure 2.3 for an illustration. Furthermore, the same holds true when $\lambda_s = 0$ and $\hat{Q}$ is fixed.

To prove this, we first assume that $N = \mathrm{Tr}(\hat{Q})$ is fixed but allow the trace-free part of $\hat{Q}$ to vary. Notice that if $\lambda_n \geq 0$ and $\lambda_s \geq 0$, then $\mathcal{E}[\psi] \geq T[\vec{\psi}] - D[n,n]$, which is known to be bounded from below when N is fixed (see, for instance, Ref. [99]). In contrast, when $\lambda_n < 0$ and $\lambda_s \geq 0$, we can choose $\vec{\psi}$ equal to a state of constant linear polarization, such that $F_s[\vec{s}] = 0$, and then it follows from Eq. (2.64) that $\mathcal{E}[\vec{\psi}_\nu]$ can be made arbitrarily negative by choosing ν large, showing that the energy functional is not bounded from below.[15] Finally, if $\lambda_s < 0$, then the inequality $|\vec{s}| \leq n$ implies that $\lambda_n F_n[n] + \lambda_s F_s[\vec{s}] \geq (\lambda_n - |\lambda_s|) F_n[n]$, with the equality sign for states of constant circular polarization. Hence, in this case, the energy functional is bounded from below if and only if $\lambda_n - |\lambda_s| \geq 0$.

When $\lambda_s = 0$ and $\hat{Q}$ is fixed it is easy to verify that one can apply the same arguments as above to show that the energy functional is bounded from below if and only if $\lambda_n \geq 0$. It should be noted that in this case one cannot always choose $\vec{\psi}$ to be a state of constant linear polarization since this requires that $\hat{Q}$ has rank 1; however, this is not needed for the scaling argument since the term $\lambda_s F_s[\vec{s}]$ in Eq. (2.64) is automatically zero when $\lambda_s = 0$. Hence, one can use again the particular variation defined in Eq. (2.63) (which fixes $\hat{Q}$) to conclude that the energy functional is unbounded from below when $\lambda_n < 0$.

B. *Energy Functional of Equilibrium States*

Second, if $\vec{\psi}(t, \vec{x})$ is an equilibrium configuration, then the first variation of the energy functional vanishes, and Eq. (2.65a) yields the relation

$$D[n,n] = 2T[\vec{\psi}] + 3\lambda_n F_n[n] + 3\lambda_s F_s[\vec{s}]. \tag{2.67}$$

This expression is valid for any equilibrium state and allows one to express the selfgravity term $D[n,n]$ as a function of the kinetic term $T[\vec{\psi}]$ and the self-interaction ones $F_n[n]$ and $F_s[\vec{s}]$, similar to the usual virial relation. Accordingly, the total energy of any equilibrium state can be expressed as

$$\mathcal{E}[\vec{\psi}] = -T[\vec{\psi}] - 2\lambda_n F_n[n] - 2\lambda_s F_s[\vec{s}], \tag{2.68}$$

which does not require the computation of the selfgravity term $D[n,n]$. Since $\lambda_n F_n[n] + \lambda_s F_s[\vec{s}] \geq \lambda_0 F_n[n]$ and $T[\vec{\psi}]$ and $F_n[n]$ are positive definite, it follows that the energy of the equilibrium states is always negative when $\lambda_0 \geq 0$.

[15] An energy functional that is unbounded from below is considered ill-defined, as it implies that an unlimited amount of energy can be extracted from the system, rendering the theory non-physical. However, in the context of effective theories, this issue is expected to be resolved by the ultraviolet completion, where higher-order operators not included in Eq. (2.7) should ensure that the energy functional becomes bounded. This is what happens, for instance, with the well-known cosine potential of the QCD axion, where expanding in a Taylor series reveals that the quartic term has a negative coefficient (indicating an attractive self-interaction), while the potential remains positive definite.

C. *Discarding Local Minima of the Energy Functional*

Third, Eq. (2.65b) implies that a critical point at $\nu = 1$ corresponds to a local minimum of $\mathcal{E}[\vec{\psi}_\nu]$ if $T[\vec{\psi}] + 3\lambda_n F_n[n] + 3\lambda_s F_s[\vec{s}]$ is positive and to a local maximum if it is negative. In particular, an equilibrium state $\vec{\psi}(t, \vec{x})$ cannot be a (local) minimum of the energy functional with respect to arbitrary variations that fix N (or $\hat{Q}$ if $\lambda_s = 0$) when $\lambda_n F_n[n] + \lambda_s F_s[\vec{s}] < -T[\vec{\psi}]/3$.

Generic Sector: Stationary Solutions

In the generic sector of the effective theory, equilibrium configurations are stationary states, which are characterized by the ansatz, c.f. Eq. (2.56):

$$\vec{\psi}(t, \vec{x}) = e^{-iEt}\vec{\sigma}^{(0)}(\vec{x}), \tag{2.69}$$

where $\vec{\sigma}^{(0)}$ is a complex vector-valued function of $\vec{x}$ and the energy eigenvalue E is a real constant. As explained previously, these states have a time-independent Hamiltonian, and consequently, they give rise to a static gravitational potential $\mathcal{U}(t, \vec{x}) = \mathcal{U}(\vec{x})$. Introducing Eq. (2.69) into the integro-differential equation (2.28) yields the nonlinear eigenvalue problem:

$$E\vec{\sigma}^{(0)} = \hat{\mathcal{H}}[\vec{\sigma}^{(0)}]\vec{\sigma}^{(0)}. \tag{2.70}$$

This equation determines the stationary solutions of the $s = 1$ Gross-Pitaevskii-Poisson system, which will be solved numerically in Section 2.3.5 under the assumption of spherical symmetry.

However, before doing so, we ask ourselves whether stationary states can arise as *global* minima of the energy functional. This question is particularly relevant since such a minimum is expected to represent a stationary state that is (orbitally) stable under small enough perturbations [100].

In order to formulate the question in a more precise way, let

$$\mathcal{A}_N := \left\{ \vec{\psi} \in H^1(\mathbb{R}^3, \mathbb{C}^3) : \int |\vec{\psi}(\vec{x})|^2 dV = N \right\}, \tag{2.71}$$

where here $H^1(\mathbb{R}^3, \mathbb{C}^3)$ denotes the space of wave functions $\vec{\psi} : \mathbb{R}^3 \to \mathbb{C}^3$ such that $\vec{\psi}$ and its first partial derivatives are (Lebesgue-) square-integrable. It can be shown that $\mathcal{E}$ is well-defined on this space [99]. Thus, we ask whether there exists a wave function $\vec{\psi}_* \in \mathcal{A}_N$ such that

$$\mathcal{E}[\vec{\psi}_*] = \inf_{\vec{\psi} \in \mathcal{A}_N} \mathcal{E}[\vec{\psi}]. \tag{2.72}$$

The first observation is that a necessary condition for the existence of such a minimum is that $\mathcal{E}$ must be bounded from below on $\mathcal{A}_N$. As has been shown in Section 2.3.3, this is the case if and only if $\lambda_0 \geq 0$, with λ_0 defined in Eq. (2.66), so for the remainder of this section we shall assume that $\lambda_0 \geq 0$.

Next, we claim that a global minimum is attained by a wave function of constant polarization and that, if multiple global minima exist, all share this form. To show this, we first decompose $\vec{\psi}(\vec{x})$ according to

$$\vec{\psi}(\vec{x}) = f(\vec{x})\hat{\epsilon}(\vec{x}), \tag{2.73}$$

where $f(\vec{x}) := |\vec{\psi}(\vec{x})|$ and $\hat{\epsilon}(\vec{x})$ has unit norm. Using the fact that $n = f^2$ and $|\nabla\vec{\psi}|^2 = |\nabla f|^2 + n|\nabla\hat{\epsilon}|^2$, and recalling the inequality $\lambda_n F_n[n] + \lambda_s F_s[\vec{s}] \geq \lambda_0 F_n[n]$, one obtains

$$\mathcal{E}[\vec{\psi}] \geq \mathcal{E}_{\text{scalar}}[f] := T_{\text{scalar}}[f] + \lambda_0 F_n[n] - D[n,n], \tag{2.74}$$

where $T_{\text{scalar}}[f] := \frac{1}{2m_0}\int |\nabla f(\vec{x})|^2 dV$. Furthermore, equality holds only if on the set of points where $f > 0$ the polarization vector $\hat{\epsilon}(\vec{x})$ is constant and satisfies $\lambda_n + \lambda_s|\hat{\epsilon}^* \times \hat{\epsilon}|^2 = \lambda_0$, which means that $\hat{\epsilon}(\vec{x})$ has linear (circular) polarization if $\lambda_s > 0$ ($\lambda_s < 0$).

One can further decrease the energy functional by replacing f by its "symmetric decreasing rearrangement" f_* (which, by definition, is spherically symmetric, nonincreasing, nonnegative and satisfies $\int f_*^p dV = \int f^p dV$ for all $p \geq 1$; see [99] and references therein). It follows from [99] that $\mathcal{E}_{\text{scalar}}[f] \geq \mathcal{E}_{\text{scalar}}[f_*]$, with strict inequality unless $f(\vec{x}) = f_*(\vec{x} - \vec{x}_0)$ with a constant vector $\vec{x}_0$.

As a consequence, any minima $\vec{\psi}_*$ of the problem (2.72) must lie in the subset of $\mathcal{A}_N$ consisting of constant polarization states for which the function $f(\vec{x}) := |\vec{\psi}(\vec{x})|$ is radially symmetric (up to translations), nonincreasing, and nonnegative and for which the polarization is linear for $\lambda_s > 0$ and circular for $\lambda_s < 0$. The function f can then be found by minimizing the functional $\mathcal{E}_{\text{scalar}}$, which is known to have a minimum [99, 101, 102] satisfying $f(\vec{x}) = f_*(\vec{x})$.

In conclusion, global minima of Eq. (2.72) exist, and (up to translations) all of them are described by stationary and spherically symmetric states of constant polarization that have the form $\vec{\psi}(t,\vec{x}) = e^{-iEt}\sigma^{(0)}(r)\hat{\epsilon}$, with $\sigma^{(0)}(r)$ monotonically decreasing and positive, the polarization $\hat{\epsilon}$ being linear when $\lambda_s > 0$ and circular when $\lambda_s < 0$. Whether or not the function $\sigma^{(0)}(r)$ characterizing the ground state is unique for $\lambda_0 > 0$ is an interesting open question that will not be addressed in this thesis work.

Figure 2.3 further illustrates the results of this section.

Symmetry-enhanced Sector: Stationary and Multi-frequency Solutions

In absence of spin-spin self-interactions ($\lambda_s = 0$), stationary configurations still exist. Following similar arguments as in Section 2.3.3 we conclude that, for fixed N and $\lambda_n \geq 0$, the energy is always minimized by a stationary and spherically symmetric state of constant polarization and no nodes. Furthermore, in the free theory ($\lambda_n = \lambda_s = 0$), the ground state is unique, up to translations and rigid unitary transformations [99].

As explained in Section 2.3.3, in the symmetry-enhanced sector there also exists the possibility of equilibrium configurations that are realized as multi-frequency states. Expanding

$$\vec{\psi}(t=0,\vec{x}) = \sum_{\lambda=1}^{3} \sigma_\lambda^{(0)}(\vec{x})\hat{e}_\lambda \tag{2.75}$$

in terms of an orthornormal basis $\hat{e}_\lambda$ of $\mathbb{C}^3$ which diagonalizes the transformation $\hat{E}$, Eq. (2.60) leads to the following expression for the multi-frequency states:

$$\vec{\psi}(t,\vec{x}) = \sum_{\lambda=1}^{3} e^{-iE_\lambda t}\sigma_\lambda^{(0)}(\vec{x})\hat{e}_\lambda, \tag{2.76}$$

where $\sigma_\lambda^{(0)}$ are complex-valued functions depending on $\vec{x}$ and E_λ denote the eigenvalues of $\hat{E}$ which are real and correspond to the frequency of oscillation associated with $\sigma_\lambda^{(0)}$. As the stationary states, these solutions have a time-independent Hamiltonian and gravitational potential. Introducing Eq. (2.76) into the integro-differential equation (2.28) yields the nonlinear eigenvalue problem:[16]

$$E_\lambda \sigma_\lambda^{(0)} = \hat{\mathcal{H}}[\vec{\psi}]\sigma_\lambda^{(0)}. \tag{2.77}$$

These equations determine the multi-frequency solutions of the symmetry-enhanced sector of the $s = 1$ Gross-Pitaevskii-Poisson system, which will be solved numerically in Section 2.3.4 under the assumption of spherical symmetry.

An open question is whether constant polarization states, which minimize the energy functional for fixed N, also minimize it for arbitrary fixed values of $\hat{Q}$. We do not address this question in this thesis work.

2.3.4 Spherically Symmetric Equilibrium Configurations

Hereafter, we further specialize on equilibrium configurations which are spherically symmetric. As discussed in Section 2.3.2, our effective theory is invariant under the rotation group, hence we expect spherically symmetric configurations to play a relevant role in our discussion. Furthermore, as we have already argued in Section 2.3.3, for fixed N and $\lambda_0 \geq 0$, all ground state configurations are stationary and spherically symmetric (up to translations).

We define a spherically symmetric configuration as one that is invariant under rotational transformations.[17] Recall that Eq. (2.7) is invariant with respect to any two of the following representations of the $SO(3)$ group: $\vec{\psi}(t,\vec{x}) \mapsto R\vec{\psi}(t,R^{-1}\vec{x})$ and $\vec{\psi}(t,\vec{x}) \mapsto \vec{\psi}(t,R^{-1}\vec{x})$. Therefore, a spherically symmetric configuration should lie in the trivial irreducible representation of any of these two representations of the rotation group.

In the first case, one obtains a state of the form

$$\vec{\psi}(t,\vec{x}) = \psi_r(t,r)\hat{e}_r, \tag{2.78a}$$

with $\hat{e}_r$ the unit radial vector and $\psi_r(t,r)$ an arbitrary complex-valued function of t and $r = |\vec{x}|$. In the second case, however, one gets

$$\vec{\psi}(t,\vec{x}) = \sum_{\lambda=1}^{3} \psi_\lambda(t,r)\hat{e}_\lambda, \tag{2.78b}$$

[16] Recall that $\hat{\mathcal{H}}[\vec{\psi}]$ depends on $\vec{\psi}$ only through the combination $n = \sum_\lambda |\sigma_\lambda^{(0)}|^2$, which is independent of t.

[17] Clearly, a spherically symmetric configuration should be associated with a radially symmetric gravitational potential. Through Poisson's equation, this implies that the particle density n should have the same symmetry. The question then is which wave functions $\vec{\psi}(t,\vec{x})$ give rise to such densities and, at the same time, are self-consistent stationary or multi-frequency solutions of the $s = 1$ Gross-Pitaevskii-Poisson system. While in this thesis report we do not provide a complete answer to this question (since we do not guarantee obtaining *all possible* such wave functions), we nevertheless identify different families of such states based on symmetry arguments.

where the three components of $\vec{\psi}(t,\vec{x})$ in an orthonormal constant basis $\hat{e}_\lambda$ of $\mathbb{C}^3$ are functions of t and r only. Note that in both cases the particle density n is radially symmetric, which, according to Poisson's equation, guarantees that the gravitational potential $\mathcal{U}$ also respects this symmetry. The spin density $\vec{s}$ vanishes in the first case, however, in the second one it may be non-zero, although its three components are functions of t and r only.

Next, we identify the different types of spherically symmetric equilibrium configurations that can exist in our effective theory. For doing this, we combine our definition of equilibrium configurations in Section 2.3.3, together with that of spherically symmetric configurations in this section.

Stationary spherical solutions

Polarization	$\lambda_n = 0$, $\lambda_s = 0$	$\lambda_n \neq 0$, $\lambda_s = 0$	$\lambda_n = 0$, $\lambda_s \neq 0$	$\lambda_n \neq 0$, $\lambda_s \neq 0$
Constant: linear	$\ell = 0$ SP [87, 49]	$\ell = 0$ GPP [49]	$\ell = 0$ SP [87, 49]	$\ell = 0$ GPP [49]
circular	$\ell = 0$ SP [87, 49]	$\ell = 0$ GPP [49]	$\ell = 0$ SP [87, 49]	$\ell = 0$ GPP [49]
arbitrary	$\ell = 0$ SP [87, 49]	$\ell = 0$ GPP [49]	non-existent	non-existent
Radial	$\ell = 1$ SP [87]	$\ell = 1$ GPP (new)	$\ell = 1$ GPP (new)	$\ell = 1$ GPP (new)

Table 2.1: **The stationary and spherical $s = 1$ Gross-Pitaevskii-Poisson system:** The stationary, spherically symmetric $s = 1$ Gross-Pitaevskii-Poisson equations as compared to other systems studied in the framework of multi-scalar field theories. The comparison depends on the polarization vector $\hat{\epsilon}$. A general constant polarization (different from the linear and circular ones) is prohibited in presence of spin-spin self-interactions. Self-interacting, radially polarized Proca stars are not related with previously known solutions. SP (Schrödinger-Poisson), GPP (Gross-Pitaevskii-Poisson).

For the following, it will be convenient to express the field $\vec{\sigma}^{(0)}(\vec{x})$ of the stationary ansatz (2.69) in the form $\vec{\sigma}^{(0)}(\vec{x}) = \sigma^{(0)}(r)\hat{\epsilon}(\vec{x})$. Here $\sigma^{(0)}$ is a real-valued function which, due to spherical symmetry, depends only on the radial coordinate r and $\hat{\epsilon}$ is a complex polarization vector that, in general, depends on $\vec{x}$ and is normalized to have unit length. Then, combining Eqs. (2.69) and (2.78a) leads to $\hat{\epsilon}(\vec{x}) = \hat{e}_r$, whereas combining Eqs. (2.69) and (2.78b) yields $\hat{\epsilon}(\vec{x}) = \hat{\epsilon}(r)$.

In addition, the wave function $\vec{\psi}(t,\vec{x})$ needs to satisfy the $s = 1$ Gross-Pitaevskii equation (2.25a), and this puts a further condition on the possible form of the polarization vector. Although we have not analyzed the full implications of this condition,[18] we identified three different types of polarization vectors that are compatible with the structure of the field equations and lead to stationary and spherically symmetric configurations:

i) A linear polarization vector, for which $\hat{\epsilon}(\vec{x}) = \hat{e}_x$; see Eq. (2.49a).

[18]However, when $\lambda_s = 0$ one can prove that $\hat{\epsilon}(r)$ must be constant since in this case the three components of $\vec{\sigma}^{(0)}(\vec{x})$ satisfy the same time-independent Schrödinger equation with the same energy level E and thus they must be proportional to each other according to the Sturm oscillation theorem [103]. Further, we have proved that under the assumption that $\hat{\epsilon}(r)$ is constant, only linear or circular polarizations are possible when $\lambda_s \neq 0$, although in this case we have not been able to demonstrate that the polarization vector is necessarily constant.

ii) A circular polarization vector, for which $\hat{\epsilon}(\vec{x}) = \hat{\epsilon}_z^{(+)}$; see Eq. (2.49b).

iii) A radial polarization vector, for which $\hat{\epsilon}(\vec{x}) = \hat{e}_r$, with $\hat{e}_r$ the unit radial vector.

The first two cases were already introduced in Section 2.3.2 and represent (up to a global symmetry transformation) the most general stationary states with constant polarization. For $\lambda_s = 0$, they degenerate; however, when $\lambda_s \neq 0$ they lead to inequivalent states. Furthermore, as discussed in the previous section, when $\lambda_0 \geq 0$ there exists a spherical and constant polarization state that minimizes the energy functional. These solutions were previously explored in Refs. [76, 77]. The radially polarized states can be obtained by substituting $\gamma_1 = \gamma_2 = 0$ and $\theta = \vartheta$ and $\phi = \varphi$ into Eq. (2.46), where ϑ and φ represent the polar and azimuthal angles in three-dimensional space, respectively. These solutions constitute the non-relativistic limit of the spherically symmetric Proca stars originally reported in [60] (see also Ref. [70], which explores radial polarization under the name of edgehog field configurations).

Introducing the ansätze i), ii), and iii) into the $s = 1$ Gross-Pitaevskii-Poisson system (2.25), we obtain that the stationary and spherically symmetric configurations of linear, circular and radial polarization must satisfy the nonlinear eigenvalue problem

$$E\sigma^{(0)} = \left[-\frac{1}{2m_0}\left(\Delta_s - \frac{2\gamma}{r^2}\right) + \frac{\lambda_n + \alpha\lambda_s}{2m_0^2}\sigma^{(0)2} + m_0\mathcal{U}\right]\sigma^{(0)}, \quad (2.79a)$$

$$\Delta_s\mathcal{U} = 4\pi G m_0 \sigma^{(0)2}. \quad (2.79b)$$

Here, $\Delta_s := \frac{1}{r}\frac{d^2}{dr^2}r$ denotes the radial part of the Laplace operator, and the parameters γ and α depend on the polarization vector $\hat{\epsilon}$ and take the following values:

i) $\gamma = 0$, $\alpha = 0$ for linearly polarized Proca stars,

ii) $\gamma = 0$, $\alpha = 1$ for circularly polarized Proca stars,

iii) $\gamma = 1$, $\alpha = 0$ for radially polarized Proca stars.

It is interesting to note that linearly and circularly polarized Proca stars are described by exactly the same equations as non-relativistic boson stars, c.f. Eqs. (32) in Ref. [49] (see also [14, 104] for previous studies of the equilibrium configurations of the $s = 0$ Gross-Pitaevskii-Poisson system). As we clarified earlier, in absence of spin-spin self-interaction, all constant polarization states are equivalent to each other; therefore, when $\lambda_s = 0$, elliptically polarized Proca stars beyond the linear and circular cases also exist and are described by Eqs. (2.79) with $\gamma = 0$. Non-selfinteracting ($\lambda_n = \lambda_s = 0$) radially polarized Proca stars, on the other hand, are described by the same equations as non-relativistic, $\ell = 1$ boson stars, c.f. Eqs. (41) in Ref. [87]. Finally, self-interacting, radially polarized Proca stars satisfy the same system of equations as self-interacting, $\ell = 1$ boson stars; however, up to our knowledge, such solutions have not been reported in the literature. We review the equivalence between these different systems in Table 2.1.

Equations (2.79) must be complemented with appropriate boundary conditions that guarantee that the solutions remain regular at the origin and possess finite total energy. Near $r = 0$, we can expand the solutions in power series of the form $\sigma^{(0)}(r) = \sigma_0 r^\alpha + \sigma_1 r^{\alpha+1} + \sigma_2 r^{\alpha+2} + \ldots$, $\mathcal{U}^{(0)}(r) = \mathcal{U}_0 r^\beta + u_1 r^{\beta+1} + \mathcal{U}_2 r^{\beta+2} + \ldots$, with $\sigma_0 \neq 0$, $\mathcal{U}_0 \neq 0$, α and β taking constant values positives values. Introducing this ansatz into Eqs. (2.79) we can write this as

$$\begin{aligned}\{\sigma_0\alpha(\alpha-1)r^{\alpha-2} + \sigma_1(\alpha+1)\alpha r^{\alpha-1} + \sigma_2(\alpha+2)(\alpha+1)r^\alpha + ...\} \\ +\frac{2\gamma}{r}\{\sigma_0\alpha r^{\alpha-1} + \sigma_1(\alpha+1)r^\alpha + \sigma_2(\alpha+2)r^{\alpha+1} + ...\} \\ -\frac{2}{r^2}\{\sigma_0 r^\alpha + \sigma_1 r^{\alpha 1+} + \sigma_2 r^{\alpha+2} + ...\} \pm \{\sigma_0 r^\alpha + ...\}^3 \\ +\{\mathcal{U}_0 r^\beta + ...\}\{\sigma_0 r^\alpha + ...\} = 0. \qquad (2.80)\end{aligned}$$

Near $r = 0$ we can neglect the terms $r^{3\alpha}$ and $r^{\alpha+\beta}$. Grouping the terms with power $r^{\alpha-2}$ and setting it to zero, we obtain a quadratic equation for α with solutions $\alpha = -1, 0$ if $\gamma = 0$ and $\alpha = -2, 1$ if $\gamma = 1$. The only solutions that are regular are given by the values $\alpha = 0, 1$. In a similar way for β using the Poisson equation (2.79b) we get the regular solution $\beta = 0, 1$. When we group the terms $r^{\alpha-1}$, we get $\sigma_1, \mathcal{U}_1 = 0$. So, when $\gamma = 0$, they have $(\alpha, \beta) = (0, 0)$ and $(\alpha, \beta) = (-1, -1)$, where the second solution needs to be discarded since it leads to divergences at the origin. For $\gamma = 1$ the two solutions have $(\alpha, \beta) = (1, 0)$ and $(\alpha, \beta) = (-2, -1)$, and again, the second one leads to a divergent behavior at $r = 0$.

This suggests the following regular boundary conditions at the center:

$$\sigma^{(0)}(r = 0) = (1 - \gamma)\sigma_0, \quad \sigma^{(0)\prime}(r = 0) = \gamma\sigma_0, \qquad (2.81a)$$

$$\mathcal{U}^{(0)}(r = 0) = \mathcal{U}_0, \qquad \mathcal{U}^{(0)\prime}(r = 0) = 0, \qquad (2.81b)$$

with σ_0 and $\mathcal{U}_0$ constants and where the primes refer to derivation with respect to r. Notice that, at the origin, linearly and circularly polarized states have a nonzero value and a vanishing first derivative. In contrast, for radially polarized Proca stars, regularity implies that the wave function vanishes at $r = 0$, whereas the first derivative at the origin does not vanish. Nonetheless, we will sometimes refer to σ_0 as the central "amplitude" of the configuration, although rigorously this is only true if the polarization is linear or circular. On the other hand, Eqs. (2.79) are invariant under simultaneous shifts of E and $\mathcal{U}(r)$, and we can use this symmetry to fix arbitrarily the value of $\mathcal{U}_0$.

At infinity, we impose $\lim_{r\to\infty} \sigma^{(0)}(r) = 0$, which is required for the solutions to have a finite total energy. This defines a nonlinear eigenvalue problem for the frequency E, where, for each central amplitude of the configuration, σ_0, there exists a discrete set of frequencies $E_n(\sigma_0)$, $n = 0, 1, 2, \ldots$, for which the boundary conditions are satisfied. We discuss this problem in more detail in Section 2.3.5, where we present our numerical results.

Multi-frequency Spherical Solutions

Next, we explore multi-frequency states, which are only possible in absence of spin-spin self-interactions ($\lambda_s = 0$).

$\lambda_n = 0$, $\lambda_s = 0$	$\lambda_n \neq 0$, $\lambda_s = 0$	$\lambda_n = 0$, $\lambda_s \neq 0$	$\lambda_n \neq 0$, $\lambda_s \neq 0$
$\ell = 0$	$\ell = 0$	$\ell = 0$	$\ell = 0$
multi-state SP [89]	multi-state GPP (new)	multi-state GPP (new)	multi-state GPP (new)

Table 2.2: **The multi-frequency and spherical $s = 1$ Gross-Pitaevskii-Poisson system:** The multi-frequency, spherically symmetric $s = 1$ Gross-Pitaevskii-Poisson equations as compared to other systems studied in the framework of multi-scalar field theories. Self-interacting, multi-frequency Proca stars are not related with previously known solutions. SP (Schrödinger-Poisson), GPP (Gross-Pitaevskii-Poisson).

Combining Eqs. (2.76) and (2.78a), we find that the only possible states are the stationary radially polarized solutions that were already discussed in the previous section. On the other hand, combining Eqs. (2.76) and (2.78b), we find

$$\vec{\psi}(t, \vec{x}) = \sum_{\lambda=1}^{3} e^{-iE_\lambda t} \sigma_\lambda^{(0)}(r) \hat{e}_\lambda, \tag{2.82}$$

where $\sigma_\lambda^{(0)}$ are complex-valued functions depending only on r. As far as we know, these solutions have not been previously reported in the literature of Proca stars.

Introducing Eq. (2.82) into the $s = 1$, $\lambda_s = 0$ Gross-Pitaevskii-Poisson system (2.25), we obtain:

$$E_i \sigma_i^{(0)} = \left[-\frac{1}{2m_0} \Delta_s + \frac{\lambda_n}{2m_0^2} \sum_j |\sigma_j^{(0)}|^2 + m_0 \mathcal{U} \right] \sigma_i^{(0)}, \tag{2.83a}$$

$$\Delta_s \mathcal{U} = 4\pi G m_0 \sum_j |\sigma_j^{(0)}|^2, \tag{2.83b}$$

where, as in Eqs. (2.79a), Δ_s denotes the radial Laplace operator, and without loss of generality we have chosen the Cartesian basis $\hat{e}_\lambda = \hat{e}_i$ with $i = x, y, z$.[19] Furthermore, it is sufficient to consider real-valued functions $\sigma_i^{(0)}(r)$,[20] and from now on we will stick to this assumption.

It is worth noting that non-selfinteracting ($\lambda_n = 0$), multi-frequency Proca stars are described by exactly the same equations as non-relativistic, multi-state boson stars with two or three occupied energy levels in which the angular momentum number ℓ vanishes, c.f. Eqs. (9) in Ref. [89]. To the best of our knowledge, the generalization of this system for $\lambda_n \neq 0$ has not been reported in the literature, with the exception of the relativistic scenario discussed in Ref. [105].

[19] By applying a unitary transformation one can always map an arbitrary orthonormal basis $\hat{e}_\lambda$ to the standard Cartesian one $\hat{e}_i$, which changes the original multi-frequency state $\vec{\psi}(t, \vec{x})$ of Eq. (2.76) to an equivalent one.

[20] Indeed, one can take the real and imaginary parts of Eq. (2.83a) and conclude that $\mathrm{Re}(\sigma_i^{(0)})$ and $\mathrm{Im}(\sigma_i^{(0)})$ satisfy the same one-dimensional Schrödinger equation. As a consequence of the nodal theorem, the imaginary part of the wave function must be proportional to the real part, which means that the functions $\sigma_i^{(0)}$ are real, up to a global phase. After applying a constant unitary transformation one achieves that all $\sigma_i^{(0)}$'s are real.

To proceed, Eqs. (2.83) must be accompanied by some appropriate boundary conditions. Near $r = 0$, we demand that the solutions remain regular. For this, we again expand the functions $\sigma_i^{(0)}(r)$ and $\mathcal{U}(r)$ in power series $\sigma_i^{(0)}(r) = \sigma_{i0} r^{\alpha_i} + \sigma_{i1} r^{\alpha_i+1} + \sigma_{i2} r^{\alpha_i+2} + \ldots$, $\mathcal{U}(r) = \mathcal{U}_0 r^{\beta_i} + \mathcal{U}_1 r^{\beta_i} + \mathcal{U}_2 r^{\beta_i+2} + \ldots$, and impose $\sigma_{i0} \neq 0$, $\mathcal{U}_0 \neq 0$, $\alpha_i \geq 0$ and $\beta_i \geq 0$. Introducing this expansion into Eqs. (2.83) results in eight solutions, although only the one for which $(\alpha_i, \beta) = (0, 0)$ and $(\sigma_{i1}, \mathcal{U}_1) = (0, 0)$ is regular. This leads to the following boundary conditions at $r = 0$:

$$\sigma_i^{(0)}(r = 0) = \sigma_{i0}, \quad \sigma_i^{(0)\prime}(r = 0) = 0, \tag{2.84a}$$

$$\mathcal{U}(r = 0) = \mathcal{U}_0, \quad \mathcal{U}'(r = 0) = 0. \tag{2.84b}$$

As for the stationary states, the system (2.83) is invariant under common constant shifts in E_i and $m_0\mathcal{U}(r)$, and we can choose arbitrarily the value of $\mathcal{U}_0$.

Finally, to guarantee finite total energy, we impose $\lim_{r\to\infty} \sigma_i^{(0)}(r) = 0$. This defines a nonlinear multi-eigenvalue problem for the frequencies E_i, where, for each combination of central amplitudes $(\sigma_{x0}, \sigma_{y0}, \sigma_{z0})$, there exists a discrete set of frequencies $E_{xn_x}(\sigma_{x0}, \sigma_{y0}, \sigma_{z0})$, $E_{yn_y}(\sigma_{x0}, \sigma_{y0}, \sigma_{z0})$, and $E_{zn_z}(\sigma_{x0}, \sigma_{y0}, \sigma_{z0})$, $n_x, n_y, n_z = 0, 1, 2, \ldots$, satisfying the boundary conditions.

For the interpretation of our results, the following observation will be important. According to the nodal (or Sturm oscillation) theorem (see [103] for a pedagogical review), the eigenfunction $\psi_n(r)$ corresponding to the nth energy level E_n of a one-dimensional Schrödinger operator has exactly n nodes. Once the nonlinear system (2.83) is solved, Eq. (2.83a) can be interpreted as a Schrödinger equation for the wave functions $\sigma_i^{(0)}(r)$ with a fixed effective potential

$$\frac{\lambda_n}{2m_0^2} \sum_j |\sigma_j^{(0)}|^2 + m_0\mathcal{U}. \tag{2.85}$$

Therefore, the frequencies E_{in_i} can be ordered according to the node number of the functions $\sigma_i^{(0)}(r)$. Consequently, two functions $\sigma_i^{(0)}(r)$ and $\sigma_j^{(0)}(r)$ with $i \neq j$ are proportional to each other if they coincide in their node numbers, whereas they are mutually orthogonal if they have different numbers of nodes. In particular, this implies that a solution whose wave functions $\sigma_i^{(0)}(r)$, $i = x, y, z$, have equal number of nodes are proportional to each other and satisfy $E_x = E_y = E_z$; therefore it yields a stationary solution. Thus, for fixed central amplitudes $(\sigma_{x0}, \sigma_{y0}, \sigma_{z0})$, multi-frequency solutions can be labeled by their node numbers (n_x, n_y, n_z) with $n_x \leq n_y \leq n_z$ and not all n_i's equal to each other.

In the next section, we numerically solve the nonlinear eigenvalue problems belonging to spherically symmetric stationary and multi-frequency states.

2.3.5 Numerical Results

In this section, we provide numerical solutions of the $s = 1$ Gross-Pitaevskii-Poisson system and discuss their properties. To proceed, we introduce the

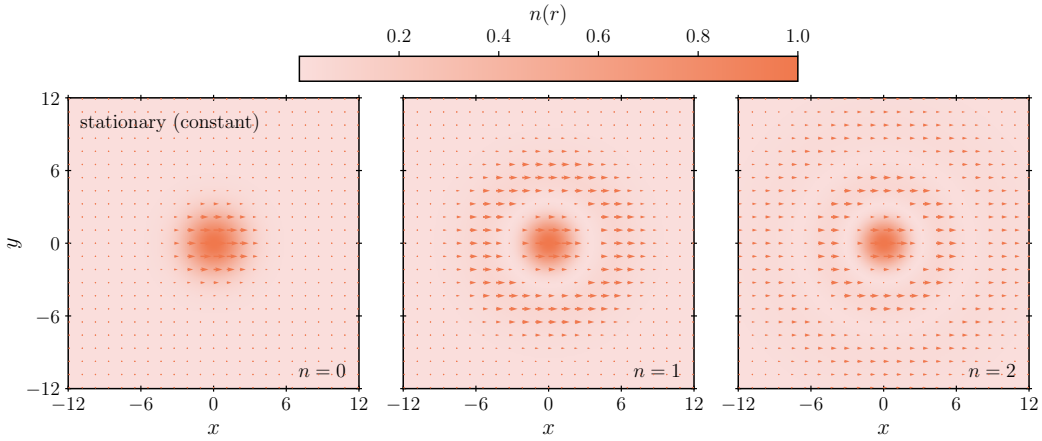

Figure 2.4: **Stationary Proca stars of constant polarization:** The normalized real part of the vector field, $\vec{\psi}_R(t,\vec{x})$, and the normalized particle number density, $n(t,\vec{x})$, for three Proca stars of constant polarization, unit central "amplitude", $\sigma_0 = 1$, and repulsive self-interaction, $\lambda_n^{phys} + \alpha\lambda_s^{phys} > 0$, at time $t = 0$. *Left panel:* No nodes, $n = 0$. *Center panel:* One node, $n = 1$. *Right panel:* Two nodes, $n = 2$. Note the appearance of an additional "layer" in the configuration for each increment of the variable n. Code variables use the scale $\lambda_* = |\lambda_n^{phys} + \alpha\lambda_s^{phys}|$.

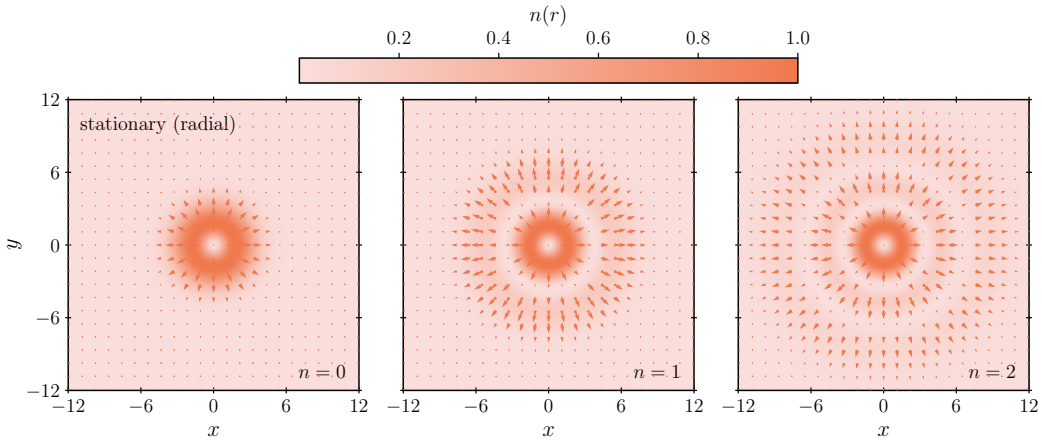

Figure 2.5: **Stationary Proca stars of radial polarization:** Same as in Figure 2.4 but for the case of radially polarized Proca stars. The main difference with respect to the linear and circular cases, apart from the fact that the vector points radially and does not pick a preferred direction, is the presence of a "hole" in the center of the configuration. This is a consequence of the regularity conditions at the origin.

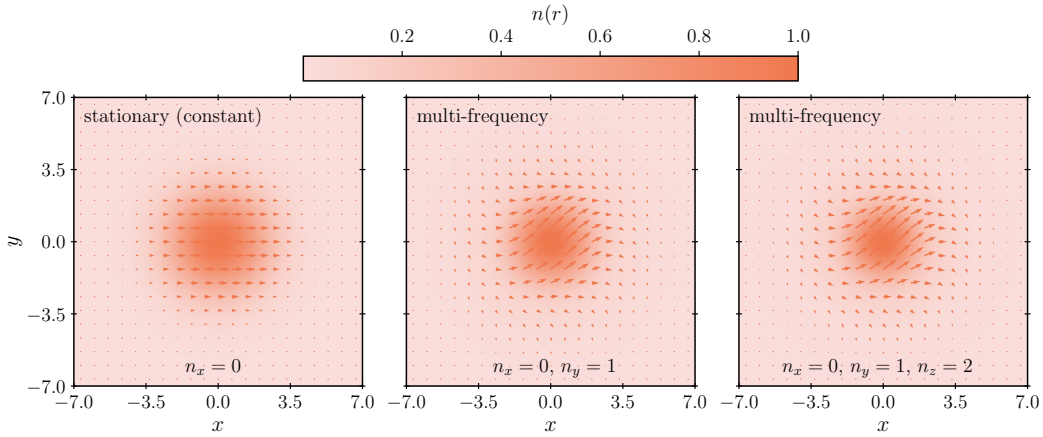

Figure 2.6: **Stationary and multi-frequency Proca stars:** Similar as in Figs. 2.4 and 2.5, but comparing a stationary Proca star with multi-frequency ones. *Left panel:* $(\sigma_{x0}, \sigma_{y0}, \sigma_{z0}) = (1, 0, 0)$ and $(n_x, n_y, n_z) = (0, 0, 0)$. *Center panel:* $(\sigma_{x0}, \sigma_{y0}, \sigma_{z0}) = (1, 1, 0)$ and $(n_x, n_y, n_z) = (0, 1, 0)$. *Right panel:* $(\sigma_{x0}, \sigma_{y0}, \sigma_{z0}) = (1, 1, 1)$ and $(n_x, n_y, n_z) = (0, 1, 2)$. Although the stationary constantly polarized and multi-frequency solutions are spherically symmetric according to the representation $\vec{\psi}(t, \vec{x}) \mapsto \vec{\psi}(t, R^{-1}\vec{x})$ of the $SO(3)$ group, this symmetry is not manifest given the pattern formed by the vector field.

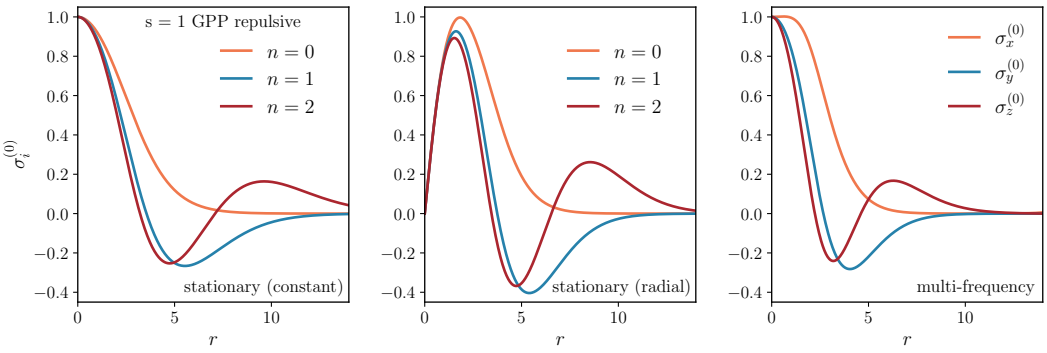

Figure 2.7: **Radial profiles of some representative stationary and multi-frequency configurations:** Radial profiles $\sigma_i^{(0)}(r)$ of some configurations reported in Figs. 2.4, 2.5 and 2.6. *Left panel:* The profiles $\sigma^{(0)}(r)$ of the three linear/circular configurations of Figure 2.4. *Center panel:* The profiles $\sigma^{(0)}(r)$ of the three radial configurations of Figure 2.5. *Right panel:* The profile $\sigma_x^{(0)}(r)$, $\sigma_y^{(0)}(r)$, and $\sigma_z^{(0)}(r)$ of the multi-frequency configuration in the right panel of Figure 2.6.

dimensionless quantities:[21]

$$t := \frac{4\pi G m_0^3}{\lambda_*} t^{phys}, \qquad \vec{x} := \frac{\sqrt{8\pi G} m_0^2}{\lambda_*^{1/2}} \vec{x}^{phys}, \tag{2.86a}$$

$$\mathcal{U} := \frac{\lambda_*}{4\pi G m_0^2} \mathcal{U}^{phys}, \qquad \vec{\psi} := \frac{\lambda_*}{\sqrt{8\pi G} m_0^{5/2}} \vec{\psi}^{phys}, \tag{2.86b}$$

$$\lambda_n := \frac{\lambda_n^{phys}}{\lambda_*}, \qquad \lambda_s := \frac{\lambda_s^{phys}}{\lambda_*}, \tag{2.86c}$$

where $\lambda_* > 0$ is a characteristic self-interaction scale that we can choose at our convenience. Note that the dimensions of E are the inverse of those of t.

In terms of the dimensionless variables, Eqs. (2.79) and (2.83) can be conveniently combined into a single system of the form

$$\Delta_s \sigma_i^{(0)} = \left(\frac{2\gamma}{r^2} \pm \sum_j \sigma_j^{(0)2} - u_i^{(0)} \right) \sigma_i^{(0)}, \tag{2.87a}$$

$$\Delta_s u_i^{(0)} = -\sum_j \sigma_j^{(0)2}, \tag{2.87b}$$

where Latin indices and summations range from 1 to 3 for multi-frequency states and are omitted for stationary states. Here, $\gamma = 0$ for multi-frequency states and stationary states with constant polarization, whereas $\gamma = 1$ for radially polarized stationary states. To simplify the numerical implementation, we have also introduced $u_i^{(0)}(r) := E_i - \mathcal{U}(r)$ as the difference between the frequencies E_i and the gravitational potential $\mathcal{U}(r)$. (Although the $u_i^{(0)}$ differ only by a constant number, for multi-frequency states we still find it convenient to solve the three Poisson equations for the shooting algorithm described below.) In addition, we have fixed the characteristic self-interaction scale of Eqs. (2.86) to $\lambda_* = |\lambda_n^{phys} + \alpha \lambda_s^{phys}|$,[22] where α was defined in Section 2.3.4. The $\pm$ signs in Eq. (2.87a) make reference to the "repulsive", $\lambda_n^{phys} + \alpha \lambda_s^{phys} > 0$, and the "attractive", $\lambda_n^{phys} + \alpha \lambda_s^{phys} < 0$, cases, respectively. These equations must be complemented with the following boundary conditions at $r = 0$; c.f. Eqs. (2.81) and (2.84):

$$\sigma_i^{(0)}(r=0) = (1-\gamma)\sigma_{i0}, \quad \sigma^{(0)\prime}(r=0) = \gamma \sigma_{i0}, \tag{2.88a}$$

$$u_i^{(0)}(r=0) = u_{i0}, \qquad u_i^{(0)\prime}(r=0) = 0. \tag{2.88b}$$

To find the appropriate values of σ_{i0} and u_{i0}, we use a methodology similar to the one described in the previous chapter (based on Ref. [87]), where, given σ_{i0}, the possible values for u_{i0} are fine-tuned using a numerical shooting method based on the conditions $\lim_{r\to\infty} \sigma_i^{(0)}(r) = 0$, which are required for the

[21] In this section, t, $\vec{x}$, $\mathcal{U}$, ... denote dimensionless variables. Whenever needed, we will label dimensionfull quantities by the superscript *phys*.

[22] In absence of self-interactions, when the polarization vector is linear or radial and $\lambda_n^{phys} = 0$, or when it is circular and $\lambda_n^{phys} = -\lambda_s^{phys}$, the second term on the right-hand side of Eqs. (2.79a) and (2.83a) vanishes. In these cases, the second term on the right-hand-side of Eq. (2.87a) should be discarded and the scale λ_* is arbitrary.

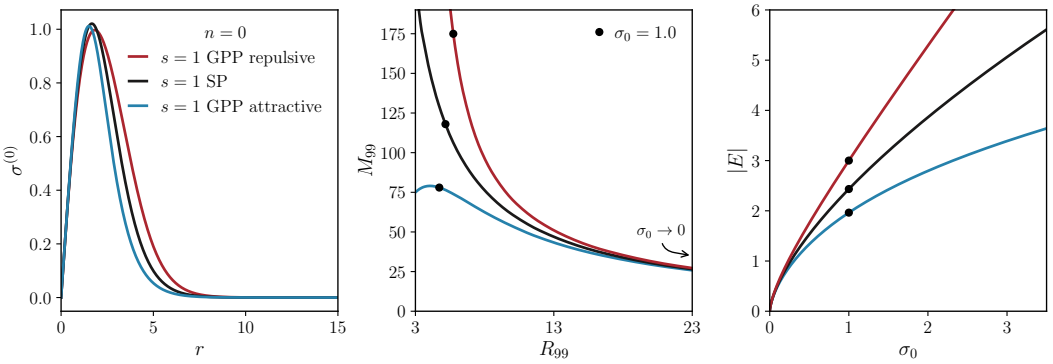

Figure 2.8: **Radially polarized Proca stars with no nodes:** Stationary and spherically symmetric solutions of the $s = 1$ Gross-Pitaevskii-Poisson system with no nodes ($n = 0$) and radial polarization. Red (blue) lines correspond to the repulsive (attractive) case, and we have included the solutions to the $s = 1$ Schrödinger-Poisson system (black lines) for reference. *Left panel:* The profile of $\sigma^{(0)}(r)$ for $\sigma_0 = 1$. *Center panel:* The effective mass of the configurations M_{99} as a function of the effective radius R_{99}. *Right panel:* The magnitude of the energy eigenvalue $|E|$ as a function of the central amplitude σ_0. The dots in the last two panels correspond to the configurations of unit amplitude. For $\sigma_0 \to 0$ the effects of the self-interactions become negligible and we recover non-self-interacting radially polarized Proca star configurations, which are equivalent to $\ell = 1$ boson star.

solutions to have finite total energy. This results in a discrete family of solutions $\sigma_i^{(0)}(\sigma_{i0}, n_i; r)$, where $n_i = 0, 1, 2, \ldots$ label the number of nodes of the functions $\sigma_i^{(0)}(r)$ in the interval $0 < r < \infty$. For the numerical integration, we use an adaptive explicit 5(4)-order Runge-Kutta routine [106, 107, 108], which requires rewriting the equations as a first-order system for the fields $(\sigma_i^{(0)}, u_i^{(0)})$, and for the shooting method we employ a technique based on bisection.

In Figs. 2.4 and 2.5 we plot some representative solutions of the stationary and spherically symmetric $s = 1$ Gross-Pitaevskii-Poisson system for $\sigma_0 = 1$, $n = 0$, 1 and 2, and different polarizations $\hat{\epsilon}$ at time $t = 0$. In addition, Figure 2.6 presents a comparison between the constantly polarized stationary configuration defined by the parameters $\sigma_0 = 1$ and $n = 0$, and two prototypical multi-frequency states, where for concreteness we have chosen $(\sigma_{x0}, \sigma_{y0}, \sigma_{z0}) = (1, 1, 0)$, $(n_x, n_y, n_z) = (0, 1, 0)$, and $(\sigma_{x0}, \sigma_{y0}, \sigma_{z0}) = (1, 1, 1)$, $(n_x, n_y, n_z) = (0, 1, 2)$, all of them evaluated at $t = 0$. For completeness, in Figure 2.7, we include the radial profiles $\sigma_i^{(0)}(r)$ associated with some of these configurations. It is important to stress that in all these figures we have focused on the repulsive case.

Mass and Radius

The mass of a Proca star can be computed as the product of m_0 with the particle number defined in Eq. (2.41), which yields $M^{phys} = m_0 N^{phys}$. Here $N^{phys} = [1/(\sqrt{8\pi G\lambda_*} m_0)]N$, where N represents the number of particles in

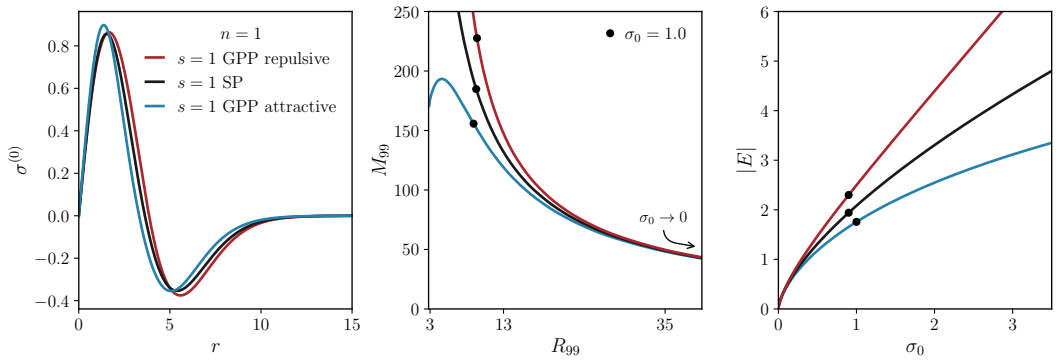

Figure 2.9: **Radially polarized Proca stars with one node:** Same as in Figure 2.8 but for the stationary and spherically symmetric solutions of the $s = 1$ Gross-Pitaevskii-Poisson system with one node ($n = 1$).

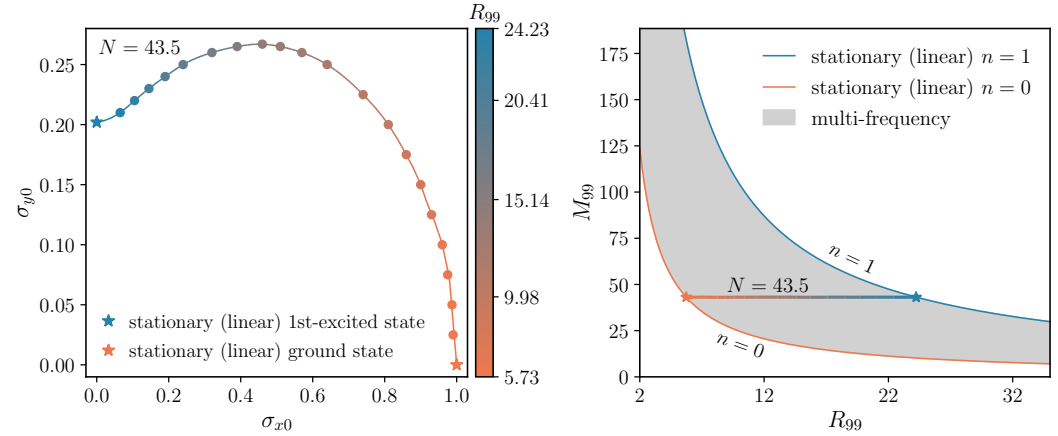

Figure 2.10: **Phase diagrams for multi-frequency states:** Multi-frequency Proca stars with amplitude $(\sigma_{x0}, \sigma_{y0}, 0)$ and node numbers $(n_x, n_y, n_z) = (0, 1, 0)$ in the free theory ($\lambda_n = \lambda_s = 0$). *Left panel:* The central amplitudes σ_{x0} and σ_{y0} that are consistent with $N = 43.5$ number of particles. *Right panel:* The M_{99} vs. R_{99} plot. Contrary to stationary states (described by the border lines), multi-frequency states correspond to a region instead of a curve.

the dimensionless variables of Eq. (2.86), and is given by

$$N = 4\pi \sum_i \int_0^\infty \sigma_i^{(0)2} r^2 dr. \tag{2.89}$$

To simplify the presentation, we have chosen the same conventions as those defined just below Eqs. (2.87).

Formally, the size of a Proca star extends to infinity, and for that reason it is usual to define an effective radius R_{99} as the one containing 99% of the total mass of the configuration, M_{99}, which in physical units is given by $R_{99}^{phys} = [\sqrt{\lambda_*}/(\sqrt{8\pi G} m_0^2)] R_{99}$.

First, we concentrate on stationary solutions. In Figs. 2.8 and 2.9, we show the profile $\sigma^{(0)}(r)$ for $\sigma_0 = 1.0$, the M_{99} vs. R_{99} plot, and the behavior of the energy eigenvalue E as a function of the central amplitude σ_0, for radially polarized Proca stars of zero and one nodes, respectively, in the attractive, repulsive, and free theories. The corresponding figures for linearly and circularly polarized Proca stars, which coincides with those of non-relativistic boson stars, can be found in Figs. 1 and 2 of Ref. [49]. In the limit $\sigma_0 \to 0$, the attractive and repulsive branches of the radially polarized Proca stars converge to those of the free theory (see the central and right panels of Figs. 2.8 and 2.9). This occurs because, at low densities, short range self-interactions (which are cubic in the fields) become negligible and the Gross-Pitaevskii equation approaches the Schrödinger one. The same property has been observed for self-interacting boson stars in Ref. [49] and thus it also holds for linearly and circularly polarized Proca stars, and for all constant polarization states when $\lambda_s = 0$. In all cases, the numerical data suggests that the mass of a stationary Proca star increases without bound as the radius of the object decreases, except when an attractive self-interaction is present. In this situation, the objects reach a state whose mass cannot be exceeded.

For multi-frequency states, the situation becomes more involved, as the configurations are labeled by the three independent amplitudes $(\sigma_{x0}, \sigma_{y0}, \sigma_{z0})$, in addition to the corresponding number of nodes (n_x, n_y, n_z). As a result, we anticipate that each curve in the M_{99} vs. R_{99} plot belonging to stationary states of fixed n transforms into a region when considering multi-frequency states of fixed (n_x, n_y, n_z).

To analyze this, we focus on the free theory ($\lambda_n = \lambda_s = 0$) for simplicity. In this case, the $s = 1$ Gross-Pitaevskii-Poisson system is invariant under the scaling transformation

$$t \mapsto \lambda_*^{-1} t, \quad \vec{x} \mapsto \lambda_*^{-1/2} \vec{x}, \quad \mathcal{U} \mapsto \lambda_* \mathcal{U}, \quad \vec{\psi} \mapsto \lambda_* \vec{\psi}, \tag{2.90}$$

where λ_* is an arbitrary nonvanishing constant. This invariance is associated with the arbitrary choice of the scale λ_* in Eqs. (2.86), which does not affect the eigenvalue problem (2.87) when both λ_n and λ_s vanish. This simplifies the analysis of the free theory, since, for any node numbers (n_x, n_y, n_z), configurations $(\sigma_{x0}, \sigma_{y0}, \sigma_{z0})$ that maintain the same ratio between the different σ_{i0} are related to each other by a rescaling transformation.

In particular, we concentrate on the case where $(n_x, n_y, n_z) = (0, 1, 0)$, which describes multi-frequency states with two components, $(\sigma_{x0}, \sigma_{y0}, 0)$. In

the left panel of Figure 2.10, we show the family of states corresponding to a fixed particle number $N = 43.5$, i.e. $M_{99} = 43.1$, leading to configurations with sizes between $5.7 \leq R_{99} \leq 24.2$. Here, the number $N = 43.5$ is the one obtained from the configuration with parameters $\sigma_{x0} = 1$ and $\sigma_{y0} = 0$, which represents a stationary state of linear polarization. As we just mentioned, this family can be rescaled to any value of N using the transformation (2.90), where every element in the family transforms according to $M_{99} \sim 1/R_{99}$. We show the M_{99} vs. R_{99} plot for multi-frequency states of $(n_x, n_y, n_z) = (0, 1, 0)$ in the right panel of Figure 2.10. Note that the left border line of this diagram corresponds to the M_{99} vs. R_{99} plot of the $n = 0$ stationary states of linear polarization, whereas the right border to the their first excited states $n = 1$ (these border lines correspond to the black curves in the central panels of Figs. 1 and 2 in Ref. [49]). As we anticipated, multi-frequency states fill whole regions in the M_{99} vs. R_{99} diagram.

Angular Momentum

All states constructed in this thesis are spherically symmetric, which inherently results in configurations of vanishing angular momentum, $\vec{L}^{phys} = 0$. This can be directly verified by substituting Eqs. (2.78a) and (2.78b) into the general expression for the orbital angular momentum. One can show that linearly, circularly, and radially polarized Proca stars possess no orbital angular momentum, $\vec{L} = -i \int [\vec{x} \times (\vec{\psi}^* \cdot \nabla \vec{\psi})] dV = 0$.

Note: If we decompose the vector field in terms of spherical harmonics as

$$\psi(t, \vec{x}) = \sum_{m=-l}^{l} Y^{1,m}(\theta, \varphi) \sigma^{(0)}(r) \tag{2.91}$$

and we concentrate on the the x-component, we can write L^x as

$$\begin{aligned} L^x = i \int \left(z \psi_m^* \partial_y \psi^m - y \psi_m^* \partial_z \psi^m \right) d^3x = i \frac{4\pi}{3} \\ \times \Bigg\{ \int \sigma^{(0)}(r) \left[z \partial_y \sigma^{(0)}(r) - y \partial_z \sigma^{(0)}(r) \right] \sum_{m=-\ell}^{\ell} Y^{1,m}(\theta, \varphi)^* Y^{1,m}(\theta, \varphi) d^3x \\ + \int z {\sigma^{(0)}}^2(r) \sum_{m=-\ell}^{\ell} Y^{1,m}(\theta, \varphi)^* \partial_y Y^{1,m}(\theta, \varphi) d^3x \\ - \int y {\sigma^{(0)}}^2(r) \sum_{m=-\ell}^{\ell} Y^{1,m}(\theta, \varphi)^* \partial_z Y^{1,m}(\theta, \varphi) d^3x \Bigg\} = 0, \end{aligned} \tag{2.92}$$

where we have made use of

$$z \partial_y \sigma^{(0)}(r) - y \partial_z \sigma^{(0)}(r) = 0, \tag{2.93}$$

and following a similar argument to that at the beginning of Appendix A

in Ref. [109]:

$$\sum_{m=-\ell}^{\ell} Y^{\ell,m}(\theta,\varphi)^* \partial_i Y^{\ell,m}(\theta,\varphi) = 0. \tag{2.94}$$

Identical arguments for L^y and L^z allows to write $\vec{L} = 0$.

On the other hand, whereas the spin angular momentum vanishes for multi-frequency states, for stationary states with circular polarization this is given by $\vec{\mathcal{S}}^{phys} = [M_{\rm Pl}/(\sqrt{8\pi\lambda_*}m_0)]\vec{\mathcal{S}}$, with[23]

$$\vec{\mathcal{S}} = -i\int(\vec{\psi}^* \times \vec{\psi})dV = \alpha N \hat{e}_z, \tag{2.95}$$

where we have used $\epsilon^{(\alpha)} \times \epsilon^{(\alpha)} = i\alpha\hat{e}_z$. And, for linear and radial polarization we have

$$\begin{aligned}\mathcal{S}^x &= -i\int\left(\psi_y^*\psi_z - \psi_z^*\psi_y\right)d^3x = -i\frac{4\pi}{3}\int_0^\infty \sigma^2(r)r^2dr \\ &\times\left(\int Y^{1,0}(\theta,\varphi)^*Y^{1,1}(\theta,\varphi)d\Omega - \int Y^{1,1}(\theta,\varphi)^*Y^{1,0}(\theta,\varphi)d\Omega\right) = 0.\end{aligned} \tag{2.96}$$

and similar for the S^y and S^z components. From a quantum perspective, the macroscopic spin angular momentum of circularly polarized Proca stars originates from the intrinsic microscopic spin of the individual particles that conform the configuration.

Global Charges

If the spin-spin self-interaction term vanishes, one can construct the charges associated with the accidental symmetry, which are also conserved in the time evolution. In physical units, Eq. (2.43) can be expressed in the form $\hat{Q}^{phys} = [1/(\sqrt{8\pi G\lambda_*}m_0)]\hat{Q}$, with

$$\hat{Q}_{ij} = 4\pi\int_0^\infty \sigma_i^{(0)*}\sigma_j^{(0)}r^2dr, \tag{2.97}$$

where $\sigma_i^{(0)}$ are the Cartesian components of $\vec{\sigma}^{(0)}(\vec{x})$.

Given that we do not distinguish between unitarily equivalent configurations, we can limit our study to states for which $\hat{Q}$ is diagonal, $\hat{Q} = \text{diag}\,(\hat{Q}_{xx}, \hat{Q}_{yy}, \hat{Q}_{zz})$. Specifically, stationary, linearly polarized Proca stars have $\hat{Q} = N\text{diag}(1,0,0)$, while stationary, radially polarized Proca stars have $\hat{Q} = \frac{N}{3}\text{diag}(1,1,1)$ (remember that in the symmetry-enhanced sector of the effective theory linearly and circularly polarized states are degenerated). In contrast, multi-frequency configurations allow the diagonal components of $\hat{Q}$ to be arbitrary, with the particle number given by $\text{Tr}(\hat{Q}) = N$.

As an illustration, we compute the global charges of the configurations that we have constructed in Figs. 2.4, 2.5, and 2.6. To do that, we assume

[23] In the absence of spin-spin self-interaction, general elliptic polarization states (2.47) have $\vec{\mathcal{S}} = N\sin(2\phi)\sin\gamma_1\hat{e}_z$.

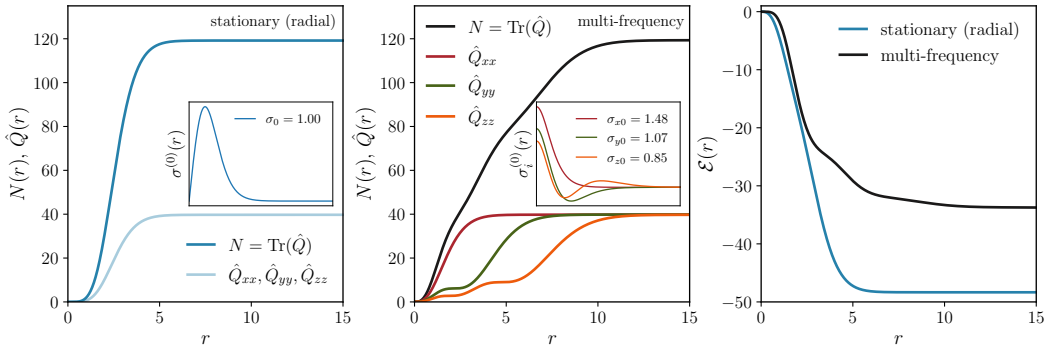

Figure 2.11: **Radial profiles of $\hat{Q}$, N, and $\mathcal{E}$:** *Left panel:* The radial profile of $\hat{Q}_{xx}$, $\hat{Q}_{yy}$, $\hat{Q}_{zz}$, and $N = \mathrm{Tr}\,\hat{Q}$ for a stationary radially polarized Proca star of $\hat{Q}_{xx} = \hat{Q}_{yy} = \hat{Q}_{zz} = 40$ and $N = 120$. *Center panel:* Same as in the left panel but for a multi-frequency state with the same values of $\hat{Q}_{xx}$, $\hat{Q}_{yy}$, $\hat{Q}_{zz}$ and N. In both panels, the insets correspond to the radial profiles of the components of $\vec{\sigma}^{(0)}(\vec{x})$ (remember that for a Proca star of radial polarization $\sigma_x^{(0)} = \sigma^{(0)}(r)\sin\vartheta\cos\varphi$, $\sigma_y^{(0)} = \sigma^{(0)}(r)\sin\vartheta\sin\varphi$, and $\sigma_z^{(0)} = \sigma^{(0)}(r)\cos\vartheta$). *Right panel:* The radial profile of $\mathcal{E}$ for both configurations. Note that the radial Proca star has a lower energy than the multi-frequency configuration. In all cases we have assumed $\lambda_n = \lambda_s = 0$. Given the rescaling symmetry of the free theory we can extend these conclusions to arbitrary values of N.

$\lambda_s = 0$. In particular, for the constant polarization states of Figure 2.4 we obtain $\hat{Q} = \mathrm{diag}(85, 0, 0)$, $\hat{Q} = \mathrm{diag}(134, 0, 0)$, and $\hat{Q} = \mathrm{diag}(190, 0, 0)$, where we have rounded the numbers to the closest integer. The radially polarized states of Figure 2.5 yield $\hat{Q} = 59\,\mathrm{diag}(1, 1, 1)$, $\hat{Q} = 81\,\mathrm{diag}(1, 1, 1)$, and $\hat{Q} = 104\,\mathrm{diag}(1, 1, 1)$, whereas the stationary and multi-frequency states of Figure 2.6 have $\hat{Q} = \mathrm{diag}(80, 0, 0)$, $\hat{Q} = \mathrm{diag}(79, 18, 0)$, and $\hat{Q} = \mathrm{diag}(79, 18, 7)$.

In the first two panels of Figure 2.11 we present, for the free theory ($\lambda_n = \lambda_s = 0$), the profiles $\hat{Q}_{ij}(r) = 4\pi \int_0^r \sigma_i^{(0)*}\sigma_j^{(0)} r'^2 dr'$ for two configurations of charge $\hat{Q} = \mathrm{diag}(40, 40, 40)$, i.e. $N = 120$, although using the rescaling of Eq. (2.90) we can extend these results to an arbitrary N: a stationary radially polarized Proca star with $\sigma_0 = 1.0$ and $n = 0$, and a multi-frequency star with $(\sigma_{x0}, \sigma_{y0}, \sigma_{z0}) = (1.48, 1.07, 0.85)$ and $(n_x, n_y, n_z) = (0, 1, 2)$. Even though the charge is distributed differently in these objects (the multi-frequency Proca star being more extended than the radially polarized one), their total charges coincide. According to Eqs. (2.67) and (2.68), when $\lambda_n = \lambda_s = 0$, the total energy is $\mathcal{E}[\vec{\psi}] = -T[\vec{\psi}] = -\frac{1}{2}D[n, n]$, which shows that for fixed N, the more extended objects have smaller values of $D[n, n]$, resulting in higher energies. This suggests that, for fixed $\hat{Q}$ proportional to the identity matrix, $(n_x, n_y, n_z) = (0, 1, 2)$ multi-frequency Proca stars are more energetic than $n = 0$ radially polarized configurations. The plots in the right panel of Figure 2.11 and the findings in Section 2.3.5 confirm this expectation.

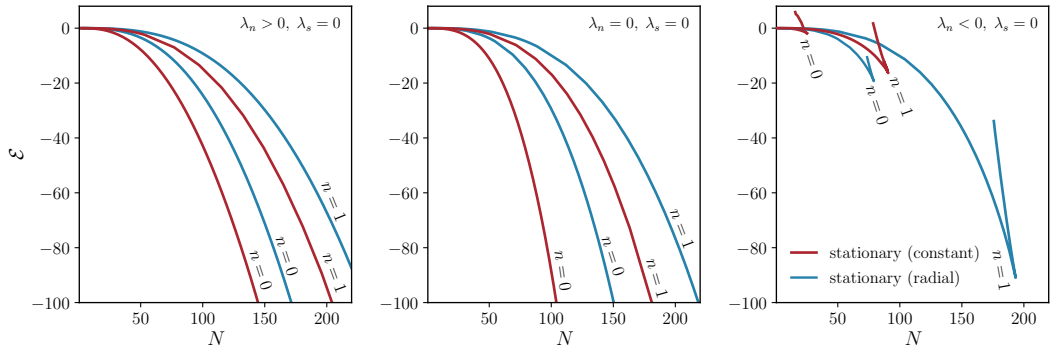

Figure 2.12: **Energy functional of stationary states (symmetry-enhanced sector):** The energy $\mathcal{E}$ of stationary Proca stars with $\lambda_s = 0$ as function of their particle number N and polarization vector $\hat{\epsilon}$. Constant polarization states are indicated by red lines and are degenerated when $\lambda_s = 0$, whereas states with radial polarization are indicated by blue lines. When the self-interaction is repulsive ($\lambda_n > 0$) or is absent ($\lambda_n = 0$) the ground state configuration is provided by nodeless Proca stars of constant polarization and negative energy, $\mathcal{E} < 0$, in agreement with the analytical results of Section 2.3.3. When the self-interaction is attractive ($\lambda_n < 0$) it is not possible to define a ground state configuration and the polarization of the lowest energy stationary state changes with N.

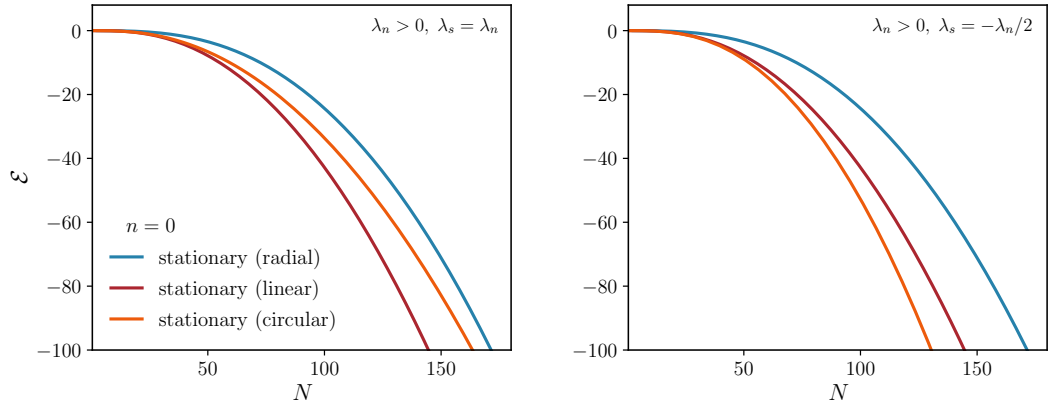

Figure 2.13: **Energy functional of stationary states (generic sector):** Similar as in Figure 2.12 but for the case in which $\lambda_s \neq 0$. The spin-spin self-interaction breaks the degeneracy of constant polarization states, which are only possible for linear (red lines) or circular (orange lines) cases. Radial polarization states are indicated in blue lines and represent excited configurations. The left panel belongs to the shaded region in the first quadrant of Figure 2.3, where $\lambda_0 > 0$, $\lambda_s > 0$, and a spherically symmetric ground state of linear polarization exists, while the right panel to the shaded triangle in the fourth quadrant of the same figure, where $\lambda_0 > 0$, $\lambda_s < 0$, and the polarization of the ground state is circular. For simplicity, we have only considered nodeless ($n = 0$) configurations. In this figure $\mathcal{E}^{phys} = [\sqrt{8\pi G} m_0^2 |\lambda_n^{phys}|^{-3/2}]\mathcal{E}$ and $N^{phys} = [1/(\sqrt{8\pi G} m_0 |\lambda_n^{phys}|^{1/2})]N$.

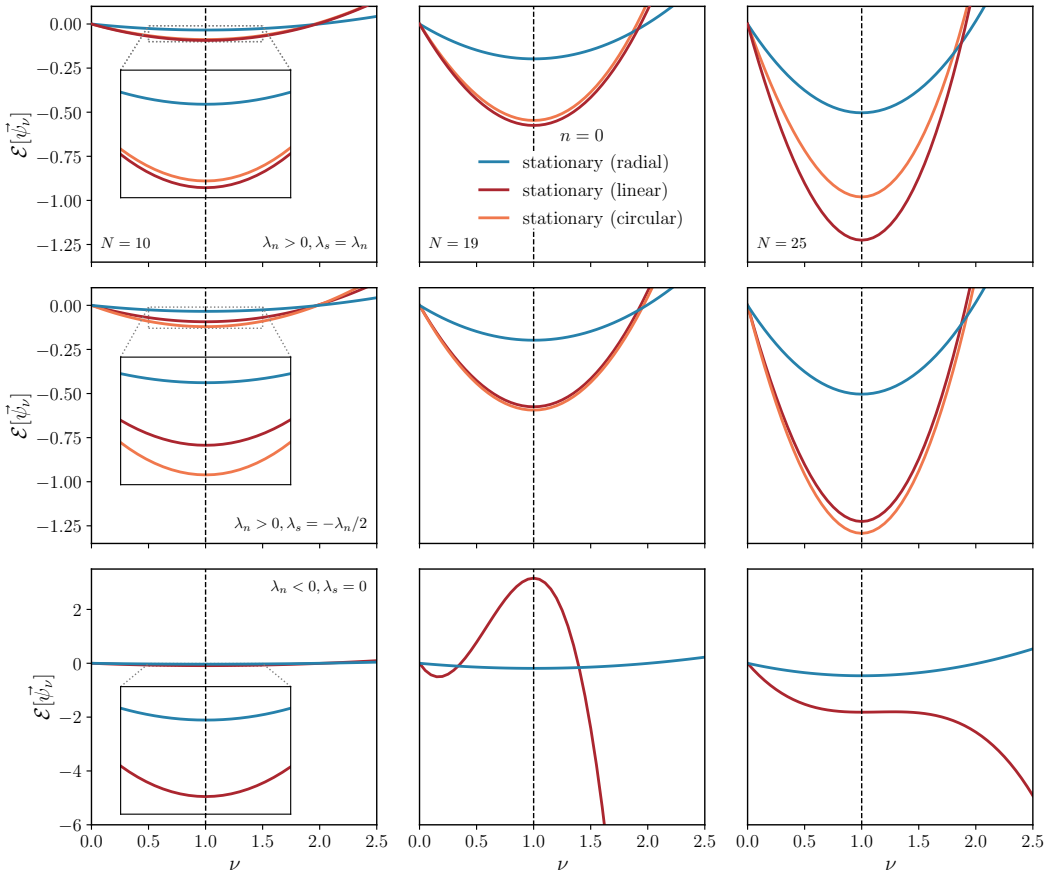

Figure 2.14: **Stationary states as critical points of the energy functional:** The energy functional $\mathcal{E}[\vec{\psi}_\nu]$ of the rescaled states $\vec{\psi}_\nu(\vec{x})$ associated to stationary configurations $\vec{\psi}_{\nu=1}(\vec{x})$ of particle number $N = 10$, 19 and 25 (see Eq. (2.63)). *First row:* For $\lambda_0 > 0$, $\lambda_s > 0$, there exists a global minimum of the energy functional provided by a stationary state of linear polarization and no nodes, where $\mathcal{E} < 0$. *Second row:* For $\lambda_0 > 0$, $\lambda_s < 0$, there is also a global minimum of the energy functional, in this case provided by a stationary state of circular polarization and no nodes, where $\mathcal{E} < 0$. *Third row:* For $\lambda_0 < 0$, $\lambda_s = 0$, stationary states of linear and circular polarization are degenerated and the energy functional is not bounded from below (this applies to the radial case as well, although the maximum of the energy functional appears for larger values of ν). In all cases, the energy functional has a critical point at $\nu = 1$, which is a global minimum if $\lambda_0 \geq 0$, and a local minimum, a saddle point or a maximum if $\lambda_0 < 0$, depending on the value of N. Here, $\mathcal{E}^{phys} = [\sqrt{8\pi G} m_0^2 |\lambda_n^{phys}|^{-3/2}]\mathcal{E}$ and $N^{phys} = [1/(\sqrt{8\pi G} m_0 |\lambda_n^{phys}|^{1/2})]N$.

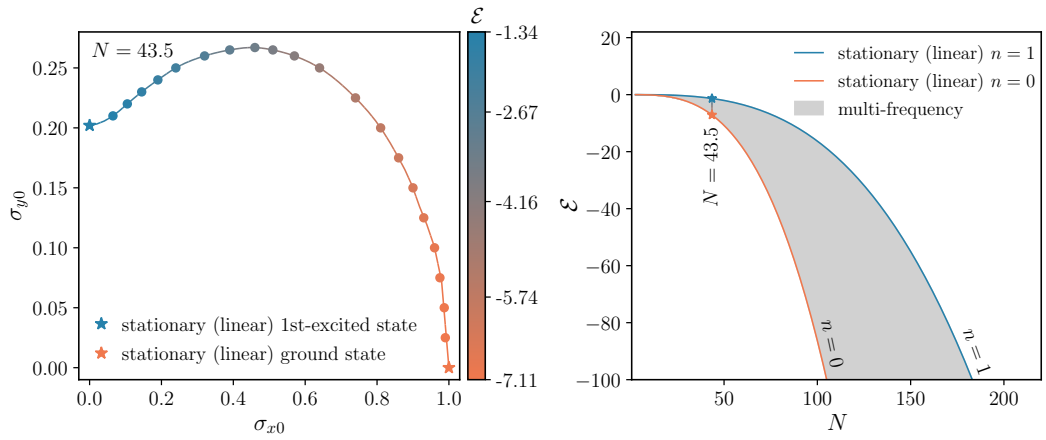

Figure 2.15: **The energy spectrum of multi-frequency states:** The energy of the same multi-frequency Proca stars as in Figure 2.10. The lowest energy state is obtained for $\sigma_{x0} = 1$ and $\sigma_{y0} = 0$ (orange star), while the highest energy state is for $\sigma_{x0} = 0$ and $\sigma_{y0} \approx 0.2$ (blue star). Both configurations correspond to a stationary, linearly polarized state of constant polarization. Multi-frequency states are represented by circle markers, with their energy values indicated by color. In addition to the discrete set of stationary states shown in the center panel of Figure 2.12, there exists a continuum of multi-frequency solutions that connect the ground state with the first excited state.

Energy Functional

The energy functional plays a central role to determine the equilibrium configurations and deserves an independent discussion. Using Eq. (2.68), the total energy of a Proca star is given by $\mathcal{E}^{phys} = [\sqrt{8\pi G m_0^2}/\sqrt{\lambda_*^3}]\mathcal{E}$, with

$$\mathcal{E} = -4\pi \sum_i \int_0^\infty \left[\frac{1}{2}\left(\sigma_i^{(0)\prime 2} + \frac{2\gamma \sigma_i^{(0)2}}{r^2} \right) \pm \frac{1}{2}\sigma_i^{(0)4} \right] r^2 dr, \tag{2.98}$$

where we have use the relation $\varepsilon[\vec{\psi}] = -T[\vec{\psi}] - 2\lambda_n F_n[\vec{\psi}] - 2\lambda_s F_s[\vec{\psi}]$, the fact that in spherical coordinates we can write $|\nabla\vec{\psi}|^2 = \sigma'^2 + 2\sigma'\sigma^{(0)}/r + \sigma^{(0)2}/r^2$, the definition $\lambda_* = |\lambda_n^{phys} + \alpha^2 \lambda_s^{phys}|$ and we have discarded the boundary terms.

As before, we first focus on stationary states. For $\lambda_s = 0$, Figure 2.12 shows the energy $\mathcal{E}$ of Proca stars as function of their particle number N and polarization vector $\hat{\epsilon}$. In absence of spin-spin self-interactions, constant polarization states are degenerated, and this is the reason why for fixed N all constantly polarized Proca stars possess the same total energy. Furthermore, if $\lambda_n \geq 0$, the ground state configuration (i.e. the lowest possible energy state that exists for a given particle number) is given by nodeless ($n = 0$), spherically symmetric constant polarization states, irrespectively of the value of N, as anticipated at the beginning of Section 2.3.3. Similarly, when N and n are fixed, radially polarized configurations have more energy than constant polarization states, signaling that radially polarized Proca stars represent excited states of the $s = 1$ Gross-Pitaevskii-Poisson system with $\lambda_n \geq 0$ and $\lambda_s = 0$. On the other hand, when the self-interaction is attractive ($\lambda_n < 0$), the energy is unbounded from below (see Section 2.3.3) and one cannot define a ground

state configuration. Nevertheless, it is interesting to note from the right panel of Figure 2.12 that for some values of N, radial polarization states possess less energy than constant polarization states whose energy can even become positive. Note that these curves exhibit a spike-like behavior, signaling an extremal point in the energy functional $\mathcal{E}$ as well as the particle number N. This feature signals the appearance of a zero mode, which is indicative of a transition in the system's stability. A more detailed discussion of this will be presented in Ref. [2]. Finally, as we argued in Section 2.3.5, when $N \to 0$ (i.e. $\sigma_0 \to 0$), the effect of the self-interaction is negligible and we recover the same results as in the free theory, no matter the value of λ_n (see the behavior of the four curves in each panel of Figure 2.12 close to the origin).

When $\lambda_s \neq 0$, the situation is more involved given that the characteristic self-interaction scale $\lambda_* = \lambda_n^{phys} + \alpha\lambda_s^{phys}$ that we have used to normalize physical quantities depends on the state of the system ($\alpha = 0$ if the polarization is linear or radial, and $\alpha = 1$ if it is circular). To proceed, we will focus on two cases: $\lambda_n > 0$, $\lambda_s = \lambda_n$, and $\lambda_n > 0$, $\lambda_s = -\frac{1}{2}\lambda_n$, both of which lie within the region shown in Figure 2.3 where the energy functional is bounded from below and a ground state exists. As is evident from Figure 2.13, the spin-spin self-interaction term breaks the degeneration between the constant polarization states that is present when $\lambda_s = 0$. This becomes more pronounced as N increases and the effects of the self-interaction grow in significance. In particular, as we anticipated in Section 2.3.3 (see Eq. (2.66)), when $\lambda_0 > 0$, $\lambda_s > 0$, the ground state configuration is given by a stationary state of linear polarization, whereas when $\lambda_0 > 0$, $\lambda_s < 0$, the polarization of the lowest energy state is circular. Moreover, in both cases radially polarized Proca stars represent excited configurations.

We further illustrate this in Figure 2.14, where we study the behavior of the energy functional under variations of the vector $\vec{\psi}$ which are consistent with the rescaling of Eq. (2.63). As we demonstrated in Section 2.3.3, when $\lambda_0 \geq 0$, the energy functional is bounded from below. Furthermore, if $\lambda_s > 0$, there exists a global minimum of the energy functional that is provided by a stationary and spherically symmetric state of linear polarization (first row of Figure 2.14), whereas if $\lambda_s < 0$ the polarization of the state that minimizes the energy is circular (second row). This suggests the existence of Proca stars that are stable under small perturbations. On the contrary, if $\lambda_0 < 0$, the energy functional is not bounded from below, as can be appreciated in the third row of Figure 2.14. Furthermore, for large N, the critical points turn into maxima, signaling the onset of an instability.

To study the multi-frequency solutions, we again concentrate on the free theory ($\lambda_n = \lambda_s = 0$). In Figure 2.15, we show the same family of multi-frequency states $N = 43.5$ that we introduced in Figure 2.10. Interestingly, this family connects the linearly polarized stationary ground state (in the x direction) with the first excited linearly polarized stationary state (in the y direction). Also shown in Figure 2.15 through the color bar is the energy of each state in this family. As can be appreciated, the configuration with $\sigma_{x0} = 1$ and $\sigma_{y0} = 0$ has the lowest energy, as expected, whereas the energy is growing monotonously when moving along the family towards the state with $\sigma_{x0} = 0$ and $\sigma_{y0} \approx 0.2$. Finally, the right panel of this figure has been constructed

from the family $N = 43.5$ using the rescaling (2.90), which implies that, when $\lambda_n = \lambda_s = 0$, the energy $\mathcal{E}$ and the particle number N are related through $\mathcal{E} \sim N^3$. As we previously identified in Figure 2.10 for the M_{99} vs. R_{99} plot, multi-frequency states with $(n_x, n_y, n_z) = (0, 1, 0)$ fill a region in the $\mathcal{E}$ vs. N diagram, which are delimited by the curves associated with the $n = 0$ and $n = 1$ stationary states of linear polarization (see the center panel of Figure 2.12).

In the right panel of Figure 2.11, we compare the energy profile of a stationary nodeless state of radial polarization and charge $\hat{Q} = \mathrm{diag}(40, 40, 40)$, with the one of the multi-frequency solution of the same charge and $(n_x, n_y, n_z) = (0, 1, 2)$, when $\lambda_n = \lambda_s = 0$. Again, this plot can be rescaled to any value of N. As was anticipated in Section 2.3.5, for fixed $\hat{Q}$, multi-frequency solutions are more energetic than $n = 0$ radially polarized states.

2.3.6 Linear Stability

In this section, we will present the general aspects and directions for the study of the linear stability of non-relativistic Proca stars, in the same way we did in Section 1.3.4, of Chapter 1. A comprehensive study of the stability of non-relativistic Proca stars is given in the forthcoming research paper *Linear stability of non-relativistic Proca stars* Ref. [2]. In order to study the stability of the equilibrium configurations that we have described in the spherically symmetric case, we follow the procedure presented in Refs. [48, 49], and we consider the behavior of small deviations of $\vec{\psi}(t, \vec{x})$ from the ansatz (2.69), which we parametrize in the form

$$\vec{\psi}(t, \vec{x}) = e^{-i\hat{E}t} \left[\vec{\sigma}^{(0)}(\vec{x}) + \epsilon \vec{\sigma}(t, \vec{x}) + \mathcal{O}(\epsilon^2) \right]. \tag{2.99}$$

Here, $(\hat{E}, \vec{\sigma}^{(0)})$ is a solution of Eq. (2.70) and $\vec{\sigma}$ is a complex vector-valued function depending on $(t, \vec{x})$ that describes the perturbation to first order in the small parameter ϵ. Recall that $\hat{E}$ is Hermitian, and further it is proportional to the identity when $\lambda_s \neq 0$. Equation (2.99) is completely analogous to the ansatz (1.61) now with $\sigma^{(0)}$ and $\sigma(t, \vec{x})$ replaced by the vector functions $\vec{\sigma}^{(0)}$, $\vec{\sigma}(t, \vec{x})$, and E replaced by a Hermitian matrix $\hat{E}$.

Substituting the expansion (2.99) into Eq. (2.27) and considering the first order terms in ϵ we obtain the following evolution equation for $\vec{\sigma}$:

$$\begin{aligned} i\frac{\partial \vec{\sigma}}{\partial t} &= \left[\hat{\mathcal{H}}^{(0)} - \hat{E} \right] \vec{\sigma} \\ &\quad + \hat{K} \left[\mathrm{Re} \left(\vec{\sigma}^{(0)*} \cdot \vec{\sigma} \right) \right] \vec{\sigma}^{(0)} + i\frac{\lambda_s}{m_0^2} \mathrm{Im} \left(\vec{\sigma}^{(0)*} \times \vec{\sigma} \right) \times \vec{\sigma}^{(0)}, \end{aligned} \tag{2.100}$$

with the linear (formally self-adjoint) operators $\hat{\mathcal{H}}^{(0)} := \hat{\mathcal{H}}[\vec{\sigma}^{(0)}]$ and

$$\hat{K} := \frac{\lambda_n}{m_0^2} + 8\pi G m_0^2 \Delta^{-1}. \tag{2.101}$$

Again, as shown in [110], one can separate the time and space parts of $\vec{\sigma}$ by means of the following mode ansatz:

$$\vec{\sigma}(t, \vec{x}) = \left[\vec{\mathcal{A}}(\vec{x}) + \vec{\mathcal{B}}(\vec{x}) \right] e^{\lambda t} + \left[\vec{\mathcal{A}}(\vec{x}) - \vec{\mathcal{B}}(\vec{x}) \right]^* e^{\lambda^* t}. \tag{2.102}$$

Here $\vec{\mathcal{A}}$ and $\vec{\mathcal{B}}$ are complex vector-valued functions depending only on $\vec{x}$ and λ is a complex number. Substituting Eq. (2.102) into Eq. (2.100) and setting the coefficients in front of $e^{\lambda t}$ and $e^{\lambda^* t}$ to zero one obtains

$$
\begin{aligned}
i\lambda\vec{\mathcal{A}} &= \left[\hat{\mathcal{H}}^{(0)} - \hat{E}\right]\vec{\mathcal{B}} + i\frac{\lambda_s}{2m_0^2}\vec{s}_0 \times (\vec{\mathcal{A}} - \vec{\mathcal{B}}) \qquad (2.103a)\\
&+ \frac{i}{2}\left\{\hat{K}\left[\vec{\sigma}^{(0)*}\cdot(\vec{\mathcal{A}}+\vec{\mathcal{B}}) + \vec{\sigma}^{(0)}\cdot(\vec{\mathcal{A}}-\vec{\mathcal{B}})\right]\right\}\text{Im }\vec{\sigma}^{(0)}\\
&+ \frac{\lambda_s}{2m_0^2}\left[\vec{\sigma}^{(0)*}\times(\vec{\mathcal{A}}+\vec{\mathcal{B}}) - \vec{\sigma}^{(0)}\times(\vec{\mathcal{A}}-\vec{\mathcal{B}})\right]\times\text{Re }\vec{\sigma}^{(0)},\\
i\lambda\vec{\mathcal{B}} &= \left[\hat{\mathcal{H}}^{(0)} - \hat{E}\right]\vec{\mathcal{A}} - i\frac{\lambda_s}{2m_0^2}\vec{s}_0 \times (\vec{\mathcal{A}} - \vec{\mathcal{B}}) \qquad (2.103b)\\
&+ \frac{1}{2}\left\{\hat{K}\left[\vec{\sigma}^{(0)*}\cdot(\vec{\mathcal{A}}+\vec{\mathcal{B}}) + \vec{\sigma}^{(0)}\cdot(\vec{\mathcal{A}}-\vec{\mathcal{B}})\right]\right\}\text{Re }\vec{\sigma}^{(0)}\\
&+ i\frac{\lambda_s}{2m_0^2}\left[\vec{\sigma}^{(0)*}\times(\vec{\mathcal{A}}+\vec{\mathcal{B}}) - \vec{\sigma}^{(0)}\times(\vec{\mathcal{A}}-\vec{\mathcal{B}})\right]\times\text{Im }\vec{\sigma}^{(0)},
\end{aligned}
$$

where $\vec{s}_0 := -i\vec{\sigma}^{(0)*}\times\vec{\sigma}^{(0)}$ is the spin density associated with the background solution. It is important to stress that in order to obtain Eqs. (2.103) we have assumed that $\hat{E}$ is real-valued; hence, for multi-frequency states, these equations are only valid in the basis that diagonalizes the operator $\hat{E}$. Equations (2.103) constitute a linear eigenvalue problem for the constant λ, where a nonvanishing real and positive part of λ indicates the existence of a linear instability of lifetime $t_{\text{life}} \sim 1/\lambda_R$, with λ_R the real part of the eigenvalue λ.

Spherical and non-spherical perturbations

Equations (2.103) describe the evolution of a general linear perturbation around an arbitrary equilibrium configuration of the $s = 1$ Gross-Pitaevskii-Poisson system. Now, if we concentrate specifically on spherical equilibrium configurations, we can decouple the linearized equations (2.103) into a family of purely radial systems by expanding the perturbations in terms of (scalar or vector) spherical harmonics, similar to what we have made in equations (1.66) for non-relativistic boson stars. The result is that for stationary states of linear, circular and radial polarization, as well as for multi-frequency states, the linearized system can be cast into the following general schematic form:

$$
i\lambda\begin{pmatrix} X_{lm}\\ Y_{lm}\\ Z_{lm}\end{pmatrix} = \begin{pmatrix} M^{11}_{lm} & M^{12}_{lm} & M^{13}_{lm}\\ M^{21}_{lm} & M^{22}_{lm} & M^{23}_{lm}\\ M^{31}_{lm} & M^{32}_{lm} & M^{33}_{lm}\end{pmatrix}\begin{pmatrix} X_{lm}\\ Y_{lm}\\ Z_{lm}\end{pmatrix}, \qquad (2.104)
$$

where l refers to the total angular momentum number of the perturbation and m to the associated magnetic quantum number where l and m assumes the values $l = 0, 1, 2, \ldots$ and $m = -l, -(l-1), \ldots, l$. The particular realization of the variables X_{lm}, Y_{lm} and Z_{lm}, and the matrix M_{lm}, which is a function of the background equilibrium configuration, depend on the case of interest. Equation (2.104) conform the eigenvalue system of the form $\hat{L}\vec{X} = i\lambda\vec{X}$ similar to the system (1.67) with $L_{ij} = M_{ij}$ and $\vec{X} = (X_{lm}, Y_{lm}, Z_{lm})$. In *Linear stability of non-relativistic Proca stars* [2], we solve numerically the system (2.104), following a generalization of the methodology described in Section 1.3.4, for

stationary Proca stars with constant, linear, and circular polarization, as well as for multi-frequency Proca stars. We invite the reader to review the detailed analysis described therein.

Part II

Gravitational Production of Dark Matter

> The idea of quantum field theory is that quantum fields are the basic ingredients of the universe, and particles are just bundles of energy and momentum of the fields. In a relativistic theory the wave function is a functional of these fields, not a function of particle coordinates.
>
> *What is Quantum Field Theory, and What Did We Think It Is?*
> S. Weinberg

Chapter 3

Scalar Fields on Curved Spacetimes

3.1 Introduction

The prediction of the *Schwinger effect* is an example of the success of applying a *semiclassical* approximation to purely quantum phenomena. When considering an external classical electric field, if it is strong enough, the presence of a quantized *spectator* matter field leads to the *particle production* of electron-positron pairs from the vacuum. This effect was first predicted by Heisenberg and Euler in 1936 [111], based on the work of Sauter in 1931 [112] and fully understood in 1951 within the framework of quantum electrodynamics by Schwinger [113]. Heuristically, an external electric field interacts with a virtual pair of particles e^+e^-, accelerating electrons in one direction and positrons in the opposite direction. If the external field is strong enough to accelerate the particles to energies greater than their mass at distances smaller than or equal to the Compton wavelength of the particle, that is, $|E| > |E_{\text{crit}}| = m_e^2/e$, then the virtual particles can be "pushed out" of the vacuum and propagate as real particles.[1] The production rate of these particles is given by $\exp\{-\pi|E_{\text{crit}}|/|E|\}$. One of the most notable lessons that was left behind by the semiclassical treatment of the Schwinger effect is that, within the regime of validity in which it can be considered, it was able to yield a prediction that was subsequently confirmed exactly within the framework of a complete quantum theory, namely, the theory of quantum electrodynamics.

Similarly, in the absence of a fully satisfactory quantum theory of gravity that incorporates the gravitational interaction with the other fundamental forces of the standard model (the electromagnetic and the weak and strong nuclear forces), a semiclassical treatment of the effects that occur in a quantum field when it interacts with a dynamical spacetime allows us to shed light on the large-scale effects we expect from a complete quantum theory of gravity. In this semi-classical treatment, the quantum aspects of gravity are negligible at effective scales, allowing for a classical description of the dynamics of the gravitational field within Einstein's theory of gravity (analogously to the way

[1] If the electric field exerts a force $\mathcal{E}$ on the pair of particles e^+e^-, and they move a distance l apart from each other, then they will receive an amount of energy $le\mathcal{E}$ from the electric field. In the case where the energy exceeds the rest mass of the particle pair, that is, $le\mathcal{E} > 2m_e$, the virtual particle pair becomes real and the particles continue moving apart. For lengths on the order of the Compton wavelength $2\pi/m_e$, the probability of creating a pair e^+e^- is given by $\exp\{-m_e^2/e\mathcal{E}\}$.

we described the electromagnetic field in the Schwinger effect above). Meanwhile, the matter fields are treated fully quantum mechanically. When this approximation is applicable, it enables us to account for important quantum effects. The purpose of this and the following chapter is to describe the phenomena that arise in the quantum treatment of scalar and fermionic fields on curved spacetimes.

First, let's consider that the quantum effects of gravity become relevant when the length and time scales of a quantum process fall below the *Planck scales*. The Planck time t_{p} and length l_{p}, therefore, mark the boundary beyond which a complete treatment of a quantum theory of gravity is necessary. When the scales of time and distance far exceed the Planck scales (e.g. at cosmological scales), we can expect that the semiclassical treatment of gravity can be applied without problem. However, when considering the nonlinearity of Einstein's equations, ignoring a complete treatment of quantum gravity implies a more subtle analysis. Since all forms of matter and energy couple equally to gravity, it implies that the *graviton* itself is subject to gravitational effects, just like any other particle (or field), such as, say, an electron. Therefore, when gravitational effects are significant (e.g. at cosmological scales), it is not possible to ignore the effects that gravity exerts on gravitons. So, when dealing with cosmological gravitational effects (or strong gravitational field), we would not be able to satisfactorily apply a semiclassical approximation.

However, if we consider, according to a classical procedure in general relativity (see for example Ref. [114], Chapter 7), that we can describe the propagation of a gravitational wave in a curved background spacetime separately according to

$$g_{\mu\nu} = \delta g_{\mu\nu} + \bar{g}_{\mu\nu}, \tag{3.1}$$

where $\delta g_{\mu\nu}$ represents the wave (perturbation) and $\bar{g}_{\mu\nu}$ the background spacetime, it is possible to consider the wave as a null fluid like any other, and its contribution to Einstein's equations can be considered as part of the energy-momentum tensor $T_{\mu\nu}$ that acts as a source. In other words, we can consider the "*graviton*"[2] field as a linear perturbation over the background spacetime through $T_{\mu\nu}$.[3] At one-loop level, the quantization of the gravitational field in the background $\bar{g}_{\mu\nu}$ is equally as important as the quantization of the matters fields [116, 117].

In this context, in curved spacetimes it will be necessary to consider a renormalization process that yields a finite value for the vacuum energy of the matter fields. For this, the number of counterterms to consider is finite. However, regarding the graviton field, when perturbatively expanding the action with respect to $\delta g_{\mu\nu}$ about $\bar{g}_{\mu\nu}$, we find an infinite number of divergent terms at each order in the expansion, so it will be necessary to consider an in-

[2] "Upon quantization, Einstein's equation predicts spin-two particles called *gravitons*. We don't know how to carry out such quantization consistently, but the existence of gravitons is sufficiently robust that it is expected to be a feature of any well-defined scheme. Since gravity couples to energy-momentum, gravitons interact with every kind of particle, including other gravitons. This provides a way of thinking about nonlinearity of Einstein's theory." Ref. [114]

[3] Let's think about the photoemission by an atom that is immersed in a classical electric or magnetic background field. Although the background field is treated classically, it is possible to talk about the emission of quanta of this same field, namely, the photon [see Ref. [115]].

finite number of counterterms. This fact renders a quantum theory of gravity non-renormalizable. Higher-order terms in the expansion of the gravitational action in powers of $\delta g_{\mu\nu}$ produce Feynman diagrams of gravitons with multiple loops. However, a theory truncated to a certain number of loops could be considered renormalizable. At one loop, for free fields, this constitute the first order quantum correction to general relativity.[4] This is the scenario we will be considering in the present thesis work: a free scalar or fermionic quantum field only coupled to gravity in an dynamical universe.

As we will see in detail in the subsequent chapters, there exist nontrivial gravitational effects in quantum field modes for which the wavelength λ is comparable with some length scale of the background spacetime (e.g. H). One of these gravitational effects is the *cosmological gravitational production of particles* from the "vacuum state". Heuristically, a pair of virtual particles being pulled apart due to the expansion of the universe can become real particles. As the spacetime expands the recessional velocity of the pair, e.g. e^+e^-, increases with distance according with the Hubble law $v = Hd$. At distance equal to m^{-1}, the velocity would be H/m. When $H \geq H_{\rm crit} \sim m$ the particles will obtain relativistic velocities within a Compton length and particles creation is possible. This is analogous to the Schwinger effect, and one might expect particle production proportional to $\exp\{-\pi H_{\rm crit}/H\}$. If there is a definitive quantum theory of gravity, the gravitational production of particles due to the expansion of the universe should be a prediction within the previously mentioned regimes.

In the semiclassical approximation to gravity at one-loop, the Einstein equations are given according to

$$\bar{G}_{\mu\nu} = 8\pi G \langle T_{\mu\nu} \rangle \tag{3.2}$$

where the gravitational field $\bar{g}_{\mu\nu}$ remains classical and the matter fields are quantum fields. Here, the important quantity to consider is the expectation value of the energy-momentum (it is a more useful probe of the physical situation than a particle count through the particle operator) and how this evolves when the spacetime is dynamical. As we have already mentioned, it is necessary to consider an appropriate renormalization process that yields a finite value for $\langle T_{\mu\nu} \rangle$ by subtraction of a finite number of physical quantities (e.g. Pauli-Villars renormalization). What are the different interpretation, in the framework of semiclassical gravity, of the renormalized value of $\langle T_{\mu\nu} \rangle$? This is an important question that play an important role in the cosmological context. We often study cosmological phenomena in terms of particles, despite assuming that the nature is described in terms of quantum fields and also, in a cosmological context, we typically ignore the quantum nature of the fields and treat them as classical fields (see, for example Ref. [118]). Dark matter models consist of non-relativistic particles, or dark energy models consist of the dynamics of classical fields. However, we effectively assume that the right-hand side of Einstein's equations, Eq. (3.2), is the expectation value of quantum

[4]Even considering mutually-interacting (or sefl-interacting) matter fields, there exist a large regime in which the one-loop level quantum gravity is still a valid approximation whereas the condition $l^{-2}G \ll 1$ is satisfied with l a typical length scale of the system under consideration.

fields. In this thesis work, we explore the limits within which a quantum field can be approximated, either by an ensemble of particles or by a classical field. This is one of the important issues to be resolved in the present thesis work focused on scalar and fermionic quantum fields on curved spacetimes. In the following chapters, we will make an effort to describe the regimes of classicality or "particle production formalism," that $\langle T_{\mu\nu} \rangle$ admits within the context of gravitational particle production. Here, will assume that the *spectator* quantum field does not have back-reaction on the dynamical geometry of spacetime (that is, the particle production is a small effect at early times). However, it is possible that the energy density of the "*produced particles*" becomes relevant at late times.

Due to the absence of direct detections, a non-interacting dark matter model [119] seems to be a model that gains strength over those in which dark matter interacts with some sector of the standard model. If this is the case, there should be a mechanism through which the relic density of dark matter is produced. In this scenario, the phenomenon of gravitational particle production can account for the abundance of matter required to explain the current cosmological observations without the need to non-gravitationally couple dark matter with any other field of the standard model. In semiclassical one-loop gravity, cosmological transitions, such as the transition from an inflationary universe to a radiation-dominated universe, can lead to the gravitational production of particles in a quantity large enough to account for the present observable universe [4, 5]. Therefore, in the context of an inflationary cosmology, justifying when "particles" or classical fields play an important role, and in which regimes it is possible to consider these approximations, is part of the discussion we present in this thesis report. An approach in this direction was made in *Cosmic Energy Density: Particles, Fields and The vacuum* Ref. [120] for a quantum scalar field. Part of its results are presented in Chapter 3. In Chapter 4, we extend this discussion to a quantum Dirac field.

The phenomenon of cosmological gravitational particle production has been investigated through multiple studies over several decades. The first paper discussing the creation of particles in the expanding universe was Schrodinger in 1939 [121]. Schrodinger suggested that the expansion of the universe can mix the positive- and negative-frequency mode solutions to the wave equations. In the subsequent works of Parker [122, 123, 124] and collaborators (Fulling, Ford and Hu [125, 126, 127, 128]) from 1968 to 1974, they emphasized the importance of gravitational particle production in a FLRW universe assuming a semiclassical approach. Also, in 1974, Hawking was developing the theory of particle creation by black holes[129]. In the context of inflationary theory, the formalism of gravitational particle production was applied to the quantum fluctuations of the inflaton scalar field and the metric fluctuations, which led to predictions about the density perturbations that account for the large-scale structure of the universe and the anisotropies in the cosmic microwave background [130]. Also, dark matter production is one of the main approaches that this phenomenon has received and its application to explain the origin of the relic density of dark matter in the present universe [131, 132, 133, 134]. The text-books of Birrel and Davies [135], Parker and Toms [136], Mukhanov and Winitzki [137] and Fulling [138], consist of excellent and comprehensive text

of this literature. We recommend to the reader the excellent reviews by Ford, [139], Kolb [140], and Jacobson [141].

The order of the present chapter is as follows: in Section 3.2, we will develop in detail the formalism of quantum scalar fields on curved spacetimes applied to a Friedmann–Lemaître–Robertson–Walker (FLRW) universe, derive the dynamic equations for the mode functions (which capture the evolution of the field as spacetime evolves), explore the solutions for asymptotically flat spacetimes, and introduce the Bogoliubov transformations. In Section 3.3, we review the construction of the number operator and the "number of particles", and in Section 3.4, we define an *adiabatic vacuum state* and *asymptotically adiabatic spacetime*. In Section 3.5, we introduce the *in* and *out* regions that allow us to define a cosmological transition, and in Section 3.6, we calculate the energy density for an arbitrary quantum state. In Section 3.7, we renormalize through the Pauli-Villars renormalization process the energy density ρ^{in} of the adiabatic vacuum state. Finally, in Section 3.8, we review the concept of "particle" and classical field description and define in which regimes *the particle production formalism* and the classical description are applicable. Here we use the signature of the metric is $(-,+,+,+)$ and the natural units $c = \hbar = 1$.

3.2 Formalism

Scalar Field Action

We are interested in the general behavior of a real quantum scalar field on expanding curved spacetimes, particularly the behavior of the energy density of this field through spacetime transitions. In a *semi*-classical context, where the dynamic gravitational field remains classical and the *spectator* scalar field is a quantum field, whose excitations consist of spin $s = 0$ particles, these conditions lead to the cosmological gravitational production of particles. In particular, we will focus on the study of transitions given by an FLRW (Friedmann-Lemaître-Robertson-Walker) type expansion, between an inflationary universe and a radiation-dominated universe.

For this purpose, we begin with the covariant action for a massive spin-0 scalar field $\Phi(x)$ coupled to gravity through the metric field $g_{\mu\nu}(x)$, given by

$$s[\Phi(x), g_{\mu\nu}] = \int d^4x\sqrt{-g}\left[\frac{M_{\text{pl}}^2}{2}R - \frac{1}{2}\partial_\mu\Phi(x)\partial^\mu\Phi(x) - \frac{1}{2}m^2\Phi(x)^2 - \frac{1}{2}\xi R\Phi(x)^2\right] \tag{3.3}$$

where g is the determinant of the metric $g_{\mu\nu}$, m is the scalar field mass, ξ is a coupling constant between the scalar field $\Phi(x)$ and the Ricci scalar R and $M_{\text{pl}}^2 = (8\pi G)^{-1/2}$ is the reduced Planck mass. In particular, we will consider only the case when $\xi = 0$, that is, the case when the scalar field is *minimally coupled* to gravity[5] (for the case $\xi = 1/6$, it is *conformally coupled* to gravity, and for other nonzero value it is *non-minimally coupled* to gravity).

[5]Conformally invariant scalar quantum field on conformally flat spacetimes (e.g. the FLRW spacetime, that is, the metric can be written down as $g_{\mu\nu} = \Omega^2(x)\eta_{\mu\nu}$) do not react to changes in the expansion history. The same occurs for massless fermion fields on conformally flat spacetimes, as we will see in the next chapter.

In the context of *inflation*, $\Phi(x)$ will represent a spectator field distinct from the *inflaton* field. Here, the field $\Phi(x)$ only interacts with gravity. As we mentioned, a dark matter model in which dark matter only interacts with the fields of the standard model through gravity is consistent with the absence of direct or indirect observations. This motivates the form of the action (3.3). Also recall that the bosonic fields of Chapter 1 and Chapters 2 that can form compact objects of dark matter interact only with the standard model through gravity.

Scalar Fields on FLRW Spacetimes

We will focus on a FLRW spacetime expansion, that is, an isotropic and homogeneous universe that expands uniformly according to the FLRW metric given by

$$ds^2 = a(\eta)^2[-d\eta^2 + dx^i dx^j \delta_{ij}], \tag{3.4}$$

where the time-dependent function $a(\eta)$ is called the scale factor, such that the *Hubble parameter* is given by $\mathcal{H} = a'(\eta)/a(\eta)$. Here we have used the *conformal time* defined as $ad\eta = dt$ and the comoving spatial coordinates defined as $x_i' = a(\eta)x_i$. The primes denote derivatives with respect to conformal time η and ∂_i denote derivatives with respect to comoving spatial coordinates.

With the metric (3.4), we have that $\sqrt{-g} = a^4$, $g^{00} = -a^{-2}$ and $g^{ij} = a^{-2}\delta^{ij}$, so after the change of variable $\Phi(x) = a^{-1}\phi(x)$, we can write the covariant action (3.3) as

$$S_{\phi(x)} = \int d\eta \int d^3x \left[\frac{\phi'^2}{2} - \frac{1}{2}(\partial_i\phi)^2 - \frac{1}{2}\partial_t[\phi^2\mathcal{H}] - \frac{1}{2}m_{\text{eff}}^2 a^2\phi^2\right] \tag{3.5}$$

where we have defined the *effective mass* as

$$m_{\text{eff}}^2(\eta) = m^2 + \left[\xi - \frac{1}{6}\right] R(\eta) \tag{3.6}$$

and we have use $R = 6(a''/a^3)$ and $\mathcal{H}' = (a''/a) - \mathcal{H}^2$. In the case of interest, where $\xi = 0$, we have an effective mass of the form $m_{\text{eff}}^{\xi=0} = m^2 - a''/a^3$.

From Eq. (3.5), we can calculate the Hamiltonian according to the relation $H = \int d^3x[\frac{\partial\mathcal{L}}{\partial\dot{\phi}}(\dot{\phi}) - \mathcal{L}]$, such that

$$H = \int d^3x \left[\frac{\phi'}{2} + \frac{1}{2}(\partial_i\phi)^2 - \phi\mathcal{H} + \frac{1}{2}\partial_\eta[\phi^2\mathcal{H}] + \frac{1}{2}m_{\text{eff}}^2 a^2\phi^2\right]. \tag{3.7}$$

Since the above Hamiltonian expression depends explicitly on time through the scale factor $a(\eta)$, the energy of the scalar field $\Phi(x)$ will not be conserved. When we quantize the field $\hat{\Phi}(x)$, the non-conservation of energy causes the gravitational production of particles, whose energy is provided by the gravitational field. We will study the details of this conclusion later.

After discarding the boundary terms and varying the action (3.5) with respect to $\phi(x)$, we have

$$\phi'' - \Delta\phi + a^2 m_{\text{eff}}^2\phi = 0, \tag{3.8}$$

where Δ is the Laplacian operator for the comoving spatial coordinate. It's worth noting that a time-dependent effective mass accounts for the interaction of the scalar field with the gravitational background. When spacetime is static a =constant, we recover the Klein-Gordon equation for a scalar field in a Minkowski spacetime.[6] So, all the information about the gravitational influence on the scalar field is encapsulated into the effective mass m^2_{eff}.

Field Quantization

Note that the action (3.5) has explicit time dependence through the effective mass $m^2_{\text{eff}}a^2$, so the energy density of the scalar field is not conserved. In the context of quantum fields on curved spacetime this time dependence leads to gravitational particle production supplied by the spacetime expansion. To characterize this behavior, we need to quantize the scalar field $\Phi(t,x)$ keeping the gravitational field classic. Canonical quantization[7] of the field imposes the equal time commutation relations

$$[\hat{\phi}(t,\vec{x}),\hat{\pi}(t,\vec{y})] = i\delta(\vec{x}-\vec{y}), \tag{3.9a}$$

$$[\hat{\phi}(t,\vec{x}),\hat{\phi}(t,\vec{y})] = [\hat{\pi}(t,\vec{x}),\hat{\pi}(t,\vec{y})] = 0, \tag{3.9b}$$

where $\hat{\pi}(x) = \partial\mathcal{L}/\partial(\phi')$ is the *conjugate momentum density*.

Introducing the mode expansion of the field $\hat{\phi}(x)$ in terms of the creation $\hat{a}^\dagger_k$ and annihilation $\hat{a}_k$ operators we can express the scalar quantum field as

$$\hat{\phi}(x) = \int \frac{d^3k}{(2\pi)^3}\left[\hat{a}_k U_{\vec{k}}(\eta,k) + \hat{a}^\dagger_k V_{\vec{k}}(\eta,k)\right] \tag{3.10a}$$

$$\text{with } U_{\vec{k}}(\eta,x) = \chi_k(\eta)e^{i\vec{k}\cdot\vec{x}} \text{ and } V_{\vec{k}}(\eta,x) = U^*_k(\eta,x), \tag{3.10b}$$

where $\vec{k} = a(\eta)\vec{k}^{phys}$ is the comoving wave vector with magnitude $k = |\vec{k}|$ and $\chi_k(\eta)$ is a complex time-dependent function called *mode function*. Here, $U_k(\eta,\vec{x})$ and $V_k(\eta,\vec{x})$ form a *complete* and *orthonormal* basis that spans the space of solutions to (3.8), and satisfies the *Wronskian condition*:

$$\int d^3x(U_{\vec{k}}V'_{\vec{q}} - V_{\vec{q}}U'_{\vec{k}}) = i(2\pi)^3\delta(\vec{k}-\vec{q}). \tag{3.11}$$

Additional to the commutation equations (3.9) the ladder operators $\hat{a}_k$ and $\hat{a}^\dagger_k$ satisfies the usual commutation relations

$$[\hat{a}_k,\hat{a}^\dagger_q] = (2\pi)^3\delta(\vec{k}-\vec{q}), \tag{3.12a}$$

$$[\hat{a}_k,\hat{a}_q] = [\hat{a}^\dagger_k,\hat{a}^\dagger_q] = 0. \tag{3.12b}$$

A ladder operator is assigned for each complex function $U_{\vec{k}}(x)$ labeled by $\vec{k}$. Note that we have written de mode function $\chi_k(\eta)$ in terms only of $k = |\vec{k}|$ because of the isotropy of the FLRW universe.

[6] In the case of a quantum fermion field we recover the usual Dirac field equations.

[7] Canonical quantization of the scalar field in action (3.3) results in a system of "single particles" that do not interact with each other. Here, we will work in the *Heisenberg picture* in which operators evolve according to the Heisenberg equation of motion and states are statics. See Ref. [36], for a comprehensive exposition of the quantization process.

The Mode Equations

Introducing Eq. (3.10b) into the Wronskian condition (3.11) implies the relation

$$\chi_k \chi_k'^* - \chi_k^* \chi_k' = i, \tag{3.13}$$

and putting Eq. (3.10a) into the wave equation (3.8) leads to the *mode equation* for $\chi_k(\eta)$ given by

$$\chi_k'' + \omega_k^2(\eta)\chi_k(\eta) = 0, \text{ where } \omega_k^2 = k^2 + a^2 m_{\text{eff}}^2 \tag{3.14}$$

is the time-dependent comoving squared *angular frequency* for each mode k.

Since the mode equation is a second order differential equation for each k, it admits a two-dimensional space of solutions. An important question is, Which basis is the "good" basis for characterize the field evolution? To determine this solution basis, additionally to the relation (3.13), we need another condition to completely specify the form of mode function $\chi_k(\eta)$. In the next subsections we analyze the conditions to give unambiguous solutions to the mode equations (3.14). The choice of the appropriate mode functions is crucial to the particle interpretation of the theory.

The Mode Function $\chi_k(\eta)$

In order to solve the mode equation (3.14) we need to specify the scale function $a(\eta)$ for the FLRW spacetime and the appropriate conditions to determine completely the mode function $\chi_k(\eta)$. For example, we are possibly interested in the cosmological expansion characterized by a quasi-de Sitter $a(t) \propto e^{H_\Lambda t}$ phase of inflation followed by a radiation dominated period with $a(t) \propto t^{1/2}$. In this case we need the conditions for the mode function $\chi^{\text{in}}(\eta) = \lim_{\eta\to-\infty}\chi(\eta)$ in the remote past and $\chi^{\text{out}}(\eta) = \lim_{\eta\to\infty}\chi(\eta)$ in the remote future. For this purpose, we begin by focusing on the simpler case of a Minkowski spacetime with $a(\eta) \sim$ constant followed by the case of an asymptotically flat spacetime.

Minkowski spacetime. For this case, we have $m_{\text{eff}}^2 = m^2$, $\mathcal{H} = 0$, $R = 0$ and $\omega^2 = k^2 + a_0^2 m^2$ with a_0^2 a constant. With these relations, we need to solve the differential equation $\chi_k'' + \omega_k^2\chi_k = 0$, which are solved by the normalized pair of solutions

$$\chi_k(\eta) = \frac{1}{\sqrt{2\omega_k}} e^{-i\omega_k\eta} \text{ and } \chi_k^*(\eta) = \frac{1}{\sqrt{2\omega_k}} e^{i\omega_k\eta}, \tag{3.15}$$

or any linear combinations of these $v_k(\eta) = \alpha_k\chi_k + \beta_k\chi_k^*$. Solutions χ_k and χ_k^* in Eqs. (3.15) are normalized according to the Wronskian condition (3.13) and are called, respectively, *positive and negative-frequency*[8] modes. If we chose $\beta_k = 0$ and $v_k = \chi_k$, w can write Eq. (3.10a) as

$$\hat{\phi}(t,x) = \frac{1}{\sqrt{2\omega_k}} \int \frac{d^3k}{(2\pi)^3} \left[\hat{a}_k e^{-i(\omega_k\eta - \vec{k}\cdot\vec{x})} + \hat{a}_k^\dagger e^{i(\omega_k\eta - \vec{k}\cdot\vec{x})}\right]. \tag{3.16}$$

[8]These terminology is motivated only on historical considerations. Positive frequency solutions refer to particles with positive energy $\omega_k > 0$ and negative frequency solutions refer to antiparticles with negative energy $\omega_k < 0$.

For this quantum field operator, we can construct a ladder operator $\hat{a}_k$ that allows us to postulate the existence of a vacuum state such that $\hat{a}_k |0\rangle = 0$ for all $\vec{k}$. The state $|0\rangle$ is interpreted as the vacuum state which minimize the energy. It is important to note that to determine the mode functions v_k unambiguously, we must define a vacuum state that allows us to set $\beta_k = 0$. Both procedures are equivalent. In the Minkowski spacetime all the inertial observers agree on the absence of particles in this vacuum state and the presence of particles in the excited states.

Contrary to the Minkowski spacetime, cosmological spacetimes like, for example, the FLRW spacetime which evolves in time (expand or contract), is generally not possible to define a positive-frequency solution, that is, in general $\beta_k \neq 0$. Thus, the notion of an empty state depends on the time at which each observer defines the state. Therefore, the vacuum state defined by an observer at time η_0 is different from the vacuum defined by an observer at time η for $\eta_0 < \eta$. On the other hand, remember that energy is not conserved for explicit time-dependent lagrangian as Eq. (3.5) and it is not possible to define a state that minimizes the energy at each instant of time.

Finally, let us emphasize that for Minkowski spacetime it is possible to choose at all times the positive (or negative) frequency solutions and therefore an associated vacuum state for which $\hat{a}_{\vec{k}} |0\rangle = 0$ is satisfied at all times. However, if the spacetime expands or contracts, it will not be possible to specify the positive (or negative) frequency solutions at all times, but rather a combination of positive and negative frequency solutions as $\chi_k^{\text{in}} = \alpha_k \chi_k + \beta_k \chi_k^*$. When $\beta_k \neq 0$, $\hat{a}_{\vec{k}}(\eta_1)$ and $\hat{a}_{\vec{k}}(\eta_2)$ will be different for $\eta_2 > \eta_1$. As a consequence, the vacuum states will be different at different times. This fact is essentially the mechanism by which gravitational particle production occurs.

Asymptotically flat spacetimes. In this case, we consider spacetimes that are asymptotically flat (e.i. Minkowski-like) at early and late times. Is such way, we can write the scaler factor as

$$a(\eta) = \begin{cases} a^{\text{in}}, \omega_k^{\text{in}} & \text{when} \quad \eta \to -\infty, \\ a(\eta), \omega_k(\eta) & \text{when} \quad -\infty < \eta < \infty, \\ a^{\text{out}}, \omega_k^{\text{out}} & \text{when} \quad \eta \to \infty \end{cases} \tag{3.17}$$

where a^{in} and a^{out} are constant and ω_k^{in} and ω_k^{out} are time-independent, real and positive. In the asymptotical regions when $\eta \to \pm\infty$, the spacetime with scale factor (3.17) are approximately Minkowski-like and admits positive-frequency solutions given by Eq. (3.15). Then, we can write two solutions that satisfy

$$\lim_{\eta \to -\infty} \chi_k^{\text{in}}(\eta) = \frac{1}{\sqrt{2\omega_k^{\text{in}}}} e^{-i\omega_k^{\text{in}}\eta}, \tag{3.18a}$$

$$\lim_{\eta \to \infty} \chi_k^{\text{out}}(\eta) = \frac{1}{\sqrt{2\omega_k^{\text{out}}}} e^{-i\omega_k^{\text{out}}\eta}, \tag{3.18b}$$

e.i., they are asymptotic to positive-frequency Minkowski solutions and are related by the linear combination $\chi_k^{\text{in}}(\eta) = \alpha_k \chi_k^{\text{out}}(\eta) + \beta_k \chi_k^{*\text{out}}(\eta)$.[9] Using

[9]Remember that, if the spacetime is always dynamic, it will not be possible to specify

these positive-frequency solutions we can construct the field mode expansion (3.10a) as

$$\begin{aligned}\hat{\phi}(t,x) &= \int \frac{d^3k}{(2\pi)^3}\left[\hat{a}^{\text{in}}_{\vec{k}}\chi^{\text{in}}_k(\eta) + \hat{a}^{\dagger\text{in}}_{-\vec{k}}\chi^{*\text{in}}_k(\eta)\right]e^{i\vec{k}\cdot\vec{x}} \\ &= \int \frac{d^3k}{(2\pi)^3}\left[\hat{a}^{\text{out}}_{\vec{k}}\chi^{\text{out}}_k(\eta) + \hat{a}^{\dagger\text{out}}_{-\vec{k}}\chi^{*\text{out}}_k(\eta)\right]e^{i\vec{k}\cdot\vec{x}},\end{aligned} \tag{3.19}$$

where we have defined the corresponding ladder operators $\hat{a}^{\text{in}}_{\vec{k}}$ and $\hat{a}^{\text{out}}_{\vec{k}}$ associated to the mode functions $\chi^{\text{in}}_k(\eta)$ and $\chi^{\text{out}}_k(\eta)$.

Bogoliubov Transformations

Eq. (3.19) establishes a relation between the ladder operators $\hat{a}^{\text{in}}_{\vec{k}}$ and $\hat{a}^{\text{out}}_{\vec{k}}$ and their complex conjugates. Writing $\hat{a}^{\text{in}}_{\vec{k}}\chi^{\text{in}}_k(\eta) + \hat{a}^{\dagger\text{in}}_{-\vec{k}}\chi^{*\text{in}}_k(\eta) = \hat{a}^{\text{out}}_{\vec{k}}\chi^{\text{out}}_k(\eta) + \hat{a}^{\dagger\text{out}}_{-\vec{k}}\chi^{*\text{out}}_k(\eta)$ and using the relation $\chi^{\text{in}}_k(\eta) = \alpha_k\chi^{\text{out}}_k(\eta) + \beta_k\chi^{*\text{out}}_k(\eta)$ and the normalization condition $|\alpha_k|^2 - |\beta_k|^2 = 1$, we have that

$$\hat{a}^{\text{out}}_{\vec{k}} = \hat{a}^{\text{in}}_{\vec{k}}\alpha_k + \hat{a}^{\dagger\text{in}}_{-\vec{k}}\beta^*_k, \quad \rightarrow \quad \hat{a}^{\text{in}}_{\vec{k}} = \hat{a}^{\text{out}}_{\vec{k}}\alpha^*_k - \hat{a}^{\dagger\text{out}}_{-\vec{k}}\beta^*_k, \tag{3.20a}$$

$$\hat{a}^{\dagger\text{out}}_{\vec{k}} = \hat{a}^{\text{in}}_{\vec{k}}\beta_k + \hat{a}^{\dagger\text{in}}_{-\vec{k}}\alpha^*_k, \quad \rightarrow \quad \hat{a}^{\dagger\text{in}}_{\vec{k}} = \hat{a}^{\dagger\text{out}}_{\vec{k}}\alpha_k - \hat{a}^{\dagger\text{out}}_{-\vec{k}}\beta_k. \tag{3.20b}$$

These relations allow us to define the linear transformation $\in SU(1,1)$

$$\begin{pmatrix} -\beta_k & \alpha_k \\ \alpha^*_k & -\beta^*_k \end{pmatrix}\begin{pmatrix} \beta^*_k & \alpha_k \\ \alpha^*_k & \beta_k \end{pmatrix} = \mathbb{I}, \tag{3.21}$$

that leaves the field operator unchanged and relates two different basis of ladder operators and mode functions. So, this matrix transformation called *Bogoliubov transformation*, relates a family of equivalent representations of the field operator $\hat{\phi}(x)$. Each ladder operator $\hat{a}^{\text{in}}_{\vec{k}}$ and $\hat{a}^{\text{out}}_{\vec{k}}$ obeys the commutation relations (3.12).

Finally, using the relation $\dot{\chi}^{\text{in}}_k = \alpha_k\dot{\chi}^{\text{out}}_k + \beta_k\dot{\chi}^{*\text{out}}_k$, we can write

$$i\alpha_k = W(\chi^{\text{in}}_k, \chi^{*\text{out}}_k), \quad i\beta_k = W(\chi^{\text{out}}_k, \chi^{\text{in}}_k), \tag{3.22}$$

where W refers to the Wronskian condition (3.11).

3.3 Particle Number Operator

Given that the ladder operators $\hat{a}^{\text{in}}_{\vec{k}}$ and $\hat{a}^{\text{out}}_{\vec{k}}$ satisfies the canonical commutation relations (3.12) and allows the field operator representation (3.10a) we can define the "vacuum states" $|0\rangle_{\text{in}}$ and $|0\rangle_{\text{out}}$ such that

$$\hat{a}^{\text{in}}_{\vec{k}}|0\rangle_{\text{in}} = 0, \quad \text{and} \quad \hat{a}^{\text{out}}_{\vec{k}}|0\rangle_{\text{out}} = 0. \tag{3.23}$$

the positive (or negative) frequency solutions at all times, but rather a combination of positive and negative frequency solutions as $\chi^{\text{in}}_k(\eta) = \alpha_k\chi_k(\eta) + \beta_k\chi^*_k(\eta)$ with $\chi(\eta)$ a general solution to Eq. (3.14). For two different times $\eta_1 \to -\infty$ and $\eta_2 \to \infty$ in an asymptotically flat spacetime, we have $\chi^{\text{in}}_k(\eta) = \alpha_k\chi^{\text{out}}_k(\eta) + \beta_k\chi^{*\text{out}}_k(\eta)$.

With these definitions, we can construct a *Fock space* of multi-particle states. So, we can talk about two definitions of the *vacuum state*: the *in*-vacuum state $|0\rangle_{\rm in}$ and the *out*-vacuum state $|0\rangle_{\rm out}$, whose excited states $|n\rangle_{\rm in}$ and $|n\rangle_{\rm out}$ describes $N_{\rm in}$ number of *in*-particles and $N_{\rm out}$ number of *out*-particles, respectively.

Since $\hat{a}^{\rm in}_{\vec{k}}$ and $\hat{a}^{\rm out}_{\vec{k}}$ are related by a Bogoliubov transformation (3.21), we can calculate the expectation value of the number of *out*-particle operator $\hat{N}^{\rm out}_{\vec{k}} = \hat{a}^{\rm out}_{\vec{k}}\hat{a}^{\dagger{\rm out}}_{\vec{k}}$ with respect to the *in*-vacuum state $|0\rangle_{\rm in}$. Using (3.20), after some straightforward algebra, we obtain

$$\langle 0|\hat{N}^{\rm out}_{\vec{k}}|0\rangle_{\rm in} = (2\pi)^3\delta(0)n, \quad \text{with} \quad n = \int \frac{d^3k}{(2\pi)^3}|\beta_k|^2 \tag{3.24}$$

where n is the comoving number density of particles that the *out*-number operator measures in the *in*-vacuum. After integration with respect to the angular variables, we have

$$n = \frac{1}{2\pi^2}\int \frac{dk}{k}k^3|\beta_k|^2 \quad \text{with} \quad n_k = \frac{k^3}{2\pi^2}|\beta_k|^2 \tag{3.25}$$

where n_k is the comoving number density spectrum; also we can write

$$n = \frac{1}{2\pi^2}\int \frac{dk}{k}\frac{d}{d\ln k}k^3|\beta_k|^2, \tag{3.26}$$

where n_k is the comoving number density of particles per logarithmic wavenumber interval. Note that, from Eq. (3.25), n is finite only if $|\beta_k|^2$ decays faster than k^{-2} for large k. This condition also guarantees that we can express the *in*-vacuum state as a normalized combination of *out*-excited states.

3.4 Adiabatic Vacuum

3.4.1 Physical Vacuum

As we have seen, the notion of real "vacuum" depends crucially on our election for the mode functions $\chi^{\rm in}_k$ and $\chi^{\rm out}_k$. For example, in the particular choice of $\chi^{\rm in}_k$ in which $\beta_k = 0$ we have that $\chi^{\rm in}_k = \chi^{\rm out}_k$, and, in this case, there exist a preferred notion of the vacuum state, namely the Minkowski vacuum state. However, in general $\beta_k \neq 0$ and there no exist a preferred notion of vacuum and the physical vacuum acquire an inherent ambiguity.

We have learned from Eq. (3.25) that in general the *out*-vacuum state $|0\rangle_{\rm out}$, being a state without *out*-particles, nevertheless contain *in*-particles. One way to see that the *out* vacuum state is populated by $N_{\rm in}$ particles, is to consider that the state that minimizes the energy at the time η_1, at the time $\eta_2 > \eta_1$ will no longer minimize the energy if the frequency ω_k is time-dependent. For these two instants η_1 and η_2, the mode functions are given by the expressions (3.15), so it is possible to define the operators $\hat{a}_k(\eta_1)$ and $\hat{a}_k(\eta_2)$ that satisfy $\hat{a}_k(\eta_1)\,|0\rangle_{\eta_1} = 0$ and $\hat{a}_k(\eta_2)\,|0\rangle_{\eta_2} = 0$. In this case, it is possible to calculate the energy density ρ_{η_2} with respect to the vacuum $|0\rangle_{\eta_1}$ from which we obtain $\rho_{\eta_2} = \langle 0_{\eta_1}|T^0_0(\eta_2)|0_{\eta_1}\rangle = \int d^3k\omega_k(\eta_2)[\frac{1}{2} + |\beta_k|^2]$. Where we obtain

a contribution to the energy coming from $\omega_k|\beta_k|^2$, that is, the energy of each particle multiplied by the number of particles in each mode. Finally, we can conclude, there is not a preferable choice of the mode functions to determine an unambiguous vacuum state or an empty state for which there no exist *in-* or *out-* particles. This is the essence of the cosmological gravitational production.

3.4.2 Asymptotically Adiabatic Spacetimes

For spacetimes that are not asymptotically flat as $\eta \to \pm\infty$ the scale factor $a(\eta)$ is always growing and the identification (3.18) is not possible, i.e., we can not identify the positive and negative frequency modes and hence the particle concept is not defined. However, in the case that the angular frequency ω_k is slowly varying at early and late times, is possible perform a WKB-*type* approximation such that

$$\chi_k = (2W_k)^{-1/2} \exp\left\{-i \int^{\eta} W_k(\eta')d\eta'\right\}, \tag{3.27}$$

where W_k satisfies the non-linear equation

$$W_k^2(\eta) = \omega_k^2 - \frac{1}{2}\left(\frac{\ddot{W}_k}{W_k} - \frac{3}{2}\frac{\dot{W}_k^2}{W_k^2}\right). \tag{3.28}$$

Since the spacetime is slowly varying, at zeroth order approximation we have $W_k^{(0)} = \omega_k$. Using Eq. (3.28), by iteration we can construct the subsequent orders of approximation with the adiabatic order given by the number of derivatives of $a(\eta)$. For example, the second adiabatic order approximation is written as

$$\left(W_k^{(2)}\right)^2 = \omega_k^2 - \frac{1}{2}\left(\frac{\ddot{\omega}_k}{\omega_k} - \frac{3}{2}\frac{\dot{\omega}_k^2}{\omega_k^2}\right). \tag{3.29}$$

Hence, one solution of adiabatic order (A) is given by $\chi_k^{(A)}$ with $W_k^{(A)}$ given by Eq. (3.28). When $a(\eta) \approx$ constant as $\eta \to \pm\infty$ we recover the asymptotically flat approximation (3.18). However, if the spacetime is varying slowly, the Minkowski solutions (3.18) and the approximate solutions $\chi_k^{(A)}$ will be different only by terms of adiabatic order higher than zero. Since the series obtained in Eq. (3.27) is asymptotic, the approximated solutions reach an optimum value at one particular order (A).

Then, for spacetimes in which $\omega_k(\eta)$ is asymptotically slowly varying or *asymptotically adiabatic*, that is when $\dot{\omega}_k \ll \omega_k$ as $\eta \to \pm\infty$, we can define the positive-(and negative) frequency approximated solutions as

$$\chi_k^{\text{in}}(\eta) = \lim_{\eta\to-\infty} \chi_k(\eta) \approx \chi_k^{(0)} = \frac{1}{\sqrt{2\omega_k^{\text{in}}(\eta)}} e^{-i\int^{\eta}\omega_k^{\text{in}}(\eta')d\eta'}, \tag{3.30a}$$

$$\chi_k^{\text{out}}(\eta) = \lim_{\eta\to\infty} \chi_k(\eta) \approx \chi_k^{(0)} = \frac{1}{\sqrt{2\omega_k^{\text{out}}(\eta)}} e^{-i\int^{\eta}\omega_k^{\text{out}}(\eta')d\eta'}. \tag{3.30b}$$

and these allows us to define an zeroth order *adiabatic vacuum* $|0\rangle_{\text{in}}^{(0)}$ associated to these solutions and the corresponding ladder operators $\hat{a}_{\vec{k}}^{\text{in}}$ and $\hat{a}_{\vec{k}}^{\dagger\text{in}}$.

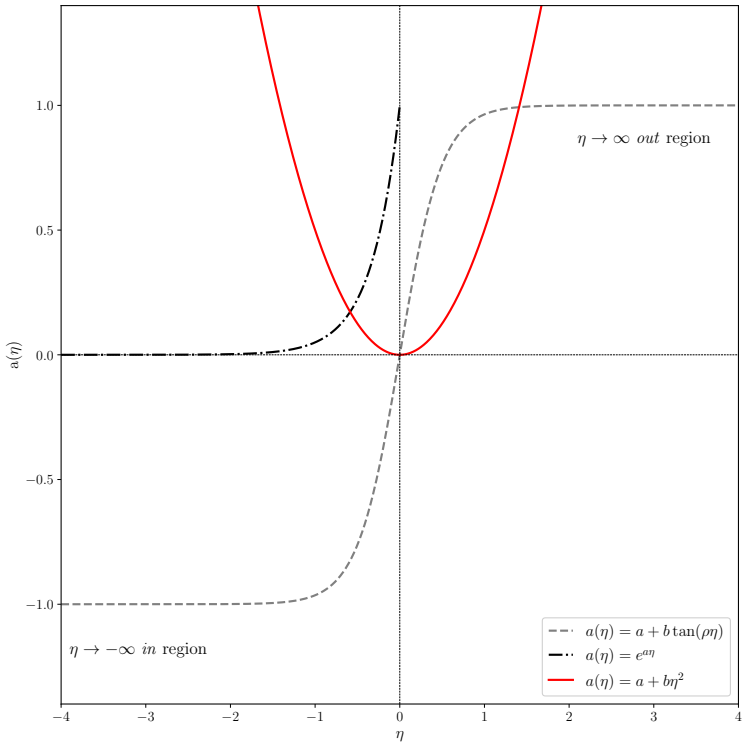

Figure 3.1: $a(\eta)$ **vs** η **for different asymptotical adiabatic spacetime**. *Black line*: asymptotically adiabatic spacetime in the remote past as $\eta \to -\infty$ and $\lim_{\eta\to-\infty} a(\eta) = e^{a\eta} = constant$ with a a constant. *Grey line*: asymptotically adiabatic spacetime in the remote past and future as $\eta \to \pm\infty$ and $\lim_{\eta\to\pm\infty} a(\eta) = a + b\tanh\rho\eta = constant$ with a, b and ρ constants. On another side, scale factor in *red line* satisfies $d^n/d\eta^n(\dot{a}/a) \to 0$ as $\eta \to \pm\infty$ for $n \leq 0$ given $a(\eta) = a^2 + b^2\eta$ with a, b constants, therefore this spacetime is asymptotically adiabatic in the remote past and future.

Consequently, it is possible to talk about "particles" and *gravitational production of particles*. Note that, actually, $|0\rangle_{\text{in}}$ is an *in* adiabatic vacuum of infinite adiabatic order $|0\rangle^{(n)}_{\text{in}}$. As we have described before in the asymptotically flat case, also for the asymptotically adiabatic case we can write the general solution $\chi_k(\eta)^{\text{in}} = \alpha_k\chi_k^{\text{out}} + \beta_k\chi_k^{\text{out}*}$ where α_k and β_k satisfy conditions $\alpha_k = 1$ and $\beta_k = 0$ as $\eta \to -\infty$ and $|\alpha_k|^2 + |\beta_k|^2 = 1$ for all time η.

Examples. Let's consider the example of a time-dependent frequency $\omega_k(\eta)$ of the form $\omega_k^2 = k^2 + a^2m_{\text{eff}}^2$ with $a(\eta) = 1 + \tanh\eta$, such that the condition of adiabaticity $\omega_k \gg \dot{\omega}_k$ is satisfied in the regions where η tends to $\pm\infty$, see Figure 3.1. The mode functions in these remote regions are given by Eqs. (3.30). This case constitutes an example of an asymptotically adiabatic spacetime. Another example of spacetime that is only adiabatic in the remote past is given by the case $a(\eta) = e^\eta$ with $\eta < 0$. However, the adiabatic approximation applies not only to spacetimes that are asymptotically static but also to those that vary slowly (e.g. $a(\eta) = a^2 + b^2\eta^2$ with $-\infty < \eta < \infty$ and a, b constants), that is, for which $\mathcal{H} \ll \omega_k$ is satisfied. In these instances, the adiabatic approximation is really useful.

3.5 Cosmological Epochs

Presumably, the universe has experienced multiple facets of uniform expansion throughout its history, characterized by different epochs of domination. The transitions between different epochs are accompanied by jumps in the behavior of the scale factor. In Figure 3.2, we draw a timeline representing the different cosmological epochs that the universe has experimented until the radiation domination. Initially, the universe experiences a period of accelerated expansion (Λ domination) called inflation at time η_i, followed by a period of decelerated expansion called radiation domination at time η_r, mediated by a highly model-dependent period of *reheating* at $\eta_e < \eta < \eta_r$. Subsequently, the universe experiments a period dominated by matter followed by a new period of accelerated expansion up to the present day. We invite the reader to review Baumman's excellent book [118], in which he reviews all these periods.

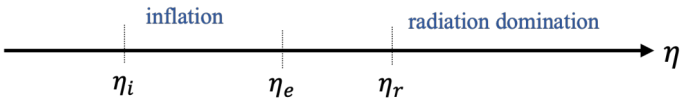

Figure 3.2: Timeline characterizing the transition experienced by the universe as it expands from an initial period of cosmic *inflation* at η_i followed by a period of radiation domination η_r mediated by a model-dependent *reheating* period $\eta_e < \eta < \eta_r$. In a sharp transition $\eta_r = \eta_e$ and there is a discontinuity in the second derivative of the scale factor.

To characterize these cosmological transitions in the context of gravitational particle production, we will consider an initial *in*-region characterized by inflation where a preferred notion of vacuum exists (the *Bunch-Davies vacuum state*, the ground state of the hamiltonian at the beginning of inflation) and a subsequent *out*-region that is generally not asymptotically adiabatic. With this in mind, we will immediately characterize both regions.

3.5.1 *in* Region

This region is characterized by an initial period of inflation. It is known that during this period we can choose a preferred notion of vacuum, since $\mathcal{H}$ tends to zero as $\eta \to -\infty$, that is $\dot{\omega}_k \ll \omega_k$, and we can approximate the solution χ_k^{in} as the zeroth order adiabatic "positive frequency" solution

$$\chi_k^{\text{in}}(\eta) \to \frac{1}{\sqrt{2\omega_k(\eta)}} e^{-i\int^\eta \omega_k(\eta')d\eta'}. \tag{3.31}$$

With this, it is possible to define an adiabatic vacuum and a concept of particles associated with this preferred notion of vacuum.

As described in Ref. [120], inflation is not a period that extends endlessly into the past. Therefore, for light or massless fields, it is necessary to introduce the scale $\Lambda_{\text{IR}} \sim \mathcal{H}_{\text{IR}}$ where $\mathcal{H}_{\text{IR}}$ is the Hubble parameter evaluated at the beginning of inflation η_i. In Figure 3.3, we draw the order of this scale. It is important to note that for superhorizon scales, there is no preferred notion of vacuum, in the sense that it is not possible to make the positive frequency

approximation (3.31). Additionally, for massive fields, that is for the case when $m \gg \mathcal{H}$, we have $\omega_k \gg \mathcal{H}$ and $\Lambda_{\rm IR} = 0$.

Let's remember that, once we have established the condition (3.31), we will be able to construct the operator $\hat{\phi}(x)$ given by Eq. (3.10a) for which it is possible to define an *in* vacuum state that satisfies $\hat{a}^{\rm in}_{\vec{k}} |0^{\rm in}\rangle = 0$, in which there is no presence of *in* "quanta/particles". Also, we can construct a number operator $\hat{N}^{\rm in}_{\vec{k}} = \hat{a}^{\rm in\dagger}_{\vec{k}} \hat{a}^{\rm in}_{\vec{k}}$ for which the state $\hat{N}^{\rm in}_{\vec{k}} |\psi\rangle = N^{\rm in}_k |\psi\rangle$ contains $N^{\rm in}_k$ number of "quanta/particles". Again, note that only the states for which the condition $k > \Lambda_{\rm IR}$ is satisfied allow us to define the notion of *in* vacuum.

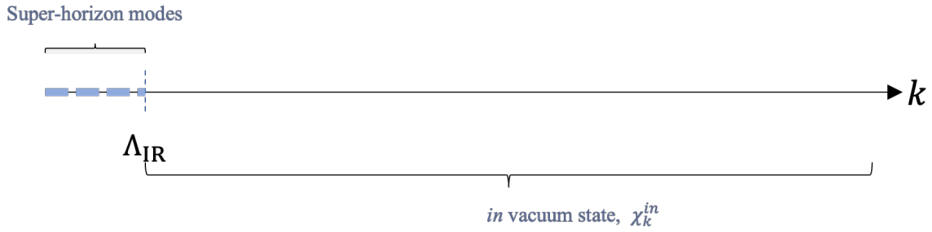

Figure 3.3: Infrared scale $\Lambda_{\rm IR} \sim \mathcal{H}_i$ at the beginning of inflation. The modes below this scale have an unknown state. Modes above $\Lambda_{\rm IR}$ are found in the preferred *in* vacuum state set by inflation at η_i. If the field is massless or light, the state of the superhorizon modes at the beginning of inflation, is not determined by inflation and remains unknown to us.

3.5.2 *out* region

As we have already mentioned, in general, the functions $\chi^{\rm out}_k(\eta)$ do not necessarily satisfy asymptotically adiabatic conditions (3.30b), and although we explicitly refer to the *out* region, the function $\chi^{\rm out}_k(\eta)$ can generally be an arbitrary function that satisfies the normalization condition (3.13) and the mode equation (3.14). Assuming that $\chi^{\rm out}_k(\eta)$ and $\chi^{\rm out*}_k(\eta)$ are linearly independent, it is possible to write $\chi^{\rm in}_k(\eta)$ as a combination of two solutions such that

$$\chi^{\rm in}_k = \alpha_k \chi^{\rm out}_k(\eta) + \beta_k \chi^{\rm out*}_k(\eta) \tag{3.32}$$

where the *Bogoliubov coefficients* satisfies the relation $|\alpha_k|^2 - |\beta_k|^2 = 1$. Furthermore, solving for α_k and β_k, we can write

$$i\alpha_k = \chi^{\rm in}_k(\eta)\dot{\chi}^{\rm out*}_k(\eta) - \dot{\chi}^{\rm in}_k(\eta)\chi^{\rm out*}_k(\eta), \tag{3.33a}$$
$$i\beta_k = -\chi^{\rm in}_k(\eta)\dot{\chi}^{\rm out}_k(\eta) + \dot{\chi}^{\rm in}_k(\eta)\chi^{\rm out}_k(\eta). \tag{3.33b}$$

When $\eta \to -\infty$, we get $\alpha_k = 1$ and $\beta_k = 0$, as expected.

Example. Asymptotically adiabatic spacetime. In the case where the spacetime is asymptotically adiabatic when $\eta \to \pm\infty$, the mode functions $\chi^{\rm out}_k(\eta)$ take the form given by Eq. (3.30b), and, substituting these solutions into Eq. (3.33b), we obtain the expression

$$|\beta_k|^2 = \frac{|\dot{\chi}^{\rm in}_k|^2}{2\omega_k} + \frac{\omega_k}{2}|\chi^{\rm in}_k|^2 - \frac{1}{2}. \tag{3.34}$$

With the expression (3.34), we can obtain the number of *out* particles that the *in* vacuum contains calculating $\langle_{\rm in}0|\hat{N}^{\rm out}_{\vec{k}}|0_{\rm in}\rangle = (2\pi^2)^{-1}\int dk k^2 |\beta_k|^2$.

3.6 Energy Density

In the semiclassical approach to gravity, the gravitational field $g_{\mu\nu}(x)$ retains its classical nature while the matter fields follow a quantum treatment. In our formalism, we need to consider the relationship

$$R_{\mu\nu} - \frac{1}{2}Rg_{\mu\nu} = M_{\rm pl}^{-2}\left\langle T_{\mu\nu}\right\rangle, \tag{3.35}$$

where the right side encodes the gravitational dynamics and the left side is the expectation value of the stress-energy tensor for the quantum field $\hat{\phi}(x)$. For the scalar field action in (3.3), the associated stress-energy tensor (for $\xi = 0$) is given by

$$T_{\mu\nu}(t,\vec{x}) = \partial_\mu\Phi\partial_\nu\Phi - \frac{1}{2}g_{\mu\nu}\partial^\beta\Phi\partial_\beta\Phi + \frac{1}{2}m^2 g_{\mu\nu}\Phi^2. \tag{3.36}$$

Given this expression, we are interested in analyzing the evolution of the expectation value on the right-hand side in Eq. (3.35) when the universe undergoes a cosmic transition as described in the previous section (e.g. the evolution of the energy density $\rho = \langle\hat{T}_{00}\rangle$ with respect to the adiabatic vacuum $|0\rangle^{\rm in}_{\rm ad}$ configured by inflation to a subsequent decelerated universe dominated by radiation).

Following the approximation in Ref. [120], we need to calculate

$$\rho = \rho_0 + \int_0^\Lambda \frac{dk}{k}\frac{d\rho}{d\log k} \tag{3.37}$$

where we have separated the energy density ρ between the contribution of the zero mode $\vec{k} = 0$ and the contribution of the modes in the range $0 < k < \Lambda$, where we have introduced the cutoff Λ. After performing the integration, we send $\Lambda \to \infty$. The zeroth mode component is given by

$$\rho_0 = \frac{1}{2a^2V}\Bigg\{\left(N_0 + \frac{1}{2}\right)\left[\left|\frac{d}{d\eta}\left(\frac{\chi_0}{a}\right)\right|^2 + m^2|\chi_0|^2\right] + L_0\left[\left(\frac{d}{d\eta}\frac{\chi_0}{a}\right)^2 + m^2\chi_0^2\right] + c.c.\Bigg\} \tag{3.38}$$

and

$$\frac{d\rho}{d\log k} = \frac{k^3}{4\pi^2a^2}\Bigg\{\left(N_k + \frac{1}{2}\right)\left[\left|\frac{d}{d\eta}\left(\frac{\chi_k}{a}\right)\right|^2 + \omega_k^2|\chi_k|^2\right] + L_k\left[\left(\frac{d}{d\eta}\frac{\chi_k}{a}\right)^2 + \omega_k^2\chi_k^2\right] + c.c.\Bigg\} \tag{3.39}$$

is the "spectral energy density" (per logarithmic interval) for the $k \neq 0$ modes. Here, the expectation value is taken with respect to an arbitrary state and χ_k are arbitrary solutions to Eq. (3.14). For the *in* adiabatic vacuum configured by inflation we have that $N_k, L_k = 0$ and $\chi_k^{\rm in} = \chi_k$ from which we can write

$$\frac{d\rho_{\rm in}}{d\log k} = \frac{k^3}{4\pi^2a^2}\left[\left|\left(\frac{d}{d\eta}\frac{\chi_k^{\rm in}}{a}\right)\right|^2 + \omega_k^2|\chi_k^{\rm in}|^2\right]. \tag{3.40}$$

Modes in range $0 \leq k < \Lambda_{\rm IR}$		
$\vec{k} = 0$ This mode admits classical interpretation	massless case	$\rho_0 \propto 1/a^6$ stiff fluid
	masive case	light field $ma \ll \mathcal{H}$ stiff fluid + " frozen field"
		$ma \gg \mathcal{H}$ adiabatic approximation pressureless fluid
$0 < k < \Lambda_{\rm IR}$	massless case	These modes not admits classical interpretation
	masive case	$\Lambda_{\rm IR} < ma$ non-relativistic
		$\Lambda_{\rm IR} > ma$ relativistic

Table 3.1: Energy density for the range of modes $0 \leq k < \Lambda_{\rm IR}$ and its behavior in different mass regimes. For these states, there is no preferred notion of vacuum, and their state is indeterminate. *The first row* corresponds to the zero mode $\vec{k} = 0$, which admits an interpretation in terms of a homogeneous classical field. For the massless case, the energy density behaves like a stiff fluid. For the massive case, if $ma \ll \mathcal{H}$, in addition to the contribution of the stiff fluid, there is the contribution of a frozen fluid, and if $ma \gg \mathcal{H}$, the density behaves like that of a pressureless fluid. *The second row* corresponds to the $0 < k < \Lambda_{\rm IR}$ modes. For the massless case $m = 0$, these modes are relativistic and do not allow for an interpretation in terms of a classical field. In the massive case, however, when $\Lambda_{\rm IR} < ma$, the modes are non-relativistic and ρ_k admits a classical interpretation.

In Table 3.1, we present the behavior of the spectral density (3.39) for the $0 \leq k < \Lambda_{\rm IR}$ modes in the massive and massless cases. Recall that $\Lambda_{\rm IR} \sim \mathcal{H}_i$ is a characteristic scale at the beginning of inflation below which the state of the field remains indeterminate or unknown to us. In Ref. [120] we can see the treatment for each different case in Table 3.1 in detail. Here we will limit ourselves to presenting as an example the massless case for the mode $\vec{k} = 0$. In the next chapter, we will perform in detail the methodology summarized here now for the case of a fermion field. To begin, let us consider the mode equation (3.14) when $m = 0$ and $k = 0$, such that $\chi_0''(\eta) + \omega_0^2 \chi_0(\eta) = 0$ with $\omega_0^2 = -\ddot{a}/a$. The solutions of this equation take the form $\chi_0^{m=0} = iAa(\eta) + Ba(\eta) \int^\eta \frac{d\tilde{\eta}}{a^2}$ with A and B two real constants. Putting these into Eq. (3.38) with $m = 0$ we have

$$\rho_0 = \frac{1}{2a^2 V} \left\{ \left(N_0 + \frac{1}{2} \right) \left[\left| \left(\frac{d}{d\eta} \frac{\chi_0}{a} \right) \right|^2 \right] + L_0 \left[\left(\frac{d}{d\eta} \frac{\chi_0}{a} \right)^2 \right] + \text{c.c.} \right\} \tag{3.41}$$

with $(\chi_0/a)^{\cdot} = B/a^2$, from which we obtain the energy density contribution coming from the zero modes given by

$$\rho_0 = \frac{B^2}{2V} \left\{ \left(N_0 + \frac{1}{2} \right) + L_0 + \text{c.c.} \right\} \frac{1}{a^6}, \tag{3.42}$$

which behaves like a stiff fluid with equation of state $\omega = 1$. Now, if we consider a classical homogeneous scalar field $\phi_{cl} = 1/a(A_0 \chi_0 + B_0 \chi_0^*)$ whose energy density is $\rho_{cl} = (|\dot{\phi}_{cl}|^2 + m^2 a^2 |\phi_{cl}|)/(2a^2)$, then we can identify the

energy density (3.42) like a classical homogeneous stiff fluid if we can solve the system of equations $(|A_0|^2+|B_0|^2)/2 = (N_0+1/2)/V$ and $A_0 B_0^* = L_0/V$. This is the result presented in the first row for the massless case of the Table 3.1.

Note: Let's briefly address the massive case ($m \neq 0$) for the zero mode $\vec{k} = 0$ (corresponding to the first row of Table 3.1). For this case, we distinguish two regimes. In the first case, when $ma \ll \mathcal{H}$, that is, when the field is *light*, we can expand the solutions to Eq. (3.14) in terms of the mass m, and progressively construct around the solution $\chi_{k=0}^{m=0}$ to Eq. (3.14). These solutions have the form $\chi_0^{m=0} = iAa(\eta)+Ba(\eta)\int^\eta \frac{d\tilde{\eta}}{a^2}$. Neglecting the term corresponding to B (which decays in an expanding universe for $-1 \leq \omega < 1$) and using into ρ_0, Eq. (3.41), and $\rho_{cl} = (|\dot{\phi}_{cl}|^2 + m^2a^2|\phi_{cl}|)/(2a^2)$, we obtain that $\rho_0 = D_0\frac{1}{a^6} + m^2E_0$ and $\rho_{\rm cl} = D\frac{1}{a^6} + m^2E$, with D_0, E_0, D and E constants dependent on N_0, L_0, A_0 and B_0. Therefore, ρ_0 admits interpretation in terms of a homogeneous classical field Φ_{cl}. On the other hand, when the field is *heavy*, that is, when $ma \gg \mathcal{H}$, we can use the adiabatic expansion (3.27) to first order, such that $\rho_0 \sim \frac{m}{a^3V}$ and $\rho_{\rm cl} \sim \frac{m}{a^3V}$, so it is also possible to interpret ρ_0 as the contribution of a homogeneous classical field ρ_{cl} as long as we can solve A_0 and B_0 in terms of N_0 and L_0.

3.7 Pauli-Villars Renormalization

In the range of modes $\Lambda_{\rm IR} < k < \infty$, as the cutoff Λ goes to infinity, the integral over all modes of Eq. (3.40) is divergent. We can see this using the zeroth adiabatic order solutions (3.31) for large k, such that $\omega_k \approx k$, so the integral

$$\rho = \lim_{\Lambda\to\infty}\int_{\Lambda_{\rm IR}}^{\Lambda}\frac{dk}{k}\frac{k^3}{4\pi^2a^2}\left[\left|\frac{d}{d\eta}\left(\frac{\chi_k^{\rm in}}{a}\right)\right|^2 + \omega_k^2|\chi_k^{\rm in}|^2\right] \tag{3.43}$$

is divergent as k^4 in the leading order term in k. To deal with these divergences, we will use the Pauli-Villars renormalization procedure, summarized in the following points:

(i) Since the mode functions $\chi_k^{\rm in}$ are built in the adiabatic regime, it is possible to expand up to fourth adiabatic order the integrand in Eq. (3.43), such that

$$\rho = \lim_{\Lambda\to\infty}\int_{\Lambda_{\rm IR}}^{\Lambda}\frac{dk}{k}\left[\left(\frac{d\rho_k}{d\log k}\right)^{(0)} + \left(\frac{d\rho_k}{d\log k}\right)^{(2)} + \left(\frac{d\rho_k}{d\log k}\right)^{(4)} + ...\right], \tag{3.44}$$

and we can identify the subsequent divergent terms as $\Lambda \to \infty$ after performing the integrals. For example, integrating the zeroth order of the adiabatic expansion of the spectral density, we have that

$$\lim_{\Lambda\to\infty}\int_{\Lambda_{\rm IR}}^{\Lambda}\frac{dk}{k}\left(\frac{d\rho_k}{d\log k}\right)^{(0)} = \lim_{\Lambda\to\infty}\frac{1}{2\pi^2}\left[\frac{\Lambda^4}{8a^4}+\frac{m^2\Lambda^2}{8a^2}+\frac{m^4}{64}\left(1-2\log\frac{4\Lambda^4}{a^2\mu^2}\right)\right] \tag{3.45}$$

where the right term is divergent as Λ tends to infinity. The same procedure applies to the second and fourth adiabatic orders in order to find the

divergent terms of the expansion. Terms with higher derivatives (sixth and more time derivatives) remain finite as the cutoff Λ tends to infinity.

(ii) In order to remove these divergences, we introduce n *Paulli-Villars Regulators* ϕ_r of mass M_r and Grassman parity σ_r, with $r = 1, , 2 \ldots, n$, in such way that we need to calculate $\sum_{i=0} \langle T_0^0 \rangle_i$, with $i = 0, 1, 2, \ldots, n$, such that

$$\rho_k = \lim_{\Lambda\to\infty} \sum_i \int_{\Lambda_{\rm IR}}^{\Lambda} \frac{dk}{k} \sigma_i \Bigg[\left(\frac{d\rho_k}{d\log k} \right)^{(0)} + \left(\frac{d\rho_k}{d\log k} \right)^{(2)} + \left(\frac{d\rho_k}{d\log k} \right)^{(4)} + ... \Bigg]. \tag{3.46}$$

Then we use the relations [10]

$$\sum_{i=0} \sigma_i = 0, \quad \sum_{i=0} \sigma_i M_i^2 = 0, \quad \sum_{i=0} \sigma_i M_i^4 = 0, \tag{3.47}$$

and we to apply the limit $\Lambda \to \infty$. For example, for the zeroth order, using the result (3.45), we have that

$$\lim_{\Lambda\to\infty} \sum_i \frac{1}{2\pi^2} \left[\frac{\sigma_i \Lambda^4}{8a^4} + \frac{\sigma_i M_i^2 \Lambda^2}{8a^2} + \frac{\sigma_i M_i^4}{64} - \frac{\sigma_i M_i^4}{32} \log \frac{4\Lambda 4}{a^2 M_i^2} \right]. \tag{3.48}$$

Now, using the relations (3.47) and applying the limit $\Lambda \to \infty$, we can see that the divergent terms in the above expression disappear. So, if Eq. (3.47) are satisfied, the theory is finite, but the expectation still depends on the otherwise arbitrary regulator masses M_r. Certainly, the expression (3.48) still depends on the term

$$\sum_r \sigma_r M_r^4 \log M_r^2 a^2 \tag{3.49}$$

which diverges when we decouple the mass of the regulators as $M_r \to \infty$.

(iii) Now, we decouple the regulator fields sending their mass to infinite $M_r \to \infty$. The only trace left are the divergent contribution stemming from the logarithms terms. They act as counterterms. For example, in order to counteract the divergence in Eq. (3.49) as $M_r \to \infty$, we introduce the counterterm

$$\delta\Lambda = \frac{1}{2\pi^2} \frac{1}{32} \sum_r \sigma_r M_r^4 \log M_r^2 a^2 + (\delta\Lambda)^f \tag{3.50}$$

where f refers to a "physical" quantity that is left after the infinity subtraction.

(iv) Finally, we can express the normalized energy density

$$\rho_{\rm ren} = \rho - \rho_{\rm sub}, \tag{3.51}$$

[10] Here, $\sum_i \sigma_i = \sigma_0 + \sum_r \sigma_r$, $\sum_i \sigma_i M_i^2 = \sigma_0 M_0^2 + \sum_r \sigma_r M_r^2$ and $\sum_i \sigma_i M_i^4 = \sigma_0 M_0^4 + \sum_r \sigma_r M_r^4$, where $\sigma_0 = 1$ and $M_0 = m$. This is possible because fermionic fields ($\sigma_i = -1$) give loop contributions with the opposite sign as those of bosonic fields ($\sigma_i = 1$).

where *sub* indicates the counterterms and the regulator fields contribution. Following the example of zeroth adiabatic order, we can express this part of the renormalized energy density $\rho_{\rm ren}$ as

$$\rho^{(0)}_{\rm ren} = \lim_{\Lambda\to\infty}\int_{\Lambda_{\rm IR}}^{\Lambda}\frac{dk}{k}\left(\frac{d\rho_k}{d\log k}\right) - \frac{1}{2\pi^2}\left\{\frac{\Lambda^4}{8a^4}+\frac{m^2\Lambda^2}{8a^2}-\left[\delta\Lambda^f-\frac{m^4}{64}\left(1-2\log\frac{4\Lambda^4}{a^2m^2}\right)\right]\right\}, \tag{3.52}$$

where, after the subtraction, when the cutoff Λ is sent to infinity, the renormalized energy remains finite and cutoff-independent by construction. We can see the totally renormalized energy density $\rho_{\rm ren}$ in Eq. (2.35) of Ref. [120].

In Eq. (3.52), $\delta\Lambda^f$ is a finite quantity with physical significance that we associate with the cosmological constant. The remaining counterterms coming from the second and fourth adiabatic orders are associated with the Einstein-Hilbert term and dimension four curvature invariants, respectively. This method makes explicit the role of counterterms and also explains the origin of the subtraction terms. It is important to emphasize that in the renormalization of Pauli-Villars, the mass of the regulators is assumed to be much larger than any accessible scale k, such that their contribution to the spectral density is highly suppressed at cosmological distances. So, only in the ultraviolet do the regulators play a role.

This procedure will be developed exhaustively in the following chapter.

3.8 Particle Interpretation

The expression (3.40) allows us to calculate the energy density of the scalar field $\phi(x)$ in the *in* vacuum through the integral (3.37) at any moment in cosmic history. However, another possible choice to obtain this expression is to use the transformation (3.32) in Eq. (3.40), and express the energy density $\rho_{\rm in}$ in terms of the arbitrary function $\chi_k^{\rm out}$ (associated or not with the *out* region) and the Bogoliubov coefficients α_k and β_k. If we perform this calculation, it is possible to identify two contributions to $\rho_{\rm in}$, one that we can identify as the contribution of the *out* vacuum independent of β_k and another contribution that depends on β_k which we can associate with the contribution of the *particles produced* in the transition between *in* and *out* regions. With this in mind, we can express $\rho_{\rm in}$ as

$$\rho_{\rm in} = \rho_{\rm out} + \rho_{\rm p}. \tag{3.53}$$

where $\rho_{\rm out}$ is the *out vacuum* contribution and $\rho_{\rm p}$ is the *produced particle* contribution.

If the spacetime is asymptotically adiabatic as $\eta \to \pm\infty$, then we can use the approximation (3.27) for $\chi_k^{\rm out}$, applicable for massive fields or large wavenumbers. Making this approximation, it is possible to demonstrate that when $\omega \gg H$ and $|\beta_k^{\rm ad}| \gg 1$ then the spectral density is well approximated by

$$\frac{d\rho_{\rm p}}{d\log k} \approx \frac{k^3}{2\pi^2a^3}|\beta_k^{\rm ad}|^2\frac{\omega_k}{a} \tag{3.54}$$

where $|\beta_k^{\rm ad}|$ are the Bogoliubov coefficients (3.33b) in the adiabatic regime. If we compare with the expression (3.25) for the number density of particles created, we can interpret the above relation in terms of particles, where $k^3/2\pi^2a^3|\beta_k^{\rm as}|^2\frac{\omega_k}{a}$ is the physical number density, the $1/a^3$ factor accounts for the physical volume of the universe and ω_k/a is the particle's energy. Here the expression (3.54) was constructed by neglecting terms with a time derivative, consequently $|\beta_k^{\rm ad}|$ will be of zeroth adiabatic order.[11]

Note: Here the spectral density for the *in* vacuum energy is given by

$$\frac{d\rho_{\rm in}}{d\log k} = \frac{d\rho_{\rm out}}{d\log k} + \frac{d\rho^{\rm p}}{d\log k} = \lim_{n\to\infty}\frac{k^3}{4\pi^2a^2}\left\{\left(|\beta_k|^2+\frac{1}{2}\right)\left[\left|\frac{d}{d\eta}\left(\frac{\chi_k^{{\rm out}(n)}}{a}\right)\right|^2+\omega_k^2|\chi_k^{{\rm out}(n)}|^2\right] + \alpha_k\beta_k^*\left[\left(\frac{d}{d\eta}\frac{\chi_k^{{\rm out}(n)}}{a}\right)^2+\omega_k^2\left(\chi_k^{{\rm out}(n)}\right)^2\right]+{\rm c.c.}\right\} \quad (3.56)$$

where (n) refers to the n adiabatic order of the adiabatic expansion for the *out* mode functions $\chi_k^{\rm out}$. From this expression is possible to relate the contribution to $\rho_{\rm in}$ from the *out* vacuum energy $\frac{d\rho_{\rm out}}{d\log k}$ given by Eq. (3.40), replacing *in* with *out* in that expression, and the contribution from the *particle production* contribution given by the remaining terms $\frac{d\rho^{\rm p}}{d\log k}$. In order to consider the approximation to $\frac{d\rho^{\rm p}}{d\log k}$ given by Eq. (3.54), it is necessary to consider only the zeroth adiabatic order $n=0$ given by the expression (3.30b), large frequencies $\omega_k \gg \mathcal{H}$, and an effective "particle production", that is, that $|\beta^{\rm ad}|^2 \geq 1$. Let's remember that $|\alpha_k|^2-|\beta_k|^2=1$, such that if $|\beta_k^{\rm ad}| \ll 1$, then $|\alpha_k^{\rm ad}\beta_k^{\rm ad}| \sim |\beta_k^{\rm ad}|$ and the relation (3.54) is not possible.

We must emphasize that the conditions under which Eq. (3.54) is valid are

(i) the mode function $\chi_k^{\rm out}$ is in the adiabatic regime where the approximation (3.27) is valid, such that $W_k^{(n)} \gg W_k^{(n+2)}$ where n is the adiabatic order,

(ii) the mode frequencies are long ($\omega_k \gg \mathcal{H}$),

(iii) and $|\beta_k^{\rm ad}| \geq 1$, that is, the "*particle production*" is effective.

In view of the above, we can express the energy density of the *in* vacuum in terms of the "particle production formalism". For this, let us rewrite Eq. (3.53)

[11] In the ultraviolet regime $k\to\infty$, that is, when $\lambda\to 0$, the expression for $\rho_{\rm p}$, Eq. (3.56) takes the form

$$\lim_{\Lambda\to\infty}\int_0^\Lambda \frac{dk}{k}\frac{d\rho_{\rm p}}{d\log k} = \frac{1}{2\pi^2a^4}\lim_{\Lambda\to\infty}\int_0^\Lambda [|\beta_k^{\rm ad}|^2k^4+\mathcal{H}|\alpha_k^{\rm ad}\beta_k^{\rm ad}|k^3\sin 2k\eta+\phi+...] \quad (3.55)$$

where we have consider $W_k \approx \omega_k \approx k$. From Eq. (3.55) it is possible to conclude that $|\beta_k|$ has to decay faster that $1/k^2$ according to the restriction for $N_k^{\rm in}$ in Eq. (3.26).

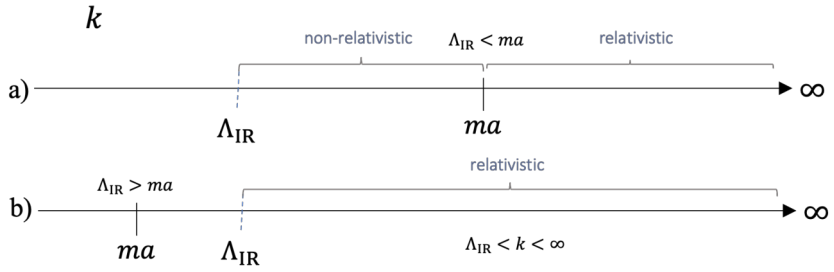

Figure 3.4: **Relativistic and non-relativistic modes**. a) Modes in the range $\Lambda_{\rm IR} < k < \infty$ for which $ma > \Lambda_{\rm IR}$ consist of modes that are relativistic and non-relativistic. b) Modes in the range $\Lambda_{\rm IR} < k < \infty$ for which $ma < \Lambda_{\rm IR}$ consist of modes that are only relativistic.

as

$$\rho_{\rm ren} = \rho_{\cancel{\rm ad}} + \rho^{\rm p}_{\rm ad} + (\rho^{\rm out}_{\rm ad})_{\rm ren}, \tag{3.57}$$

where we have separated the contribution of the modes that are in the adiabatic regime "ad" from those that are not "$\cancel{\rm ad}$". Regarding the modes that are in the adiabatic regime, as we have already seen, we can express these as $\rho_{\rm ad} = \rho^{\rm p}_{\rm ad} + (\rho^{\rm out}_{\rm ad})_{\rm ren}$, where we have considered the contribution of the created particles $\rho^{\rm p}_{ad}$ and the contribution of the renormalized energy density of the adiabatic vacuum given by $(\rho^{\rm out}_{\rm ad})_{\rm ren} = \rho^{\rm out}_{\rm ad} - \rho_{\rm sub}$.

Moreover, if we consider that the dominant modes in Eq. (3.57) are those that satisfy conditions i), ii) and iii), then we can write this as

$$\rho_{\rm ren} \approx \int \frac{dk}{k} \frac{k^3}{2\pi^2 a^3} |\beta^{\rm ad}_k|^2 \frac{\omega_k}{a}. \tag{3.58}$$

Classical Field Interpretation

Let's now briefly see if it is possible to identify $\rho_{\Lambda_{\rm IR}<k}$, the contribution to the energy density coming from the modes $\Lambda_{\rm IR} < k < \infty$, with the contribution of an homogeneous classical field, as happens for the zero mode $\vec{k} = 0$ and for the modes in the range $0 < k < \Lambda_{\rm IR}$ when these are non-relativistic (see Table 3.1, second row). For this purpose, we consider dividing $\rho_{\rm ren}$ for the modes in the range $\Lambda_{\rm IR} < k < \infty$ into the contribution from the non-relativistic modes and the contribution from the relativistic modes (see Figure 3.4), that is, $k < ma$ and $k > ma$, respectively, in such a way that

$$\rho_{\rm ren} = \rho_{<ma} + \rho_{>ma}, \tag{3.59}$$

where $\rho_{<ma}$ refers to the energy density contributions from the modes in $\Lambda_{\rm IR} < k < ma$ and $\rho_{<ma}$ to the modes from $ma < k < \infty$. The energy density of these last modes needs to be renormalized according to the Pauli-Villars renormalization procedure. Here, $\rho^{>ma}_{\rm ren}$ refers to the renormalized energy density of the *in* vacuum state (3.43). With this classification, in Table 3.2, we summarize the conditions under which it is possible to apply the classical field description for each contribution.

Modes in range $\Lambda_{\rm IR} < k < \infty$			
$\rho_{<ma}$	non-relativistic modes $\Lambda_{\rm IR} < k < ma$	$\omega_k^2 \approx m^2a^2$, $\chi_k^{\rm in} \approx \alpha_k\chi_0^{\rm out} + \beta_k\chi_0^{\rm out*}$	It admits classical homogeneous field interpretation
$\rho_{>ma}$	relativistic modes $ma < k < \infty$	gradients contribute to the energy density	no admits classical homogeneous interpretation

Table 3.2: Energy density for the modes in the range $\Lambda_{\rm IR} < k < \infty$, when $\Lambda_{\rm IR} < ma$. *In the first row* $\rho_{<ma}$ is the contribution to ρ_{ren} from the non-relativistic modes $\Lambda_{\rm IR} < k < ma$, for which $\omega_k^2 \approx m^2a^2$. These modes can be interpreted in terms of a homogeneous classical field. The second row corresponds to the relativistic modes for which $ma < k < \infty$. These modes do not allow for a classical interpretation.

As an example, we will briefly analyze the result shown in the first column of Table 3.2. There, $\rho_{<ma}$ refers to the contribution of the non-relativistic modes to the energy density $\rho_{\rm ren}^{\rm in}$, given by

$$\rho_{<ma} = \int_{\Lambda_{\rm IR}}^{ma} \frac{dk}{k} \frac{d\rho}{d\log k}. \tag{3.60}$$

For these modes the dispersion relation is given by $\omega_k \approx ma$ since $k \ll ma$, whose mode functions correspond to $\chi_k^{\rm in} \approx \alpha_k\chi_0^{\rm out} + \beta_k\chi_0^{\rm out*}$. Using these solutions in (3.43) we have that

$$\rho_{<ma} = \frac{1}{4\pi^2a^2}\int_{\Lambda_{\rm IR}}^{ma}\frac{dk}{k}k^3\Bigg\{\left(|\beta_k|^2+\frac{1}{2}\right)\left[\left|\frac{d}{d\eta}\left(\frac{\chi_0}{a}\right)\right|^2 + m^2|\chi_0|^2\right] + \alpha_k\beta_k^*\left[\left(\frac{d}{d\eta}\frac{\chi_0}{a}\right)^2 + m^2\chi_0^2\right] + \text{c.c.}\Bigg\}. \tag{3.61}$$

When we compare this result with the zero mode expression (3.38), we observe that it is possible to interpret this contribution to the energy density $\rho_{<ma}$ as that of a homogeneous classical field $\phi_{cl} = 1/a(A_0\chi_0 + B_0\chi_0^*)$ as long as we make the identification

$$\frac{1}{V}\left(N_0+\frac{1}{2}\right) \equiv \frac{1}{2\pi^2}\int_{\Lambda_{\rm IR}}^{ma}\frac{dk}{k}k^3\left(|\beta_k|^2+\frac{1}{2}\right),\ \frac{L_0}{V} \equiv \frac{1}{2\pi^2}\int_{\Lambda_{\rm IR}}^{ma}\frac{dk}{k}k^3\alpha_k\beta_k^*, \tag{3.62}$$

and if we are able to solve the system of equations $(|A_0|^2 + |B_0|^2)/2 = (N_0 + 1/2)/V$ and $A_0B_0^* = L_0/V$. Let's note that for N_0 and L_0 to be constant, the integration between the limits $\Lambda_{\rm IR} < k < ma$ must be constant, which, in general, does not happen. When the $\rho_{>ma}$ contribution to $\rho_{\rm ren}$ is subdominant, then is possible write Eq. (3.59) as

$$\rho_{\rm ren} = \frac{1}{2a^2}\left(|\dot{\phi}_{cl}|^2 + m^2a^2|\phi_{cl}|^2\right). \tag{3.63}$$

In the next chapter, we will extend this discussion to the case of a Dirac field.

3.8.1 The Concept of Particle

As a final section, we will review the concept of particle according to the main authors we have examined for this chapter, which will serve as the basis for the study of fermion fields in curved spaces.

As we have already reviewed, according to Ref. [120], to discuss a particle production formalism, it is necessary for the three conditions we have reviewed in Section 3.8 to be satisfied, that is, i) that the mode functions χ_k^{out} is in the adiabatic regime when the approximation (3.27) is valid, such that $W_k^{(n)} \gg W_k^{(n+2)}$ where n is the adiabatic order, ii) the mode frequencies are long ($\omega_k \gg \mathcal{H}$) and iii) the particle production is effective (that is $|\beta_k|^2 \gg 1$). With these conditions, and always that the adiabatic modes are dominant, we can consider the particle production energy density as

$$\rho_{\text{p}} = \frac{1}{2\pi^2}\int_0^\infty \frac{\omega_k}{a}|\beta_k|^2 k^2 dk. \tag{3.64}$$

On the other hand, according to Ref. [140], several conditions are required in order to talk about the number density of particles interpreted in a Minkowskian context, that is, i) the spacetime is asymptotically adiabatic ($\omega_k \gg \dot{\omega}_k$) in the remote past and future (for intermediate times the particle interpretation is ambiguous because positive and negative frequency solutions are mixing), ii) the spacetime curvature must not vary across the spatial size of the wavepacket of momentum k/a (in FLRW spacetime this implies $k/a > H$), and iii) $\omega_k^2 > 0$, that is, the mode must be oscillatory (if this condition is not satisfied the mode equation does not have oscillatory solutions).

Finally, according to Ref. [135], the concept of a particle is associated with the best possible description of a *physical vacuum* (also understood as the absence of particles). Birrell and Davis associate the presence of particles with *what* a quantum detector can register, therefore the concept of a particle is tied to the state of the detector. Particles can register their presence in some detectors but not in others, so they have an essentially observer-dependent quality. However, if spacetime is asymptotically adiabatic, it is possible to define the state of the detector unambiguously in the *in* and *out* regions and associate $|\beta_k|^2$ with the number density n_k of the particles produced due to the dynamics of spacetime.

Chapter 4

Fermion Fields on Curved Spacetimes

4.1 Introduction

In the context of semiclassical gravity, that we have outlined in the previous chapter, a "spectator" quantum field in presence of a dynamic background spacetime leads to the gravitational production of particles. As we have seen for a quantum scalar field on FLRW spacetime, there are circumstances in which it is possible to speak of a "particle production" interpretation and a *classical field* description for the vacuum energy density of the scalar field. In the present chapter, we explore whether these conditions hold when dealing with a quantum field of spin ½. Since a fermion quantum field introduces the condition of the Pauli exclusion principle, we will observe that a parallelism with the scalar field is not immediate. This chapter follows the results derived from the forthcoming research paper *Cosmic Spinors and the Weight of the Vacuum* [3].

Given the absence of direct detections of dark matter and the growing cosmological and astrophysical evidence of its gravitational presence in the universe, a plausible line of investigation about its nature is to consider that dark matter only interacts gravitationally with the rest of the universe. However, a dark matter model with these characteristics faces the challenge of accounting for a *production mechanism* that yields the correct abundance to satisfy observational constraints, as well as meeting the stability criterion (minimum the age of the universe). It is in this scenario that the gravitational particle production mechanism enters as a natural mechanism in the evolution of the universe, depending only on the mass of the particle and the nature of its coupling to gravity, without depending on how dark matter couples to other sectors of the standard model.[1] This is one of the main motivations for systematically exploring the behavior of the energy density, both of a scalar field and a fermionic field, in a dynamical spacetime.

The gravitational production of particles has been studied in various contexts. For quantum scalar fields during inflation, this phenomenon has been studied in Refs. [4, 142, 143, 144], as well as during the *reheating* period

[1] Different species of particles can be created by various mechanisms in the early universe. For any spin number (integer or half-integer), the most familiar mechanism is through collisions or decays of other particles. Also, in the case of spin-0 particles, they can be produced through topological defects or through the oscillations of a scalar field.

[145, 146]. In turn, for example, the gravitational production of particles on spacetimes that depend on a particular equation of state has been studied in Ref. [147], as well as for radiation-dominated universes [148]. For quantum fermionic fields, gravitational particle productions have been studied in standard cosmology scenarios [149, 150, 151], and for the inflationary period of expansion [144, 152, 5, 153, 154, 155, 156]. The renormalization of the energy-momentum tensor in FRLW universes has also been studied in the works of Navarro et al. [157, 158, 159, 160, 161, 162, 163, 164].

In the present thesis work, we focus on studying the phenomenon of gravitational particle production as a result of the expansion of a FLRW universe for a Dirac quantum field that only interacts (minimally coupled) with gravity. The fermionic field does not interact with the *inflaton* field nor with any other field of the standard model. We set the initial conditions to those that correspond to an early universe of inflationary expansion characterized by a De Sitter spacetime followed by a post-inflationary universe dominated by radiation. In general, our results can be applied to any transition that takes place in a FLRW universe.

The main objective is to characterize the evolution of the energy density of the Dirac field when a cosmic transition occurs in the universe. We analyze the contribution of the modes for the ranges $0 \leq k < \Lambda_{\text{IR}}$ and $\Lambda_{\text{IR}} < k < \infty$ where Λ_{IR} is the characteristic scale at the beginning of inflation $\mathcal{H}_i = \Lambda_{\text{IR}}$. We also consider the contribution of the relativistic modes and the non-relativistic modes, as well as the adiabatic and non-adiabatic modes, which allows us to analyze the density energy according to the contribution of the different modes. We also calculated analytically the solutions in a De Sitter and radiation-dominated universe, as well as solutions for a massless field and a homogeneous field, and we calculated approximate solutions when it is possible to make an adiabatic approximation. We characterize the energy density with respect to the *in* vacuum as $\rho = \rho_{\text{out}} + \rho_{\text{p}}$, where ρ_{out} is the contribution of the *out* vacuum, which we will renormalize using the Pauli-Villars procedure, and ρ_{p} is the contribution of the "gravitationally produced particles". We found that in general it is not possible to consider ρ as the contribution of gravitationally produced *particles* due to the restrictions imposed by the Pauli exclusion principle. However, under certain circumstances, it is possible to talk about the classical field description of the energy density.

The value of the mass m of the "produced particles" plays a central role in the analysis. Depending on the value of m, these particles can account for dark matter in the universe. For example, for a scalar field in the context of inflation, it has been found that the density of the particles produced is given by $n \sim H_{\text{inf}}^3$ if $m \leq H_{\text{inf}}$ where H_{inf} denotes the Hubble parameter during inflation. For the case of fermions, Chung et al. [5] have found that when the mass of the gravitationally produced particles is much smaller than the Hubble expansion rate at the end of inflation, i.e., $m \ll H_{\text{inf}}$, then $n_k = |\beta_k|^2 \sim 1/2$ when $k \sim ma(t)$, an identical result to the case of a conformally coupled scalar field. Here we address the form of the number density $n_k = |\beta_k|^2$ for different orders of approximation and mode contribution. As we shall see, when the fermionic field is massless, there is no gravitational particle production.

Regarding the process of renormalization of the expectation value of the

energy-momentum tensor, we use Pauli-Villars renormalization based on the adiabatic expansion of the mode functions (which contain information about how the fermionic field evolves on time). In curved spacetime, the renormalization process is more complicated than in Minkowski spacetime, as curvature introduces new types of divergences. To identify and deal with these divergences, we use the adiabatic expansion proposed by Barbero et al [159] based on a WKB-type expansion of the mode functions. On the other hand, the same authors have developed another method not based on a WKB-type expansion that overcomes some ambiguities of this expansion [164]. However, both methods allow for the determination of the subtraction terms and produce the same results for the renormalized quantities. The subtracted terms can be interpreted in terms of renormalization of coupling constants in the gravitational action functional. In the present work, we used this methodology to renormalize the energy density ρ_{in} and pressure p_{in} with respect to the *in* vacuum and we calculated the value of the *conformal anomaly*. In the previous chapter, we summarized the Pauli-Villars renormalization process using the work [120] as a reference.

The present chapter is organized as follows: in Section 4.2, we introduce the formalism of spin ½ Dirac fields on curved spaces and derive the mode equations for a FLRW spacetime. In Section 4.3, we derive exact and approximate solutions for the mode functions in different regimes of approximation. In Section 4.4, we define a cosmic transition and introduce the Bogoliubov transformations. In Section 4.5 and 4.6, we calculate the energy density for the modes $0 \geq k < \Lambda_{\text{IR}}$ and $\Lambda_{\text{IR}} < k < \infty$, in the same way we did in the previous chapter 3, and we calculate the renormalized value of ρ_{in} and p_{in} and the *trace anomaly*. Finally, in Sections 4.7-4.8, we review under what conditions (if they exist) it is possible to apply the "particle production formalism" and the classical field description. We use the signature $(+,-,-,-)$ and work with natural units $\hbar = c = 1$.

Literature Review: In the work of Barbero et al. [165], the authors propose an adiabatic regularization method based on a WKB-type expansion of the mode functions $u_k(\eta)$ and $u_k(\eta)$ (similar to that applied in adiabatic regularization for the scalar field (3.27)) to calculate the energy density ρ_{ψ}^{in} and the number density N_{ψ} of the gravitationally produced particles for a quantum Dirac field $\hat{\psi}(x)$. In our work, we recover the WKB-type expansion for the mode functions introduced by the authors in this work. This regularization method was applied to an expanding universe without regions that are asymptotically Minkowskian. In this particular case, the integral of the number of particles density n_k leads to divergences that need to be removed. This calculation was extended to the energy density and pressure in a de Sitter universe during the inflationary expansion, not only during asymptotically static regions. In particular, they confirm the adiabatic regularization method by calculating the conformal anomaly and the axial anomaly. Subsequent works extend the analysis to consider universes dominated by radiation in Ref. [159] and Yukawa-type interactions with a scalar field using the same adiabatic regularization process in Ref. [164]. Other proposals for adiabatic expansion to regularize the energy density are given in later works by Suman Ghosh [162, 161], similarly applied to a de Sitter and radiation dominated universe

in the same framework as the previous works. In Ref. [164], they move away from a WKB-like expansion, proposing an iterative method involving unitary transformations. Regarding this, in Herring et al. [148], the authors propose an expansion in the same spirit as Barbero et al. for adiabatic regularization of the energy density. We will discuss these authors more specifically later. Here, we use the original WKB-expansion of Ref. [165] for the Pauli-Villars regularization of the energy density.

In Chung et al. [5], they analyze the gravitational production of spin ½ particles directly related to $|\beta_k|^2$ for the heavy and light mass regimes compared to the inflation scale. In this study, they do not perform the adiabatic regularization treatment of the energy density or any other regularization method. The main result of this work is that for light masses $|\beta_k|^2 \to ½$. They apply the particle production formalism to a toy inflationary model with instant transition from a de Sitter universe to a radiation-dominated universe. In a numerical analysis of $|\beta_k|^2$, the authors confirm that most of the contribution to $|\beta_k|^2$ comes from non-relativistic modes with light mass relative to the inflation scale. Chung et al. also perform an analysis of the particle production resulting from the rapid oscillation of the inflaton after inflation. In Herring et al. [148], they recover the same analysis by considering an adiabatic expansion for mode functions beyond the zeroth order. On the other hand, the works by Ema et al. [154] perform a quite similar analysis to Ref. [5], recovering the expression for n_ψ in line with the latter. Similarly, they analyze particle production due to the rapid expansion related to coherent inflaton oscillations at the end of inflation. Unlike all previous analyses, Ema et al. [154] include a study of gravitational production for vector fields. In a separate work Stahl and Strobel [156], calculate the number of particles created in a de Sitter universe for an asymptotically adiabatic spacetime. Especially, they calculate β_k through iterative integration, considering a WKB-like ansatz similar to that used in Ref. [165].

In summary, all the previous works attempt to address whether a Dirac field of dark matter can account for the observed dark matter energy density. With the exception of Ref. [148], the distinction between the concepts of field and particle plays a rather superficial role, and the authors limit themselves to using the expression for $N_k \sim |\beta_k|^2$ to account for the production of dark matter particles through the expansion of the universe. A treatment that is closer to distinguishing between the concepts of particle and field is found in Herring et al [148]. As mentioned earlier, Ref. [148] follows a similar approach to Chung et al. [5], with a particular emphasis on the concept of particle production and adiabatic regularization through a WKB-like approximation (different from the proposal of Refs. [164, 162]). In this work, they calculate $|\beta_k|^2$ as in [5], obtaining a spectrum close to Maxwell-Boltzmann and applying it to the same toy inflationary model with instant reheating. In comparison to previous works, our study aims to emphasize the more general conditions under which the "particle production" formalism is applicable and when it is possible to speak of a classical field description that can play the role of dark matter (as in some axion dark matter models). It is also important to emphasize that in this thesis we renormalize using the Pauli-Villars method, with the original WKB-like adiabatic expansion proposed by Ref. [165], in order to

identify divergences. Our goal is to analyze the behavior of a minimally coupled and non-interacting Dirac quantum field, undergoing a cosmic transition as mentioned above. In addition, we aim to determine under what conditions the interpretation of particle production yields the correct estimated value of energy density, and under what conditions the latter can be considered as the contribution of a homogeneous classical Dirac field.

Pauli-Villars Regularization: In this work, we develop the Pauli-Villars renormalization of the energy density of a spin 1/2 field in an expanding universe. In this regard, we differentiate ourselves from the previously mentioned works. In those, the authors develop energy density regularization through adiabatic regularization. The adiabatic method identifies UV divergences by initially considering a slow variation of the scale factor, i.e., by considering a slow expansion of the universe. The Pauli-Villars regularization adopts this criterion to identify the divergences. For this purpose, it is natural to require a WKB-like expansion of the mode functions. When the adiabatic regularization method is applied to renormalize local expectation values, such as the energy-momentum tensor, it is equivalent to the DeWitt-Schwinger point-splitting method. This method has been extended to spin 1/2 fields in Ref. [166]. On the other hand, in Ref. [167], the authors demonstrated that adiabatic regularization is equivalent to n-wave regularization (which is essentially a variant of the Pauli-Villars regularization method (see Birrel and Davis Ref. [135]). Here, we make use of Pauli-Villars renormalization, supported by the work of Weinberg [168]. As mentioned earlier, Pauli-Villars utilizes a WKB-like approximation to analyze the divergences that are controlled by the introduction of Pauli-Villars regulators.

4.2 Formalism

Our main purpose is to analyze the evolution of the energy density of a free fermion field ψ minimally coupled to gravity, through the action

$$S_\psi = \int d^4x\sqrt{-g}\left\{\frac{i}{2}[\bar{\psi}\gamma^\mu(\nabla_\mu\psi) - (\nabla_\mu\bar{\psi})\gamma^\mu\psi] - m\bar{\psi}\psi\right\}, \tag{4.1}$$

where γ^μ are the global gamma matrices, related to the usual Minkowski ones by the vierbein field e^μ_a as $\gamma^\mu = e^\mu{}_a\gamma^a$, m is the mass of the field, $\bar{\psi}(x)$ denotes *Dirac conjugation* of the field $\psi(x)$ and $\nabla_\nu = \partial_\nu + \Omega_\nu$ denotes its covariant derivative (for the covariant representation of Dirac fields on curved spacetime see Refs. [169, 170, 171, 172]). The global gamma matrices satisfy the generalized Clifford algebra $\{\gamma^\mu(x), \gamma^\nu(x)\} = 2g^{\mu\nu}(x)$, where $g_{\mu\nu}$ is a general metric tensor and g its determinant. We use the convention that Latin indices $a, b, \ldots$ are used to label local inertial coordinates and Greek indices $\mu, \nu, \ldots$ for general coordinates. From here on, we will use the notation $\gamma^\mu = e^\mu{}_a\tilde{\gamma}^a$.

The covariant derivative is define in terms of the *connection coefficient* $\Omega_\nu(x)$ for the spinor field $\psi(x)$ which is given by

$$\Omega_\nu = -\frac{i}{4}\omega_{ab\nu}(x)\sigma^{ab}, \tag{4.2}$$

where $\sigma^{ab} = i[\tilde{\gamma}^a, \tilde{\gamma}^b]/2$ and the *spinor connection* (a generalization of the affine connection) is

$$\omega_{ab\nu} \equiv \eta_{ac} e^c{}_\mu e^\sigma{}_b \Gamma^\mu{}_{\sigma\nu} + \eta_{ac} e^c{}_\mu \partial_\nu e^\mu{}_b, \tag{4.3}$$

where η_{ac} is the Minkowski metric and $\Gamma^\mu{}_{\sigma\nu}$ are the Christoffel's symbols. The spin connection is antisymmetric in the first two indices, i.e., $\omega_{ab\nu} = -\omega_{ba\nu}$. The *vierbein* and the inverse vierbein matrices (defined at point $x^\mu = X^\mu$ by $e^\mu{}_a(X) = (\partial x^\mu/\partial y^a)|_{x^\mu = X^\mu}$ and $e^a{}_\mu(X) = (\partial y^a/\partial x^\mu)|_{x^\mu = X^\mu}$), which diagonalizes the metric $g_{\mu\nu}(x)$, obey the relations

$$\eta_{ab} = e^\mu{}_a e^\nu{}_b g_{\mu\nu} \quad \text{and} \quad g_{\mu\nu} = e^a{}_\mu e^b{}_\nu \eta_{ab}. \tag{4.4}$$

The action (4.1) describes how a spinor field $\psi(x)$ is coupled to gravity. If we assume the latter is governed by the Einstein-Hilbert action, then the spinor field minimally coupled to gravity is given by the action

$$S = S_m + S_\psi + \frac{M_{\rm pl}^2}{2} \int d^4x \sqrt{-g} R, \tag{4.5}$$

where R is the Ricci scalar and $S_m[g_{\mu\nu}, \psi]$ describes additional matter fields. Here $g_{\mu\nu}(x)$ is regarded as a classical external field, whereas the Dirac field $\psi(x)$, as well as the matter fields in the action of the standard model S_m, will be treated as quantum fields. Gauge fields and massless fermion fields are conformally invariant and do not react to changes in the expansion history. After varying with respect to the field $\bar{\psi}(x)$, the dynamical equation is provided by a generalization of the Dirac equation to curved spacetime given by

$$[i\gamma^\mu \nabla_\mu - m]\psi(x) = 0. \tag{4.6}$$

4.2.1 Dirac Fields on FLRW Spacetimes

In particular, for the conformal FLRW metric

$$ds^2 = a^2(\eta)[d\eta^2 - \delta_{ij} dx^i dx^j], \tag{4.7}$$

where η is the conformal time $\eta = \int dt/a(t)$ and $a(\eta)$ is the scale factor, we get according to Eq. (4.4) the vierbein coefficients $e^0{}_0 = e^1{}_1 = e^2{}_2 = e^3{}_3 = 1/a$ (the vierbein inherit the same symmetry as the metric) and the Christoffel symbols $\Gamma^0{}_{00} = \mathcal{H}$, $\Gamma^0{}_{ij} = \mathcal{H}\delta_{ij}$, $\Gamma^i{}_{j0} = \mathcal{H}\delta^i_j$. In these coordinates, the Hubble parameter is $\mathcal{H} = \dot{a}/a$, which is related to the "physical" Hubble constant H by $\mathcal{H} = aH$, where from now on a dot represents the derivative with respect to conformal time.

Inserting the above results into Eq. (4.3), these leads to the non-vanishing spin connections $\omega_{0ij} = -\mathcal{H}\delta_{ij}$, and $\omega_{i0j} = \mathcal{H}\delta_{ij}$ (note that $\omega_{\mu ab}$ depends on the signature of the metric). Plugging these results in Eq. (4.2), we get $\Omega_j = \frac{\mathcal{H}}{4}[\tilde{\gamma}^0, \tilde{\gamma}^j]$ and $\Omega_0 = 0$. Noticing that $\gamma^\mu = e^\mu{}_a \tilde{\gamma}^a$, then we can write

$$\gamma^0 = (1/a)\tilde{\gamma}^0, \quad \gamma^1 = (1/a)\tilde{\gamma}^1, \quad \gamma^2 = (1/a)\tilde{\gamma}^2, \quad \gamma^3 = (1/a)\tilde{\gamma}^3. \tag{4.8}$$

Inserting the above results into Eq. (4.6) and multiplying with $a\tilde{\gamma}^0$ from the left, we get the Dirac equation in a flat conformal FLRW spacetime as

$$i\partial_0\psi + \tilde{\gamma}^0\tilde{\gamma}^i\partial_i\psi + \frac{i\mathcal{H}}{4}\tilde{\gamma}^0\tilde{\gamma}^k[\tilde{\gamma}^0, \tilde{\gamma}^k]\psi - m\tilde{\gamma}^0 a\psi = 0. \tag{4.9}$$

Now, using the relation $\tilde{\gamma}^c\tilde{\gamma}^a\tilde{\gamma}^b - \tilde{\gamma}^c\tilde{\gamma}^b\tilde{\gamma}^a = 2\eta^{ca}\tilde{\gamma}^b - 2\eta^{cb}\tilde{\gamma}^a - 2i\epsilon^{cabd}\tilde{\gamma}_d\tilde{\gamma}^5$, where ϵ^{cabd} is the Levi-Civita connection, we can recast the commutator in Eq. (4.9) and get

$$i\tilde{\gamma}^0\left(\partial_0 + \frac{3\mathcal{H}}{2}\right) + i\tilde{\gamma}^k\partial_k\psi - ma\psi = 0. \tag{4.10}$$

Finally, upon defining $\psi \equiv a^{-3/2}\tilde{\psi}$, we can obtain

$$i\tilde{\gamma}^0\partial_0\tilde{\psi} + i\tilde{\gamma}^k\partial_k\tilde{\psi} - ma\tilde{\psi} = 0 \quad \longrightarrow i\tilde{\gamma}^\mu\partial_\mu\tilde{\psi} - m_{\text{eff}}\tilde{\psi} = 0, \tag{4.11}$$

where $m_{\text{eff}} = ma$ is called the *effective mass* or *conformal mass*. So, the field $\tilde{\psi}$ solves the regular Dirac equation with effective mass $m_{\text{eff}} = ma$.

Once we have written the Dirac equation in an FLRW spacetime, we proceed to quantize the field $\psi(x)$ and calculate the expectation value of the energy-momentum tensor, which is the source of Einstein's semiclassical equations. Our objective is to analyze the evolution of the energy density as the universe experiments a transition between an *in*-region to a subsequent *out*-region (similar to a scattering process in QFT) like, for example, from an *in* region during which the universe accelerates exponentially (an inflationary period) to a subsequent *out* region during which the expansion is decelerating, namely, during the radiation domination era. In general, the *in* and *out* regions refer to two different epochs of a transition and are not *apriori* related to the *"particle production formalism"*. In the *in* region, the field ψ is considered as a *spectator* field, which allows us to control the "initial" conditions for field fluctuations.

4.2.2 Field Quantization

In the semiclassical treatment of gravity, the gravitational field remains classical while the other matter fields obey a quantum formulation. In order to quantize the Dirac field ψ, we proceed according to the canonical quantization recipe introducing the ladder operators for the creation and annihilation of "*particles*" and "*antiparticles*", denoted as $\hat{a}_{\vec{k}\lambda}$ and $\hat{b}^\dagger_{\vec{k}\lambda}$ [2] , and their anti-commutation relations $\{\hat{a}_{\lambda,\vec{k}}, \hat{a}^\dagger_{\lambda',\vec{k}'}\} = \{\hat{b}_{\lambda,\vec{k}}, \hat{b}^\dagger_{\lambda',\vec{k}'}\} = \delta_{\lambda,\lambda'}\delta'_{k\vec{k}\vec{k}}$ and $\{\hat{a}_{\lambda,\vec{k}}, \hat{b}^\dagger_{\lambda',\vec{k}'}\} = 0$. With these, the Dirac field $\hat{\psi}$ can be written as

$$\hat{\psi} = \sum_\lambda \int d^3k \left[\hat{a}_{\vec{k}\lambda}U_{\vec{k}\lambda} + \hat{b}^\dagger_{\vec{k}\lambda}V_{\vec{k}\lambda}\right], \tag{4.12}$$

[2]The annihilation and creation operators can be interpreted as creating particles and antiparticles of comoving momentum $\vec{k}$. Actually, these "particles-antiparticles" do not represent localized particles, these are eigenvectors of the momentum operator.

where the momentum expansion of the eigenspinors $U_{\vec{k}\lambda}(x)$ and $V_{\vec{k}\lambda}(x)$ are given by

$$U_{\vec{k}\lambda} = \frac{e^{i\vec{k}\cdot\vec{x}}}{(2\pi a)^{3/2}} \begin{pmatrix} u_k \xi_\lambda \\ v_k \frac{\vec{\sigma}\cdot\vec{k}}{k} \xi_\lambda \end{pmatrix}, \quad \text{or} \quad U_{\vec{k}\lambda} = \frac{e^{i\vec{k}\cdot\vec{x}}}{(2\pi a)^{3/2}} \begin{pmatrix} u_k \xi_\lambda \\ v_k \lambda \xi_\lambda \end{pmatrix}, \tag{4.13a}$$

$$V_{\vec{k}\lambda} = \frac{e^{-i\vec{k}\cdot\vec{x}}}{(2\pi a)^{3/2}} \begin{pmatrix} -v_k^* \xi_{-\lambda} \\ -u_k^* \frac{\vec{\sigma}\cdot\vec{k}}{k} \xi_{-\lambda} \end{pmatrix}, \qquad V_{\vec{k}\lambda} = \frac{e^{-i\vec{k}\cdot\vec{x}}}{(2\pi a)^{3/2}} \begin{pmatrix} -v_k^* \xi_{-\lambda} \\ \lambda u_k^* \xi_{-\lambda} \end{pmatrix}, \tag{4.13b}$$

where ξ_λ is the normalized two-component spinor stisfying $\xi^\dagger_{\lambda'}\xi_\lambda = \delta_{\lambda'\lambda}$ and the property $\frac{\vec{\sigma}\cdot\vec{k}}{2k}\xi_\lambda = (\lambda/2)\xi_\lambda$ where $\lambda = \pm 1$ represents the helicity. Also $U_{\vec{k}\lambda}$ and $V_{\vec{k}\lambda}$ are related by *charge conjugation* operation (e.g. $V_{\vec{k}\lambda} = CU_{\vec{k}\lambda} = i\gamma^2 U^*_{\vec{k}\lambda}$) [3] with $u_k(\eta)$ and $v_k(\eta)$ two time-dependet functions known as *mode functions*[4]. In particular, because of the homogeneity and isotropy of the metric (4.7), we may assume that the mode functions only depend on $k \equiv |\vec{k}|$.

Note: To write the solutions (4.13), we have used the ansatz of the form

$$\psi_k(x) = \begin{pmatrix} u_k(\eta) \\ v_k(\eta) \end{pmatrix} \otimes \begin{pmatrix} \psi_L \\ \psi_R \end{pmatrix} e^{i\vec{k}\cdot\vec{x}}, \tag{4.14}$$

where we have chosen the *positive frequency* solutions and $\begin{pmatrix} \psi_L \\ \psi_R \end{pmatrix}$ correspond to the Weyl eigenspinors of the helicity operator $(\hat{k}\cdot\vec{\sigma}/k)\psi_{R,L} = \pm\psi_{R,L}$ which have two eigenvalues $\lambda = \pm 1$. This corresponds to the massless Dirac equations $i\tilde{\gamma}^\mu k_\mu \tilde{\psi} = 0$ with $k_\mu = \partial_\mu$ for $\tilde{\psi} = \begin{pmatrix} \psi_L \\ \psi_R \end{pmatrix}$ which have the solutions $\psi_L = i\vec{\sigma}\cdot\vec{k}/k\psi_R$ and $\psi_R = -i\vec{\sigma}\cdot\vec{k}/k\psi_L$. With these, we can write Eq. (4.14) as

$$\psi_{k,\lambda}(x) = \begin{pmatrix} u_k(\eta)\xi_\lambda \\ v_k(\eta)\frac{\hat{k}\cdot\vec{\sigma}}{k}\xi_\lambda \end{pmatrix} e^{i\vec{k}\cdot\vec{x}}, \quad \text{with} \quad \xi_{\lambda=\pm1} = \psi_{R,L}. \tag{4.15}$$

It makes sense that the helicity operator captures the spin information (which is a conserved quantity) through the constant eigenspinors ξ_λ (solutions of the massless Dirac equation) since the time dependence comes from the effective mass $m_{\text{eff}} = ma$ in Eq. (4.11) whose effect is captured by the time-dependent functions $u_k(\eta), v_k(\eta)$. Finally, we have that the

[3] In order to obtain the expression Eq. (4.13), we need to take into account the expression $-i\sigma^2\xi^*_\lambda = \lambda\xi_{-\lambda}$. For example, if we consider Eq. (4.16) we can write $-i\sigma^2\xi_{+1} = \xi_{-1}$ where we have used the Pauli matrix $\sigma^2 = \begin{pmatrix} 0 & -i \\ i & 0 \end{pmatrix}$.

[4] Because the mode function $V_{\vec{k}\lambda}$ arises from the charge conjugation matrix acting on $U_{\vec{k}\lambda}$ we can impose the Majorana condition on ψ simply by setting $b_{\vec{k}\lambda} = a_{\vec{k}\lambda}$. It is hence straightforward to extend our analysis to Majorana fermions. Weyl fermions (massless) are also easy to deal with. In that case, we can set $u = v$, which effectively yields two independent massless fields, one for each chirality.

normalized spinors written are

$$\xi_{+1} = \frac{1}{\sqrt{2k(k+k_3)}}\begin{pmatrix} k+k_3 \\ k_1+ik_2 \end{pmatrix} \text{ and } \xi_{-1} = \frac{1}{\sqrt{2k(k+k_3)}}\begin{pmatrix} -k_1+ik_2 \\ k+k_3, \end{pmatrix} \tag{4.16}$$

with $\vec{k} = (k_1, k_2, k_3)$ and $\xi_\lambda^\dagger \xi_{\lambda'} = \delta_{\lambda,\lambda'}$. When $k_1 = k_2 = 0$ we have $\xi_{+1} = \begin{pmatrix} 1 \\ 0 \end{pmatrix}$ and $\xi_{-1} = \begin{pmatrix} 0 \\ 1 \end{pmatrix}$.

The Dirac product on the solution ψ to equations (4.11) is given by

$$(\psi|\psi) = \int_\Sigma \bar{\psi}\gamma^\alpha(x)\psi n_\alpha d\Sigma, \tag{4.17}$$

where the vector n_α is the future-directed normal to the spacelike Cauchy hypersurface Σ, and $d\Sigma$ is the invariant "volume element" on Σ. It is easy to calculate Eq. (4.17) if we choose Σ to be a slice of constant conformal time η, then the future-directed normal vector n_α has components $(a(\eta), 0, 0, 0)$. In this case we have

$$(\psi|\psi) = \int_\Sigma \psi^\dagger\psi\sqrt{-g}d^3x. \tag{4.18}$$

where $\bar{\psi} = \psi^\dagger\tilde{\gamma}^0$ is the Dirac adjoint and where the integration is over a constant $x^0 = \eta$ Cauchy hypersurface ($d\Sigma = \sqrt{-g}d^3xa^3d^3x$). Also we have use the relations $(\gamma^0)^2 = I$ and $\gamma^0 = (1/a)\tilde{\gamma}$.

Finally, with the ansatz (4.12) into Eq. (4.18) we have $(U_{\vec{k}\lambda}|U_{\vec{k}'\lambda'}) = (V_{\vec{k}\lambda}|V_{\vec{k}'\lambda'}) = \delta_{\lambda\lambda'}\delta^{(3)}(\vec{k}-\vec{k}')$, which implies the normalization condition for the mode functions as [5]

$$|u_k(\eta)|^2 + |v_k(\eta)|^2 = 1. \tag{4.19}$$

This condition assures the standard anticommutation relations for the creation and annihilation operators given by [6] $\{a_{\vec{k}\lambda}, a^\dagger_{\vec{k}'\lambda'}\} = \{b_{\vec{k}\lambda}, b^\dagger_{\vec{k}'\lambda'}\} = \delta^3(\vec{k}-\vec{k}')\delta_{\lambda\lambda'}$ with all the others combinations equal to zero.

4.2.3 Mode Equations

Now, we will derive the dynamic equations for the mode functions, $u_k(\eta)$ and $v_k(\eta)$, which encapsulate the information about how the field $\hat{\psi}(x)$ evolves as spacetime evolves over time. From Eq. (4.13), we observe that the dynamic evolution of the field depends on the mode functions $u_k(\eta)$ and $v_k(\eta)$. To

[5] Here we have use the integral $\int_\Sigma d^3x e^{i\vec{x}\cdot(\vec{k}-\vec{k}')} = (2\pi)^3\delta^{(3)}(\vec{k}-\vec{k}')$ and the normalization condition $\xi_\lambda^\dagger\xi_\lambda = \delta_\lambda\delta_{\lambda'}$.

[6] These relations are established imposing the anticommutation relation for the Dirac field $\{\psi_\lambda(x)\psi^\dagger_{\lambda'}(x')\} = \delta(x-x')\delta_{\lambda,\lambda'}$. Using the Fourier decomposition (4.12), the solutions (4.13) and the normalization condition (4.19), the Dirac field anticommutation relation is satisfied if $\{a_{\vec{k}\lambda}, a^\dagger_{\vec{k}'\lambda'}\} = \{b_{\vec{k}\lambda}, b^\dagger_{\vec{k}'\lambda'}\} = \delta^3(\vec{k}-\vec{k}')\delta_{\lambda\lambda'}$ are satisfied. Also, we have used the delta Dirac definition given by $(1/(2\pi)^3)\int d^3k \exp[ik(x-x')] = \delta^{(3)}(x-x')$.

obtain their dynamical equations, we put Eq. (4.13) into Eq. (4.11) and using the gamma matrix given by

$$\tilde{\gamma}^0 = \begin{pmatrix} 1 & 0 \\ 0 & -1 \end{pmatrix} \text{ and } \tilde{\gamma}^i = \begin{pmatrix} 0 & \sigma^i \\ -\sigma^i & 0 \end{pmatrix}, \tag{4.20}$$

we can write the Dirac equations as $i\dot{u}_k\xi_\lambda + i\lambda v_k \vec{\sigma}\cdot\vec{k}\xi_\lambda - mau_k\xi_\lambda = 0$ and $-i\dot{v}_k\lambda\xi_\lambda - iu_k\vec{\sigma}\cdot\vec{k}\xi_\lambda - mav_k\lambda\xi_\lambda = 0$. Now, using the eigen-equation $(\vec{\sigma}\cdot\vec{k}/k)\xi_\lambda = \lambda\xi_\lambda$ and the normalization condition for the eigen-spinors $\xi^\dagger_\lambda\xi_{\lambda'} = \delta_{\lambda,\lambda'}$ we get the following first-order coupled differential equations

$$\dot{u}_k + imau_k + ikv_k = 0, \tag{4.21a}$$
$$\dot{v}_k - imav_k + iku_k = 0. \tag{4.21b}$$

Next, multiplying Eq. (4.21a) by v^*_k and subtracting the complex conjugation of Eq. (4.21b) multiplied by u_k, and using the normalization condition (4.19) we get the Wronskian condition given by $\dot{u}_k v^*_k - u_k\dot{v}^*_k = -ik$.

Finally, deriving equations (4.21a) and using $\dot{v}_k = imav_k - iku_k$ and $\dot{u}_k = -imau_k - ikv_k$, and similarly for (4.21b), we obtain the following two decoupled second-order equations for u_k a and v_k:

$$\ddot{u}_k + [\omega_k^2 + im\dot{a}]u_k = 0, \tag{4.22a}$$
$$\ddot{v}_k + [\omega_k^2 - im\dot{a}]v_k = 0, \tag{4.22b}$$

where $\omega_k = \sqrt{m^2a^2 + k^2}$. Here, the expression $\tilde{\omega}^2_{k\pm} = \omega_k^2 \pm im\dot{a}$ corresponds to the frequency of the mode functions u_k and v_k, respectively, and ω_k^2 is the frequency of the fermion field $\hat{\psi}(x)$. Note that a solution for v_k can be obtained from a solution for u_k by the replacement $m \to -m$. From now on, we will refer to these equations as the *mode equations* of first (4.21) and second differential order (4.22).

It turns out to be convenient to recast Eq. (4.21) as the Schrodinger equation for a non-relativistic spin-1/2 particle in a time-dependent magnetic field $\vec{B}$. Namely, setting by defining the two-component spinor $\psi \equiv (u_k, v_k)$, equations (4.21) can be cast as

$$i\dot{\psi} = H\psi, \text{ where } H = \vec{B}\cdot\vec{\sigma} \text{ and } \vec{B} = (k, 0, ma). \tag{4.23a}$$

The latter admits the formal solution

$$\psi(t) = T\exp\left(-i\int_{t_0}^{t} d\tilde{t}\tilde{H}\right)\psi_0, \tag{4.23b}$$

which is particularly useful in the cases in which exact solutions are ready found, namely, when $k = 0$ or when $m = 0$.

Finally, we remark that for conformal fields on conformal spacetimes, there is no gravitational particle production as gravity does not influence the dynamical equations. In the case of a spin 1/2 field on a conformal spacetime (like Eq. (4.7)), this occurs when the field is massless. If in the mode equations (4.22), we set $m = 0$, these reduce to the trivial expression for Minkowskian spacetime; therefore, gravitational effects do not exist in this case.

4.3 Approximate and Exact Solutions

In this section, we will discuss approximate and exact solutions to the dynamical equations (4.22) for the u_k and v_k mode functions. For the cases of a massless $m = 0$ and homogeneous $k = 0$ Dirac field, and for a spinor on inflationary and radiation dominated universe, we found exact solutions that describes the evolution of ψ on a FLRW spacetime. However, in general, there are no exact analytical solutions to the mode equation (4.22), so we shall rely on approximate solutions instead. We present high-frequency and low-frequency solutions to the mode functions in the next two subsections. In the first case, we will consider solutions for frequencies that satisfy $\omega_k \gg \mathcal{H}$, when an adiabatic approximation of $u_k,\ v_k$ is possible. In the second case, we will discuss the regime in which $ma \ll \mathcal{H}$ and $k \ll \mathcal{H}$, such that a small mass and small momentum approximation is possible.

4.3.1 Exact Solutions

Massless Dirac Field

In the case of a massless Dirac field, the dynamical equations (4.22) take the form $\ddot{u}_k + k^2 u_k = 0$ and $\ddot{v}_k + k^2 v_k = 0$. The solutions to these equations are given by

$$u_k^{m=0} = C\exp(-ik\eta) + D\exp(ik\eta), \tag{4.24a}$$
$$v_k^{m=0} = E\exp(-ik\eta) + F\exp(ik\eta). \tag{4.24b}$$

These solutions satisfy the normalization condition (4.19) and the Wronskian condition $\dot{u}_k v_k^* - u_k \dot{v}_k^* = -ik$. Putting Eq. (4.24) into Eq. (4.22) we find that $E = C$ and $D = -F$. If we choose the defined solution "positive frequency" we obtain, after normalization, that at zeroth order in mass

$$u_k^{m=0} = \frac{1}{\sqrt{2}}\exp(-ik\eta), \quad v_k^{m=0} = \frac{1}{\sqrt{2}}\exp(-ik\eta), \tag{4.25a}$$

and for defined solution "negative frequency"

$$u_k^{m=0} = -\frac{1}{\sqrt{2}}\exp(ik\eta), \quad v_k^{m=0} = \frac{1}{\sqrt{2}}\exp(ik\eta). \tag{4.25b}$$

This is equivalent to choosing initial conditions to determine the coefficients C and D for the system of equations (4.24). Negative and positive frequency solutions are related by charge conjugation. When $m = 0$, the Dirac field is conformally coupled. In this case, the field evolves as in Minkowski spacetime, and it does not experience the expansion of the universe, hence there is not room for gravitational particle production.

Homogeneous Dirac Field

In this case let's consider solutions to Eq. (4.22) with $k = 0$ and $\omega_k \sim ma$. One can also solve exactly the system (4.22) with $k = 0$ and arbitrary m. Two linearly independent solutions are, for instance,

$$u_{k=0} = \exp\left(-i\int ma\, d\eta\right), \quad v_{k=0} = 0. \tag{4.26a}$$

and

$$u_{k=0} = 0, \quad v_{k=0} = \exp\left(i \int ma\, d\eta\right). \tag{4.26b}$$

Again, one solution is "positive-frequency" and the other "negative-frequency," and both solutions are related by "charge conjugation". When $k = 0$ the Hamiltonian in equation (4.23a) is diagonal and equation (4.23b) immediately leads to the positive frequency exact solution (4.26a). As opposed to what happens in the scalar case, such positive frequency solutions exist even when the field is homogeneous. A negative frequency solution can be found by charge conjugation of the previous solution, as usual.

Dirac Spinor in de Sitter spacetime

De Sitter universe is characterized by the scale factor $a(t) = e^{Ht}$ where H is the Hubble constant. In terms of the conformal time η we have $a(\eta) = (-H\eta)^{-1}$ and $\eta = (-He^{Ht})^{-1}$. Solutions to Eq. (4.22) in a De Sitter universe that satisfies the appropriate asymptotic conditions in the remote past are given by

$$u(z) = i\frac{\sqrt{z\pi}}{2} e^{\pi\mu/2} H^{(1)}_{\nu_+}(z), \tag{4.27a}$$

$$v(z) = \frac{\sqrt{z\pi}}{2} e^{\pi\mu/2} H^{(1)}_{\nu_-}(z), \tag{4.27b}$$

where $z = -k\eta$, $\mu = m/H$, $\nu_\pm = \pm\frac{1}{2} - i\mu$ and $H_{\nu_\pm}(z)$ are the Hankel functions of the first kind. See Appendix C.1 for details.

Dirac Spinor in Radiation Dominated Universe

A radiation dominated universe is characterized by the scale factor $a(t) = a_0\sqrt{t}$ where a_0 is a constant with t the *cosmic time*. In terms of the conformal time η we have $a(\eta) = \frac{a_0^2}{2}\eta$ with $\eta = \frac{2}{a_0}\sqrt{t}$ and $\dot{a}_0 \equiv \dot{a}(t_0) = \frac{a_0^2}{2} \equiv H_R$. Solutions to Eq. (4.22) in a radiation dominated universe that satisfies the asymptotic conditions (4.29) in the remote future are given by

$$u_k = \exp\left(-\frac{\pi k^2}{8mH_R}\right) D_\alpha\left(\sqrt{2}e^{i\pi/4} z\right), \tag{4.28a}$$

$$v_k = \frac{e^{i\pi/4}k}{\sqrt{2mH_R}} \exp\left(-\frac{\pi k^2}{8mH_R}\right) D_{\alpha-1}\left(\sqrt{2}e^{i\pi/4} z\right). \tag{4.28b}$$

where $z = \sqrt{mH_R}\eta$, $\alpha = -ik^2/mH_R$ and $D_\alpha(z)$ are the cylindrical parabolic functions. See Appendix C.2 for details.

4.3.2 High Frequencies Approximation

When the field frequency ω_k is much greater than the Hubble parameter $\omega_k \gg \mathcal{H}$, it is possible to rely on approximate solutions given by an *adiabatic expansion*. We found in the literature a variety of approximate solutions to the second-order differential equations (4.22), by adopting an "adiabatic" expansion in the number of time derivatives of the scale factor. Similar to the

case of a scalar field on curved spacetime, these solutions make use of a WKB-expansion for the mode functions $u_k(\eta)$ and $v_k(\eta)$ (see for example Refs. [165], [173] and [174]). Here, we use the first proposal given by Ref. [165], where the authors propose an ansatz with the form

$$u_k = \sqrt{\frac{\omega_k + ma}{2\omega_k}} \exp\left(-i\int \Omega(\tilde{\eta})d\tilde{\eta}\right) F(\eta), \tag{4.29a}$$

$$v_k = \sqrt{\frac{\omega_k - ma}{2\omega_k}} \exp\left(-i\int \Omega(\tilde{\eta})d\tilde{\eta}\right) G(\eta), \tag{4.29b}$$

where $\omega_k = \sqrt{m^2a^2 + k^2}$ and the time-dependent function $\Omega(\eta)$, $F(\eta)$ and $G(\eta)$ are expanded adiabatically as

$$\Omega(\eta) = \omega_k + \omega_k^{(1)} + \omega_k^{(2)} + \omega_k^{(3)} + \omega_k^{(4)} + \ldots, \tag{4.30a}$$

$$F(\eta) = 1 + F^{(1)} + F^{(2)} + F^{(3)} + F^{(4)} + \ldots, \tag{4.30b}$$

$$G(\eta) = 1 + G^{(1)} + G^{(2)} + G^{(3)} + G^{(4)} + \ldots, \tag{4.30c}$$

where the superscripts indicate the adiabatic order, that is $F^{(n)}$, $G^{(n)}$ and $\omega_k^{(n)}$ are functions of adiabatic order n, i.e. they contain n derivatives of the scale factor $a(\eta)$. The time-dependent functions $F^{(n)}$ and $G^{(n)}$ are complex functions and we can write these like $F^{(n)} = f_x^{(n)} + if_y^{(n)}$ and $G^{(n)} = g_x^{(n)} + ig_y^{(n)}$.[7] This expansion is generally applicable when $\omega_k \gg \mathcal{H}$, that is, for short wavelengths modes or massive fields. Strictly speaking, the "adiabatic regime" holds whenever expressions (4.29) is a valid approximation of the mode equation, no matter what the value of the frequency ω_k is. In general when the mode frequency becomes small, $\omega_k \ll \mathcal{H}$, the approximate solution (4.29) stops working. Then the approximate solution for low frequencies (small mass or long wavelength) is applicable. As an example of the procedure described in Ref. [165], we will calculate the approximate solutions u_k and v_k to first-order adiabatic (in Appendix C.3 we calculate these solutions up to fourth-order adiabatic). For this, it is useful to write the coupled differential equations for u_k and v_k, Eq. (4.21), as

$$ku_k = i\dot{v}_k + mav_k, \tag{4.31a}$$

$$kv_k = i\dot{u} - mau_k. \tag{4.31b}$$

Now, substituting the ansatz (4.29) for u_k and v_k into Eq. (4.31a) we obtain the expression

$$k\left(\frac{W_+}{W_-}\right)F = i\left[\left(\frac{\dot{W}_-}{W_-}\right)G - i\Omega G + \dot{G}\right] + maG, \tag{4.32}$$

[7] One more formal solution was given in Refs. [174] and [175] overcoming the arbitrariness in the adiabatic expansion of the mode function that is somewhat inconvenient. However, all these works obtain exactly the same results for the renormalized expressions ρ_k and p_k.

where $W_\pm = \sqrt{\frac{\omega_k \pm ma}{2\omega_k}}$ and similarly for Eq. (4.31b). After some straightforward algebra and recalling that $\omega_k^2 = k^2 + m^2a^2$, we can write both equations as

$$(\omega_k - ma)G = \frac{i}{2}\frac{1}{(\omega_k + ma)}\left(m\dot{a} - \frac{ma\dot{\omega}_k}{\omega_k}\right)F + \Omega F + i\dot{F} - maF, \quad (4.33a)$$

$$(\omega_k + ma)F = \frac{i}{2}\frac{1}{(\omega_k - ma)}\left(\frac{ma\dot{\omega}_k}{\omega_k} - m\dot{a}\right)G + \Omega G + i\dot{G} + maG, \quad (4.33b)$$

$$F^*F(\omega_k + ma) + G^*G(\omega_k - ma) = 2\omega_k, \quad (4.33c)$$

where we have used the relation $m^2a\dot{a} = \dot{\omega}_k\omega_k$ and the third equation follows from the normalization condition (4.19). By keeping only terms in first adiabatic order in Eq. (4.33) and taking into account Eq. (4.30) we obtain

$$(\omega_k - ma)G^{(1)} = (\omega_k - ma)F^{(1)} + \omega_k^{(1)} + \frac{i}{2}\frac{1}{(\omega_k + ma)}\left(m\dot{a} - \frac{ma\dot{\omega}_k}{\omega_k}\right), \quad (4.34a)$$

$$(\omega_k + ma)F^{(1)} = (\omega_k + ma)G^{(1)} + \omega_k^{(1)} + \frac{i}{2}\frac{1}{(\omega_k - ma)}\left(\frac{ma\dot{\omega}_k}{\omega_k} - m\dot{a}\right), \quad (4.34b)$$

$$(\omega_k + ma)(F^{(1)} + F^{(1)*}) + (\omega_k - ma)(G^{(1)} + G^{(1)*}) = 0. \quad (4.34c)$$

Now, using the decomposition $F^{(0)} = f_x^{(0)} + if_y^{(0)}$ and $G^{(0)} = g_x^{(0)} + ig_y^{(0)}$, and working the real part, we have $(\omega_k - ma)(g_x^{(1)} - f_x^{(1)}) = \omega_k^{(1)}$, $(\omega_k + ma)(g_x^{(1)} - f_x^{(1)}) = -\omega_k^{(1)}$, and $(\omega_k + ma)f_x^{(1)} + (\omega_k - ma)g_x^{(1)} = 0$, from which after some straightforward manipulations we obtain $f_x^{(1)} = g_x^{(1)} = \omega_k^{(1)} = 0$. On other hand, the imaginary part gives two dependent equations

$$(\omega_k - ma)(g_y^{(1)} - f_y^{(1)}) = \frac{1}{2}\frac{1}{(\omega_k + ma)}\left(m\dot{a} - \frac{ma\dot{\omega}_k}{\omega_k}\right), \quad (4.35a)$$

$$(\omega_k + ma)(g_y^{(1)} - f_y^{(1)}) = -\frac{1}{2}\frac{1}{(\omega_k - ma)}\left(\frac{ma\dot{\omega}_k}{\omega_k} - m\dot{a}\right), \quad (4.35b)$$

from which the solution is given by $g_y^{(1)} - f_y^{(1)} = \frac{1}{2}\frac{m\dot{a}}{\omega_k^2}$. To alleviate this ambiguity we can use the fact that $u_k(-m) = v_k(m)$[8], that is equivalent to $F^{(n)}(-m) = G^{(n)}(m)$. This fact implies that $f_y^{(1)}(-m) - f_y^{(1)} = \frac{1}{2}\frac{m\dot{a}}{\omega_k^2}$ and from here is necessary to write $f_y^{(1)}(-m) = -f_y^{(1)}(m)$. From a direct manipulation we obtain

$$g_y^{(1)} = \frac{m\dot{a}}{4\omega_k^2}, \quad f_y^{(1)} = -\frac{m\dot{a}}{4\omega_k^2}. \quad (4.36)$$

With the results above is possible to write the adiabatic expansion (4.29) up to first order as

$$u_k^{(1)} = \sqrt{\frac{\omega_k + ma}{2\omega_k}}\exp\left(-i\int\omega_k(\tilde{\eta})d\tilde{\eta}\right)\left[1 - \frac{im\dot{a}}{4\omega_k^2}\right], \quad (4.37a)$$

$$v_k^{(1)} = \sqrt{\frac{\omega_k - ma}{2\omega_k}}\exp\left(-i\int\omega_k(\tilde{\eta})d\tilde{\eta}\right)\left[1 + \frac{im\dot{a}}{4\omega_k^2}\right]. \quad (4.37b)$$

In Appendix C.3, we write the complete expressions for u_k and v_k up to fourth-order adiabatic.

[8]This symmetry comes from the differential equation (4.22) under the change $m \to -m$.

4.3.3 Low Frequencies Approximation

In order to find approximate solutions to the system of equations (4.22) when $ma \ll \mathcal{H}$ and $k \ll \mathcal{H}$, that is, when the field has small mass or small momentum, we can consider two regimes: in the first case we can consider m as a perturbation in the Hamiltonian (4.23a). In this case, we can search for approximate solutions in which $m = 0$ is the lowest order of approximation and proceed successively by searching for corrections in perturbation theory around the mass m. In the second case we can consider k as a perturbation in the Hamiltonian (4.23a), from which it is possible to obtain corrections to the approximate solutions in perturbation theory in a similar way to the previous case.

First Case. We will develop the solution to Eq. (4.22) with $m = 0$ as the lowest order approximation when the mass of the field is sufficiently small. In this case equations (4.22) have solutions $u_k^{m=0}$ and $v_k^{m=0}$, and take the form of Eq. (4.25). If $m \neq 0$ the relations (4.24) is not a solution of the mode equation (4.22). In this case Eq. (4.24) can be regarded as solutions of the lowest order to the massless mode equation at the limit of small mass, with corrections, $\Delta u_k \equiv u_k^{(n)} - u_k^{m=0}$ and $\Delta v_k \equiv v_k^{(n)} - v_k^{m=0}$, given by

$$\Delta u_k = -\int^{\eta} d\tilde{\eta} G_1(\eta;\tilde{\eta}) \left(m^2 a^2 u_k^{(n-2)} + im\dot{a} u_k^{(n-1)} \right), \tag{4.38a}$$

$$\Delta v_k = -\int^{\eta} d\tilde{\eta} G_2(\eta;\tilde{\eta}) \left(m^2 a^2 v_k^{(n-2)} - im\dot{a} v_k^{(n-1)} \right), \tag{4.38b}$$

where $G_{1,2}(\eta;\tilde{\eta})$ is the Green's function of the zero-mass equation, which can be readily constructed as a linear combination of the two solutions $\exp(-ik\eta)$ and $\exp(ik\eta)$. We obtain an explicit solution of the mode equation by recursively expanding $u_k,\ v_k$ in powers of m. The n-th order in such an expansion thus contain n powers of the mass m and is related to the next one by

$$u_k^{\mathrm{low}(n)}(\eta) = u_k^{\mathrm{low}(0)}(\eta) - \int^{\eta} d\tilde{\eta} G_{1,2}(\eta;\tilde{\eta}) \left[a^2 u_k^{\mathrm{low}(n-2)}(\tilde{\eta}) + i\dot{a} u_k^{\mathrm{low}(n-1)}(\tilde{\eta}) \right], \tag{4.39}$$

and similarly for $v_k^{\mathrm{low}(n)}$, where $u^{\mathrm{low}(0)} = u_k^{m=0}$ and $n > 1$.

Small mass. In order to extend the exact solution (4.25) at $m = 0$ to cases where m is non-zero but "small", we shall treat the mass term in the Hamiltonian as a perturbation,

$$H = H_0 + V,\ H_0 = k\sigma_1,\ V = ma\sigma_3. \tag{4.40}$$

Then, turning to the interaction picture, the "exact" solution (4.23b) can be cast as

$$\psi = U_0(t) T \exp\left(-i \int^t d\tilde{t} \tilde{V}_I \right) \psi_0,\ \ U_0 = T \exp\left(-i \int^t d\tilde{t} \tilde{H}_0 \right), \tag{4.41}$$

where $V_I = U_0^{\dagger} V U_0$ is the interaction V in the interaction picture. It is worth noting that, at least formally, Eq. (4.41) is still an exact solution of

the Schrodinger equation (4.23a), so the validity of Eq. (4.41) does not require m to be small. When m is "small," however, it ought to suffice to expand Eq. (4.41) to first order in the interaction V_I. We shall deem the approximation "accurate" when the first order correction is much smaller than the zeroth order term. Because both depend on the common but arbitrary initial vector ψ_0, we hence arrive at the operator norm condition

$$\| \int^t d\tilde{t} \tilde{V}_I \| \ll 1. \tag{4.42}$$

The eigenvalues of the integrated interactions obey

$$\lambda^2 = m^2 \left[\left(\int^t \tilde{a} \cos\big(2k\tilde{t}\big) d\tilde{t} \right)^2 + \left(\int^t \tilde{a} \sin\big(2k\tilde{t}\big) d\tilde{t} \right)^2 \right] \leq 2m^2 \left(\int^t \tilde{a} d\tilde{t} \right)^2 \tag{4.43}$$

and, therefore, the condition for the validity of our small mass approximation is $ma \ll H$, which, somewhat surprisingly, does not depend on the magnitude of k, but on the size of the comoving horizon. As hinted above, this is because our approximation does not rely on ma begin smaller than k, but, rather, that the series in Eq. (4.41) be correctly approximated by its leading term. In summary, the zero mass approximation works when the field is light, that is, when $ma \ll H$.

Second Case. In this case we consider an expansion around k, to solutions for low frequencies, with $k = 0$ the lowest order of the approximation, when $\omega_k \sim ma$. These solutions are given by Eq. (4.26). As before, we can obtain corrections to these approximate solutions in perturbation theory. In the same way, we can write the n-th order in such expansion that contain n powers of k and is related to the next one by

$$u_k^{\mathrm{low}(n)}(\eta) = u_0^{\mathrm{low}}(\eta) - \int^\eta d\tilde{\eta} \exp\left(-i \int^{\tilde{\eta}} ma(\eta') d\eta' \right) u_k^{\mathrm{low}(n-2)}, \tag{4.44}$$

$$v_k^{\mathrm{low}(n)}(\eta) = v_0^{\mathrm{low}}(\eta) - \int^\eta d\tilde{\eta} \exp\left(i \int^{\tilde{\eta}} ma(\eta') d\eta' \right) v_k^{\mathrm{low}(n-2)}, \tag{4.45}$$

where $u_0^{\mathrm{low}}, v_0^{\mathrm{low}} = u_{k=0}^{\mathrm{low}}, v_{k=0}^{\mathrm{low}}$, $n > 2$ and we have used the explicit form of the Green's function. In this case, the solutions (4.26a) and (4.26b) correspond to the case $k = 0$ of the zeroth order of the adiabatic approximation (4.29).

Small Momentum. To find an approximate solution when the momentum k is small, we employ again first order perturbation theory in the interaction picture. Setting

$$H_0 = ma\sigma_3, \; V = k\sigma_1, \tag{4.46}$$

and proceeding exactly like in the small mass case we arrive at the eigenvalues of the first order correction

$$\lambda^2 = k^2 \left\| \int^t d\tilde{t} \exp\left(2i \int^{\tilde{t}} d\tilde{t} m\tilde{a} \right) \right\|^2 \leq k^2 (\eta - \eta_0)^2. \tag{4.47}$$

Hence, in this case the condition for the validity of the small momentum approximation is $k \ll H$, once more, regardless of how k compares to ma.

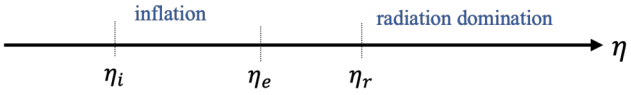

Figure 4.1: Timeline characterizing the transition experienced by the universe as it expands from an initial period of cosmic *inflation* at η_i followed by a period of radiation domination η_r mediated by a model-dependent *reheating* period $\eta_e < \eta < \eta_r$. In a sharp transition $\eta_r = \eta_e$ and there is a discontinuity in the second derivative of the scale factor.

4.4 Cosmological Epochs

4.4.1 *in* and *out* Regions

The notion of *vacuum* and the *number of particles*, associated with the number of quanta for the number operator and the creation and annihilation operators introduced by the expansion (4.12), depends on the particular choice we make of the mode functions $u_k(\eta)$ and $v_k(\eta)$. In a spacetime that experiments a transition from an initial *in* inflationary region to a subsequent *out* region where the universe expands as a FLRW spacetime, the *in* vaccum is determined by the Bunch-Davis vacuum (see Figure 4.1). So, this *in* region is determined by the existence of a preferred notion of vacuum. This is the case if the solutions of the mode equations (4.22) for any fixed k, that in the remote past matches the adiabatic zero order of the expansion (4.29), are given by

$$u_k^{\text{in}} \to \sqrt{\frac{\omega_k + ma}{2\omega_k}} \exp\left(-i \int \omega_k d\eta\right), \tag{4.48a}$$

$$v_k^{\text{in}} \to \sqrt{\frac{\omega_k - ma}{2\omega_k}} \exp\left(-i \int \omega_k d\eta\right). \tag{4.48b}$$

This condition is characteristic of a universe experiencing an early period of inflation. With these initial conditions we can characterize the mode functions u_k^{in} and v_k^{in}, which in turn characterize a preferred vacuum, that is, the *in* adiabatic vacuum. However, we must rule out a scenario of eternal inflation, that is, inflation is not expected to be past eternal. With this in mind, we cannot consider that the conditions are determined by an *in* region that extends indefinitely into the past. Taking this into account, it is convenient to introduce an initial time η_i at which inflation starts characterized by $\mathcal{H}_i = \mathcal{H}(\eta_i)$. With this scale, if the field is massless or light we must introduce an infrared cutoff such that $\Lambda_{\text{IR}} \sim \mathcal{H}_i$, since at these scales there is no preferred quantum state for the modes that are higher than the horizon at the start of inflation. On the other hand, if the field is heavy, we can set $\Lambda_{\text{IR}} = 0$. See Figure (4.2).

Once we have determined the *in* initial conditions for the mode functions in the decomposition (4.12), it is possible to associate the ladder operators $\hat{a}^{\text{in}}_{\vec{k}\lambda}$ and $\hat{b}^{\text{in}}_{\vec{k}\lambda}$ to those states corresponding to the *in* region. With this we can talk about a number operator $\hat{N}^{a,\text{in}}_{\vec{k}\lambda}$ and $\hat{N}^{b,\text{in}}_{\vec{k}\lambda}$ associated with the mode $\vec{k}$. The *in* vacuum $a^{\text{in}}_{\vec{k}\lambda} |0_{\text{in}}\rangle = 0$ has no *in* quanta $\hat{N}^{a,\text{in}}_{\vec{k}\lambda} |0_{\text{in}}\rangle = 0$, while $\hat{N}^{a,\text{in}}_{\vec{k}\lambda} |\psi\rangle = N^{a,\text{in}}_{\lambda} |\psi\rangle$ can be thought of as containing a definite number of quanta $N^{a,\text{in}}_{\lambda}$, and similarly

for the operator $\hat{N}^{b,\mathrm{in}}_{\vec{k}\lambda}$. This is how inflation allows us to identify the quantum state of all modes within the range $\Lambda_{\mathrm{IR}} < k < \infty$, e.i., the *in* vacuum.

Now we consider an *out* region that for example, contains a radiation-dominated universe starting at $\eta = \eta_r > \eta_e$, where e means the end of inflation and r the begin of the radiation-dominated universe. To determine the mode functions in the *out* region, we need to find the solution of equation (4.22) that evolved through the transition from the one in the *in* region. Let u_k and v_k be arbitrary solutions to the equation (4.22). Since u_k and v_k are linearly independent we can express the solutions u^{in}_k and v^{in}_k as a linear combination of u_k and v_k as

$$u^{\mathrm{in}}_k(\eta) = \alpha_k u_k - \beta_k v^*_k, \tag{4.49a}$$

$$v^{\mathrm{in}}_k(\eta) = \alpha_k v_k + \beta_k u^*_k, \tag{4.49b}$$

where α_k and β_k are the Bogoliubov coefficient and u_k and v_k are arbitrary solutions to equation (4.22) that do not necessarily satisfy the initial conditions set by inflation. In general, the solutions u_k and v_k are not necessarily associated with the *out* region. At this point the nature of u_k and v_k are irrelevant, we only need these to satisfy the equation (4.22) and the normalization condition (4.19). If $u_k = u^{\mathrm{in}}_k$ and $v_k = v^{\mathrm{in}}_k$ these equations imply that $\beta_k = 0$ and $\alpha_k = 1$, as expected.

Expressions in Eq. (4.49) are useful to define a two mode expansion similar to that Eq. (4.12), now with the *out* conterpart of the annihilation and creations operators $a^{\mathrm{in}}_{\vec{k}\lambda}$ and $b^{\dagger\mathrm{in}}_{\vec{k}\lambda}$ (see Appendix C.6). These set of operators defines, respectively, a number operator of *out* particles and antiparticles, given by $\hat{N}^a_{\vec{k}\lambda} = \hat{a}^\dagger_{\vec{k}\lambda}\hat{a}_{\vec{k}\lambda}$ and $\hat{N}^b_{\vec{k}\lambda} = \hat{b}^\dagger_{\vec{k}\lambda}\hat{b}_{\vec{k}\lambda}$. This set of number operators $\hat{N}^a_{\vec{k}\lambda}$, $\hat{N}^b_{\vec{k}\lambda}$, $\hat{N}^{a,\mathrm{in}}_{\vec{k}\lambda}$ and $\hat{N}^{b,\mathrm{in}}_{\vec{k}\lambda}$ allows define the *in* vacuum $|0_{\mathrm{in}}\rangle$ which no contain *in* particles and the *out* vacuum $|0_{\mathrm{out}}\rangle$ which no contain *out* particles. But, when β_k is nonzero, the *in* vacuum does contain *out* particles given by $\langle 0_{\mathrm{in}}|N^{ab}_{\vec{k}}|0_{\mathrm{in}}\rangle = \int dk^3|\beta_k|^2$. Note that the Bogolubov coefficients do not have an independent meaning by themselves, since they are inherently linked to the choice of the mode functions u_k and v_k through Eq. (4.49). Only in the adiabatic regime do the Bogolubov coefficients acquire a context-independent meaning. Then, in the adiabatic regime we can say that the mode functions u^{ad}_k and v^{ad}_k are uniquely determined. If this approximation is applicable then we can refer to these mode functions as "*out* adiabatic mode functions" and to the vacuum state as "*out* adiabatic vacuum". The exact solution to the mode equation that matches with Eq. (4.29) and its first derivative at any chosen and fixed time η implicitly defines the n-th order adiabatic vacuum at that time. As stressed in Ref. [135], this defines a two-parameter family of vacuum, characterized by the adiabatic order n and the time η. In general, we are not interested in determining the *out* mode basis functions. Only when we need to renormalize the energy density of the *out* vacuum is that we must determine the adiabatic mode functions up to order $n \geq 4$.

4.4.2 Transitions

Once the nature of the *in* and *out* regions is established, we must establish the nature of the transition between the two regions. In a scenario determined

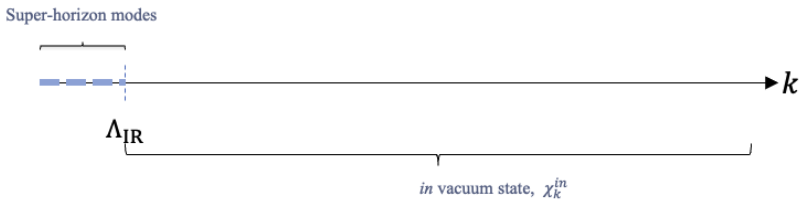

Figure 4.2: Infrared scale $\Lambda_{\rm IR} \sim \mathcal{H}_i$ at the beginning of inflation. The modes below this scale have an unknown state. Modes above $\Lambda_{\rm IR}$ are found in the preferred *in* vacuum state set by inflation at η_i. If the field is massless or light, the state of the superhorizon modes at the beginning of inflation, is not determined by inflation and remains unknown to us.

by the transition from an inflationary universe to a universe dominated by radiation, the nature of this transition is determined by the relatively unknown phenomenology of the period called reheating, see Figure 4.1. To describe the inflationary period, we can use the parametrization $a(\eta) \sim \eta^p$ with $p \leq -1$ where the effective equaion of satate in such universe is $\omega_k = (2-p)/3p$. Here, the slow-roll parameter $\epsilon = -\dot{H}/(aH^2) = p^2 + p$. The case $p = -1$, for example, correspond to a Cosmological Constant Λ dominated universe and $\epsilon = 0$. After Inflation, in a radiadion dominated universe the scale factor evolves as $a(\eta) \sim \eta$ or $a(t) \sim t^{1/2}$. In the following, unless a specific example is required we will only assume that $\mathcal{H}_r \leq \mathcal{H} \leq \mathcal{H}_e$.

In order to determine the form of the *in* mode functions after a *jump* in the derivates of the scale factor $a(\eta)$, we need to find the solution of equation (4.22) that matches the one in the *in* region at the transition time $\eta = \eta_e$. We use arbitrary solutions u_k and v_k to the mode equations, and we impose continuity of the solutions and its derivatives at the future boundary of the *in* region, that is η_e. If the mode functions $u_k^{\rm in}$ and $v_k^{\rm in}$ remains in the adiabatic regime throughout the *in* region, and we assume that the mode functions u_k and v_k are well approximated by the adiabatic expansion (4.29), the Bogolubov coefficients in Eq. (4.49) after such transition are given by

$$\alpha_k^{\rm ad} \approx 1 + \left(\frac{\omega_k + ma}{2\omega}\right)\left(F^{-,(1)*} + F^{+,(1)} + F^{+,(1)}F^{-,(1)*} + F^{+,(2)}F^{-,(2)} + ...\right) + \left(\frac{\omega_k - ma}{2\omega}\right)\left(G^{-,(1)*} + G^{+,(1)} + G^{+,(1)}G^{-,(1)*} + G^{+,(2)}G^{-,(1)*} + ...\right), \tag{4.50a}$$

$$\beta_k^{\rm ad} \approx \frac{k}{2\omega}\Big[\left(F^{-,(1)} - F^{+,(1)}\right) + \left(G^{+,(1)} - G^{-,(1)}\right) + \left(G^{+,(1)}F^{-,(1)} - G^{-,(1)}F^{+,(1)}\right) + ...\Big], \tag{4.50b}$$

where the plus and minus superscripts denote the limits in which η approaches η_e from above and below, respectively. The different terms are organized by growing number of time derivatives. If $F^{-,(1)} = F^{+,(1)}$, $G^{-,(1)} = G^{+,(1)}$,

that is, there is no jump in the derivatives of the scale factor, and using $|F|^2(\omega_k + ma) + |G|^2(\omega_k - ma) = 2\omega_k$, then we have to $\alpha_k = 1$ and $\beta_k = 0$, as we expected. From this, we infer that the scale factor must at least make a jump in the first derivative of the scale factor to obtain a value of $|\beta_k|$ different from zero. At first adiabatic order we have $\beta_k^{(1)} \approx (ikm/4\omega_k^3)[\dot{a}^+ - \dot{a}^-]$ and $\alpha_k^{(1)} \approx 1 - (ma/k)\beta_k^{(1)}[\dot{a}^+ - \dot{a}^-]$ where $[\dot{a}^+ - \dot{a}^-]$ is always positive. Now, taking into account that $0 \leq |\alpha_k|, |\beta_k| \leq 1$, and given that $[\dot{a}^+ - \dot{a}^-] = [1 + p/\eta_e^{-p-1}] \approx 1$, we expect particle production to be effective when $k \sim ma$, i.e, the fermion becomes non-relativitic. On the other hand, from the expression $\beta_k = u_k v_k^{\rm in} - v_k u_k^{\rm in}$, evaluating u_k, v_k in the asymptotic region $\eta \to \eta_{eq}$ where η_{eq} is the time at matter-radiation equality, $\beta_k = u_k v_k^{\rm in} - v_k u_k^{\rm in}$ are given by the adiabatic approximation (4.29) to zeroth order in the late radiation-dominated universe, and evaluating $u_k^{\rm in}, v_k^{\rm in}$ in the asymptotic past determined by the early inflation stage where $u_k^{\rm in}, v_k^{\rm in} = \frac{1}{\sqrt{2}} e^{-ik\eta}, \frac{1}{\sqrt{2}} e^{ik\eta}$, in the limit $k \to 0$, we obtain $|\beta_k|^2 \sim \frac{1}{2}$. This result coincides with the result reported in Refs. [173, 176]. These formulas establish a link between the smoothness of the transition and the behavior of the Bogolubov coefficients in the adiabatic regime. If the transition remains differentiable, the coefficients β_k vanish in the adiabatic regime, as expected. As we have previously argued, the modulus square $|\beta_k|^2$ is the expected number density of *out* particles and antiparticles in that mode, and particle and antiparticle production hence requires departures from adiabaticity. Up to third adiabatic order the Bogoliubov coefficient are given by

$$\beta_k^{(3)} \approx \frac{km}{8\omega_k^4}\left(\ddot{a}_{\rm in} - \ddot{a}_{\rm out}\right) + \frac{i19km^3 a_0 \dot{a}_0}{32\omega^7}(\ddot{a}_{\rm in} - \ddot{a}_{\rm out}) - \frac{ikm}{16\omega^5}(\dddot{a}_{\rm in} - \dddot{a}_{\rm out}) + ... \tag{4.51}$$

4.5 Energy Density

We are interested in the evolution of the energy density of the quantum fermion field $\hat{\psi}$ as the universe experiences transition from the *in* to the *out* region, as described in Section 4.4. In the semiclassical approximation to gravity, the energy density of the field ψ is related to the expectation value of the time-time component of its energy-momentum tensor as $\rho = \langle T^{00} \rangle$, which acts as a source for the classical gravitational field, c.f. Eq. (3.2). According to the action (4.1) the energy-momentum tensor is given by $T^m_{\mu\nu} = \frac{i}{2}[\bar{\psi}\gamma_{(\mu}\nabla_{\nu)}\psi - (\nabla_{(\mu}\bar{\psi})\gamma_{\nu)}\psi]$, where we are using de definition $A_{(i}B_{j)} = 1/2(A_i B_j + A_j B_i)$. Now, using $\Omega_0 = 0$, $\gamma^0 = (1/a)\tilde{\gamma}^0$ and $\gamma_0 = (1/a)\tilde{\gamma}_0$, the 00-component of the stress-energy tensor can be written as

$$T_0^0 = \frac{i}{2}\left(\bar{\psi}\gamma^0\partial_0\psi - \partial_0\bar{\psi}\gamma^0\psi\right). \tag{4.52}$$

In order to calculate the vacuum expectation value $\langle T_0^0 \rangle$ with respect to the vacuum state $|0\rangle$, we use the expressions (4.12) and (4.13) into Eq. (4.52) (see Appendix C.4 for details), and after some calculations we obtain

$$\rho = \frac{1}{2\pi^2 a^3}\int^{\infty} dk k^2 \rho_k, \tag{4.53a}$$

where the *spectral density* is given by

$$\rho_k = \frac{i}{a}\left[u_k^{\rm in}\partial_0 u_k^{\rm in*} + v_k^{\rm in}\partial_0 v_k^{\rm in*} - u_k^{\rm in*}\partial_0 u_k^{\rm in} - v_k^{\rm in*}\partial_0 v_k^{\rm in}\right]. \tag{4.53b}$$

On other hand, if we calculate $\langle T_0^0\rangle$ with respect to an arbitrary state $|\psi\rangle$, after some calculations, we can write the energy density expression $\rho = \langle\psi|T_0^0|\psi\rangle$ with the spectral density given by

$$\rho_k = \frac{i}{2a}\Big[2i\left(2-[n_k^b+n_k^a]\right)\mathfrak{Im}\{u_k\dot{u}_k^* + v_k\dot{v}_k^*\} + 2m_k^b(\dot{u}_k^* v_k^* - u_k^*\dot{v}_k^*) + 2m_k^a(u_k\dot{v}_k - \dot{u}_k v_k)\Big] \tag{4.53c}$$

or, eliminating the time derivatives using the equations (4.21), we can write

$$\rho_k = \frac{i}{2a}\Big[2i\left(2-[n_k^b+n_k^a]\right)\mathfrak{Im}\{ima(|u_k|^2-|v_k|^2) + ik(u_k v_k^* + v_k u_k^*)\} + 2m_k^a(ik(u_k^2-v_k^2) - 2imau_k v_k) - 2m_k^b(-ik(u_k^{*2}-v_k^{*2}) + 2imau_k^* v_k^*)\Big]. \tag{4.53d}$$

Here, the mode functions u_k and v_k are arbitrary solutions to the mode equations (4.21) and we have defined $\langle\hat{a}^\dagger_{\vec{k}'\lambda'}\hat{a}_{\vec{k}\lambda}\rangle = \delta(\vec{k}-\vec{k}')n^a_{\lambda\lambda'}$, $\langle\hat{a}^\dagger_{\vec{k}'\lambda'}\hat{b}^\dagger_{\vec{k}\lambda}\rangle = \delta(\vec{k}+\vec{k}')m^b_{\lambda\lambda'}$, $\langle\hat{b}_{\vec{k}'\lambda'}\hat{a}_{\vec{k}\lambda}\rangle = \delta(\vec{k}+\vec{k}')m^a_{\lambda\lambda'}$, $\langle\hat{b}_{\vec{k}'\lambda'}\hat{b}^\dagger_{\vec{k}\lambda}\rangle = \delta(\vec{k}-\vec{k}')\delta_{\lambda\lambda'} - \delta(\vec{k}-\vec{k}')n^b_{\lambda\lambda'}$ where $n_k^a = \sum_\lambda n^a_{\lambda\lambda}$, $n_k^b = \sum_\lambda n^b_{-\lambda-\lambda}$, $m_k^a = \sum_\lambda m^a_{-\lambda-\lambda}$, $m_k^b = \sum_\lambda m^b_{\lambda\lambda}$, see Appendix C.4 for details. If $|\psi\rangle$ is the vacuum state then $n_k^a = n_k^b = m_k^b = m_k^a = 0$.

In order to analyze the energy density ρ of the fermionic field it is convenient to separate the contributions from the $\vec{k}=0$ and $\vec{k}>0$ modes.[9] Starting from a sum over the modes in a volume V and subsequently replacing it with an integral taking the continuous limit $V\to\infty$, we can write ρ as

$$\rho = \rho_{\vec{k}=0} + \frac{1}{2\pi^2 a^3}\int^\infty dk k^2 \rho_k, \tag{4.54}$$

where $\rho_{\vec{k}=0}$ and $\rho_{\vec{k}>0}$ are the zeroth and $k>0$ mode contribution, respectively, to the total energy density. Here, if the expectation value $\langle T_0^0\rangle$ is respect to the states $|0\rangle$ or $|\psi\rangle$, ρ is given in term of the spectral density (4.53b) or (4.53b), respectively.

Finally, motivated by the discussion in Section (4.4.1), we will divide the integral in Eq. (4.54) in two pieces

$$\rho_{<\Lambda_{\rm IR}} \equiv \int_0^{\Lambda_{\rm IR}} dk k^2\rho_k, \quad \text{and} \quad \rho_{>\Lambda_{\rm IR}} \equiv \int_{\Lambda_{\rm IR}}^{\Lambda} dk k^2\rho_k, \tag{4.55}$$

where $\Lambda_{\rm IR}\sim\mathcal{H}_i$ is of the order the Hubble radius at the beginning of inflation and plays the role of an infrared cutoff. Here $\rho_{<\Lambda_{\rm IR}}$ contains the contribution of

[9] Since for a free field the modes evolve in a decoupled manner, we can treat these separately. In particular, the zero mode $k=0$ requires separate treatment. In the case when $0\le k<\Lambda_{\rm IR}$, there is no preferred state for these modes.

those modes in the interval $0 < k < \Lambda_{\rm IR}$, that were already outside the horizon at the beginning of inflation and whose state remains undetermined. On the other hand, modes in the range $\Lambda_{\rm IR} < k < \infty$ do have a preferred state, though we have limited their contribution up to those below an ultraviolet cutoff Λ that we have introduced for convenience (in the integration process we will apply the limit $\lim \Lambda \to \infty$).

Reformulation of ρ_k. We can also recast the spectral energy density in terms of the "state vector" ψ. Using equation (4.21) in order to eliminate the time derivatives, we find that the energy of a single momentum mode (two polarizations) is

$$\rho_k = -\frac{2}{Va^4}\psi^\dagger H \psi, \tag{4.56}$$

where H is the Hamiltonian above, c.f. Eq. (4.23a). In other words, the Hamiltonian and the energy density are proportional to each other. The proportionality factor contains the volume factor a^3V expected from a density, and the additional redshift of the energy inversely proportional to a.

4.5.1 Adiabatic Expansion of the Spectral Density

Now, we will calculate the spectral density ρ_k for the *in* vacuum whose state is characterized by the solutions $u_k^{\rm in}$ and $v_k^{\rm in}$, which satisfy the conditions (4.48). To calculate the integral (4.53a) we must expand its integrand (that is, the spectral density $\rho_k^{\rm in}$, Eq. (4.53b)) adiabatically. By dimensional analysis, we need to calculate up to the fourth adiabatic order. So, once we get the adiabatic expression for the mode functions $u_k^{(n)}$ and $v_k^{(n)}$, up to adiabatic order $n = 4$, we can obtain, after some straightforward algebra, the expression for $\rho^{(n)}$ putting

$$u_k^{(n)} = \sqrt{\frac{\omega_k + ma}{2\omega_k}}\left[1 + \sum_{i=1}^{n} F(\eta)^{(i)}\right] \exp\left(-i\int \Omega^{(n)} d\eta'\right), \tag{4.57a}$$

$$v_k^{(n)} = u_k^{(n)}(-m), \tag{4.57b}$$

into Eq. (4.53b), with $F^{(n)}$, $G^{(n)} = F^{(n)}(-m)$ and $\Omega^{(n)}$ given by Eqs. (4.30). For example, at the zeroth adiabatic order, the mode functions are given by

$$u_k^{(0)} = \sqrt{\frac{\omega_k + ma}{2\omega_k}} \exp\left(-i\int \omega_k(\eta')d\eta'\right), \quad \text{and} \quad v_k^{(0)}(\eta) = u_k^{(0)}(-m), \tag{4.58}$$

form which the spectral density $\rho_k^{(0)}$, remaining at zeroth adiabatic order, can be written as

$$\rho_k^{(0)} = \frac{i}{a}\left[\left(\frac{\omega_k + ma}{\omega_k}\right) i\omega_k\right] + (F \to G) = -\frac{2\omega_k}{a}, \tag{4.59}$$

where $(F \to G)$ refers to adding the first term by changing the functions F for $G = F(-m)$, or making the change $m \to -m$. In the appendix (C.5), we explain in more detail how to obtain the second and fourth adiabatic orders of the spectral density ρ_k (the odd adiabatic orders vanish).

Finally, using the equations (C.22), (C.35) and (C.36), the full expression for the spectral density $\rho_k^{(4)}$ up to fourth adiabatic order is given by

$$\rho_k \approx \rho_k^{(0)} + \rho_k^{(1)} + \rho_k^{(2)} + \rho_k^{(3)} + \rho_k^{(4)}, \tag{4.60}$$

where

$$\rho_k^{(0)} = -\frac{2\omega_k}{a},\ \rho_k^{(1)} = \rho_k^{(3)} = 0, \tag{4.61a}$$

$$\rho_k^{(2)} = -\frac{\dot{a}^2 m^4 a}{4\omega_k^5} + \frac{\dot{a}^2 m^2}{4a\omega_k^3}, \tag{4.61b}$$

$$\begin{aligned}\rho_k^{(4)} = {} & \frac{105m^8 a^3 \dot{a}^4}{64\omega_k^{11}} - \frac{63m^6 a\dot{a}^4}{32\omega_k^9} + \frac{21m^4\dot{a}^4}{64a\omega_k^7} - \frac{7m^6 a^2\dot{a}^2\ddot{a}}{8\omega_k^9} + \frac{7m^4\dot{a}^2\ddot{a}}{8\omega_k^7} \\ & + \frac{m^4 a\ddot{a}^2}{16\omega_k^7} + \frac{m^2\ddot{a}^2}{16a\omega_k^5} + \frac{m^4 a\dot{a}\dddot{a}}{8\omega_k^7} - \frac{m^2\dot{a}\dddot{a}}{8a\omega_k^5}.\end{aligned} \tag{4.61c}$$

4.5.2 Modes $0 \leq k < \Lambda_{\rm IR}$

Now, let us consider the contribution to the energy density coming from the modes $0 \leq k < \Lambda_{\rm IR}$, that is, from those modes below the infrared cutoff $\Lambda_{\rm IR}$ at the start of inflation. As we already mentioned, these modes are outside the horizon $\mathcal{H}_i$ at the star of inflation and do not have a preferred state. We will divide the discussion by analyzing separately the zero mode $\vec{k} = 0$ and the modes in range $0 < k < \Lambda_{\rm IR}$.

Zero mode. According to Eq. (C.33), the spectral density for the zero mode can be written as

$$\begin{aligned}\rho_0 = \frac{i}{2a^4 V}\Big[& (2 - [n_0^b + n_0^a])(2i\mathfrak{Im}\{u_0\dot{u}_0^* + v_0\dot{v}_0^*\}) \\ & + 2m_0^a\,(u_0\dot{v}_0 - v_0\dot{u}_0) - 2m_0^b\,(u_0^*\dot{v}_0^* - v_0^*\dot{u}_0^*)\Big].\end{aligned} \tag{4.62}$$

If into Eq. (4.62) we consider V goes to infinity then $\rho_{k=0} \to 0$, since $|n_0^a|, |n_0^b| \leq 1$ and $|m_0^a|, |m_0^b| \leq 1$. It may be useful to cast the energy density of the zero mode as function of the critical density: it is of order $(n_0^a + n_0^b - 1)(mH/M_{\rm pl}^2)(V_H/V)$ where V_H is the Hubble volume. This is typically very small. Otherwise, for the scalar field it is possible to obtain a macroscopic Boson condensate as $V \to \infty$. In any case, for a value of V different from zero, the energy density seems to coincide with that of a classical homogeneous Dirac field $\Psi_{\rm cl} = \sum_\lambda \left[A_\lambda U_{0\lambda} + B_\lambda V_{0\lambda}\right]$ whose energy density is $\rho_{\rm cl} = i/2a(\bar{\Psi}_{\rm cl}\gamma^0\partial_0\Psi_{\rm cl} - \partial_0\bar{\Psi}_{\rm cl}\gamma^0\Psi_{\rm cl})$, such that

$$\begin{aligned}\rho_{\rm cl} = \frac{i}{2a^4}\Bigg[& \left(\sum_\lambda |B_\lambda|^2 - |A_\lambda|^2\right)(u_0\dot{u}_0^* + v_0\dot{v}_0^* - u_0^*\dot{u}_0 - v_0^*\dot{v}_0) \\ & + \sum_\lambda A_\lambda^* B_{-\lambda}(v_0^*\dot{u}_0^* - u_0^*\dot{v}_0^*) + \sum_\lambda A_{-\lambda}B_\lambda^*(u_0\dot{v}_0 - v_0\dot{u}_0)\Bigg].\end{aligned} \tag{4.63}$$

Comparing the last expression with Eq. (4.62), such a classical description works provided that we are able to identify

$$\sum_{\lambda} |B_\lambda|^2 - |A_\lambda|^2 = \frac{1}{V}\left[2 - \left(n_0^b + n_0^a\right)\right],$$
$$\sum_{\lambda} A_{-\lambda} B_\lambda^* = \frac{m_0^a}{V}, \quad \sum_{\lambda} A_\lambda^* B_{-\lambda} = \frac{m_0^b}{V}, \tag{4.64}$$

and there exists a solution to the system. As long as there is a solution for Eq. (4.64) the classical description for $\Psi_{\rm cl}$ works, in the sense that there exists a *classical field* configuration with the same energy density like Eq. (4.62). In general, there is no preferential choice of the functions v_0, u_0. Any solution of the mode equation for $k = 0$ is equally valid, such that the coefficients B_λ, A_λ, n_0, m_0, do not have a particular meaning for themselves.

On the other hand, we can see that if the field is massless, the zero mode u_0 and v_0 is described by the equation (4.25) with $\vec{k} = 0$ which have solutions $v_0^{m=0}$, $u_0^{m=0} =$ constant subject to Eq. (4.21). Then, the energy density vanishes. If the mass is different from zero, on the other hand, there are two different regimes. In the first case, if now we consider the "*positive frequencies*" solutions (4.25a) with $ma \ll \mathcal{H}$, that is, whereas the field remains *light*, we have from Eq. (4.62) that the energy density also vanishes.

After some time, when the field becomes heavy, $ma \gg \mathcal{H}$, the frequency approximation (4.25a) breaks down, then we need to make use of the adiabatic approximation, that is, the equation (4.29). With these solutions, we can write

$$\rho_{k=0} = \frac{1}{a^4 V}\left(n_{k=0}^a + n_{k=0}^b - 2\right)\left[\Omega |F_{k=0}|^2 + \mathfrak{Im}(F\dot{F}^*)_{k=0}\right], \tag{4.65}$$

from which the zero adiabatic order is given by $\rho_{k=0} = \frac{2\omega_k}{a^4 V}[(n_{k=0}^a + n_{k=0}^b) - 2] = \frac{2m}{a^3 V}[N_0^{\rm ad} - 2]$, that is, we obtain that, at zeroth order in the adiabatic approximation, the oscillating zero mode behaves like a pressureless fluid, whose overall density is proportional to the value of $N_0^{\rm ad}$, where the superscript indicates that we have chosen the mode functions (4.29) in the field expansion (4.12). As we discussed in Section 4.7 this is precisely the behavior that would be expected of $N_0^{\rm ad}$ particles with zero space momentum.

In the case of a massless classical field, we obtain $\rho_{\rm cl} = 0$, and if the fields is massive, we can write the classical energy density as $\rho_{\rm cl} = \frac{m}{a^3}\bar{\Psi}_0\Psi_0 = \rho_{0m}/a^3$ where Ψ_0 is a constant spinor. Since the expectation of the energy density of the zero mode (4.65) also scales like $1/a^3$, by a appropriate choice of Ψ we can always cast it as that of classical field

$$\rho_{\rm cl} = -\left(\sum_{\lambda} |B_\lambda|^2 - |A_\lambda|^2\right)\frac{m}{a^3}. \tag{4.66}$$

If there exists a solution to Eq. (4.64), Eq. (4.65) admits a *classical interpretation* in terms of a classical field ψ_{cl} as Eq. (4.66). But, as we have already mentioned, given that $n_0^a, n_0^b \leq 1$, the contribution of the zero mode, for the massive or massless case, is generally negligible. Otherwise, for the case of the

scalar field, when V grows $N_0^{\rm ad}$ must grow so that its energy density approaches a value other than zero. Of course in the case of fermions this contribution tends to zero.

Continuum $0 < k < \Lambda_{\rm IR}$. Now, let's analyze the energy density $\rho_{k<\Lambda_{\rm IR}}$ which captures the contribution of modes $0 < k < \Lambda_{\rm IR}$ whose state, like the case $\vec{k} = 0$, we also ignore. In the massless case, as long as $\Lambda_{\rm IR} < \mathcal{H}$, we can set $u_k, v_k \approx u_k^{m=0}, v_k^{m=0}$ like the solutions (4.25a), $u_k, v_k \approx (1/\sqrt{2})\exp\{-ik\eta\}$ as discussed in Section (4.3.3), and substitute into Eq. (4.53c) we find

$$\rho_{k<\Lambda_{\rm IR}} = \frac{1}{\pi^2 a^4}\int_0^{\Lambda_{\rm IR}} dk k^3 \left[(n_k^a + n_k^b) - 1\right], \tag{4.67}$$

where the value of the integral is finite. Let's note that if we express $\rho_{k<\Lambda_{\rm IR}}$ in the form $\rho_{k<\Lambda_{\rm IR}} = \rho_{0,r}/a^4$, we can conclude that the energy density (4.67) behaves *classically* like cosmological radiation. Later, in Section (4.7), we will associate $2-(n_k^a+n_k^b) = 2-4|\beta_k|^2$ for $\Lambda_{\rm IR} < k < \infty$ with the density number of *out* particles plus the contribution of the *out* vacuum in the case of an asymptotically adiabatic spacetime in the *out* region. With these conditions, we can associate $\rho^{\rm p}_{k<\Lambda_{\rm IR}} = \frac{1}{\pi^2 a^4}\int_0^{\Lambda_{\rm IR}} dk k^3 |\beta_k|^2$ as the value of the density energy of created particles whose behavior does not admit classical interpretation. Let's remember that $0 \leq |\beta_k|^2 \leq 1$, therefore $\rho^{\rm p}_{k<\Lambda_{\rm IR}}$ is always positve.

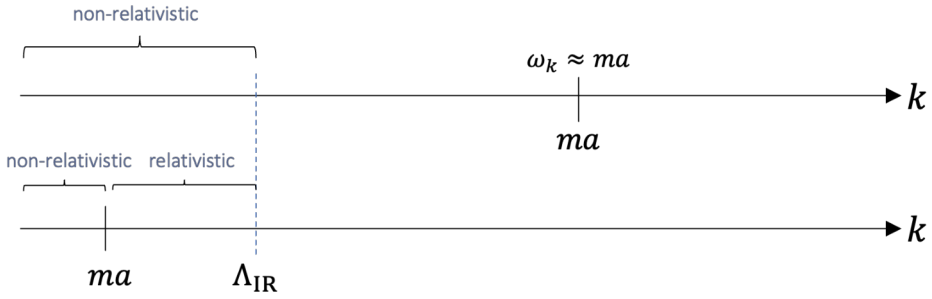

Figure 4.3: **Relativistic and non-relativistic modes**. a) Modes in the range $0 < k < \Lambda_{\rm IR}$ for which $ma > \Lambda_{\rm IR}$ consist of non-relativistic modes. b) Modes in the range $0 < k < \Lambda_{\rm IR}$ for which $ma < \Lambda_{\rm IR}$ consist of relativistic and non-relativistic modes.

In the massive case, we need to distinguish between two possible limits. When $\Lambda_{\rm IR} < ma$ all the relevant modes are non-relativistic, so we can approximate the dispersion relation $\omega_k \approx ma$ (see Figure 4.3, first arrow). When $ma \ll \mathcal{H}$, that is, when the field is *light*, the mode functions are well approximated by the expression (4.25a), so from Eq. (4.53c),

$$\rho_{k<\Lambda_{\rm IR}} \sim \frac{1}{a^4}\left[\frac{1}{\pi^2}\int_0^{\Lambda_{\rm IR}} dk k^3 (n_k^a + n_k^b - 1)\right] \tag{4.68}$$

which we can express as $\rho_{k<\Lambda_{\rm IR}} \sim \rho_r/a^4$ with $\rho_r = \frac{m}{\pi^2}[\int_0^{\Lambda_{\rm IR}} dk k^3 (n_k^a + n_k^b - 1)]$. Again, this is the cosmological *classical* behavior of relativistic matter. In the second limit, when $\mathcal{H} \ll ma$, the mode functions are well approximated

by the adiabatic approximation (4.29) and the energy density at zero adiabatic order scales like non-relativistic matter as $\rho_{k<\Lambda_{\rm IR}} \sim \rho_m/a^3$ with $\rho_m = \frac{m}{\pi^2}[\int_0^{\Lambda_{\rm IR}} dk k^2(n_k^a + n_k^b - 1)]$, which admits a classical interpretation in terms of the classical field ψ_{cl}. Since the comoving mass grows monotonically, we expect $\Lambda_{\rm IR} < ma$ to hold at sufficiently late times, and this is the relevant limit then.

If the mass satisfies $ma \leq \Lambda_{\rm IR}$ (see Figure 4.3, second row), the modes in the interval $0 < k < ma$ are non-relativistic, so their spectral density behaves like that of the massive case just discussed above, with $\rho_{k<ma} = \rho_m(\eta)/a^3 = \frac{m}{\pi^2 a^3}\int_0^{ma} dk k^2(n_k^a + n_k^b - 1)$. Similarly, modes in the interval $ma < k < \Lambda_{\rm IR}$ are relativistic, and their spectral density behaves like that of a massless field, $\rho_{ma<k<\Lambda_{\rm IR}} = \rho_r(\eta)/a^4 = \frac{1}{\pi^2 a^4}\int_{ma}^{\Lambda_{\rm IR}}(n_k^a + n_k^b - 1)$. Note that the behavior of the energy for these modes is that of a time-dependent *classical* cosmological component, of non-relativistic and relativistic matter, respectively. But since the boundary between the two regimes at $k = ma$ changes with time, we cannot, in general, make definite predictions about the time evolution of $\rho_{k<\Lambda_{\rm IR}}$ for these modes. Therefore, we will not study this case explicitly here, although the methods we have presented so far could be similarly applicable.

Modes in range $0 \leq k < \Lambda_{\rm IR}$		
$\rho_{\vec{k}=0}$ These modes are negligible due to the exclusion principle.	massless case	The energy density vanishes
	masive case	It admits *classical interpretation* as non-relativistic matter $\sim \rho_{0,m}/a^3$.
$\rho_{k<\Lambda_{\rm IR}}$	massless case	It admits *classical interpretation* only as non-relativistic matter $\sim\rho_{0,m}/a^3$.
	masive case	

Table 4.1: Energy density for modes in the range $0 \leq k < \Lambda_{\rm IR}$ and its behavior in different mass regimes. For these states, there is no preferred notion of vacuum, and their state is indeterminate. *The first row* corresponds to the zero mode $\vec{k} = 0$, which admits an interpretation in terms of a homogeneous classical field $\rho_{k=0} \sim \rho_{0m}/a^3$ in the massive case for *heavy* mass $ma \gg \mathcal{H}$. For the massless case, the energy density vanishes. *The second row* corresponds to the $0 < k < \Lambda_{\rm IR}$ modes. For the massless case $m = 0$, these modes are relativistic and behaves like that of relativistic matter $\rho_{k<\Lambda_{\rm IR}} \sim \rho_r/a^4$, and does not admit classical interpretation. In the massive case, however, when $\Lambda_{\rm IR} < ma$, in the *heavy* mass regimes, the modes are non-relativistic and $\rho_{k<\Lambda_{\rm IR}}$ behaves like that of a classical field for non-relativistic matter $\sim \rho_m/a^3$.

4.6 Modes in Range $\Lambda_{\rm IR} < k < \infty$

4.6.1 Renormalization of $\rho_{\Lambda_{\rm IR}<k}$

Modes in the range $\Lambda_{\rm IR} < k < \infty$ find themselves effectively in Minkowski space at the beginning of inflation, where a preferred choice of state exists: the *in* vacuum. If, as opposed to a general state, the field is in the *in* vacuum,

with solutions $u_k = u_k^{\rm in}$ and $v_k = v_k^{\rm in}$, then the energy density simplifies to

$$\rho^{\rm in}_{>\Lambda_{\rm IR}} = \frac{1}{2\pi^2 a^3}\int_{\Lambda_{\rm IR}}^{\infty} dk k^2 \rho_k^{\rm in}, \tag{4.69}$$

with

$$\rho_k^{\rm in} = \frac{i}{a}\left[u_k^{\rm in}\partial_0 u_k^{\rm in*} + v_k^{\rm in}\partial_0 v_k^{\rm in*} - u_k^{\rm in*}\partial_0 u_k^{\rm in} - v_k^{\rm in*}\partial_0 v_k^{\rm in}\right]. \tag{4.70a}$$

Let us remember that within the Heisenberg picture, the states remain static, while the operators obey a dynamic equation. A system configured in the state $|0^{\rm in}\rangle$ remains in this state all time. From now on, unless stated otherwise, the energy density $\rho_{>\Lambda_{\rm IR}}$ and the spectral density ρ_k will be those of modes above the infrared cutoff $\Lambda_{\rm IR}$ in the *in* vacuum, but for notational simplicity, we shall omit the labels "$>\Lambda_{\rm IR}$" and *in* form our expressions.

The Einstein gravitational semiclassical equations are given by the approximation $M_{\rm pl}^2\bar{G}_{\mu\nu} = \langle T_{\mu\nu}\rangle$, where $\bar{G}_{\mu\nu}$ behaves classically, and $T_{\mu\nu}$ is the energy-momentum tensor associated with the $s = 1/2$ quantum field $\hat{\psi}$. In this context, the expectation value of $\langle T_{\mu\nu}\rangle$ is the quantity we are interested in calculating. From this, we shall restrict our attention to the time-time component to calculate the renormalized vacuum energy density. This 00 component is the semiclassical "Friedman" equation $\mathcal{H}^2/a^2 = a^2\langle 0|T_0^0|0\rangle/3M_p^2$. As it stands, the energy density (4.69) diverges in the ultraviolet regime, when $\Lambda \to \infty$. This follows from the solutions (4.48), in the adiabatic regime, wich implies that at large k the leading term in the spectral density is proportional to k. Pictorially, this divergence arises from a *Feynman Loop diagram* in which a particle is crated and annihilated at the same spacetime location.

In order to renormalize the integral $(1/2\pi^2a^3)\int dk k^2\rho_k^{\rm in}$ in the range of modes $\Lambda_{\rm IR} < k < \infty$, we will follow the *Puilli-Villars renormalization* procedure that is described in Ref. [168], and as we have described in Section 3.7, where it is possible to regularize this quantity while preserving diffeomorphism invariance by introducing a set of Pauli-Villars regulator fields. The contribution of these regulator fields and the counterterms leads to the renormalized energy density

$$\rho_{\rm ren} = \rho - \rho_{\rm sub}, \tag{4.71}$$

where $\rho_{\rm sub}$ consists of the subtraction terms that leave the integral free of divergences when $\Lambda \to \infty$, and the contribution of the counterterms coming from the regulator fields as their mass is decoupled.

The first step is then to adiabatically expand the spectral density ρ_k and identify the divergent terms as the cutoff Λ tends to infinity. That is, we need to calculate

$$\rho = \lim_{\Lambda\to\infty}\frac{1}{2\pi^2a^3}\int_{\Lambda_{\rm IR}}^{\Lambda} dk k^2(\rho_k^{(0)} + \rho_k^{(2)} + \rho_k^{(4)} + ...), \tag{4.72}$$

and identify the divergent terms. This adiabatic expansion was given in the last Section (4.61). In the particular case of a fermion field in *conformal spacetime*, the divergent terms come from the zeroth and second adiabatic order. Higher

orders remain finite when $\Lambda \to \infty$. However, we will calculate up to fourth order by analogy with the scalar case. These divergent terms are given by

$$\rho^{(0)} = \frac{-1}{\pi^2}\left[\frac{\Lambda^4}{4a^4} + \frac{\Lambda^2 m^2}{4a^2} + \frac{m^4}{32} - \frac{1}{8}m^4 \log\left(\frac{2\Lambda}{ma}\right)\right], \tag{4.73}$$

$$\rho^{(2)} = \frac{\dot{a}^2 m^2}{8\pi^2 a^4}\left[-\frac{4}{3} + \log\left(\frac{2\Lambda}{ma}\right)\right]. \tag{4.74}$$

Again, all the subsequent adiabatic terms are convergent as the cutoff Λ tends to infinity. Next, in the second step (see Section 3.7), we shall regulate the divergent ρ_k integrand in Eq. (4.72) through the introduction of a set of n Pauli-Villars regulator fields ψ_r of Grassmann parity σ_r, with the same couplings as ψ, but with different masses M_r, where $r = 1, ..., n$. So, the actual expectation that enters the 00-component of the energy-momentum tensor in equation (4.53a) is $\rho = \sum_{i=0}^{n} \langle T_0^0 \rangle_i$. At the end of the calculation we shall decouple the regulator fields by sending their masses M_r to infinity, leaving a finite, renormalized theory behind. Remember, the adiabatic approximation is only valid at large values of k or large values of M_r^2. Hence, we shall only be able to analytically recover the ultraviolet behavior of the original mode integral (4.72), or the magnitude of ρ_{ren} when the regulators become sufficiently heavy. Fortunately, these are the only regimes at which we shall need to renormalize the divergences we shall encounter. Hence, we need to perform the integral

$$\sum_{i=0} \langle T_0^0 \rangle_i = \lim_{\Lambda\to\infty} \frac{1}{2\pi^2 a^3} \sum_i \sigma_i \int_{\Lambda_{\rm IR}}^{\Lambda} dk k^2 \rho_{k,i}. \tag{4.75}$$

Using the expressions (4.73) and (4.74) we obtain

$$\rho^{(0)} = \sum_i \sigma_i \frac{-1}{\pi^2}\left[\frac{\Lambda^4}{4a^4} + \frac{\Lambda^2 M_i^2}{4a^2} + \frac{M_i^4}{32} - \frac{1}{8}M_i^4 \log\left(\frac{2\Lambda}{M_i a}\right)\right], \tag{4.76a}$$

$$\rho^{(2)} = \sum_i \sigma_i \frac{\dot{a}^2 M_i^2}{8\pi^2 a^4}\left[-\frac{4}{3} + \log\left(\frac{2\Lambda}{M_i a}\right)\right], \tag{4.76b}$$

and the convergent term

$$\rho^{(4)} = -\frac{1}{4\pi^2}\sum_i \sigma_i \left[\frac{11}{240}\frac{\dot{a}^4}{a^8} - \frac{1}{10}\frac{\ddot{a}\dot{a}^2}{a^7} - \frac{1}{40}\frac{\ddot{a}^2}{a^6} + \frac{1}{20}\frac{\dddot{a}\dot{a}}{a^6}\right], \tag{4.76c}$$

where $\rho^{(0)}$ contains no derivatives of the scale factor, $\rho^{(2)}$ contains two, and $\rho^{(4)}$ has four. Next, if the regulator masses and parities obey the relations

$$\sum_i \sigma_i = 0, \quad \sum_i \sigma_i M_i^2 = 0, \quad \sum_i \sigma_i M_i^4 = 0, \tag{4.77}$$

as we send Λ to infinity the first three terms in Eq. (4.76a) and the first term in Eq. (4.76c) disappear, however, they still depend on the regulator masses M_r through the terms $8\pi^2 \sum_r \sigma_r M_r^4 \log\left(\frac{M_r}{\mu}\right)$ and $\frac{1}{8\pi^2}\sum_r \sigma_r M_r^2 \log\left(\frac{M_r}{\mu}\right)$, and hence the integral diverge when the regulators are decoupled $M_r \to \infty$. However, if these surviving contributions are of the same form as those from the additional counterterms

$$S_{ct} = \int d^4x \sqrt{-g}\left[\delta\Lambda + \delta M_{\rm pl}^2\right] \tag{4.78}$$

which are given by

$$\delta\Lambda = \frac{1}{8\pi^2}\sum_r \sigma_r M_r^4 \log\left(\frac{M_r}{\mu}\right) + (\delta\Lambda)^f, \tag{4.79}$$

$$\delta M_{\rm pl}^2 = \frac{R}{6}\frac{1}{8\pi^2}\sum_r \sigma_r M_r^2 \log\left(\frac{M_r}{\mu}\right) + (\delta M_{\rm pl}^2)^f, \tag{4.80}$$

the integral will be UV divergent. Here we have introduced the arbitrary renormalization scale μ, and $\delta\Lambda^f$ and $\delta(M_{\rm pl}^2)^f$ are the finite pieces of the counterterms associated with a cosmological constant and the Einstein-Hilbert term, respectively. On dimensional grounds, terms with a higher number of time derivatives vanish as the cutoff Λ is sent to infinity. Finally, with the counterterms given by the previous expressions, the one-loop "exact" renormalized value of the energy density have the form

$$\begin{aligned}\rho_{\rm ren} = \lim_{\Lambda\to\infty}\Bigg\{ & \frac{1}{2\pi^2 a^3}\int_0^\Lambda dk k^2 \rho_k \\ & + \frac{\Lambda^4}{4\pi^2 a^4} + \frac{\Lambda^2 M_0^2}{4\pi^2 a^2} + \frac{M_0^4}{8(4\pi^2)} - \frac{M_0^4}{2(4\pi^2)}\log\left(\frac{2\Lambda}{a\mu}\right) + (\delta\Lambda)^f \\ & - \frac{4}{3}\frac{1}{8\pi^2}\frac{\dot a^2}{a^4}M_0^2 + \frac{1}{8\pi^2}\frac{\dot a^2}{a^4}M_0^2\log\left(\frac{2\Lambda}{a\mu}\right) + \frac{1}{8\pi^2}\frac{\dot a^2}{a^4}(\delta M_{\rm pl}^2)^f \\ & - \frac{1}{4\pi^2}\left[\frac{11}{240}\frac{\dot a^4}{a^8} - \frac{1}{10}\frac{\ddot a \dot a^2}{a^7} - \frac{1}{40}\frac{\ddot a^2}{a^6} + \frac{1}{20}\frac{\dddot a \dot a}{a^6}\right]\Bigg\},\end{aligned} \tag{4.81}$$

where $M_0 = m$ is the mass of the field ψ. Then after the substraction in equation (4.81), $\rho_{\rm ren}$ is UV divergent. Changes in the arbitrary renormalization scale μ effectively amount to changes in the finite values of these constants, which are determined by appropriate renormalization conditions. In that sense, observables that depend on the values of the counterterms are not predictions of the quantum theory. Note that, the subtraction terms in Eq. (4.81) arise from an adiabatic expansion of the vacuum energy of the regulators. Leaving the counterterms aside, it is in fact straightforward to check that, when the field is massive, $\rho_{\rm sub}$ is just the integral of the adiabatic expansion up to fourth order of the vacuum integrand in Eq. (4.69).

Our regularization scheme reproduces and justifies the often employed adiabatic scheme, but it goes beyond it because it makes the role of the counterterms explicit and it also explains the origin of the subtraction terms. Yet, from the perspective of Pauli-Villars regularization, the subtraction of adiabatic approximations to the spectral density is not fully justified [168]. In Pauli-Villars the masses of the regulators are assumed to be much larger than any accessible scale k, so their contribution to the spectral energy density at long distances is highly suppressed. For this reason, we shall not distinguish between the unrenormalized and renormalized spectral densities, as long as cosmological scales k are concerned. The regularization and renormalization afforded by the Pauli-Villars regulators is only of consequence in the ultraviolet, and only there does it play a role. Hence, we shall subtract $\rho_{\rm sub}$ from the energy density only when the mode integral includes the contributions of the ultraviolet.

4.6.2 The Conformal Anomaly

The trace of the energy-momentum tensor for a classical Dirac field is given by $T^{\mu}_{\mu} = m\bar{\psi}\psi$. In the limit where $m \to 0$ this trace vanishes. However, after quantizing the field $\hat{\psi}$, the renormalized value of $\langle T^{\mu}_{\mu}\rangle = \langle m\bar{\hat{\psi}}\hat{\psi}\rangle$ yields a non-zero value. This phenomenon is known as *the conformal anomaly*. To see this we need to renormalize the integral

$$\langle T^{\mu}_{\mu}\rangle_{\rm ren} = \frac{1}{2\pi^2 a^3}\int^{\infty} dk k^2[\rho^{\rm in}_k + 3p^{\rm in}_k], \text{ with } p_k = \frac{2k}{3a}\left[u^{\rm in}_k v^{\rm in*}_k + u^{\rm in*}_k v^{\rm in}_k\right], \quad (4.82)$$

and ρ^{in}_k given by Eq. (4.70a). In order to renormalize the vacuum expectation value of the trace, we use the Pauli-Villars procedure. For this, we need to expand the expression $\rho^{\rm in}_k + 3p^{\rm in}_k$ up to fourth adiabatic order. We have already calculated $\rho^{\rm in}_k$ up to fourth adiabatic order in Eq. (4.76). While $p^{(0)}_k$, $p^{(2)}_k$, and $p^{(4)}_k$ are given by

$$p^{(0)}_k = -\frac{2k^2}{3a\omega_k}, \quad (4.83a)$$

$$p^{(2)}_k = -\frac{k^2m^2\ddot{a}}{6\omega^5} + \frac{5k^2m^4a\dot{a}^2}{12\omega^7} + \frac{k^2m^2\dot{a}^2}{12\omega^5 a}, \quad (4.83b)$$

$$\begin{aligned} p^{(4)}_k = {} & \frac{k^2m^2a^{(4)}}{24\omega^7} - \frac{7k^2m^4a\ddot{a}^2}{16\omega^9} + \frac{k^2m^2\ddot{a}^2}{48\omega^7 a} - \frac{385k^2m^8a^3\dot{a}^4}{64\omega^{13}} \\ & + \frac{359k^2m^6a\dot{a}^4}{192\omega^{11}} + \frac{7k^2m^4\dot{a}^4}{128\omega^9 a} - \frac{7k^2m^4aa^{(3)}\dot{a}}{12\omega^9} \\ & - \frac{k^2m^2a^{(3)}\dot{a}}{48\omega^7 a} + \frac{77k^2m^6a^2\dot{a}^2\ddot{a}}{16\omega^{11}} - \frac{61k^2m^4\dot{a}^2\ddot{a}}{96\omega^9}. \end{aligned} \quad (4.83c)$$

Following the same procedure in Section (4.6.1) for the renormalization of the energy density $\rho_{\rm in}$, we cut off all momentum integrals to render them finite, and introduce a set of massive regulator fields to keep the pressure finite as the cutoff is removed. At zero, two and fourth derivatives, by also including the contribution of all the regulator fields, we arrive at

$$p^{(0)} = -\sum_i \frac{\sigma_i}{2\pi^2}\left[\frac{\Lambda^4}{6a^4} - \frac{\Lambda M_i^2}{6a^2} + \frac{7}{48}M_i^4 + \frac{M_i^4}{4}\log\left(\frac{\Lambda}{M_i a}\right)\right], \quad (4.84a)$$

$$p^{(2)} = -\sum_i \frac{\sigma_i M_i^2}{2\pi^2}\left[\left(\frac{\dot{a}^2}{36a^4} - \frac{\dot{a}^2}{12a^4}\log\left(\frac{2\Lambda}{M_i a}\right)\right) - \left(\frac{2\ddot{a}}{9a^3} - \frac{\ddot{a}}{6a^3}\log\left(\frac{2\Lambda}{M_i a}\right)\right)\right], \quad (4.84b)$$

$$p^{(4)} = \sum_i \frac{\sigma_i}{\pi^2 a^3}\left[-\frac{11\dot{a}^4}{576a^5} + \frac{a^{(4)}}{240a^2} - \frac{\ddot{a}^2}{96a^3} - \frac{a^{(3)}\dot{a}}{48a^3} + \frac{7\dot{a}^2\ddot{a}}{144a^4}\right], \quad (4.84c)$$

which remain finite as the cut-off is sent to infinity, as long as equations (4.77) are satisfied. Just like what happens with $\rho^{(4)}_k$, the integral of $p^{(4)}_k$ in Eq. (4.82) is divergent and independent of m. Furthermore, as the regulators are decoupled, by sending their masses to infinity, the counterterms that were needed to cancel the divergent contributions in the energy density, also cancel the divergencies in the pressure. Finally, by collecting the contributions of the

original spinor, the regulator fields and the counterterms we arrive at the final renormalized pressure

$$\begin{aligned} p_{\rm ren} &= \left\{ \frac{1}{2\pi^2 a^3} \int dk k^2 p_k \right. \\ &+ \frac{1}{2\pi^2}\left[\frac{\Lambda^4}{6a^4} - \frac{\Lambda m^2}{6a^2} + \frac{7}{48}m^4 + \frac{m^4}{4}\log\left(\frac{\Lambda}{\mu a}\right)\right] \\ &+ \left. \frac{m^2}{2\pi^2}\left[\left(\frac{\dot{a}^2}{36a^4} - \frac{\dot{a}^2}{12a^4}\log\left(\frac{2\Lambda}{\mu a}\right)\right) - \left(\frac{2\ddot{a}}{9a^3} - \frac{\ddot{a}}{6a^3}\log\left(\frac{2\Lambda}{\mu a}\right)\right)\right] \right\} \\ &- \frac{1}{\pi^2 a^3}\left[-\frac{11\dot{a}^4}{576a^5} + \frac{a^{(4)}}{240a^2} - \frac{\ddot{a}^2}{96a^3} - \frac{a^{(3)}\dot{a}}{48a^3} + \frac{7\dot{a}^2\ddot{a}}{144a^4}\right]. \end{aligned} \tag{4.85}$$

With these results, the trace (4.82) in the massless limit $m \to 0$ is given by

$$\langle T^{\mu}_{\ \mu}\rangle^{(4)} = \frac{1}{2\pi^2 a^3}\left[-\frac{a^{(4)}}{40a^2} + \frac{3\ddot{a}^2}{40a^3} + \frac{11\dot{a}^4}{240a^5} + \frac{a^{(3)}\dot{a}}{20a^3} - \frac{29\dot{a}^2\ddot{a}}{240a^4}\right] \tag{4.86}$$

In the Wolfram Mathematica notebook `https://www.wolframcloud.com/obj/e330fbd3-e35b-4abf-bf98-f8974492f127`, the reader can review the previous calculations in detail.

4.7 Particle Production Formalism

Equation (4.53a) is sufficient to compute the energy density of the Dirac field in the *in* vacuum at any time in cosmic history. All one needs is an *in* region to single out the appropriate state of the field. Given the *in* region, we can set up initial condition for the mode function $u_k^{\rm in}$ and $v_k^{\rm in}$ in the asymptotic past, and equations (4.22) then determines its evolution all the way to the asymptotic future. However, the use of $u_k^{\rm in}$ and $u_k^{\rm in}$ in equation (4.53a) is only a possible choice, and the energy density can be expressed in any other basis of mode functions.

Spectral Density. In order to write the spectral density of the *in* vacuum in terms of the arbitrary functions u_k, v_k, is sufficient to plug the expressions (4.49), that is $u_k^{\rm in} = \alpha_k u_k - \beta_k v_k^*$ and $v_k^{\rm in} = \alpha_k v_k + \beta_k u_k^*$, into the equation (4.53b). Clearly, by construction, the final result does not depend on the nature of the chosen mode functions u_k and u_k, as long the state of the field remains unchanged. After some algebra, and using the relation $|\alpha_k|^2 + |\beta_k|^2 = 1$, we can to rewrite the spectral density (4.53b) as

$$\rho_k = -(2/a)\left[(1-2|\beta_k|^2)\mathfrak{Im}\{u_k\dot{u}_k^* + v_k\dot{v}_k^*\} + 2\mathfrak{Im}\{\alpha_k\beta_k^*(v_k\dot{u}_k - u_k\dot{v}_k\}\right]. \tag{4.87}$$

Comparing the above result with the expression (4.53c), reveals that the *in* vacuum appears to effectively contain $n_k^a + n_k^b = 4|\beta_k|^2$ *out* particles that are not in an eigenvector of the *out* number operator, and $m_k^a = \alpha_k\beta_k^*$ and $m_k^b = \alpha_k^*\beta_k$. This formal similarity is behind what is referred to as "*particle production*". In this approach, we can consider the spectral energy density expression (4.87) as

the contribution of the *out* vacuum $\rho_{\rm out}$ plus the energy density of *out* produced particles $\rho^{\rm p}_k$, such that $\rho_k = \rho_{\rm out} + \rho^{\rm p}_k$, where

$$\rho_{\rm out} = (i/a)\big[u_k\dot{u}^*_k + v_k\dot{v}^*_k - u^*_k\dot{u}_k - v^*_k\dot{v}_k\big] \tag{4.88}$$

and

$$\rho^{\rm p}_k = -(2/a)\left[(-2|\beta_k|^2)\mathfrak{Im}\{v_k\dot{v}^*_k + u_k\dot{u}^*_k\} + 2\mathfrak{Im}\{\alpha_k\beta^*_k(v_k\dot{u}_k - u_k\dot{v}_k\}\right]. \tag{4.89}$$

Note that the contribution of $\rho^{\rm p}_k$ left over when $\beta_k = 0$. The above expression would associate the spectral energy density $\rho^{\rm p}_k$ to the "produced particles". Hence, one could regard equation (4.89) as the spectral density of the field (4.87) from which the spectral density of the *out* vacuum (4.88) has been subtracted. As a matter of fact, however, the *out* vacuum plays no role in our analysis, first because it depends on the arbitrary choice of mode functions u_k and v_k, and second because we assume that the field is in the *in* vacuum. Furthermore, since we are interested in the gravitational effects of the field, there is no physical basis for the removal of the *out* vacuum energy density. In the adiabatic scheme, if the field is massive, renormalization amounts to the subtraction in the spectral density given in equation (4.81). But the latter is the spectral density of the *out* vacuum only when the *out* adiabatic vacuum is actually defined, in the adiabatic regime, and only up to factors of fourth adiabatic order.

In any case, we shall no adopt adiabatic regularization here, and equation (4.89) is not usually associated with particle production formalism. Instead, see for instance Refs. [177, 178], the energy density is usually approximated by

$$\rho = \frac{4}{(2\pi a)^3}\int d^3k E_{\rm out}|\beta_k|^2 = \frac{4}{2\pi^2 a^4}\int dk k^2\omega_{\rm out}|\beta_k|^2, \tag{4.90}$$

where $E_{\rm out} = \omega_k/a$ is the energy of a particle in the *out* region and the four factor come from the sum of particles and antiparticles, which neglects the *out* vacuum contribution and assumes that the *in* vacuum is an eigenvector of the *out* number operator, with eigenvalue $|\beta_k|^2$. To explore the potential applicability of equation (4.90) it is useful to consider the spectral density when the corresponding modes are in the adiabatic regime, and we can approximate u_k and v_k by equation (4.29). This does not generally hold, but applies, for instance, for massive fields at late times or sufficiently large wavenumbers. Now, using Eq. (4.29) into Eq. (4.89) and using the fact that $\alpha_k\beta^*_k = \alpha^*_k\beta_k$, we can write Eq. (4.89) as

$$\begin{aligned}\rho^{\rm p}_k = \frac{i}{a}\Bigg\{(-2|\beta_k|^2)\Bigg[&\left(\frac{\omega_k + ma}{2\omega_k}\right)\Big(2i\Omega|F|^2 + 2i\mathfrak{Im}(\dot{F}^*F)\Big)\\ &+\left(\frac{\omega_k - ma}{2\omega_k}\right)\Big(2i\Omega|G|^2 + 2i\mathfrak{Im}(\dot{G}^*G\Big)\Bigg]\\ &- 4i\alpha_k\beta^*_k\mathfrak{Im}\Bigg[\left(\frac{-km\dot{a}}{2\omega^2_k}\right)\exp\left(-2i\int\Omega d\tilde{\eta}\right)FG\\ &+\frac{k}{2\omega}\exp\left(-2i\int\Omega d\tilde{\eta}\right)\Big(F\dot{G} - G\dot{F}\Big)\Bigg]\Bigg\}.\end{aligned} \tag{4.91}$$

Which, up to second adiabatic order have the form

$$\rho_k^{\rm p} = \frac{i}{a}\Bigg\{(-2|\beta_k|^2)\left(2i\omega_k + 2i\omega_k\frac{m^2\dot{a}^2}{16\omega^4}\right) - 4i\alpha_k\beta_k^*\mathfrak{Im}\Bigg[\left(\frac{-km\dot{a}}{2\omega_k^2}\right)\exp\left(-2i\int\Omega d\tilde{\eta}\right) + \exp\left(-2i\int\Omega d\tilde{\eta}\right)\frac{i}{4}\left[\frac{km\ddot{a}}{\omega_k^3} - \frac{2k\dot{a}^2m^3a}{\omega_k^5}\right]\Bigg\}. \quad (4.92)$$

In the adiabatic limit, when frequencies are large $\omega_k \gg \mathcal{H}$, we can proximate $\Omega_k \approx \omega_k$, $F(\eta) \approx 1$ and $G(\eta) \approx 1$. In this approximation we can rewrite the expression (4.91) as

$$\rho_k^{\rm p} \approx \frac{4\omega_k}{a}|\beta_k^{\rm ad}|^2 + \alpha_k\beta_k^*\frac{4km\dot{a}}{2\omega_k^2}\sin\left(2\int\omega_k d\tilde{\eta}\right). \quad (4.93)$$

In this expression the second term is doubly suppressed: first because opposed to the first term proportional to ω_k, this is proportional to $\mathcal{H}$, and second because this rapidly oscillates with time. But adiabaticity and high frequencies are still not sufficient to guarantee the validity of the particle production formula (4.90). In the limit $|\beta_k^{\rm ad}|^2 \to 1$ when particle production is "effective", the second term in Eq. (4.93), is $|\alpha_k^{\rm ad}\beta_k^{*\rm ad}| \approx 0$. Therefore, we can only claim that the terms on the first line in Eq. (4.92) are necessary "dominant" if, in addition, particle production is "effective", $|\beta_k^{\rm ad}|^2 \to 1$. So, if this is the case, in the mode range in which these conditions are simultaneously met, the energy density is well approximated by

$$\rho^p \approx \frac{4}{2\pi^2a^4}\int_0^\infty dk k^2|\beta_k^{\rm ad}|^2\omega_k, \quad (4.94)$$

which possesses an interpretation in terms of particles, once we identify $4|\beta_k|^2$ with the number density of the particles n_a and the antiparticles n_b created in the mode k. We are referring to Eq. (4.94) whenever we invoke the "particle production formalism". For massless particles the dispersion relation is $\omega_k = k$, and $\rho_k^{\rm p}$ scales like radiation. For massive particles $\omega_k \approx ma$ at late times, and $\rho_k^{\rm p}$ would scale like dust. Those are the two behaviors usually attributed to free particles. Although the meaning of the Bogoliubov coefficients α_k and β_k is tied in general to the arbitrary choice of mode functions u_k and v_k in equation (C.44), in order to arrive at Eq. (4.94) we have employed the adiabatic approximation (4.29). Hence, the $\beta_k^{\rm ad}$ in equation (4.94) are uniquely determined by that choice of mode functions. Since Eq. (4.94) neglects terms with one derivative, it is inconsequential to calculate β_k beyond the zeroth order adiabatic approximation. However, strictly speaking, even at the limit of effective particle production $|\beta_k^{\rm ad}|^2 \to 1$, it is not possible to neglect the contribution of the vacuum $\rho_{\rm out}$ (unlike what we did for the scalar case), so the approximation $\rho_{ren} \approx \rho^p$ is not valid even at this limit. For this reason, we have used quotation marks around the terms "effective" production and "dominant" contribution. This is a consequence derived from Fermi-Dirac statistics, so it is not possible, in general, to approximate $\rho_{ren} \approx \rho_p$ even when the three conditions mentioned are satisfied.

It is also worth pointing out that equation (4.94) fails at small frequencies even when the modes themselves are in the adiabatic regime and particle production is effective, because to justify it we need to assume that $\omega_k \gg \mathcal{H}$. Conversely, since the validity of the adiabatic approximation demands that $\Omega_k^{(n)} \gg \Omega_k^{(n+1)}$, $F^{(n)} \gg F^{(n+1)}$, $G^{(n)} \gg G^{(n+1)}$, for all n, it is conceivable for one of these conditions to be violated even when frequencies are large.

In conclusion, the particle production formula (4.94) is "well-justified" provided that

i) *particle production* is effective ($|\beta_k^{\rm ad}|^2 \to 1$),

ii) the relevant modes are in te abiabatic regime (that is $\Omega_k^{(n)} \gg \Omega_k^{(n+1)}$, $F^{(n)} \gg F^{(n+1)}$, $G^{(n)} \gg G^{(n+1)}$),

iii) the modes frequencies are large ($\omega_k \gg \mathcal{H}$).

Even then one should recognize that the approximation (4.94) does not extend beyond the leading adiabatic order, since the terms that are neglected in equation (4.91) are of first order. Note that when particle production is ineffective, that is $|\beta_k^{\rm ad}|^2 = 0$, the spectral density of the field is dominated by that of the *out* vacuum equation (4.88). Table (4.3) lists the conditions under which the various equations in this subsection are valid approximations to the fermion field energy density. Again, we have used quotes around the expression "well-defined" because even when the three conditions i), ii), and iii) are satisfied, due to Fermi-Dirac statistics, it is in general not possible to disregard the contribution of the vacuum $\rho_{\rm out}$, so, in general, the approximation $\rho \approx \rho_{\rm p}$ is not valid.

The adiabatic limit of the *out* mode functions in the ultraviolet also allows us to determine under what conditions the renormalized energy density after the transition remains finite. By construction, the terms in equation (4.87) that survive when $|\beta_k|^2$ is set to zero give rise to a ultraviolet divergent integral that is regulated and renormalized by the subtraction terms in Eq. (4.76). Therefore, the remaining terms must yield a finite contribution to the energy density. To estimate their behavior in the ultraviolet, we substitute the leading approximation $\Omega_k \approx \omega_k \approx k$ into equation (4.93). At leading order we obtain

$$\rho_k^{\rm p} \approx \frac{4}{a}|\beta_k|^2 k + \alpha_k \beta_k^* \frac{4ma^2\mathcal{H}}{2k} \sin(2k\eta + \varphi), \tag{4.95}$$

which implies that $|\beta_k|^2$ has to decay faster than $1/k^2$ in order for the integral (4.53a) to remain finite, since $\alpha_k \approx 1$ in the ultraviolet[10]. On the other hand, note that the expression (4.50b) for β_k, the above implies that it is not necessary for the second derivative of the scale factor $\ddot{a}(t)$ to be continuous to avoid divergences in ρ unlike the case for the scalar field. With $|\beta_k| \sim 1/k^3$, the energy density (4.94) is ultraviolet finite.

A look at Cosmological Gravitational Particle Production. Now, let's consider the expression for $\beta_k^{(\rm ad)}$ up to first adiabatic order $n = 1$. Using the

[10]Given the normalization condition $|\alpha_k|^2 + |\beta_k|^2 = 1$, in the ultraviolet $|\beta_k|^2 \ll 1$ and $\alpha_k \approx 1$.

expression (4.50b) and the first order solutions (4.36), we can we see that $\beta_k^{(1)} \approx \frac{ikm}{4\omega_k^3}[\dot{a}^{(+)} - \dot{a}^{(-)}]$. From this last expression, we can see that $\beta_k^{(1)}$ vanishes when $m \to 0$, so we can anticipate that cosmological gravitational particle production will be suppressed when dealing with spin 1/2 particles of light masses. Also, let's observe that $\beta_k^{(1)}$ vanishes when $k \to 0$, so we expect particle production to be suppressed for long-wavelength modes. So, an *effective* particle production requires considering the *superheavy regime* and short-wavelength modes. We had already anticipated in previous sections that large modes and light mass modes are suppressed in ρ_k. In Ref. [176], the authors found, within the framework of inflationary cosmology, that $|\beta_k|^2 \sim 1$ if the field is light $H > m$ and $k \sim ma$, that is, for a small mass compared to the Hubble parameter, particle production is significant. Gravitational production for spin 1/2 particles is typically more efficient for masses in the superheavy regime, around the inflationary Hubble scale, $m \sim H_{\rm inf} \sim 10^{14}$GeV. Finally, let us note that this behavior is also expected for a conformally-coupled scalar field.

Energy Density. Even though the spectral density ρ_k is particularly convenient to study the contribution of the different modes to the total energy density, it is not an actual observable. The Einstein gravitational equations $\mathcal{H}^2/a^2 = a^2\rho/3M_p^2$ are sourced by the renormalized total energy density, which is given by the integral of the spectral density once we have removed the subtraction terms $\rho_{\rm ren} = \rho - \rho_{\rm sub}$. It is convenient to split $\rho_{\rm ren}$ in terms of those modes which are adiabatic, that is, the modes for which the adiabatic *out* vacuum is defined $\rho_{\rm ad}$, which we shall label by "ad", and those for which it is not $\rho_{\cancel{\rm ad}}$, which we shall denote by "$\cancel{\rm ad}$". The former are precisely those that satisfy condition ii) above, whereas the latter typically include those beyond the horizon when the field is light or massless. Then we can write

$$\rho_{\rm ren} = \rho_{\cancel{\rm ad}} + \rho_{\rm ad}, \tag{4.96a}$$

where

$$\rho_{\rm ad} = \rho_{\rm ad}^{\rm p} + \left(\rho_{\rm ad}^{\rm out}\right)_{\rm ren}, \text{ with } \left(\rho_{\rm ad}^{\rm out}\right)_{\rm ren} \equiv \rho_{\rm ad}^{\rm out} - \rho_{\rm sub} \tag{4.96b}$$

and

$$\rho_{\cancel{\rm ad}} \equiv \frac{1}{2\pi^2 a^3}\int_{\cancel{\rm ad}} dk k^2 \rho_k^{\cancel{\rm ad}},\ \rho_{\rm ad}^{\rm p} \equiv \frac{1}{2\pi^2 a^3}\int_{\rm ad} dk k^2 \rho_k^{\rm p},\ \rho_{\rm ad}^{\rm out} \equiv \frac{1}{2\pi^2 a^3}\int_{\rm ad} dk k^2 \rho_{\rm out}.$$

The energy density of the adiabatic modes is divided in two contributions, one of "produced particles" $\rho_{\rm ad}^{\rm p}$ and the other one of the renormalized *out* vacuum for these modes, $(\rho_{\rm ad}^{\rm out})_{\rm ren}$. It is important to stress that the spectral density that enters the energy density $\rho_{\rm ad}^{\rm p}$, here is the one in Eq. (4.89), since only then is the quoted expression for $\rho_{\rm ren}$ in Eq. (4.96a) exact. Because $|\beta_k^{\rm ad}|^2$ has to decay faster than $1/k^2$, the adiabatic energy density $\rho_{\rm ad}^{\rm p}$ is ultraviolet finite, and we can directly set the cutoff Λ to infinity therein. On the other hand, both $\rho_{\rm ad}^{\rm out}$ and $\rho_{\rm sub}$ are ultraviolet divergent, and only the difference between $\rho_{\rm ad}^{\rm out}$ and $\rho_{\rm sub}$ remains finite as $\Lambda \to \infty$. The value of $\rho_{\cancel{\rm ad}}$ does not depend on our choice of mode functions, since it corresponds to the energy density of the non-adiabatic modes in the *in* vacuum, and neither does the sum $\rho_{\rm ad}^{\rm p} + (\rho_{\rm ad}^{\rm out})_{\rm ren}$, which is that of the adiabatic modes in the same state. In

the last case the individual $\rho^{\rm p}_{\rm ad}$ and $(\rho^{\rm out}_{\rm ad})_{\rm ren}$ do actually depend on the election of mode functions, but adiabaticity singles out a "preferred" state, the *out* adiabatic vacuum.

In the end, though, which of the three components in $\rho_{\rm ren}$ dominates the energy density, depends on the properties of the *in* vacuum and the evolution of the universe since the beginning of inflation. But the applicability of the "*particle production formalism*" requires the validity of conditions i), ii) and iii). Just as we did above, it is hence useful to split the adiabatic modes into those that additionally satisfy conditions i) and iii) from those that do not. When the terms of $\rho_{\rm ren}$ that satisfies these conditions are dominant, we can approximate

$$\rho_{\rm ren} \approx \frac{4}{2\pi^2 a^4}\int_{\rm pp} dk k^2 |\beta_k|^2 \omega_k \tag{4.97}$$

where "pp" denotes that the integral only runs over the modes that satisfy condition i), ii), and iii), and only under those circumstances it is then justified to write. With the integration range replaced by all modes, Eq. (4.97) is the "particle production" equation often used in the literature. However, since one or several of the conditions stated above typically fails, the latter is in general not a valid approximation to the field energy density. In general, it is not possible to neglect the vacuum energy density $\rho_{\rm out}$, so, in that case, the expression (4.97) is not always applicable.

Combining Eq. (4.53b) with Eqs. (4.87) and (4.89) we obtain an alternative expression for the effective particle number density that appears in equation (4.97) as

$$|\beta^{\rm ad}_k|^2 = \frac{i}{4\omega_k}(u^{\rm in}_k \partial_0 u^{\rm in*}_k + v^{\rm in}_k \partial_0 v^{\rm in*}_k - u^{\rm in*}_k \partial_0 u^{\rm in}_k - v^{\rm in*}_k \partial_0 v^{\rm in}_k) + \frac{1}{2}. \tag{4.98}$$

This expression is an adiabatic invariant, that is, it is a constant in the limit of a constant scale factor. It is only useful when Eq. (4.97) is a valid approximation to the particle $\rho^{\rm p}_k$, that is, when the three condition i), ii) and iii) are satisfied.

At this point it becomes clear that in most cases the particle production formalism is just an approximation at best. As far as the spectral density is concerned, equation (4.87) remains true no matter whether the notion of particle exists, and regardless of how the mode functions u_k and v_k are chosen. Furthermore, if we knew the form of the *in* mode functions throughout cosmic history, $u^{\rm in}_k$ and $v^{\rm in}_k$, there would be no need to go through the process of introducing Bogolubov coefficients and evaluating Eq. (4.87) or its approximations, Eqs. (4.89) to (4.94); it would just suffice to evaluate equations (4.53a) at any desired time. The "particle production formalism" is useful in the adiabatic regime and at high frequencies, where we can interpret the field excitations as actual particles on top of the *out* adiabatic vacuum. However, it does not universally apply to all modes of the field, as it is sometimes implicitly assumed in the literature, nor its use is restricted to asymptotically flat spacetimes, as it is often presented in the standard monographs.

4.8 Classical Field Description

In which cases can the classical field formalism be applied? We have already seen that if there is a solution to equation (4.64), the excitation of the mode with $\vec{k} = 0$ is macroscopic and its contribution to the energy density can be considered as that of a homogeneous classical field of Dirac when $m \neq 0$. We have also seen that this treatment can be extended to the range $0 < k < \Lambda_{\rm IR}$ when the modes are relativistic or non-relativistic or if the modes are *light* or *heavy*, we can also talk about *particle production*. Let's now investigate whether it is possible to extend this treatment to the range $\Lambda_{\rm IR} < k < \infty$, where the state of the field is assumed to be the *in* vacuum.

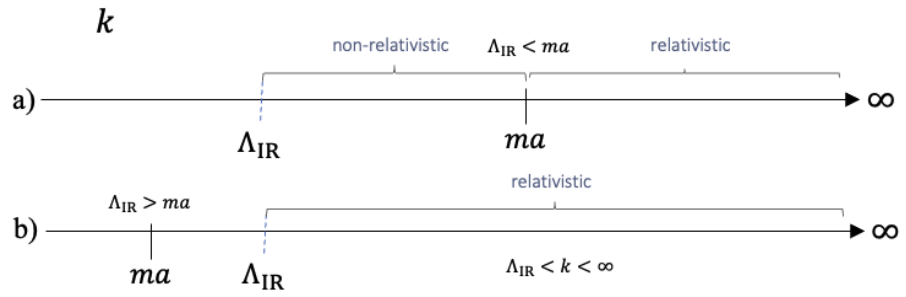

Figure 4.4: **Relativistic and non-relativistic modes**. a) Modes in the range $\Lambda_{\rm IR} < k < \infty$ for which $ma > \Lambda_{\rm IR}$ consist of modes that are relativistic and non-relativistic. b) Modes in the range $\Lambda_{\rm IR} < k < \infty$ for which $ma < \Lambda_{\rm IR}$ consist of modes that are only relativistic.

We consider for this purpose that $\rho_{\rm ren}$ is given by Eq. (4.81) such that, if we split into the non-relativistic and relativistic modes, we obtain

$$\rho_{\rm ren} = \rho_{<ma} + \rho_{\rm ren}^{>ma}, \text{ where } \rho_{\rm ren}^{>ma} \equiv \rho_{>ma} - \rho_{\rm sub}^{>ma} \tag{4.99a}$$

and

$$\rho_{<ma} \equiv \frac{1}{2\pi^2 a^3}\int_{\Lambda_{\rm IR}}^{ma} dk k^2 \rho_k, \quad \rho_{>ma} \equiv \frac{1}{2\pi^2 a^3}\int_{ma}^{\infty} dk k^2 \rho_k. \tag{4.99b}$$

Note that there is no ambiguity in this decomposition, as the energy density refers to that of the *in* vacuum, as opposed to that of the particle and *out* vacuum in Eq. (4.96a). In Eq. (4.99a) we have assumed that $\Lambda_{\rm IR} < ma$, that is, the modes in $\Lambda_{\rm IR} < k < ma$ are non-relativistic, see Figure 4.4. Remember that in the relativistic case the dispersion relation is approximate by $\omega_k \approx k$, and in the non-relativistic case is approximate by $\omega_k \approx ma$. So for $\rho_{<ma}$, the energy density corresponding to the modes that are non-relativistic and their dispersion relation is k-independent, their mode functions must be of the form $u_k^{\rm in}(\eta) \approx \alpha_k^* u_0 + \beta_k v_0^*$, $v_k^{\rm in}(\eta) \approx \alpha_k^* v_0 - \beta_k u_0^*$. Substituting this into Eq. (4.70a), we find that we can cast the energy density of the non-relativistic modes as that of the *homogeneous classical Dirac field*, provided that

$$\rho_{<ma} = \frac{\rho_{m,0}(\eta)}{a^3} = -\frac{m}{\pi^2 a^3}\int_{\Lambda_{\rm IR}}^{ma} dk k^2 \left(1 - 2|\beta_k|^2\right). \tag{4.100a}$$

Note that with $n_k^a + n_k^b = 2|\beta_k|^2$ these equation differ from Eq. (4.68) only in the integration limits. If we assume that the upper limit is constant, and if we make the identification $[\sum_\lambda |A_\lambda|^2 - |B_\lambda|^2] = \frac{1}{\pi^2}\int_{\Lambda_{\rm IR}}^{ma} dk k^2\,(1 - 2|\beta_k|^2)$, we can think of the field as a homogeneous classical Dirac field with $\rho_{<ma} = \rho_{m,0}/a^3$. This is the case where spacetime is asymptotically adiabatic, that is, $ma \sim$ constant and $\mathcal{H} \ll \omega_k$ as $\eta \to \infty$. In particular, for a universe that experiences a transition from an inflationary period to a radiation-dominated universe, we have that $a(t) = t^{1/2}$ and $H \to 0$ as $t \to \infty$. In Ref. [165], the authors have calculated the renormalized energy density of the *created particles* for late times $t \gg m^{-1}$ in this particular universe. The result they report is analogous to Eq. (4.100) differing by the integration limits. There, the authors integrate over all modes $0 < k < \infty$.

Now, let's analyze the contribution $\rho_{>ma}$, that is, the relativistic contribution to the energy density. Since the contribution to the energy density $\rho_{>ma}$ comes from the relativistic modes and their dispersion relation is approximate by $\omega_k \approx k$ we can use the approximated solutions $u_k^{m\approx 0}$ and $v_k^{m\approx 0}$. With these we can write

$$\rho_{>ma} = \frac{\rho_{r,0}(\eta)}{a^4} = -\frac{1}{\pi^2 a^4}\int_{ma}^{\infty} dk k^3\left(1 - 2|\beta_k|^2\right), \tag{4.100b}$$

Again, note that if $n_k^a + n_k^b = 2|\beta_k|^2$ these equation differ from Eq. (4.67) only in the integration limits. However, we can't think of the this contribution as that of homogeneous classical Dirac field of the form $\rho_{>ma} = \rho_{r,0}/a^4$, since massless fields do not admit classical field interpretation. In Ref. [165], the authors have calculated the renormalized energy density of the *created particles* for the relativistic modes in a radiation-dominated universe at early times $t \ll m^{-1}$, where they report a behavior analogous to Eq. (4.100b) differing again at the integration limits. When, $\Lambda_{\rm IR} > ma$, the modes in the range $\Lambda_{\rm IR} < k < \infty$, are relativistic (see Figure 4.4). In this case $\rho_{>ma} = \rho_{\rm ren}^{\rm out} + \rho_{r,0}/a^4$ where $\rho_{\rm ren}^{\rm out}$ is the renormalized vacuum contribution and $\rho_{r,0}/a^4 = (1/\pi^2 a^4)\int_{\Lambda_{\rm IR}}^{\infty} dk k^3 |\beta_k|^2$ is the contribution of the relativistic *created particles* if conditions i), ii), and iii) are satisfied. We summarize the previous results in Table 4.2.

So, when $\Lambda_{\rm IR} < ma$ and the classical contribution $\rho_{<ma}$ are well defined and dominant, we can approximate ρ_{ren} like that of a homogeneous classical field whose energy density is given by

$$\rho_{\rm cl} = i/2a(\bar{\Psi}_{\rm cl}\gamma^0\partial_0\Psi_{\rm cl} - \partial_0\bar{\Psi}_{\rm cl}\gamma^0\Psi_{\rm cl}) \tag{4.101}$$

with $\Psi_{\rm cl} = \sum_\lambda \left[A_\lambda U_\lambda + B_\lambda V_\lambda\right]$. It is under these circumstances that the classical field formalism becomes really useful. When the dominant modes are adiabatic and non-relativistic and particle production is effective, the "particle production" and classical field formalisms yield the same results. We conclude by emphasizing that, although we have discussed the energy density of the Dirac field within the specific context of cosmic transitions, many of the results in Section (4.5) are applicable to a much wider class of scenarios almost without modification. All that is essentially needed is for a subset of the Dirac field modes to be in a preferred state $|0_{\rm in}\rangle$ such that $\hat{a}_{\vec{k}}^{\rm in}\,|0_{\rm in}\rangle = 0$. In Table 4.3, we summarize the main results of this chapter.

Modes in range $\Lambda_{\rm IR} < k < \infty$			
$\rho_{<ma}$	non-relativistic modes $\Lambda_{\rm IR} < k < ma$	$\omega_k^2 \approx m^2 a^2$, $\chi_k^{\rm in} \approx \alpha_k \chi_0^{\rm out} + \beta_k \chi_0^{\rm out*}$	These modes admits classical field interpretation $\rho(\eta) = \rho_{m,0}/a^3$
$\rho_{>ma}$	relativistic modes $ma < k < \infty$	$\omega_k \approx k$, $\chi_k^{\rm in} \approx \alpha_k \chi_k^{\rm out} + \beta_k \chi_k^{\rm out*}$	These modes do not admit classical field interpretation $\rho(\eta) = \rho_{r,0}/a^4$

Table 4.2: Energy density for the modes in the range $\Lambda_{\rm IR} < k < \infty$, when $\Lambda_{\rm IR} < ma$. *In the first row* $\rho_{<ma}$ is the contribution to ρ_{ren} from the non-relativistic modes $\Lambda_{\rm IR} < k < ma$, for which $\omega^2 \approx m^2 a^2$. These modes can be interpreted in terms of a homogeneous classical field. *The second row* corresponds to the relativistic modes for which $ma < k < \infty$. These modes does not allow for a classical interpretation. When, $\Lambda_{\rm IR} > ma$, the modes in the range $\Lambda_{\rm IR} < k < \infty$, are relativistic, see Figure (4.4).

Mode	state	formalism
$k = 0$	unknown	negligible contribution
$0 < k < \Lambda_{\rm IR}$	unknown	particles: posibly at high frequencies (Sec. 4.5.2) classical field: non-relativistic modes (Sec. 4.5.2)
$\Lambda_{\rm IR} < k < \Lambda$	*in* vacuum	particles: posibly at high frequencies (Sec. 4.7) classical field: non-relativistic modes (Sec. 4.7)

Table 4.3: Conditions under which the energy density of the different modes of the quantum fermion field ψ admits a description in terms of particles or a classical field. In the range $\Lambda_{\rm IR} < k < \Lambda$ the state of the field is determined by the *in* a vacuum configured by inflation, so we can predict its contribution to the energy density, which in some cases can be computed using the particle or classical field formalisms, whichever is applicable. See the quoted sections for further details.

Chapter 5

Conclusions

In Chapters 1 and 2 of this thesis, we have studied the equilibrium configurations known as boson and Proca stars in the non-relativistic regimes. These configurations constitute compact, self-gravitating, self-interacting objects of finite energy that do not disperse over time and constitute minima of the energy functional for a fixed number of particles, whose ground state (or minimum-energy state) is given by spherically symmetric configurations. Due to their non-interacting nature (i.e., being fields that interact only with gravity and themselves, see Ref. [119]) and their mass and length ranges (that may reach to astrophysical scales), they can serve as dark matter models that could alleviate small-scale problems, such as the "cuspy" and "missing satellite" problems. However, since they do not interact directly with any other field, these models must account for the mechanism by which dark matter is produced. In this vein, in Chapters 3 and 4 we study the gravitational particle production mechanism for scalar and fermion quantum fields undergoing a cosmic transition. Within this framework, we make an effort to characterize the energy density of the gravitationally produced particles and to distinguish their contribution from the vacuum energy. To properly renormalize the vacuum contribution of these fields, we introduce Pauli-Villars renormalization, which allows us to handle divergences in the vacuum energy density. We also make an effort to determine in which regimes it is possible to speak of a classical field description for this quantum phenomenon. In Chapters 2 and 4, we recover the results obtained in the published and forthcoming papers *Nonrelativistic Proca stars: Spherical stationary and multi-frequency states* [1], *Linear stability of nonrelativistic Proca stars* [2] and *Cosmic Spinors and the Weight of the Vacuum* [3]. Chapters 1 and 3 are intended to introduce the concepts and methodologies used throughout the thesis, making its presentation more comprehensible.

The first part of the thesis, concerning self-gravitating objects, captures the phenomenology of non-relativistic equilibrium configurations for massive, complex, self-interacting scalar and vector fields (for boson stars, we have introduced the relativistic treatment for illustrative purposes and briefly outlined the relativistic treatment for Proca stars). The parameter space for non-relativistic boson stars is determined by the value of the field mass m_0 and the value of the self-interaction constant λ_n. The configurations that minimize the energy functional evolve harmonically in time and constitute *stationary boson stars*. Depending on whether the self-interaction is attractive or repulsive, the energy of these configurations may be bounded from below. For an attrac-

tive self-interaction, the energy value is not bounded from below. Spherically symmetric configurations constitute solutions that minimize the energy. For non-relativistic Proca stars, the parameter space grows, and the spectrum of configurations is more diverse. The spectrum of Proca star solutions depends on the spin-spin self-interaction parameter λ_s, which captures the effect of the spin of the field. When $\lambda_s \neq 0$ (called *generic sector* of the parameter space) the Proca star's wave function evolves in time harmonically with a single frequency. These configurations constitute *stationary* (or single-frequency) Proca stars. However, when $\lambda_s = 0$, the effective theory acquires an additional (accidental) symmetry, resulting in a reduced parameter space called *symmetry-enhanced sector*. In this sector, new types of equilibrium configurations appear in addition to stationary states in which the wave function oscillates with two or three distinct frequencies. These configurations constitute *multi-frequency* Proca stars. This spectrum of configurations differs from that of a boson star, where we only find stationary configurations that evolve harmonically with a frequency. The important difference is the spin term introduced by the vector field theory. Analogously to a boson star, depending on the nature of the particle-particle λ_n and spin-spin λ_s self-interactions, the energy functional may be bounded from below. We find that, for the cases when $\lambda_n, \lambda_s \geq 0$ or $\lambda_n - |\lambda_s| \geq 0$ (with $\lambda_n \geq 0$ and $\lambda_s < 0$), the energy functional is bounded from below. Furthermore, we find that spherically symmetric configurations with constant polarization constitute the minimum-energy state (i.e. the ground state configuration). When $\lambda_n > 0$ and $\lambda_s > 0$, the state that minimize the energy is spherically symmetric with linear polarization. When $\lambda_n > 0$, $\lambda_s < 0$ and $\lambda_n - |\lambda_s| \geq 0$ the state that minimizes the energy is spherically symmetric with circular polarization. Radially polarized and multi-frequency states represent higher energy solutions. All of the above results have been implemented and verified numerically.

The second part of the thesis, concerning the gravitational particle production of dark matter, studies the quantum phenomenon of cosmological particle production for non-interacting scalar and fermion quantum fields as a result of cosmic transitions in an FLRW universe. In the semi-classical formalism, the gravitational field is treated classically, while the matter fields are treated quantum mechanically. In this context, for scalar and spin-1/2 fermion fields, we find that, given a cosmic transition from an *in* (inflationary) region to a subsequent *out* (radiation-dominated) region, for asymptotically adiabatic FLRW spacetimes, it is possible to characterize the energy density of the created particles, ρ^{p}, as the integral of the energy per particle ω_k times the number of particles N_k for each mode k, distinct from the vacuum energy density that we renormalized using the Pauli–Villars scheme. However, whereas for bosons an indeterminate number of particles can occupy the same quantum state, for fermions the number of particles is limited to two per state. This implies that for a scalar field, it will be possible to neglect the vacuum contribution when the number of particles per mode k is large, whereas for the fermion case, this is generally not possible; instead, it will depend on how the vacuum energy compares to ρ^{p}. In any case, it is possible to interpret the energy density ρ_{ren} in terms of a classical field for non-relativistic modes if we can neglect the contribution from relativistic modes. Finally, in both cases, for bosons

and fermions, when the vacuum contribution is negligible and the dominant modes are adiabatic and non-relativistic, the classical field interpretation and the particle formalism may coincide, as might be expected in some dark-matter models (as in some axion dark matter models).

Appendix A

Appendix Chapter I

In this appendix, we will review in detail the derivation of the nonrelativistic action from the relativistic Einstein-Klein-Gordon action (1.1). For this, we will carry out the analysis in three steps. First, we will analyze the nonrelativistic limit of the free theory, which excludes self-interactions and the effects of gravity. Next, we will analyze the term with self-interaction, and finally, we will analyze the part of the action corresponding to the gravitational effects coming from the Einstein-Hilbert action and the kinetic term of the scalar field. We will develop an identical process when dealing with the nonrelativistic limit of the Einstein-Proca action in Chapter 2.

A.1 Nonrelativistic Limit of the Relativistic action

In the non-relativistic regime is convenient to write the spacetime line element as

$$ds^2 = -[1 + 2\Phi(t, \vec{x})]dt^2 + [1 - 2\Psi(t, \vec{x})]\delta_{ij}dx^i dx^j, \tag{A.1}$$

and to assume the complex scalar field in the form

$$\phi(t, \vec{x}) = \frac{1}{\sqrt{2m_0}} e^{-im_0 t}\psi(t, \vec{x}), \tag{A.2}$$

where $\Phi(t, \vec{x})$ and $\Psi(t, \vec{x})$ are scalar gravitational potentials in the Newtonian gauge (we have neglected the traceless *strain* tensor s_{ij} and vector perturbations ω_j since these do not couple to nonrelativistic matter) and $\psi(t, \vec{x})$ is the wave function, whose role is clarified bellow. In the non-relativistic limit the different quantities in the action (1.1) scales like $\Phi(t, \vec{x}) \sim \Psi(t, \vec{x}) \sim \epsilon$, $\psi \sim \sqrt{M_{\rm pl}^2 m_0}\epsilon$ and $\partial_t \sim \epsilon^{1/2}\partial_i \sim \epsilon m_0$, with ϵ a small positive number. In order to explore the non relativistic limit of the action (1.1) we will separate the action (1.1) into the free theory $S_{\lambda=0}$, which excludes the effects of the self-interactions and gravity, the self-interacting terms S_λ and the gravity terms S_G which are codified in the spacetime line element (A.1).

First, we analyze the free theory, that is when gravity and self-interactions are absent. In this case we can obtain the system of equations by varying $S_{\lambda=0}$ with respect to the wave function $\psi(t, \vec{x})$. The free theory is described in terms

of the action

$$S_{\lambda=0} = \int dt \int d^3x \left[\frac{1}{2m_0} \Big(2im_0 \dot{\psi}\psi^* - im_0 \partial_0(\psi^*\psi) + \dot{\psi}\dot{\psi}^* - [\partial_i(\psi^* \partial_i \psi) - \psi^* \Delta \psi] \Big) \right], \quad \text{(A.3)}$$

where we have expanded $-\partial_\mu \phi^* \partial^\mu \phi - m_0^2 |\phi|^2$ in terms of the wave function $\psi(t, \vec{x})$ and their derivatives, lowered indices with the flat spacetime metric $\eta_{\mu\nu}$ and use the relations $\partial_0(\psi^*\psi) = \dot{\psi}^*\psi + \psi^*\dot{\psi}$ and $\partial_i(\psi^* \partial_i \psi) = \partial_i \psi^* \psi + \psi^* \partial^2 \psi$.[1] Now, discarding the boundary terms and keeping to leading order in ϵ (neglecting $\dot{\psi}\dot{\psi}^*$) we can approximate:

$$S_{\lambda=0} = \int dt \int d^3x \left[i\psi^* \left(\partial_0 \psi + \frac{1}{2m_0} \Delta \right) \psi \right]. \quad \text{(A.4)}$$

This is the Schrodinger action for a scalar wave function that describes a particle of spin $s = 0$.

Second, we analyze the self-interacting theory, which include the self-interacting term

$$S_\lambda = \int dt \int d^3x \left[i\psi^* \left(\partial_0 \psi + \frac{1}{2m_0} \Delta + \frac{\lambda}{4m_0^2} |\psi|^2 \right) \psi \right]. \quad \text{(A.5)}$$

The only difference with respect to the free theory (A.4) is the appearance of one self-interaction term that depends of the particle density $n = |\psi|^2$.

Third, in the Newtonian Gauge and in the non-relativistic limit, the Einstein equations take the form

$$\Delta \Psi = 4\pi G \rho \quad \text{(A.6)}$$

$$(\delta_{ij} \Delta - \partial_i \partial_j)(\Phi - \Psi) = 0. \quad \text{(A.7)}$$

where Δ is the three-dimansinal flat Laplace operator. The first equation is the conventional Poisson equation for the static source ρ. Also, if we take the trace of the second equation (that is, summing over δ^{ij}), we can write $2\Delta(\Phi - \Psi) = 0$. Since we are looking for solutions that ere non-singular and well-behaved at infinity, then only these fields that are sourced by the right-hand side will be non-vanishing. So, this enforces the equality of the scalars potential $\Phi(t, \vec{x}) = \Psi(t, \vec{t}) \equiv \mathcal{U}(t, \vec{x})$ where $\mathcal{U}(t, \vec{x})$ is the Newtonian potential. Note that in the Newtonian limit the the sources are static and the time derivatives of the gravitational potential $\dot{\mathcal{U}}$ vanish. It is also important to note that we have discarded the vector and tensor modes of the metric for simplicity, since in the non-relativistic limit, matter does not couple to these modes. Next, we need to perform the kinetic terms considering the covariant derivatives $\nabla_\mu \phi \nabla^\mu \phi$ in terms of the metric components in Eq. (A.1). The procedure is a little more involved. We need to calculate $\sqrt{-g}$ in term of the metric potential $\Psi(t, \vec{x}) = \Phi(t, \vec{x}) = \mathcal{U}(t, \vec{x})$ at leading order in ϵ, that is

[1] Note that in the absence of gravity, covariant derivatives ∇_μ are replaced by partial derivatives ∂_μ.

$\sqrt{-g} = 1 + 2\Psi - 2\Psi^2$, where the second term is of order $[\epsilon]$ and the third term of order $[\epsilon^2]$. Expanding the kinetic term of the action (1.1) we obtain

$$S_G = \int dt \int d^3x \sqrt{-g} \Bigg[\frac{1}{8\pi G} \mathcal{U} \Delta \mathcal{U} + \frac{1}{2m_0} \Bigg(\Big[1 + 2\mathcal{U} \Big] \Big\{ m_0^2 |\psi|^2 + 2 i m_0 \dot{\psi} \psi^* - i m_0 \partial_0 (\psi^* \partial_0 \psi) \Big\} - (1 - 2\mathcal{U}) [\partial_i (\psi \partial_i \psi) - \psi^* \Delta \psi] - m_0^2 |\psi|^2 + 2 m_0 |\psi|^4) \Bigg) \Bigg]$$

where we have use the fact that $g^{\mu\nu} \nabla_\mu \phi^* \nabla_\nu \phi$ whee $g^{00} = [1 + 2\mathcal{U}]$ and $g^{ij} = [1 - 2\mathcal{U}] \delta^{ij}$. Keeping with the lowest orders in ϵ, and discarding the boundary terms, we can write the gravity term of action as

$$S_G = \int dt \int d^3x \left[\frac{1}{8\pi G} \mathcal{U} \Delta \mathcal{U} + \mathcal{U} m_0 |\psi|^2 \right] \tag{A.8}$$

where the first term comes from the Newtonian limit of the Einstein-Hilbert action.

Finally, adding the previous results, we can write the non-relativistic limit of the action (1.1) as

$$S[\mathcal{U}, \psi] = \int dt \int d^3x \left[\frac{1}{8\pi G} \mathcal{U} \Delta \mathcal{U} + \psi^* \left(i \frac{\partial}{\partial t} + \frac{1}{2m_0} \Delta - \frac{\lambda}{4 m_0^2} |\psi|^2 \right) \psi - m_0 \mathcal{U} |\psi|^2 \right]. \tag{A.9}$$

First term describes the Newtonian gravity, terms in the parentheses describe the sector of matter and the last term describes the interaction of the field with the gravitational potential. In particular, we will consider a sefl-interacting potential $V = \lambda |\phi|^4$ with λ a dimensionless coupling constant, which can take the values $\lambda > 0$ if the self-interaction is repulsive or $\lambda < 0$ if the self-interaction is attractive. When $\lambda = 0$ we recover the case with no self-interaction, in which the scalar field is only coupled to gravity. Variations with respect to the gravitational potential $\mathcal{U}(t, \vec{x})$ produce the Poisson equation (A.6), and variations with respect to the scalar field $\psi(t, \vec{x})$ produce the Gross-Pitaevskii equation (1.37a). Both equations constitute the $s = 0$ Gross-Pitaevski-Poisson system (1.37).

Appendix B

Appendix Chapter II

B.1 Example: Stationary Proca Star of Constant Polarization.

In this section we present the numerical construction for a stationary Proca star with constant polarization $\hat{\epsilon}$. This configuration is given by the system (2.87) with Latin indices omitted and $\gamma = 0$. Let us remember that this configuration is characterized by only one frequency given through the shifted potential $u^{(0)} = E - \mathcal{U}(r)$. We will present the numerical implementation of the *shooting method* for the first excited state configuration with $n = 1$ number of nodes, in the repulsive, free and attractive cases $\lambda_* = -1, 0, 1$ and central amplitude $\sigma^{(0)} = 1.0$.

In order to solve the system numerically, we need to rewrite the system (2.87) as four first-order differential equation given by

$$f_0 = \frac{d\sigma_0}{dr}, \tag{B.1a}$$

$$f_1 = \lambda[\sigma_0]^3 r^{2\gamma} - 2(1+\gamma)\frac{f_0}{r} - u_0\sigma_0, \tag{B.1b}$$

$$f_2 = \frac{du_0}{dr}, \tag{B.1c}$$

$$f_3 = -[\sigma_0]^2 r^{2\gamma} - \frac{2f_2}{r}, \tag{B.1d}$$

for $r > 0$, and

$$f_0 = \frac{d\sigma_0}{dr}, \tag{B.1e}$$

$$f_1 = [\lambda[\sigma_0]^3 r^{2\gamma} - u_0\sigma_0]/(2\gamma+3), \tag{B.1f}$$

$$f_2 = \frac{du_0}{dr}, \tag{B.1g}$$

$$f_3 = -\frac{[\sigma_0]^2 r^{2\gamma}}{3}, \tag{B.1h}$$

for $r = 0$, where we have use the ansatz $\sigma^{(0)}(r) = \sigma_0 r^\gamma$, $u^{(0)} = u_0$, L'Hôpital's rule and we have use the boundary conditions (2.88). We have characterized this system through the function `System_Stationary` in the `Python` language. Given the parameters `Lambda` and `gamma` and the `Vector` of the boundary

values $(\sigma^{(0)}(r), d\sigma^{(0)}/dr, u^{(0)}(r), du^{(0)}/dr)|_{r=0}$, we solve the system of first-order equations using the `Scipy` package called `solve_ivp`. Solving the value of $u_0(r = 0)$ that satisfies the boundary conditions (2.88) will depend on the shooting function `Stationary_Shooting`.

```
def System_Stationary(r, Vector, arg):
    """
    ##### System of equations (B.1) #####
    [sigma(r), sigma'(r), u(r), u'(r)] ==> [sigma_0, sigma_1, u_0, u_1],
    r ==> radial coordinate,
    u_0 ==> u_0 = E-V(r),
    Lambda = -1 (atractive case), 0 (free case), 1 (repulsive case),
    gamma  = 0 (circular or linear polarization), 1 (radial polarization).
    """
    sigma_0, sigma_1, u_0, u_1 = Vector
    Lambda, gamma = arg

    if r > 0:
        f0 = sigma_1
        f1 = Lambda*sigma_0**3*r**(2*gamma)-2*(1+gamma)*sigma_1/r-u_0*sigma_0
        f2 = u_1
        f3 = -r**(2*gamma)*sigma_0**2-2*u_1/r
    else:
        f0 = sigma_1
        f1 = (Lambda*sigma_0**3*r**(2*gamma)-u_0*sigma_0)/(2*gamma+3)
        f2 = u_1
        f3 = -r**(2*gamma)*sigma_0**2/3

    return [f0, f1, f2, f3]
```

We show the algorithm of the shooting method in the `Python` function `Stationary Shooting`. As we have already explained in the previous Chapter 2, given the boundary conditions (2.88) for $\gamma = 0$, we must now determine the value of $u^{(0)} = E - \mathcal{U}(r)$ for Eqs. (B.1) that satisfies these conditions. These values will be given by an infinite number of discrete values for $n = 0, 1, 2...$ number of nodes in $\sigma^{(0)}(r)$. The state that minimizes the energy will be characterized by the solution $\sigma^{(0)}_{n=0}(r)$ with $n = 0$ number of nodes. Solutions $\sigma_n(r)$ for which E_n with $n = 1, 2, 3...$ different from zero will constitute states of higher energy.

Given the value $\sigma^{(0)}(r = 0) = \sigma_0$, we choose a *seed* value for u_0 and we solve the system (B.1) accordingly. If we choose u_0 very large, then $d\sigma^{(0)}/dr$ becomes negative at a finite value of the radius, and if we choose u_0 very small, $d\sigma(r)/dr$ becomes positive at a finite radius, which causes the condition $\lim_{r\to\infty} \sigma(r) = 0$ to be broken. Then, we most chose a more appropriate value for the seed u_0. We can do this by bisecting $u_0 = (u_{0,max} + u_{0,min}/2)$ in a range $[u_{0,max}, u_{0,min}]$ for a sufficient number of iterations until that we reach the desired precision. These iterations based on the number of zeros present in the profile $\sigma^{(0)}(r)$ and its derivative $\sigma^{(0)\prime}(r)$ are encoded in the shooting algorithm presented below.

```
def Stationary_Shooting(sigma_0, u_max, u_min, Lambda, gamma, rmax_, rmin_, nodes,
     sigma_1 = 0, u_1=0, met='RK45', Rtol=1e-09, Atol=1e-10):
    """
     ###### Shooting Algorithm  #####

     rmax ==> We must choose a maximum value for the radius r large enough so that
          the code always stops due to the limit of numerical precision.
    Events ==> The solve_ivp function can detect and respond to "events" in the
        integration of a set of differential equations. One or more functions can
        be provided in the events argument, which should return zero when the
        state of the system to the event to be triggered. SEE [Learning Scientific
         Programmming With Python, Christian Hill].  The functions for which we
        are interested in finding the zeros are given by sigma(r) and sigma'(r).
        For example, a solution that satisfies the boundary conditions for n=0
```

```
        will have 0 events in sigma(r) and 1 event in sigma'(r) given that sigma'(
        r=0) =0.

    U0 = [sigma_0, sigma_1, u0_, u_1] ==> Values at the boundary with the seed u0_
        .
    """

    arg = [Lambda, gamma]
    def Sig(r, U, arg): return U[0]
    def dSig(r, U, arg): return U[1]
    Sig.direction = 0
    dSig.direction = 0

    while True:
        u0_ = (u_max+u_min)/2
        U0 = [sigma_0, df0, u0_, du0]
        sol_ = solve_ivp(system, [rmin_, rmax_], U0, events=(Sig, dSig),
                         args=(arg,), method=met,  rtol=Rtol, atol=Atol)

        # If the solution satisfies the condition sigma'(r) ==> [n] = nodes+1 and
            sigma(r) ==> [n] = nodes, we have found the sought solution. Here
            t_events[1].size = [number of nodes] for sigma'(r) and t_events[0].
            size = [number of nodes] for sigma(r).

        if sol_.t_events[1].size == nodos+1 and sol_.t_events[0].size == nodos:

            print('Found', u0_)
            return u0_, rmax_, sol_.t_events[0]

        # If sigma'(r) have [n]> nodes+1 and sigma(r) have [n]> nodes we have
            chosee u_0 too much large. We need to reduce it u_max = u0_. If sigma
            '(r) have [nodos]> n+1 and sigma(r) have [nodos]<= n we have chosee
            u_0 too small. We need to increase it u_min = u0_.

        elif sol_.t_events[1].size > nodos+1:

            if sol_.t_events[0].size > nodos:
                u_max = u0_
                rTemp_ = sol_.t_events[0][-1]
            else:
                u_min = u0_
                rTemp_ = sol_.t_events[1][-1]

        # If sigma'(r) have [n]=< nodes+1 and sigma(r) have [n]> nodes we have
            chosee u_0 too much large. We need to reduce it u_max = u0_. If sigma
            '(r) have [n]=< nodes+1 and sigma(r) have [n]<= nodes we have chosee
            u_0 too small. We need to increase it u_min = u0_.

        elif sol_.t_events[1].size <= nodos+1:
            # si hay menos nodos aumentar la energía
            if sol_.t_events[0].size > nodos:  # dos veces por nodo
                u_max = u0_
                rTemp_ = sol_.t_events[0][-1]
            else:
                u_min = u0_
                rTemp_ = sol_.t_events[1][-1]

        # If we have achieved the maximum precision:

        if abs((u_max-u_min)/2) <= 1e-14: #1e-14
            print('maximum precision achieved', u0_, 'radio', rTemp_)
            return u0_, rTemp_, sol_.t_events[0]
```

Due to the numerical precision (about 16 decimal digits in our code), the shooting method `Stationary_Shooting` only allows us to reach a finite radius. Beyond this radius, we utilize the asymptotic solutions

$$\sigma_i^{(0)}(r) \approx \frac{C_i}{r^{1+\gamma}} e^{-\sqrt{|E_i|}r}, \quad u_i^{(0)}(r) \approx E_i + \frac{N}{4\pi r} \tag{B.2}$$

of Eqs. (2.87), with C_i, E_i, and N constants, where E_i and N represent the dimensionless frequencies and trace of the Hermitian operator $\hat{Q}$, respectively,

and C_i is an amplitude scale. The value of E_i and N are computed according to[1]

$$E_i = u_{i0} - \sum_i \int_0^\infty \sigma_i^{(0)2}(r) r^{2\gamma+1} dr, \tag{B.3a}$$

$$N = 4\pi \sum_i \int_0^\infty \sigma_i^{(0)2}(r) r^{2(\gamma+1)} dr, \tag{B.3b}$$

whereas the C_i coefficients are obtained using a linear fitting methodology. The value of γ is one for radial polarization and zero for all other cases. For more details, see App. C in Ref. [87]. In the `Energy` function, we present the algorithm to calculate the quantities (B.3a) and (B.3b). Given the solutions obtained through the shooting method, we interpolate and integrate $\sigma^{(0)}$ using the `interp1d` and `quad` packages, respectively.

```
def Energy(r, sigma_0, gamma, V0):
    """
    #### Mass and Energy ####
    sigma_0 ==> The solution sigma_0(r) that we obtained from Stationary_Shooting
        and the solve_ivp package.
    V0 ==> Value at the boundary of the gravitational potential. This is the u0_
        value obtained in Stationary_Shooting.
    """

    sigF = interp1d(r, sigma_0, kind='quadratic')
    #sigF: An interpolation of sigma_0 that we will use in the subsequent
        integration.

    Af = lambda r: r**(2*gamma+1)*sigF(r)**2
    # Af: Integrand in the equations (4.83a).  To calculate the value of the
        Energy.

    Bf = lambda r: r**(2*(gamma+1))*sigF(r)**2
    # Bf: Integrand into equations (4.83b). To calculate the value of the Mass (
        m_0*N).

    # Integration Intervals.
    rmin = r[0]
    rfin = r[-1]

    # Eq. (4.91a).
    Energy = V0 - quad(Af, rmin, rfin)[0]

    # Eq. (4.91b).
    Mass = quad(Bf, rmin, rfin)[0]

    return Energy, Mass
```

Again, given that the numerical precision is limited and the shooting method `Stationary_Shooting` only allows us to reach a finite radius, we need to use asymptotic solutions given by Eqs. (B.2). We present the implementation of this concatenation in the `extend` function and in Figure (B.1) we present the radial profile $\sigma^{(0)}(r)$ for a starionary Proca star with constant polarization in the repulsive, free and attractive case. In the same figure, we show the relationship of the effective mass M_{99} as a function of the effective radius R_{99} and the relation of the energy eigenvalue $|E|$ with the central amplitude σ_0.

```
def extend(gamma, r, sigma_0, sigma_1, u_0, u_1, Ext, Np=1000, inf=False, ptos
    =400):
```

[1] Alternatively, one can use the asymptotic form described in Eq. (B.2) to obtain E_i. This alternative form to compute the energy eigenvalue was used to check the validity of the results obtained from Eq. (B.3a).

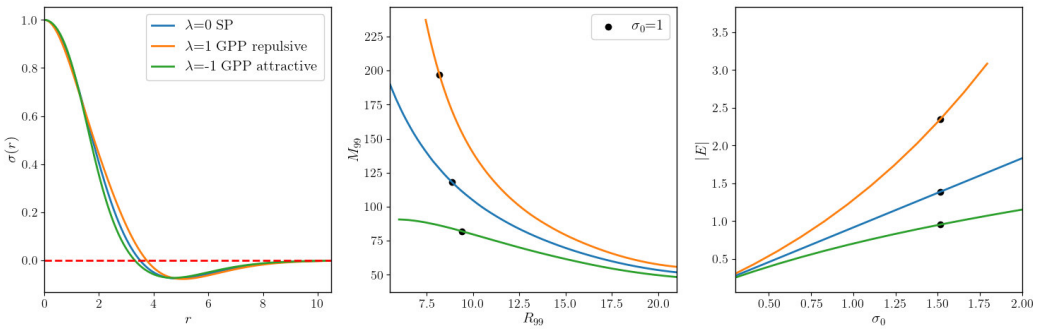

Figure B.1: **Constant polarized stationary Proca star with $n = 1$ nodes**: Stationary and spherically symmetric solutions of the $s = 1$ Gross-Pitaevskii-Poisson system with $n = 1$ nodes. Red (blue) lines correspond to repulsive (attractive) case, and we have included the solutions to the $s = 1$ Schrodinger-Poisson system (black lines) for reference. *Left panel*: The profile $\sigma^{(0)}(r)$ for $\sigma_0 = 1$. *Center panel*: The effective mass of the configuration M_{99} as a function of the effective radius R_{99}. *Right panel*: The magnitude of the energy eigenvalue $|E|$ as a function of the central amplitude σ_0. The dots in the last two panel correspond to the configurations of unit amplitude. For $\sigma_0 \to 0$ the effects of the self-interactions become negligible.

```
"""
### Extended solutions ###
We concatenate the asymptotic solutions with the solutions derived from
    Stationary_Shooting.
"""
# Parameters k and C in (B.2).
def parametrosS(r, S):
    yr1, yr2 = S[-2], S[-1]
    r1, r2 = r[-2], r[-1]

    k = np.real(np.log(np.abs(yr1*r1/(yr2*(r2)))))
    s = np.exp(-k*r1)/r1
    C = yr1/s
    return C, k

# Asymptotic solutions (B.2).
def sigm_asym(r, C, k):
    y = C*np.exp(-k*r)/r
    dy = -(C*np.exp(-k*r)*(1+k*r))/r**2
    return y, dy

def U_asym(r, A, B):
    y = A+B/r
    dy = -B/r**2
    return y, dy

# Extended radius
rad = np.linspace(r[-1], r[-1]+Ext, Np)

# Calculating Parameters
En, Mas = energ(rD, sigma_0, gamma, u_0[0])
Ap, k = parametrosS(r, sigma_0)

# Joining data
sigma_0_Ext, sigma_1_Ext = sigm_asym(rad, Ap, k)
u_0_Ext, u_1_Ext = U_asym(rad, En, Mas)

r_new = np.concatenate((r[:-1], rad), axis=None)
sigma_0_new = np.concatenate((sigma_0[:-1], sigma_0_Ext), axis=None)
sigma_1_new = np.concatenate((sigma_1[:-1], sigma_1_Ext), axis=None)
u_0_New = np.concatenate((u_0[:-1], u_0_Ext), axis=None)
```

```
u_1_New = np.concatenate((u_1[:-1], u_1_Ext), axis=None)

# Quadratic interpolation.
fsN = interp1d(r_new, sigma_0_new, kind='quadratic')
fprof = lambda x: x**2*fsN(x)**2
masa = quad(fprof, r_new[0], r_new[-1])[0]
# checking
if inf:
    print('checking ')
    print('Energia: ', En, ' ', uExt[-1]) #, ' ', k**2)
    print('Masa: ', Mas,  ' ', masa)


return r_new, sigma_0_new, sigma_1_new, u_0_New, u_1_New, [masa, En, sigma_0
    [0]]
```

When $\gamma = 0$ and $\lambda_s = 0$ the system of dimensionless equations (B.1) is identical to the system of equations (1.55a) for a non-relativistic, spherically symmetric, and self-interacting boson star that we presented in Section 1.3, of Chapter 1. Procedures analogous to those we have presented in this Appendix B.1 were used to compute the solutions we present in Chapter 1, for relativistic and non-relativistic configurations. In the repositories `https://github.com/edgargovea/Relativistic-Boson-Stars.git` and `https://github.com/edgargovea/Nonrelativistic-Boson-Stars.git`, the reader can review these procedures in detail.

B.2 Example: Multi-frequency Proca Star for $\sigma_{x0} = 1.0$, $\sigma_{y0} = 0.8$, and $\sigma_{z0} = 0$ with $n_x = 1, n_y = 0, n_z = 0$.

In this section, we analyze the shooting method implemented for a multi-frequency Proca star in the case where $\sigma_x^{(0)}(r=0) = 1.0$, $\sigma_y^{(0)}(r=0) = 0.8$ and $\sigma_z^{(0)}(r=0) = 0$ with $(n_x = 1, n_y = 0, n_z = 0)$ nodes. For this, we must reduce the dimensionless system (2.87) to a system of first-order differential equations given by:

$$f_0 = \frac{d\sigma_x^{(0)}}{dr}, \tag{B.4a}$$

$$f_1 = \lambda \sum_j \left[\sigma_j^{(0)}\right]^2 - 2\frac{d\sigma_x^{(0)}}{dr}\frac{1}{r} - \sigma_x^{(0)} u_x^{(0)}, \tag{B.4b}$$

$$f_6 = \frac{du_x^{(0)}}{dr}, \tag{B.4c}$$

$$f_7 = \lambda \sum_j \left[\sigma_j^{(0)}\right]^2 - 2\frac{du_x^{(0)}}{dr}\frac{1}{r}, \tag{B.4d}$$

and similarly for the y and z components on $\vec{\sigma}$. We have written this system in the function `SystemMultiFrequency` for $r > 0$ and $r = 0$ following the same procedure as the previous example. The system depends on the values at the boundary for the components $[\sigma_{x0}, \sigma_{y0}, \sigma_{z0}]$ and the values of the frequencies $[u_{x0}, u_{y0}, u_{z0}]$. We have to solve this system numerically using the `scipy` package in `Python` called `solve_ivp` with the method `'RK45'`: Explicit

Runge-Kutta method of order 5(4) [107]. Particularly we consider `rtol` and `atol`, optional relative and absolute tolerances, as `Rtol=1e-07` and `Atol=1e-8`.[2] The purpose is to solve the system numerically for the values $[u_{x0}, u_{y0}, u_{z0}]$ that satisfy the boundary conditions (2.88). These solutions will constitute an infinite and discrete set of frequencies $E_n = [E_{nx}, E_{ny}, E_{nz}]$ that will conform a mult-ifrequency configuration with $E_{nx} \neq E_{ny} \neq E_{nz}$. In order to find this configuration, we use the function `MultFreq_Shooting`.

```
def SystemMultiFrequency(r, Vector, arg):
    """
    ##### Multifrequency System of Equiations #####
    [phi_x, phi_x', phi_y, phi_y', phi_z, phi_z', u_x, u_x', u_y, u_y', u_z, u_z']
         ==> [p0x, p1x, p0y, p1y, p0z, p1z, u0x, u1x, u0y, u1y, u0z, u1z]
    Lambda ==> Atractive case: -1, SP = 0, Repulsive case = 1
    """
    p0x, p1x, p0y, p1y, p0z, p1z, u0x, u1x, u0y, u1y, u0z, u1z = Vector
    Lambda, = arg

    # System of equations (B.4).
    if r > 0:
        sumpi = p0x**2 + p0y**2 + p0z**2
        f0 = p1x
        f1 = LambT*sumpi*p0x - (2*p1x)/r - p0x*u0x
        f2 = p1y
        f3 = LambT*sumpi*p0y - (2*p1y)/r - p0y*u0y
        f4 = p1z
        f5 = LambT*sumpi*p0z - (2*p1z)/r - p0z*u0z
        f6 = u1x
        f7 = -sumpi-(2*u1x)/r
        f8 = u1y
        f9 = -sumpi - (2*u1y)/r
        f10 = u1z
        f11 = -sumpi - (2*u1z)/r
    else:
        sumpi = p0x**2 + p0y**2 + p0z**2
        f0 = p1x
        f1 = (LambT*sumpi*p0x - p0x*u0x)/3
        f2 = p1y
        f3 = (LambT*sumpi*p0y - p0y*u0y)/3
        f4 = p1z
        f5 = (LambT*sumpi*p0z - p0z*u0z)/3
        f6 = u1x
        f7 = -sumpi/3
        f8 = u1y
        f9 = -sumpi/3
        f10 = u1z
        f11 = -sumpi/3

    return [f0, f1, f2, f3, f4, f5, f6, f7, f8, f9, f10, f11]
```

To implement the function `MultFreq_Shooting`, we must introduce a *seed value* for $[u_{x0}, u_{y0}, u_{z0}]$ given by $u_{0x} = [u_{max,x} + u_{min,x}]/2$, $u_{0y} = [u_{max,y} + u_{min,y}]/2$ for a certain range $[u_{min,x}, u_{max,x}]$,$[u_{min,y}, u_{max,y}]$ and $[u_{min,z}, u_{max,z}]$ and solve the system `SystemMultiFrequency` accordingly. Then we analyze the zeros for the profile $\sigma_j^{(0)}(r)$ and its derivative $d\sigma_j^{(0)}(r)/dr$ trough the functions `events =(Sigx , dSigx , Sigy , dSigy , Sigz , dSigz)` for each component x, y and z. So, as we explain below, the component that first reaches one of the zeros according to the `identify()` function will be subjected to the shooting algorithm described in the `Stationary_Shooting` function above. If we have chosen $u0_x$ (or $u0_y$ or $u0_z$) very large or very small,

[2]The solver keeps the local error estimates less than `atol` + `rtol` * abs(y). Here `rtol` controls a relative accuracy (number of correct digits), while `atol` controls absolute accuracy (number of correct decimal places).

we will need to expand or reduce the range in $[u_{min,x}, u_{max,x}]$ and repeat the process.

```
def MultFreq_Shooting(Initial0, Uintx, Uinty, Uintz, rmax, rmin=0, Lambda=1, nodes
    =[1, 0, 0], met='RK45', Rtol=1e-09, Atol=1e-10, lim=1e-6, info=False, klim
    =500, outval=13, delta=0.4):
    """
    ##### Multifrequency Shooting Algorithm #####
    #Range of values Umin, Umax in which the Shooting will perform the search for
        each component phi_x, phi_y, phi_z:
    Uintx -> [Umin_x, Umax_x]
    Uinty -> [Umin_y, Umax_y]
    Uintz -> [Umin_z, Umax_z]

    Initial0 -> [p0x, p1x, p0y, p1y, p0z, p1z, u1x, u1y, u1z] # Vector of initial
        values for phi_x(r=0), phi_x'(r=0), u_x'(r=0), etc.
    rmax, rmin -> Maximum and minimum radius values.
    nodes ==> [nodos_p0x, nodos_p0y, nodos_p0z] # Number of nodes for each
        component phi_x(r)==> n_x, etc.
    klim ==> Maximum number of iterations for the shooting cycle.
    outval ==> Number of times it moves once the <<shoot>> function has returned a
         result.
    delta ==> Amount we move the values returned by the <<shoot>> function,
        defined below.

    Order of the variables
    [phi_x, phi_x', phi_y, phi_y', phi_z, phi_z', u_x, u_x', u_y, u_y', u_z, u_z']
         -> [p0x, p1x, p0y, p1y, p0z, p1z, u0x, u1x, u0y, u1y, u0z, u1z]
    """

    nodes = np.array(nodes)
    p0x, p1x, p0y, p1y, p0z, p1z, u1x, u1y, u1z = Initial0

    # Vector with central profiles phi_x(r=0), phi_y(r=0), phi_z(r=0)
    p0Data = [p0x, p0y, p0z]

    Uminx, Umaxx = Uintx
    Uminy, Umaxy = Uinty
    Uminz, Umaxz = Uintz

    #Finding a profile with [nx, ny, nz] numer of nodes for phi_x(r), phi_y(r) and
         phi_z(r).

    # Events. Analogous to the case of a stationary Proca star, we base the
        shooting algorithm on the number of zeros that exist in the profiles phi_x
        (r), phi_y(r), and phi_z(r), and their derivatives phi_x'(r), phi_y'(r),
        and phi_z'(r).  To see when these zeros occurs, we define:

    def Sigx(r, U, arg): return U[0]
    def dSigx(r, U, arg): return U[1]
    def Sigy(r, U, arg): return U[2]
    def dSigy(r, U, arg): return U[3]
    def Sigz(r, U, arg): return U[4]
    def dSigz(r, U, arg): return U[5]
    Sigx.direction = 0; dSigx.direction = 0
    Sigy.direction = 0; dSigy.direction = 0
    Sigz.direction = 0; dSigz.direction = 0

    k = 0

    arg = [Lambda]
    Uintrs = np.array([[Uminx, Umaxx], [Uminy, Umaxy], [Uminz, Umaxz]])

    out = 0
    while True:
        # As in the previous case, we start with a seed value u0_x, u0_y and u0_z
            for each one of the components phi_x, phi_y and phi_z and solve the
            system of equations accordingly.
        ##def shoot(imin, imax):##
        #######return (imin+imax)/2#######
        u0 = np.array([shoot(*i) for i in Uintrs])
        V0 = [p0x, p1x, p0y, p1y, p0z, p1z, u0[0], u1x, u0[1], u1y, u0[2], u1z]
```

```
sol = solve_ivp(MultFreq_Shooting, [rmin, rmax], V0, events=(Sigx, dSigx,
    Sigy, dSigy, Sigz, dSigz),
                args=(arg,), method=met,  rtol=Rtol, atol=Atol)

# Next, we list the zeros of the solutions for u0.
eventos = np.array([[sol.t_events[0], sol.t_events[1]],
           [sol.t_events[2], sol.t_events[3]],
           [sol.t_events[4], sol.t_events[5]]], dtype=object)

#Next, we proceed to increase or decrease the value of u0_x, u0_y, or u0_z
     according to the same criteria we described for a stationary Proca
    star.  Which of the different u0_x, u0_y, or u0_z we modify first is
    determined by the component that reaches a zero in its profile (e.g.,
    phi_x(r)) or its derivative (e.g., phi_x'(r)) before any other
    component (e.g., phi_y(r) or phi_y'(r)).  The function indentify()
    allows this selection.

sigModif = identify(sol.t_events, nodes, pODataa, info=info)

# For axample sigModif = [True, False, False] if \phi_x(r=0) reaches a
    zero in its profile or its derivative before any other component. So,
    we use the previously described shooting algorithm (here the function
    freq_shoot) if we need to increase or decrease u0_x. From this, we
    obtain the new values u0 in iInterv and rTemp.

# Here, freq_shoot follows the shooting algorithm in Stationary_Shooting.
iInterv, rTemp = freq_shoot(eventos[sigModif], nodos[sigModif], u0[
    sigModif], Uintrs[sigModif], rmax)

# If we have reached the maximum precision:
if abs((iInterv[1]-iInterv[0])/2) <= lim:
    if info:
        print(out)
        print('We have reached the maximum precision: U0x = ', V0[6], '
            U0y = ', V0[8], ' U0z = ', V0[10], 'radio', rTemp)

    if out==outval:
        print('Maxima precisión alcanzada: U0x = ', V0[6], ' U0y = ', V0
            [8], ' U0z = ', V0[10], 'radio', rTemp)
        return V0[6], V0[8], V0[10], rTemp, sol.t_events[0], sol.t_events
            [2], sol.t_events[4]
    else:

        Uintrs[sigModif] = [iInterv[0]-delta, iInterv[1]+delta]
        out += 1
#If we still haven't reached maximum precision, we rewrite u0.
else:
    Uintrs[sigModif] = iInterv


if np.all(np.array([shoot(*i) for i in Uintrs])==u0):
    print('Found: U0x = ', V0[6], ' U0y = ', V0[8], ' U0z = ', V0[10], '
        radio', rTemp)
    return V0[6], V0[8], V0[10], rTemp, sol.t_events[0], sol.t_events[2],
        sol.t_events[4]

if k==klim:
    print('loop limit reached')
    break

k += 1
```

The use of the function `identify` allows us to identify which of the components $\sigma_x^{(0)}(r)$, $\sigma_y^{(0)}(r)$ or $\sigma_z^{(0)}(r) = 0$ has reached a zero (`event`) first. For example, let's suppose that in the j-th iteration for a given u_{0x} and u_{0y} we obtain the results described in the Figure (B.2). Given that the solutions we are looking for in this example satisfy $\sigma_x(r = 0) = 1.0$, $\sigma_y(r = 0) = 0.8$ and $\sigma_z(r = 0) = 0$ with $(n_x = 1, n_y = 0, n_z = 0)$, we observe that the solution for $\sigma_x(r)$ satisfies $n_x = 1$ but the zeros in the derivative function $\sigma_x'(r)$

are greater than $n_x + 1$ with the value of the n_x zero at $r = 4.022$. On the other hand, $\sigma_y(r)$ satisfies $n_y = 0$, but similarly, the number of zeros of the derivative function $\sigma_y'(r)$ is greater than $n_y + 1$ with the value of n_y zero at $r = 0.0$. Then, the component that first reaches zero is $\sigma_y(r)$, so `sigModif = [False, True, False]` and $\sigma_y(r)$ will be the next component subjected to the shooting method. The logical sequence of this process is described below.

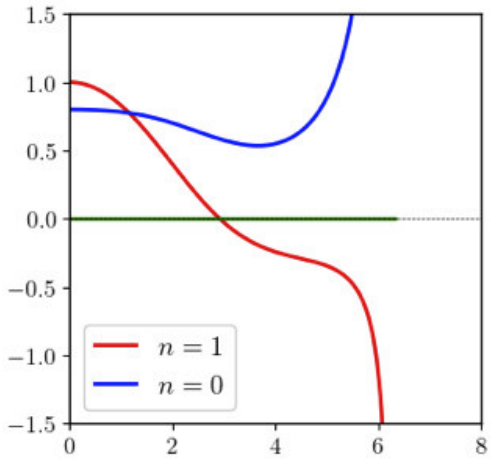

Figure B.2: **`identify` function.** The use of the function `identify` allows us to identify which of the components $\sigma_x^{(0)}(r)$ (red line), $\sigma_y^{(0)}(r)$ (blue line) or $\sigma_z^{(0)}(r) = 0$ has reached a zero (`event`) first.

The shooting method replicates the same procedure that we have described for a stationary Proca star. We emphasize that the difference is that for a multi-frequency Proca star this process is done successively for each component $\sigma_x(r)$, $\sigma_y(r)$, and $\sigma_z(r)$, as each one first reaches one of the zeros for the profile or the derivative of the profile according to the `identify` function. The result of this particular example for $\sigma_{0x} = 1.0$ and $\sigma_{0y} = 0.8$ with $n_x = 1$ and $n_y = 0$ (the component in the z direction equal to zero) is shown in Figure (B.3).

```
def identify(events, nodes, pODataa, info=False):
    """
```

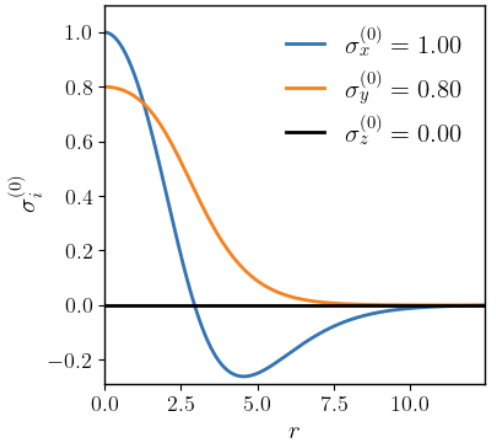

Figure B.3: **Multi-frequency Proca star**. Multi-frequency configuration for $\sigma_{0x} = 1.0$ and $\sigma_{0y} = 0.8$ with $n_x = 1$ and $n_y = 0$

```
##### identify function #####
Identifying which components have zeros in successive order. When a component
    is taken as zero and excluded from the analysis
"""
dicNod = {'0': nodes[0], '2': nodes[1], '4': nodes[2]}
indices = np.fromiter(map(int, dicNod.keys()), dtype=int)
ind = list(map(bool, p0Data))
posit = indices[ind]
# posit = [0,2,4]

valR = [np.infty, np.infty, np.infty]
for i in posit:
    valtemp = []
    node = dicNod[str(i)]
    numNod = events[i].size; numdSig = events[i+1].size
    if numNod == node and numdSig == node+1:
        valtemp.append(0)
    elif numNod == node:
        if numdSig < node+1:
            valtemp.append(events[i+1][node-1])
        elif numdSig > node+1:
            valtemp.append(events[i+1][node])
    elif numNod > node:
        valtemp.append(events[i][node])
    else:
        if numNod != 0:
            valtemp.append(events[i][-1])
        else:
            valtemp.append(0)

    if i==0:
        valR[0] = min(valtemp)
    elif i==2:
        valR[1] = min(valtemp)
    elif i==4:
        valR[2] = min(valtemp)


sigModif = [False, False, False]
test = np.min(valR)
for i in range(3):
    if valR[i]==test:
        sigModif[i]=True
        break

return sigModif
```

Appendix C

Appendix Chapter IV

C.1 Dirac Spinor in a de Sitter Universe

In a De Sitter universe, the scale factor is give by

$$a(\eta) = (-H_{ds}\eta)^{-1} \quad \text{and} \quad \frac{da(\eta)}{d\eta} = \frac{1}{H_{ds}\eta^2}. \tag{C.1}$$

With such a scale factor, the modified Dirac equation (4.22) are given by

$$\left[\frac{d^2}{d\eta^2} + k^2 + \frac{m^2}{H_{ds}^2\eta^2} + i\frac{m}{H_{ds}\eta^2}\right] u_k = 0, \tag{C.2a}$$

$$\left[\frac{d^2}{d\eta^2} + k^2 + \frac{m^2}{H_{ds}^2\eta^2} - i\frac{m}{H_{ds}\eta^2}\right] v_k = 0. \tag{C.2b}$$

Making the appropriate change of variable given by

$$z = -k\eta, \quad \text{and} \quad \mu = \frac{m}{H_{ds}}, \quad -\nu_\pm^2 + \frac{1}{4} = \mu^2 \pm i\mu \tag{C.3}$$

we can recast Eq. (C.2) as

$$\left[\frac{d^2}{dz^2} + 1 + \frac{\nu_+^2 + \frac{1}{4}}{z^2}\right] u_k = 0, \tag{C.4a}$$

$$\left[\frac{d^2}{dz^2} + 1 + \frac{\nu_-^2 + \frac{1}{4}}{z^2}\right] v_k = 0. \tag{C.4b}$$

where $\nu_\pm = -i\mu \pm \frac{1}{2}$. These equations admit solutions in terms of the Hankel functions of the first $\sqrt{z}H_{\nu_+}^{(1)}$ and second kind $\sqrt{z}H_{\nu_+}^{(2)}$ for u_k and $\sqrt{z}H_{\nu_-}^{(1)}$ and $\sqrt{z}H_{\nu_-}^{(2)}$ for v_k. The normalized solutions that has the correct asymptotic behavior solutions (4.48) as $\eta \to -\infty$ are given by Eq. (4.27). When $\eta \to -\infty$ the asymptotic expression of Hankel function of first is given by $H_\nu^{(1)}(z) = \sqrt{\frac{2}{\pi z}}\exp\left[i(z - \frac{\nu\pi}{2} - \frac{\pi}{4})\right]$, such that

$$u_k^{(0)} = \lim_{\eta\to-\infty} i\frac{\sqrt{z\pi}}{2}e^{\pi\mu/2}H_{\nu_+}^{(1)}(z) = \frac{1}{\sqrt{2}}e^{-ik\eta}, \tag{C.5}$$

$$v_k^{(0)} = \lim_{\eta\to-\infty} \frac{\sqrt{z\pi}}{2}e^{\pi\mu/2}H_{\nu_-}^{(1)}(z) = \frac{1}{\sqrt{2}}e^{-ik\eta}, \tag{C.6}$$

which are the asymptotic adiabatic solutions (4.48) in the remote past.

C.2 Dirac Spinor in a Radiation Dominated Universe

In a radiation dominated universe, the scale factor is a linear function of conformal time as

$$a(\eta) = H_R\eta, \quad \text{with} \quad \frac{da(\eta)}{d\eta} = H_R. \tag{C.7}$$

With such a scale factor, the modified Dirac equation (4.22) are given by

$$\left[\frac{d^2}{d\eta^2} + k^2 + m^2H_R^2\eta^2 + imH_R\right] u_k = 0, \tag{C.8a}$$

$$\left[\frac{d^2}{d\eta^2} + k^2 + m^2H_R^2\eta^2 - imH_R\right] v_k = 0. \tag{C.8b}$$

Making the appropriate change of variable given by

$$z = \sqrt{mH_R}\eta, \quad q = \frac{k}{\sqrt{mH_R}}, \quad \text{and} \quad \lambda_{(\pm)} = q^2 \pm i, \tag{C.9}$$

we can recast (C.8) as

$$\left[\frac{d^2}{dz^2} + z^2 + \lambda_{(+)}\right] u_k = 0, \tag{C.10a}$$

$$\left[\frac{d^2}{dz^2} + z^2 + \lambda_{(-)}\right] v_k = 0. \tag{C.10b}$$

The modified Dirac equation above immediately admits solutions in terms of the parabolic cylinder functions $D_\alpha(z)$. These are given by

$$u_k = c_1 D_\alpha\left(\sqrt{2}e^{i\pi/4}z\right) + c_2 D_{-\alpha-1}\left(\sqrt{2}e^{i3\pi/4}z\right), \tag{C.11a}$$

$$v_k = c_3 D_{\alpha-1}\left(\sqrt{2}e^{i\pi/4}z\right) + c_4 D_{-\alpha}\left(\sqrt{2}e^{i3\pi/4}z\right). \tag{C.11b}$$

with $\alpha = -iq^2/2$. By imposing that equations (4.21) be satisfied at late times, and normalizing according to (4.19) we arrive at

$$u_k = \exp\left\{\left(-\frac{\pi k^2}{8mH_R}\right)\right\} D_\alpha\left(\sqrt{2}e^{i\pi/4}z\right), \tag{C.12a}$$

$$v_k = \frac{e^{i\pi/4}k}{\sqrt{2mH_R}} \exp\left\{\left(-\frac{\pi k^2}{8mH_R}\right)\right\} D_{\alpha-1}\left(\sqrt{2}e^{i\pi/4}z\right). \tag{C.12b}$$

As in the scalar field case, the structure of this solution, through the value α, reveals the presence of a new momentum scale, $k_J \equiv \sqrt{mH_R}$, the Jeans length of a self-gravitating field. In addition, the argument of the cylinder functions suggests different behaviors the light field ($ma \ll H$) and heavy field ($ma \gg H$) limits.

C.3 Adiabatic Expansion for u_k and v_k up to Fourth Order

Zeroth order In the adiabatic limit, following the reasoning of S. Gosh [174, 161], we can propose the following ansatz to the differential equations (4.22) such that

$$u_k(\eta) \sim \exp\left[\int \big(X_k(\tilde{\eta}) - iY_k(\tilde{\eta})\big)d\tilde{\eta}\right] \tag{C.13}$$

where

$$X_k(\tilde{\eta}) = \frac{1}{\hbar}\sum_{n=0}^{\infty}\hbar^n X_n(\tilde{\eta}), \;\; Y_k(\tilde{\eta}) = \frac{1}{\hbar}\sum_{n=0}^{\infty}\hbar^n Y_n(\tilde{\eta}) \tag{C.14}$$

where n indicates the adiabatic order expansion, and similarly for $v_k(\eta)$. Putting Eq. (C.14) into Eq. (4.22a), we obtain, for the zero and first order in n, respectively

$$X_0^2 - Y_0^2 + \omega_k^2 = 0, \;\; 2X_0Y_0 - Q = 0,$$
$$\dot{X}_0 + 2X_0X_1 - 2Y_0Y_1 = 0, \;\; \dot{Y}_0 + 2X_0Y_1 + 2X_1Y_0 = 0.$$

where $Q = m\dot{a}$. Solving this set of coupled differential equations up to first adiabatic order, we obtain

$$\begin{aligned} X_0 &\approx \frac{m\dot{a}}{2\omega_k}, \;\; X_1 \approx -\frac{\dot{\omega}_k}{2\omega_k}, \\ Y_0 &\approx \omega_k, \;\; Y_1 \approx 0. \end{aligned}$$

Then, the ansatz (C.13) can be written as

$$u_k \sim \exp\left[\int \big(\frac{m\dot{a}}{2\omega_k} - \frac{\dot{\omega}_k}{2\omega_k}\big)d\tilde{\eta}\right]\exp\left[-i\int \omega_k d\tilde{\eta}\right]. \tag{C.15}$$

The expression in the first integral can be recast as

$$\frac{m\dot{a}}{2\omega_k} - \frac{\dot{\omega}_k}{2\omega_k} = \frac{m\dot{a}}{2\omega_k}\left[\frac{ma+\omega_k}{ma+\omega_k}\right] - \frac{\dot{\omega}_k}{2\omega_k} = \frac{d}{dt}\left[\left(\frac{\omega_k+ma}{2\omega_k}\right)^{1/2}\right]\left(\frac{\omega_k+ma}{2\omega_k}\right)^{-1/2}.$$

So, the solution $u_k^{(0)}$ at zero adiabatic order finally is

$$u_k^{(0)} \sim \sqrt{\frac{\omega_k+ma}{\omega_k}}\exp\left[-i\int \omega_k d\tilde{\eta}\right], \tag{C.16}$$

and similarly for $v_k^{(0)}$.

Second order. Now, working up to adiabatic second order, from the expression (4.33) and using Eq. (4.22), we can write

$$(\omega_k - ma)G^{(2)} = (\omega_k - ma)F^{(2)} + \omega_k^{(2)} + i\dot{F}^{(1)} + \frac{i}{2}\frac{1}{(\omega_k+ma)}\left(m\dot{a} - \frac{ma\dot{\omega}_k}{\omega_k}\right)F^{(1)},$$
$$(\omega_k + ma)F^{(2)} = (\omega_k + ma)G^{(2)} + \omega_k^{(2)} + i\dot{G}^{(1)} + \frac{i}{2}\frac{1}{(\omega_k - ma)}\left(\frac{ma\dot{\omega}_k}{\omega_k} - m\dot{a}\right)G^{(1)},$$
$$(\omega_k + ma)(F^{(2)} + F^{(1)}F^{(1)*} + F^{(2)*}) + (\omega_k - ma)(G^{(2)} + G^{(1)}G^{(1)*} + G^{(2)*}) = 0.$$

Similar to the above process we recast these equations as

$$(\omega_k - ma)(g_x^{(2)} - f_x^{(2)}) = \omega_k^{(2)} - \dot{f}_y^{(1)} - \frac{f_y^{(1)}}{2}\frac{1}{(\omega_k + ma)}\left(m\dot{a} - \frac{ma\dot{\omega}_k}{\omega_k}\right),$$
$$(\omega_k + ma)(g_x^{(2)} - f_x^{(2)}) = -\omega_k^{(2)} + \dot{g}_y^{(1)} + \frac{g_y^{(1)}}{2}\frac{1}{(\omega_k - ma)}\left(\frac{ma\dot{\omega}_k}{\omega_k} - m\dot{a}\right),$$
$$(\omega_k + ma)(2f_x^{(2)} + (f_y^{(1)})^2) + (\omega_k - ma)(2g_x^{(2)} + (g_y^{(1)})^2) = 0,$$

and after some manipulations, we can write

$$\begin{aligned} 2\omega_k(g_x^{(2)} - f_x^{(2)}) &= \dot{g}_y^{(1)} - \dot{f}_y^{(1)} - \frac{1}{2}\left(m\dot{a} - \frac{ma\dot{\omega}_k}{\omega_k}\right)\left(\frac{g_y^{(1)}}{\omega_k - ma} + \frac{f_y^{(1)}}{\omega_k + ma}\right), \\ f_x^{(2)} &= -\frac{(f_y^{(1)})^2}{2} - \frac{1}{2}\frac{\omega_k - ma}{\omega_k + ma}(2g_x^{(2)} + (g_y^{(1)})^2). \end{aligned}$$

From this we obtain the second order expression for $g_x^{(2)}$ as

$$g_x^{(2)} = -\frac{(f_y^{(1)})^2}{2} + \frac{\omega_k + ma}{4\omega_k^2}\Bigg[\dot{g}_y^{(1)} - \dot{f}_y^{(1)} - \frac{1}{2}\left(m\dot{a} - \frac{ma\dot{\omega}_k}{\omega_k}\right)\left(\frac{g_y^{(1)}}{\omega_k - ma} + \frac{f_y^{(1)}}{\omega_k + ma}\right)\Bigg].$$

The function $f_x^{(2)}$ is obtained using the condition $f_x^{(2)}(-m) = g_x^{(2)}(m)$, and from these we obtain $\omega_k^{(2)}$. On other hand, we calculate the imaginary part as

$$(\omega_k - ma)(g_y^{(2)} - f_y^{(2)}) = \dot{f}_x^{(1)} + \frac{f_x^{(1)}}{2}\frac{1}{(\omega_k + ma)}\left(m\dot{a} - \frac{ma\dot{\omega}_k}{\omega_k}\right), \quad \text{(C.17a)}$$
$$(\omega_k + ma)(g_y^{(2)} - f_y^{(2)}) = -\dot{g}_x^{(1)} - \frac{g_x^{(1)}}{2}\frac{1}{(\omega_k - ma)}\left(\frac{ma\dot{\omega}_k}{\omega_k} - m\dot{a}\right). \quad \text{(C.17b)}$$

From here is straightforward to write

$$2\omega_k\left(g_y^{(2)} - f_y^{(2)}\right) = 0 \to g_y^{(2)} = f_y^{(2)}. \quad \text{(C.18)}$$

Here, the functions $g_y^{(2)}$ and $f_y^{(2)}$ remain undetermined. However, since the local observables, e.g. the energy density ρ, regardless of the required adiabatic order n, remains independent of these functions, this ambiguity can be resolved by choosing $g_y^{(2)} = f_y^{(2)} = 0$. All the tedious calculus are more easily made in *Wolfram Mathematica*, after some computational work we get

$$\omega_k^{(2)} = \frac{5m^4a^2\dot{a}^2}{8\omega_k^5} - \frac{m^2\dot{a}^2}{8\omega_k^3} - \frac{m^2a\ddot{a}}{4\omega_k^3}, \quad \text{(C.19a)}$$
$$F^{(2)} = -\frac{5m^4a^2\dot{a}^2}{16\omega_k^6} + \frac{5m^3\dot{a}^2a}{16\omega_k^5} - \frac{m^2\dot{a}^2}{32\omega_k^4} + \frac{m^2a\ddot{a}}{8\omega_k^4} - \frac{m\ddot{a}}{8\omega_k^3}. \quad \text{(C.19b)}$$

and $G^{(2)} = g_x^{(2)}(m) = f_x^{(2)}(-m) = F^{(2)}(-m)$.

With the above results now is possible to write

$$u_k^{(2)} = \sqrt{\frac{\omega_k + ma}{2\omega_k}} \exp\left(-i \int \left[\omega_k(\tilde{\eta}) + \frac{5m^4a^2\dot{a}^2}{8\omega_k^5} - \frac{m^2\dot{a}^2}{8\omega_k^3} - \frac{m^2a\ddot{a}}{4\omega_k^3}\right] d\tilde{\eta}\right)$$
$$\times \left[1 - \frac{im\dot{a}}{4\omega_k^2} - \frac{5m^4a^2\dot{a}^2}{16\omega_k^6} + \frac{5m^3\dot{a}^2a}{16\omega_k^5} - \frac{m^2\dot{a}^2}{32\omega_k^4} + \frac{m^2a\ddot{a}}{8\omega_k^4} - \frac{m\ddot{a}}{8\omega_k^3}\right], \quad \text{(C.20)}$$

and similarly for $v_k^{(2)}$ using the fact that $u_k^{(2)}(-m) = v_k^{(2)}(m)$. The third and fourth adiabatic order are calculated next.

Third and fourth adiabatic order. For completeness, we write the third and fourth adiabatic order expression to get $F^{(3)}$, $G^{(3)}$ and $F^{(4)}$ and $G^{(4)}$. Up to third adiabatic order, the real part of Eq. (4.33) is given by

$$(\omega_k - ma)(g_x^{(3)} - f_x^{(3)}) = \omega_k^{(3)} - \dot{f}_y^{(2)} + \omega^{(2)} f_x^{(1)} - \frac{f_y^{(2)}}{2} \frac{1}{(\omega_k + ma)} \left(m\dot{a} - \frac{ma\dot{\omega}_k}{\omega_k}\right),$$
$$(\omega_k + ma)(g_x^{(3)} - f_x^{(3)}) = -\omega_k^{(3)} + \dot{g}_y^{(2)} - \omega^{(2)} g_x^{(1)} + \frac{g_y^{(2)}}{2} \frac{1}{(\omega_k - ma)} \left(\frac{ma\dot{\omega}_k}{\omega_k} - m\dot{a}\right),$$
$$(\omega_k + ma)(2f_x^{(3)} + 2f_y^{(2)} f_y^{(1)}) + (\omega_k - ma)(2g_x^{(3)} + 2g_y^{(2)} g_y^{(1)}) = 0.$$

Using the fact that $g_y^{(2)} = f_y^{(2)} = 0$ in the above expressions, we have the result $f_x^{(3)} = g_x^{(3)}$. Using the relation $G^{(n)}(m) = F^{(n)}(-m)$ then we have $g_x^{(3)} - f_x^{(3)}(-m) = g_x^{(3)} - g_x^{(3)}(-m) = 0$ that is $g_x^{(3)}(m)$ and $f_x^{(3)}(m)$ are even functions of m and using the third relation above we have $f_y^{(3)} = g_y^{(3)} = 0$. With these we find $\omega_k^{(3)} = 0$. On the other hand, the imaginary part results in the expressions

$$(\omega_k - ma)(g_y^{(3)} - f_y^{(3)}) = \dot{f}_x^{(2)} + \frac{f_x^{(2)}}{2} \frac{1}{(\omega_k + ma)} \left(m\dot{a} - \frac{ma\dot{\omega}_k}{\omega_k}\right) + \omega_k^{(2)} f_y^{(1)},$$
$$(\omega_k + ma)(g_y^{(3)} - f_y^{(3)}) = -\dot{g}_x^{(2)} - \frac{g_x^{(2)}}{2} \frac{1}{(\omega_k - ma)} \left(\frac{ma\dot{\omega}_k}{\omega_k} - m\dot{a}\right) - \omega_k^{(2)} g_y^{(1)}.$$

Recasting the expressions above, we obtain

$$2\omega_k(g_y^{(3)} - f_y^{(3)}) = \dot{f}_x^{(2)} - \dot{g}_x^{(2)} + \omega^{(2)}(f_y^{(1)} - g_y^{(1)})$$
$$+ \frac{1}{2}\left(m\dot{a} - \frac{ma\dot{\omega}_k}{\omega_k}\right)\left(\frac{g_x^{(2)}}{\omega_k - ma} + \frac{f_x^{(2)}}{\omega_k + ma}\right), \quad \text{(C.21)}$$

from which, we can determine $g_y^{(3)}$ and $f_y^{(3)}$ with the condition $f_y^{(3)}(-m) = g_y^{(3)}(m)$. [1]

[1] In order to get $f_y^{(3)}$ we define $A \equiv g_y^{(3)} - f_y^{(3)}$ and we use the relation $g_y^{(3)}(m) = f_y^{(3)}(-m)$. With these we can write $A = f_y^{(3)}(-m) - f_y^{(3)(m)}$ and we calculate the right side of (C.21). If A is odd in m then $f_y^{(3)}(m)$ is odd and $f_y^{(3)}(m) = -1/2A$ which is the case.

In the same way, we can calculate the fourth adiabatic order. The real part is

$$(\omega_k - ma)(g_x^{(4)} - f_x^{(4)}) = \omega_k^{(4)} + \omega^{(2)} f_x^{(2)} - \dot{f}_y^{(3)} - \frac{f_y^{(3)}}{2} \frac{1}{(\omega_k + ma)} \left(m\dot{a} - \frac{ma\dot{\omega}_k}{\omega_k} \right),$$

$$(\omega_k + ma)(g_x^{(4)} - f_x^{(4)}) = -\omega_k^{(4)} - \omega^{(2)} g_x^{(2)} + \dot{g}_y^{(3)} + \frac{g_y^{(3)}}{2} \frac{1}{(\omega_k - ma)} \left(\frac{ma\dot{\omega}_k}{\omega_k} - m\dot{a} \right),$$

$$(\omega_k + ma)(2f_x^{(4)} + 2f_y^{(1)} f_y^{(3)} + (f_x^{(2)})^2) + (\omega_k - ma)(2g_x^{(4)} + 2g_y^{(1)} g_y^{(3)} + (g_x^{(2)})^2) = 0,$$

and the imaginary part is

$$(\omega_k - ma)(g_y^{(4)} - f_y^{(4)}) = \omega^{(2)} f_y^{(2)} + \dot{f}_x^{(3)} + \frac{f_x^{(3)}}{2} \frac{1}{(\omega_k + ma)} \left(m\dot{a} - \frac{ma\dot{\omega}_k}{\omega_k} \right),$$

$$(\omega_k + ma)(g_y^{(4)} - f_y^{(4)}) = -\omega^{(2)} g_y^{(2)} - \dot{g}_x^{(3)} - \frac{g_x^{(3)}}{2} \frac{1}{(\omega_k - ma)} \left(\frac{ma\dot{\omega}_k}{\omega_k} - m\dot{a} \right).$$

Using the fact that $f_y^{(2)} = g_y^{(2)} = f_x^{(3)} = g_x^{(3)} = 0$ into the above expression for the imaginary part we have $g_y^{(4)} - f_y^{(4)} = 0$ where, again, the functions $g_y^{(4)}$ and $f_y^{(4)}$ remains undetermined. However, since the local observables are independent of these functions, this ambiguity can be resolved by choosing $g_y^{(4)} = f_y^{(4)} = 0$. Next, from the real part we obtain

$$\begin{aligned} f_x^{(4)} = -f_y^{(1)} f_y^{(3)} &- \left(\frac{\omega_k + ma}{2\omega_k} \right) \frac{(f_x^{(2)})^2}{2} - \left(\frac{\omega_k - ma}{2\omega_k} \right) \frac{(g_x^{(2)})^2}{2} \\ &- \frac{\omega_k - ma}{4\omega_k^2} \Bigg[\omega_k^{(2)} (f_x^{(2)} - g_x^{(2)}) + \dot{g}_y^{(3)} - \dot{f}_y^{(3)} \\ &\qquad + \frac{1}{2} \left(\frac{ma\dot{\omega}_k}{\omega_k} - m\dot{a} \right) \left(\frac{g_y^{(3)}}{\omega_k - ma} + \frac{f_y^{(3)}}{\omega_k + ma} \right) \Bigg], \end{aligned}$$

from which, again, is possible to obtain g_x^4 with the condition $f_x^{(4)}(-m) = g_x^{(4)}(m)$ and once done this we can obtain $\omega_k^{(4)}$ through

$$\omega_k^{(4)} = ma(f_x^{(4)} - g_x^{(4)}) - \frac{w_k^{(2)}}{2} \left(f_x^{(2)} + g_x^{(2)} \right) + \frac{m\dot{a} f_y^{(3)}}{2w_k}.$$

Finally, up to fourth adiabatic order the mode functions are given by

$$\begin{aligned} u_k^{(4)} \sim \sqrt{\frac{\omega_k + ma}{2\omega_k}} \left[1 + \sum_{i=1}^{4} F(\eta)^{(i)} \right] \times \\ \exp\left(-i \int \left(\omega_k + \omega_k^{(1)} + \omega_k^{(2)} + \omega_k^{(3)} + \omega_k^{(4)} \right) d\tilde{\eta} \right) \end{aligned} \quad \text{(C.22)}$$

where

$$F^{(3)} = \frac{65im^5a^2\dot{a}^3}{64\omega_k^8} - \frac{21im^3\dot{a}^3}{128\omega_k^6} - \frac{19im^3a\dot{a}\ddot{a}}{32\omega_k^6} + \frac{im\dddot{a}}{16\omega_k^4}, \tag{C.23}$$

$$\begin{aligned} F^{(4)} = {} & \frac{2285m^8a^4\dot{a}^4}{512\omega_k^{12}} - \frac{565m^7a^3\dot{a}^4}{128\omega_k^{11}} - \frac{349m^6a^2\dot{a}^4}{256\omega_k^{10}} + \frac{803m^5a\dot{a}^4}{512\omega_k^9} - \frac{85m^4\dot{a}^4}{2048\omega_k^8} \\ & - \frac{457m^6a^3\dot{a}^2\ddot{a}}{128\omega_k^{10}} + \frac{113m^5a^2\dot{a}^2\ddot{a}}{32\omega_k^9} + \frac{113m^4a\dot{a}^2\ddot{a}}{256\omega_k^8} - \frac{141m^3\dot{a}^2\ddot{a}}{256\omega_k^7} \\ & + \frac{41m^4a^2\ddot{a}^2}{128\omega_k^8} - \frac{5m^3a\ddot{a}^2}{16\omega_k^7} - \frac{m^2\ddot{a}^2}{128\omega_k^6} + \frac{7m^4a^2\dot{a}\dddot{a}}{16\omega_k^8} - \frac{7m^3a\dot{a}\dddot{a}}{16\omega_k^7} \\ & - \frac{m^2\dot{a}\dddot{a}}{64\omega_k^6} - \frac{m^2a\ddddot{a}}{32\omega_k^6} + \frac{m\ddddot{a}}{32\omega_k^5}. \end{aligned} \tag{C.24}$$

and

$$\begin{aligned} \omega_k^{(4)} = {} & -\frac{1105m^8a^4\dot{a}^4}{128\omega_k^{11}} + \frac{29m^6a^2\dot{a}^4}{8\omega_k^9} - \frac{11m^4\dot{a}^4}{128\omega_k^7} + \frac{221m^6a^3\dot{a}^2\ddot{a}}{32\omega_k^9} - \frac{89m^4a\dot{a}^2\ddot{a}}{64\omega_k^7} \\ & - \frac{19m^4a^2\ddot{a}^2}{32\omega_k^7} - \frac{7m^4a^2\dot{a}\dddot{a}}{8\omega_k^7} + \frac{m^2\dot{a}\dddot{a}}{32\omega_k^5} + \frac{m^2a\ddddot{a}}{16\omega_k^5}. \end{aligned} \tag{C.25}$$

with $\omega_k^{(1)} = \omega_k^{(3)} = 0$, and similarly for $v_k^{(4)}$ remembering the condition $u_k^{(n)}(-m) = v_k^{(n)}(m)$.

C.4 Energy Density

The Dirac field ψ can be written in terms of creation and annihilation operators for particles and antiparticles, $\hat{a}_{\vec{k},\lambda}$ and $\hat{b}_{\vec{k},\lambda}$ respectively, as

$$\psi = \sum_\lambda \int d^3k \left[\hat{a}_{\vec{k}\lambda} U_{\vec{k}\lambda} + \hat{b}^\dagger_{\vec{k}\lambda} V_{\vec{k}\lambda}\right], \tag{C.26}$$

where the eigenfunctions $U_{\vec{k}\lambda}(x)$ and $V_{\vec{k}\lambda}(x)$ are given by

$$U_{\vec{k}\lambda} = \frac{e^{i\vec{k}\cdot\vec{x}}}{(2\pi a)^{3/2}} \begin{pmatrix} u_k\xi_\lambda \\ v_k \frac{\vec{\sigma}\cdot\vec{k}}{k}\xi_\lambda \end{pmatrix} \quad \text{or} \quad U_{\vec{k}\lambda} = \frac{e^{i\vec{k}\cdot\vec{x}}}{(2\pi a)^{3/2}} \begin{pmatrix} u_k\xi_\lambda \\ v_k\lambda\xi_\lambda \end{pmatrix}, \tag{C.27a}$$

$$V_{\vec{k}\lambda} = \frac{e^{-i\vec{k}\cdot\vec{x}}}{(2\pi a)^{3/2}} \begin{pmatrix} -v_k^*\xi_{-\lambda} \\ -u_k^* \frac{\vec{\sigma}\cdot\vec{k}}{k}\xi_{-\lambda} \end{pmatrix} \quad \text{or} \quad V_{\vec{k}\lambda} = \frac{e^{-i\vec{k}\cdot\vec{x}}}{(2\pi a)^{3/2}} \begin{pmatrix} -v_k^*\xi_{-\lambda} \\ \lambda u_k^*\xi_{-\lambda} \end{pmatrix}, \tag{C.27b}$$

and ξ_λ is the normalized two-component spinor satisfying $\xi^\dagger_{\lambda'}\xi_\lambda = \delta_{\lambda'\lambda}$ with the property $\frac{\vec{\sigma}\cdot\vec{k}}{2k}\xi_\lambda = (\lambda/2)\xi_\lambda$ where $\lambda = \pm 1$ represents the helicity. Also $U_{\vec{k}\lambda}$ and $V_{\vec{k}\lambda}$ are related by charge conjugation operation (e.g. $V_{\vec{k}\lambda} = CU_{\vec{k}\lambda} = i\gamma^2 U^*_{\vec{k}\lambda}$) [2] with $u_k(\eta)$ and $v_k(\eta)$ the two time-dependent mode functions.

[2] In order to obtain the expression (C.27b), we need to take into account the expression $-i\sigma^2\xi^*_\lambda = \lambda\xi_{-\lambda}$.

Let's compute the expectation value of the energy-momentum tensor using the Dirac field decomposition (C.26) such that

$$\psi = \sum_{\lambda} \int d^3k \left[\hat{a}_{\vec{k}\lambda} U_{\vec{k}\lambda} + \hat{b}^{\dagger}_{\vec{k}\lambda} V_{\vec{k}\lambda} \right], \tag{C.28}$$

$$\bar{\psi} = \psi^{\dagger}\gamma^0 = \sum_{\lambda} \int d^3k \left[\hat{a}^{\dagger}_{\vec{k}\lambda} U^{\dagger}_{\vec{k}\lambda} + \hat{b}_{\vec{k}\lambda} V^{\dagger}_{\vec{k}\lambda} \right] \gamma^0. \tag{C.29}$$

Putting these in the expectation value of $T^m_{00} = \frac{i}{2}[\bar{\psi}\gamma_{(0}\nabla_{0)}\psi - (\nabla_{(0}\bar{\psi})\gamma_{0)}\psi]$, we get

$$\begin{aligned}
&\langle \psi^{\dagger}\partial_0\psi\rangle - \langle \partial_0\psi^{\dagger}\psi\rangle = \\
&\quad \int d^3\vec{k} \int d^3\vec{k'} \sum_{\lambda}\sum_{\lambda'} \left(U^{\dagger}_{\vec{k}\lambda}\partial_0 U_{\vec{k'}\lambda'} - \partial_0 U^{\dagger}_{\vec{k}\lambda} U_{\vec{k'}\lambda'} \right) \delta(\vec{k}-\vec{k'}) n^a_{\lambda\lambda'} \\
&\quad + \int d^3\vec{k} \int d^3\vec{k'} \sum_{\lambda}\sum_{\lambda'} \left(U^{\dagger}_{\vec{k}\lambda}\partial_0 V_{\vec{k'}\lambda'} - \partial_0 U^{\dagger}_{\vec{k}\lambda} V_{\vec{k'}\lambda'} \right) \delta(\vec{k}+\vec{k'}) m^b_{\lambda\lambda'} \\
&\quad + \int d^3\vec{k} \int d^3\vec{k'} \sum_{\lambda}\sum_{\lambda'} \left(V^{\dagger}_{\vec{k}\lambda}\partial_0 U_{\vec{k'}\lambda'} - \partial_0 V^{\dagger}_{\vec{k}\lambda} U_{\vec{k'}\lambda'} \right) \delta(\vec{k}+\vec{k'}) m^a_{\lambda\lambda'} \\
&\qquad + \int d^3\vec{k} \int d^3\vec{k'} \sum_{\lambda}\sum_{\lambda'} \left(V^{\dagger}_{\vec{k}\lambda}\partial_0 V_{\vec{k'}\lambda'} - \partial_0 V^{\dagger}_{\vec{k}\lambda} V_{\vec{k'}\lambda'} \right) \times \\
&\qquad\qquad \left[\delta(\vec{k}-\vec{k'})\delta_{\lambda,\lambda'} - \delta(\vec{k}-\vec{k'}) n^b_{\lambda\lambda'} \right],
\end{aligned}$$

where for an arbitrary state $|\psi\rangle$,

$$\langle a^{\dagger}_{\vec{k'}\lambda'} a_{\vec{k}\lambda}\rangle = \delta(\vec{k}-\vec{k'}) n^a_{\lambda\lambda'}, \tag{C.30a}$$

$$\langle a^{\dagger}_{\vec{k'}\lambda'} b^{\dagger}_{\vec{k}\lambda}\rangle = \delta(\vec{k}+\vec{k'}) m^b_{\lambda\lambda'}, \tag{C.30b}$$

$$\langle b_{\vec{k'}\lambda'} a_{\vec{k}\lambda}\rangle = \delta(\vec{k}+\vec{k'}) m^a_{\lambda\lambda'} \tag{C.30c}$$

$$\langle b_{\vec{k'}\lambda'} b^{\dagger}_{\vec{k}\lambda}\rangle = \delta(\vec{k}-\vec{k'})\delta_{\lambda\lambda'} - \delta(\vec{k}-\vec{k'}) n^b_{\lambda\lambda'}. \tag{C.30d}$$

If we choose the $|in, 0\rangle$ vacuum state, then $n^a_{\lambda\lambda'}, m^b_{\lambda\lambda'}, m^a_{\lambda\lambda'}, n^b_{\lambda\lambda'} = 0$. Using the eigenfunctions (4.13) we can write

$$\begin{aligned}
&\langle \bar{\psi}\gamma^0\partial_0\psi\rangle - \langle \partial_0\bar{\psi}\gamma^0\psi\rangle = \\
&\quad \frac{1}{(2\pi)^3 a^3}\Big[\int d^3\vec{k} \sum_{\lambda}\sum_{\lambda'} \delta_{\lambda\lambda'}(u^*_k\dot{u}_k + \lambda\lambda' v^*_k\dot{v}_k - \dot{u}^*_k u_k - \lambda\lambda' v\dot{v}^*_k) n^a_{\lambda\lambda'} \\
&\quad + \int d^3\vec{k} \sum_{\lambda}\sum_{\lambda'} \delta_{-\lambda-\lambda'}(v_k\dot{v}^*_k + \lambda\lambda' u_k\dot{u}^*_k - v^*_k\dot{v}_k - \lambda\lambda' u^*_k\dot{u})[1 - n^b_{\lambda\lambda'}] \\
&\qquad - \int d^3\vec{k} \sum_{\lambda}\sum_{\lambda'} (\dot{u}^*_k v^*_k(1+\lambda\lambda') - u^*_k\dot{v}^*_k(1+\lambda'\lambda)) \xi^{\dagger}_{\lambda\vec{k}}\xi_{-\lambda'-\vec{k}} m^b_{\lambda\lambda'} \\
&\qquad\quad - \int d^3\vec{k} \sum_{\lambda}\sum_{\lambda'} (u_k\dot{v}_k(1+\lambda'\lambda) - \dot{u}_k v_k(1+\lambda\lambda')) \xi^{\dagger}_{-\lambda\vec{k}}\xi_{\lambda'-\vec{k}} m^a_{\lambda\lambda'} \Big].
\end{aligned}$$

After some straightforward algebra, and using the relations $\xi^{\dagger}_{\lambda\vec{k}}\xi_{-\lambda'-\vec{k}} = -\xi^{\dagger}_{\lambda\vec{k}}\xi_{\lambda'\vec{k}} = \delta_{\lambda\lambda'}$ and $\xi^{\dagger}_{-\lambda\vec{k}}\xi_{\lambda'-\vec{k}} = -\xi^{\dagger}_{-\lambda\vec{k}}\xi_{-\lambda'\vec{k}} = \delta_{-\lambda-\lambda'}$ (where in the relation $\xi_{-\lambda-\vec{k}} = e^{i\phi}\xi_{\lambda\vec{k}}$ we have choose $\phi = \pi$) we can write the energy density

expression as

$$\rho = \frac{1}{2\pi^2 a^3}\int_0^\infty dk k^2 \rho_k \tag{C.31}$$

where

$$\rho_k = \frac{i}{2a}\Big[2i\left(2-[n^b+n^a]\right)\mathfrak{Im}\{u_k\dot{u}_k^* + v_k\dot{v}_k^*\} + 2m^b(\dot{u}_k^* v_k^* - u_k^*\dot{v}_k^*) + 2m^a(u_k\dot{v}_k - \dot{u}_k v_k)\Big] \tag{C.32}$$

or for a finite volume V we have

$$\rho = \frac{i}{2a^4 V}\sum_{\vec{k},\lambda}\Big[2i\left(1-[n^b_{-\lambda-\lambda}+n^a_{\lambda\lambda}]\right)\mathfrak{Im}\{u_k\dot{u}_k^* + v_k\dot{v}_k^*\} - 2m^b_{\lambda\lambda}(\dot{u}_k^* v_k^* - u_k^*\dot{v}_k^*) - 2m^a_{-\lambda-\lambda}(u_k\dot{v}_k - \dot{u}_k v_k)\Big] \tag{C.33}$$

with

$$n^a_k = \sum_\lambda n^a_{\lambda\lambda},\ n^b_k = \sum_\lambda n^b_{-\lambda-\lambda},\ m^a_k = \sum_\lambda m^a_{-\lambda-\lambda},\ m^b_k = \sum_\lambda m^b_{\lambda\lambda},$$

or

$$\rho = \frac{i}{2a^4 V}\sum_{\vec{k},\lambda}\Big[2i\left(\langle a^\dagger_{\vec{k}\lambda}a_{\vec{k}\lambda}\rangle - \langle b_{\vec{k}\lambda}b^\dagger_{\vec{k}\lambda}\rangle\right)\mathfrak{Im}\{u_k\dot{u}_k^* + v_k\dot{v}_k^*\} - 2\langle a^\dagger_{\lambda\vec{k}}b^\dagger_{\lambda\vec{k}}\rangle(\dot{u}_k^* v_k^* - u_k^*\dot{v}_k^*) - 2\langle b_{\vec{k}-\lambda}a_{\vec{k}-\lambda}\rangle(u_k\dot{v}_k - \dot{u}_k v_k)\Big].$$

C.5 Second and Fourth Adiabatic Expansion of $\rho_k^{\mathbf{in}}$

Up to second adiabatic order, $u_k^{(2)}$ can be written as

$$u_k^{(2)} \sim \sqrt{\frac{\omega_k + ma}{2\omega_k}}\left[1 + F^{(1)} + F^{(2)}\right]\exp\left\{\left(-i\int(\omega_k + \omega_k^{(2)})d\tilde{\eta}\right)\right\} \tag{C.34}$$

and $v_k^{(2)}(\eta) = u_k^{(2)}(-m)$. Putting these in (4.53b) we get

$$\rho_k^{(2)} = \frac{1}{a}\left(\frac{\omega_k + ma}{\omega_k}\right)\left[\mathfrak{Im}\dot{F}^{(1)} - |F^{(1)}|^2\omega_k - 2F^{(2)}\omega_k - \omega_k^{(2)}\right] + \frac{1}{a}\left(\frac{\omega_k - ma}{\omega_k}\right)[F\to G]. \tag{C.35}$$

With the same steps, we can write the fourth-order term of ρ_k^{in} as

$$\rho_k^{(4)} = \frac{\omega_k + ma}{a\omega_k}\Big[\mathfrak{Im}\dot{F}^{(3)} - \dot{F}^{(2)}\mathfrak{Im}F^{(1)} - (F^{(2)})^2\omega_k$$
$$-(F^{(3)*}F^{(1)} + F^{(1)*}F^{(3)} + 2F^{(4)})\omega_k + F^{(2)}(\mathfrak{Im}\dot{F}^{(1)} - 2\omega_k^{(2)}) - |F^{(1)}|^2\omega_k^{(2)} - \omega_k^{(4)}\Big]$$
$$+ \frac{\omega_k - ma}{a\omega_k}[F \to G]. \quad \text{(C.36)}$$

C.6 Bogoliubov Transformation

The set of orthonormal basis (4.13), that is $\{U^{\text{in}}_{\vec{k},\lambda}, V^{\text{in}}_{\vec{k},\lambda}\}$, is not unique. Let's consider a different orthonormal basis $\{U_{\vec{k},\lambda}, V_{\vec{k},\lambda}\}$, with the following relations

$$U^{\text{in}}_{\vec{k},\lambda} = \alpha_k U_{\vec{k},\lambda} + \beta_k V_{\vec{k},\lambda}, \quad V^{\text{in}}_{\vec{k},\lambda} = \alpha_k^* V_{\vec{k},\lambda} - \beta_k^* U_{\vec{k},\lambda} \quad \text{(C.37)}$$

where $V_{\vec{k},\lambda} = i\gamma^2 U^*_{\vec{k},\lambda}$. Using the fact that

$$\hat{\Psi} = \sum_{\vec{k}}\sum_{\lambda}[\hat{a}^{\text{in}}_{\vec{k},\lambda}U^{\text{in}}_{\vec{k},\lambda} + \hat{b}^{\text{in}\dagger}_{\vec{k},\lambda}V^{\text{in}}_{\vec{k},\lambda}] = \sum_{\vec{k}}\sum_{\lambda}[\hat{a}_{\vec{k},\lambda}U_{\vec{k},\lambda} + \hat{b}^{\dagger}_{\vec{k},\lambda}V_{\vec{k},\lambda}] \quad \text{(C.38)}$$

and substituting in this the relations (C.37) we obtain

$$\hat{a}_{\vec{k},\lambda} = [\hat{a}^{\text{in}}_{\vec{k},\lambda}\alpha_k - \hat{b}^{\text{in}\dagger}_{\vec{k},\lambda}\beta_k^*], \quad \text{(C.39a)}$$
$$\hat{b}^{\dagger}_{\vec{k},\lambda} = [\hat{a}^{\text{in}}_{\vec{k},\lambda}\beta_k + \hat{b}^{\text{in}\dagger}_{\vec{k},\lambda}\alpha_k^*]. \quad \text{(C.39b)}$$

With these relations, we can rewrite (C.39) as

$$\begin{pmatrix}\hat{a}_{\vec{k},\lambda}\\ \hat{b}^{\dagger}_{\vec{k},\lambda}\end{pmatrix} = \begin{pmatrix}\alpha_k & -\beta_k^*\\ \beta_k & \alpha_k^*\end{pmatrix}\begin{pmatrix}\hat{a}^{\text{in}}_{\vec{k},\lambda}\\ \hat{b}^{\text{in}\dagger}_{\vec{k},\lambda}\end{pmatrix} \quad \text{and}$$
$$\begin{pmatrix}\alpha_k & -\beta_k^*\\ \beta_k & \alpha_k^*\end{pmatrix}^{\dagger}\begin{pmatrix}\alpha_k & -\beta_k^*\\ \beta_k & \alpha_k^*\end{pmatrix} = \begin{pmatrix}1 & 0\\ 0 & 1\end{pmatrix}. \quad \text{(C.40)}$$

On other hand, using the relations

$$U^{\text{in}}_{\vec{k}\lambda}(\vec{x},\eta) = \frac{e^{i\vec{k}\cdot\vec{x}}}{(2\pi a)^{3/2}}\begin{pmatrix}u^{\text{in}}_k\xi_\lambda\\ v^{\text{in}}_k\lambda\xi_\lambda\end{pmatrix}, \; V^{\text{in}}_{\vec{k}\lambda}(\vec{x},\eta) = \frac{e^{-i\vec{k}\cdot\vec{x}}}{(2\pi a)^{3/2}}\begin{pmatrix}-v^{\text{in}*}_k\xi_{-\lambda}\\ u^{\text{in}*}_k\lambda\xi_{-\lambda}\end{pmatrix}. \quad \text{(C.41a)}$$

and the orthogonality of ξ_λ, the relation $U^{\text{in}}_{\vec{k},\lambda} = \alpha_k U_{\vec{k},\lambda} + \beta_k V_{\vec{k},\lambda}$, imply, after some manipulations, that the solution corresponding to u_k^{in} and v_k^{in} are given according to the transformation

$$u^{\text{in}}_k(\eta) = \alpha_k u_k - \beta_k v_k^* \quad \text{and} \quad v^{\text{in}}_k(\eta) = \alpha_k v_k + \beta_k u_k^*, \quad \text{(C.42)}$$

where again the functions u^{in}_k and v^{in}_k are those mode functions that satisfy the *in* initial conditions and α_k and β_k are the Bogoliubov coefficients of a Bogoliubov transformation (C.40).

Putting these into the normalization condition $|u_k^{\rm in}|^2 + |v_k^{\rm in}|^2 = 1$ we have directly that

$$|\alpha_k|^2 + |\beta_k|^2 = 1, \tag{C.43}$$

provided that $|u_k|^2 + |v_k|^2 = 1$ is satisfied. Then, the Bogoliubov coefficients α_k and β_k are constant. On other hand, using Eq. (C.43) and after some manipulations we have

$$u_k = \alpha_k^* u_k^{\rm in} + \beta_k v_k^{\rm in*}, \quad v_k = \alpha_k^* v_k^{\rm in} - \beta_k u_k^{\rm in*}. \tag{C.44}$$

Finally, using the normalization condition for $|u_k^{\rm in}|^2 + |v_k^{\rm in}|^2 = 1$ and manipulating Eq. (C.44) we can write

$$\alpha_k = u_k^{\rm in} u_k^* + v_k^{\rm in} v_k^*, \quad \beta_k = u_k v_k^{\rm in} - v_k u_k^{\rm in}. \tag{C.45a}$$

We can also calculate β_k considering the inner product between $V_{\vec{k},\lambda}^{\rm in}$ and $U_{\vec{k},\lambda}$ given by Eq. (4.17), from which

$$\beta_k = (V_{\vec{k}\lambda}^{\rm in}, U_{\vec{k}'\lambda'}) = \int dx^3 a^3 V_{\vec{k}\lambda}^{\rm in\dagger} U_{\vec{k}'\lambda'} = [v_k u_k^{\rm in} - u_k v_k^{\rm in}] e^{i\phi} \tag{C.46}$$

with $e^{i\phi} = \xi^\dagger_{\lambda,\vec{k}} \xi_{-\lambda,-\vec{k}}$. To make the Bogoliubov coefficients independent of λ and $\vec{k}$ as Eq. (C.44), we need to choose $\phi = \pi$. Since $|\beta_k|^2$ is the quantity that determines an observable, we can do this without loss of generality.

Bibliography

[1] Emmanuel Chávez Nambo, Alberto Diez-Tejedor, Edgar Preciado-Govea, Armando A. Roque, and Olivier Sarbach. Nonrelativistic Proca stars: Spherical stationary and multi-frequency states. 12 2024.

[2] Emmanuel Chávez Nambo, Alberto Diez-Tejedor, Edgar Preciado-Govea, Armando A. Roque, and Olivier Sarbach. Linear stabilty of non-relativistic Proca stars.

[3] A. Diez-Tejedor C. Armendariz-Picon and E. Preciado-Govea. work in progress.

[4] Daniel J.H. Chung, Edward W. Kolb, and Antonio Riotto. Superheavy dark matter. *Physical Review D*, 59(2):023501, 1998.

[5] Daniel J.H. Chung, Lisa L. Everett, Hojin Yoo, and Peng Zhou. Gravitational fermion production in inflationary cosmology. *Physics Letters B*, 712(3):147–154, 2012.

[6] Julio F. Navarro, Carlos S. Frenk, and Simon D. M. White. The structure of cold dark matter halos. *The Astrophysical Journal*, 462:563, May 1996.

[7] Andreas Burkert. The structure of dark matter halos in dwarf galaxies. *The Astrophysical Journal*, 447(1):L25, 1995.

[8] Guinevere Kauffmann, Simon D.M. White, and Bruno Guiderdoni. The formation and evolution of galaxies within merging dark matter haloes. *Monthly Notices of the Royal Astronomical Society*, 264(1):201–218, 1993.

[9] Luca Visinelli. Boson stars and oscillatons: A review. *International Journal of Modern Physics D*, 30(15), November 2021.

[10] John Archibald Wheeler. Geons. *Physical Review*, 97(2):511, 1955.

[11] Remo Ruffini and Silvano Bonazzola. Systems of selfgravitating particles in general relativity and the concept of an equation of state. *Phys. Rev.*, 187:1767–1783, 1969.

[12] Stuart L Shapiro and Saul A Teukolsky. *Black holes, white dwarfs and neutron stars: the physics of compact objects*. John Wiley & Sons, 2024.

[13] Wayne Hu, Rennan Barkana, and Andrei Gruzinov. Fuzzy cold dark matter: The wave properties of ultralight particles. *Physical Review Letters*, 85(6):1158–1161, August 2000.

[14] Pierre-Henri Chavanis. Mass-radius relation of Newtonian self-gravitating Bose-Einstein condensates with short-range interactions: I. Analytical results. *Phys. Rev. D*, 84:043531, 2011.

[15] David J. Kaup. Klein-Gordon Geon. *Phys. Rev.*, 172:1331–1342, 1968.

[16] Monica Colpi, Stuart L. Shapiro, and Ira Wasserman. Boson stars: Gravitational equilibria of self-interacting scalar fields. *Phys. Rev. Lett.*, 57:2485–2488, Nov 1986.

[17] Jochum J. Van der Bij and Marcelo Gleiser. Stars of bosons with non-minimal energy-momentum tensor. *Physics Letters B*, 194(4):482–486, 1987.

[18] Ph. Jetzer and J.J. Van Der Bij. Charged boson stars. *Physics Letters B*, 227(3):341–346, 1989.

[19] Marcelo Gleiser. Stability of boson stars. *Phys. Rev. D*, 38:2376–2385, Oct 1988.

[20] T.D. Lee and Yang Pang. Stability of mini-boson stars. *Nuclear Physics B*, 315(2):477–516, 1989.

[21] Philippe Jetzer. Gravitational equilibria of self-interacting charged scalar fields. *Nuclear Physics B - Proceedings Supplements*, 16:653–655, 1990.

[22] Marcelo Gleiser and Richard Watkins. Gravitational stability of scalar matter. *Nuclear Physics B*, 319(3):733–746, 1989.

[23] Fjodor V. Kusmartsev, Eckehard W. Mielke, and Franz E. Schunck. Gravitational stability of boson stars. *Phys. Rev. D*, 43:3895–3901, Jun 1991.

[24] Phillippe Jetzer. Boson stars. *Physics Reports*, 220(4):163–227, 1992.

[25] Remo Ruffini and Silvano Bonazzola. Systems of self-gravitating particles in general relativity and the concept of an equation of state. *Phys. Rev.*, 187:1767–1783, Nov 1969.

[26] R. Friedberg, T. D. Lee, and Y. Pang. Scalar soliton stars and black holes. *Phys. Rev. D*, 35:3658–3677, Jun 1987.

[27] Andrew R. Liddle and Mark S. Madsen. The Structure and Formation of Boson Stars. *International Journal of Modern Physics D*, 1(1):101–143, January 1992.

[28] Franz E. Schunck and Eckehard W. Mielke. General relativistic boson stars. *Classical and Quantum Gravity*, 20(20):R301–R356, September 2003.

[29] Miguel Alcubierre, Juan Barranco, Argelia Bernal, Juan Carlos Degollado, Alberto Diez-Tejedor, Miguel Megevand, Darío Núñez, and Olivier Sarbach. ℓ-boson stars. *Classical and Quantum Gravity*, 35(19):19LT01, September 2018.

[30] Steven L. Liebling and Carlos Palenzuela. Dynamical boson stars. *Living Reviews in Relativity*, 26(1), February 2023.

[31] Emmanuel Chávez Nambo, Alberto Diez-Tejedor, Armando A. Roque, and Olivier Sarbach. Linear stability of nonrelativistic self-interacting boson stars. *Physical Review D*, 109(10), May 2024.

[32] Joshua Eby, Madelyn Leembruggen, Lauren Street, Peter Suranyi, and L. C. R. Wijewardhana. Approximation methods in the study of boson stars. *Phys. Rev. D*, 98:123013, Dec 2018.

[33] Jiajun Chen, Xiaolong Du, Erik W. Lentz, David J. E. Marsh, and Jens C. Niemeyer. New insights into the formation and growth of boson stars in dark matter halos. *Physical Review D*, 104(8), October 2021.

[34] R van Breukelen. *Topological and nontopological solitons*. PhD thesis, Faculty of Science and Engineering, 2012.

[35] Tsung-Dao Lee and Yang Pang. Nontopological solitons. *Physics Reports*, 221(5-6):251–350, 1992.

[36] Tom Lancaster and Stephen J. Blundell. *Quantum Field Theory for the Gifted Amateur*. Oxford University Press, 04 2014.

[37] G. H. Derrick. Comments on nonlinear wave equations as models for elementary particles. *J. Math. Phys.*, 5:1252–1254, 1964.

[38] Eckehard W. Mielke and Franz E. Schunck. Boson stars: Early history and recent prospects, 1998.

[39] R. Friedberg, T.D. Lee, and Y. Pang. Mini-soliton stars. *Physical Review D*, 35(12):3640, 1987.

[40] Andrew R. Liddle and Mark S. Madsen. The Structure and formation of boson stars. *Int. J. Mod. Phys. D*, 1:101–144, 1992.

[41] Marcelo Gleiser. Stability of boson stars. *Physical Review D*, 38(8):2376, 1988.

[42] Edward Seidel and Wai-Mo Suen. Dynamical evolution of boson stars: Perturbing the ground state. *Phys. Rev. D*, 42:384–403, Jul 1990.

[43] Franz E. Schunck and Eckehard W. Mielke. General relativistic boson stars. *Classical and Quantum Gravity*, 20(20):R301–R356, September 2003.

[44] Robert Ferrell and Marcelo Gleiser. Gravitational atoms: Gravitational radiation from excited boson stars. *Phys. Rev. D*, 40:2524–2531, Oct 1989.

[45] AB Henriques, Andrew R Liddle, and RG Moorhouse. Combined boson-fermion stars: configurations and stability. *Nuclear Physics B*, 337(3):737–761, 1990.

[46] Philippe Jetzer. Boson stars. *Phys. Rept.*, 220:163–227, 1992.

[47] Marcelo Gleiser and Richard Watkins. Gravitational Stability of Scalar Matter. *Nucl. Phys. B*, 319:733–746, 1989.

[48] Emmanuel Chávez Nambo, Armando A. Roque, and Olivier Sarbach. Are nonrelativistic ground state ℓ-boson stars only stable for ℓ=0 and ℓ=1? *Phys. Rev. D*, 108(12):124065, 2023.

[49] Emmanuel Chávez Nambo, Alberto Diez-Tejedor, Armando A. Roque, and Olivier Sarbach. Linear stability of nonrelativistic self-interacting boson stars. *Phys. Rev. D*, 109(10):104011, 2024.

[50] Steven L. Liebling and Carlos Palenzuela. Dynamical boson stars. *Living Rev. Rel.*, 26(1):1, 2023.

[51] Hong Zhang. Axion Stars. *Symmetry*, 12(1):25, 2019.

[52] Luca Visinelli. Boson stars and oscillatons: A review. *Int. J. Mod. Phys. D*, 30(15):2130006, 2021.

[53] Abril Suárez, Victor H. Robles, and Tonatiuh Matos. *A Review on the Scalar Field/Bose-Einstein Condensate Dark Matter Model*, page 107–142. Springer International Publishing, November 2013.

[54] Bohua Li, Tanja Rindler-Daller, and Paul R. Shapiro. Cosmological constraints on bose-einstein-condensed scalar field dark matter. *Physical Review D*, 89(8), April 2014.

[55] Abril Suárez, Victor H. Robles, and Tonatiuh Matos. A Review on the Scalar Field/Bose-Einstein Condensate Dark Matter Model. *Astrophys. Space Sci. Proc.*, 38:107–142, 2014.

[56] David J. E. Marsh. Axion Cosmology. *Phys. Rept.*, 643:1–79, 2016.

[57] L. Arturo Ureña López. Brief Review on Scalar Field Dark Matter Models. *Front. Astron. Space Sci.*, 6:47, 2019.

[58] Elisa G. M. Ferreira. Ultra-light dark matter. *Astron. Astrophys. Rev.*, 29(1):7, 2021.

[59] D. Antypas et al. New Horizons: Scalar and Vector Ultralight Dark Matter. 3 2022.

[60] Richard Brito, Vitor Cardoso, Carlos A. R. Herdeiro, and Eugen Radu. Proca stars: Gravitating Bose–Einstein condensates of massive spin 1 particles. *Phys. Lett. B*, 752:291–295, 2016.

[61] Ignacio Salazar Landea and Federico García. Charged Proca Stars. *Phys. Rev. D*, 94(10):104006, 2016.

[62] Y. Brihaye, Th. Delplace, and Y. Verbin. Proca Q Balls and their Coupling to Gravity. *Phys. Rev. D*, 96(2):024057, 2017.

[63] Masato Minamitsuji. Vector boson star solutions with a quartic order self-interaction. *Phys. Rev. D*, 97(10):104023, 2018.

[64] Carlos A. R. Herdeiro, Grigoris Panotopoulos, and Eugen Radu. Tidal Love numbers of Proca stars. *JCAP*, 08:029, 2020.

[65] Carlos A. R. Herdeiro and Eugen Radu. Asymptotically flat, spherical, self-interacting scalar, Dirac and Proca stars. *Symmetry*, 12(12):2032, 2020.

[66] C. A. R. Herdeiro, E. Radu, N. Sanchis-Gual, N. M. Santos, and E. dos Santos Costa Filho. The non-spherical ground state of Proca stars. *Phys. Lett. B*, 852:138595, 2024.

[67] Carlos Joaquin and Miguel Alcubierre. Proca stars in excited states. *Gen. Rel. Grav.*, 57(2):45, 2025.

[68] Nicolas Sanchis-Gual, Carlos Herdeiro, Eugen Radu, Juan Carlos Degollado, and José A. Font. Numerical evolutions of spherical Proca stars. *Phys. Rev. D*, 95(10):104028, 2017.

[69] Nicolas Sanchis-Gual, Carlos Herdeiro, José A. Font, Eugen Radu, and Fabrizio Di Giovanni. Head-on collisions and orbital mergers of Proca stars. *Phys. Rev. D*, 99(2):024017, 2019.

[70] Zipeng Wang, Thomas Helfer, and Mustafa A. Amin. General relativistic polarized Proca stars. *Phys. Rev. D*, 109(2):024019, 2024.

[71] Juan Calderón Bustillo, Nicolas Sanchis-Gual, Alejandro Torres-Forné, José A. Font, Avi Vajpeyi, Rory Smith, Carlos Herdeiro, Eugen Radu, and Samson H. W. Leong. GW190521 as a Merger of Proca Stars: A Potential New Vector Boson of 8.7×10^{-13} eV. *Phys. Rev. Lett.*, 126(8):081101, 2021.

[72] Carlos A. R. Herdeiro, Alexandre M. Pombo, Eugen Radu, Pedro V. P. Cunha, and Nicolas Sanchis-Gual. The imitation game: Proca stars that can mimic the Schwarzschild shadow. *JCAP*, 04:051, 2021.

[73] Nicolas Sanchis-Gual, Juan Calderón Bustillo, Carlos Herdeiro, Eugen Radu, José A. Font, Samson H. W. Leong, and Alejandro Torres-Forné. Impact of the wavelike nature of Proca stars on their gravitational-wave emission. *Phys. Rev. D*, 106(12):124011, 2022.

[74] João Luís Rosa and Diego Rubiera-Garcia. Shadows of boson and Proca stars with thin accretion disks. *Phys. Rev. D*, 106(8):084004, 2022.

[75] Ivo Sengo, Pedro V. P. Cunha, Carlos A. R. Herdeiro, and Eugen Radu. The imitation game reloaded: effective shadows of dynamically robust spinning Proca stars. *JCAP*, 05:054, 2024.

[76] Mudit Jain and Mustafa A. Amin. Polarized solitons in higher-spin wave dark matter. *Phys. Rev. D*, 105(5):056019, 2022.

[77] Hong-Yi Zhang, Mudit Jain, and Mustafa A. Amin. Polarized vector oscillons. *Phys. Rev. D*, 105(9):096037, 2022.

[78] Mustafa A. Amin, Mudit Jain, Rohith Karur, and Philip Mocz. Small-scale structure in vector dark matter. *JCAP*, 08(08):014, 2022.

[79] Mudit Jain and Mustafa A. Amin. i-SPin: an integrator for multicomponent Schrödinger-Poisson systems with self-interactions. *JCAP*, 04:053, 2023.

[80] Mudit Jain, Wisha Wanichwecharungruang, and Jonathan Thomas. Kinetic relaxation and nucleation of Bose stars in self-interacting wave dark matter. *Phys. Rev. D*, 109(1):016002, 2024.

[81] Peter Adshead and Kaloian D. Lozanov. Self-gravitating Vector Dark Matter. *Phys. Rev. D*, 103(10):103501, 2021.

[82] Marco Gorghetto, Edward Hardy, John March-Russell, Ningqiang Song, and Stephen M. West. Dark photon stars: formation and role as dark matter substructure. *JCAP*, 08(08):018, 2022.

[83] Jiajun Chen, Le Hoang Nguyen, and David J. E. Marsh. Vector Dark Matter Halo: From Polarization Dynamics to Direct Detection. 7 2024.

[84] Hong-Yi Zhang. *Probing ultralight dark fields in cosmological and astrophysical systems*. PhD thesis, Rice U., 2023.

[85] Hong-Yi Zhang. Unified view of scalar and vector dark matter solitons. 6 2024.

[86] `https://youtube.com/playlist?list=PLtSeM9Y95qPbmOVgqq1Gy0Kag8DJ7ZKZB&si=hg_tYzoFmDI6KwGN`, 2024.

[87] Armando A. Roque, Emmanuel Chávez Nambo, and Olivier Sarbach. Radial linear stability of nonrelativistic ℓ-boson stars. *Phys. Rev. D*, 107(8):084001, 2023.

[88] Emmanuel Chávez Nambo. Sobre la existencia de estrellas de bosones newtonianas con momento angular en simetría esférica. Master's thesis, Universidad Michoacana de San Nicolás de Hidalgo, 2021.

[89] Tonatiuh Matos and L. Arturo Urena-Lopez. Flat rotation curves in scalar field galaxy halos. *Gen. Rel. Grav.*, 39:1279–1286, 2007.

[90] Carlos A. R. Herdeiro and Eugen Radu. Asymptotically flat, spherical, self-interacting scalar, dirac and proca stars, 2020.

[91] Ignacio Salazar Landea and Federico García. Charged proca stars. *Physical Review D*, 94(10), November 2016.

[92] Eugen Merzbacher. *Quantum Mechanics*. Wiley, USA, 1998.

[93] Katy Clough, Thomas Helfer, Helvi Witek, and Emanuele Berti. Ghost Instabilities in Self-Interacting Vector Fields: The Problem with Proca Fields. *Phys. Rev. Lett.*, 129(15):151102, 2022.

[94] Zong-Gang Mou and Hong-Yi Zhang. Singularity Problem for Interacting Massive Vectors. *Phys. Rev. Lett.*, 129(15):151101, 2022.

[95] Andrew Coates and Fethi M. Ramazanoğlu. Intrinsic Pathology of Self-Interacting Vector Fields. *Phys. Rev. Lett.*, 129(15):151103, 2022.

[96] Enrico Barausse, Miguel Bezares, Marco Crisostomi, and Guillermo Lara. The well-posedness of the Cauchy problem for self-interacting vector fields. *JCAP*, 11:050, 2022.

[97] Katsuki Aoki and Masato Minamitsuji. Resolving the pathologies of self-interacting Proca fields: A case study of Proca stars. *Phys. Rev. D*, 106(8):084022, 2022.

[98] Marcelo E. Rubio, Guillermo Lara, Miguel Bezares, Marco Crisostomi, and Enrico Barausse. Fixing the dynamical evolution of self-interacting vector fields. *Phys. Rev. D*, 110(6):063015, 2024.

[99] E. H. Lieb. Existence and Uniqueness of the Minimizing Solution of Choquard's Nonlinear Equation. *Studies in Applied Mathematics*, 57(2):93–105, 1977.

[100] T. Cazenave and P. L. Lions. Orbital stability of standing waves for some nonlinear Schrödinger equations. *Communications in Mathematical Physics*, 85:549–561, 2017.

[101] P.L. Lions. The concentration-compactness principle in the calculus of variations. The locally compact case, part 1. *Annales de l'Institut Henri Poincaré C, Analyse non linéaire*, 1(2):109–145, 1984.

[102] P.L. Lions. The concentration-compactness principle in the calculus of variations. The locally compact case, part 2. *Annales de l'Institut Henri Poincaré C, Analyse non linéaire*, 1(4):223–283, 1984.

[103] Barry Simon. *Sturm Oscillation and Comparison Theorems*, pages 29–43. Birkhäuser Basel, Basel, 2005.

[104] P. H. Chavanis and L. Delfini. Mass-radius relation of Newtonian self-gravitating Bose-Einstein condensates with short-range interactions: II. Numerical results. *Phys. Rev. D*, 84:043532, 2011.

[105] Hong-Bo Li, Yan-Bo Zeng, Yan Song, and Yong-Qiang Wang. Self-interacting multistate boson stars. *JHEP*, 04:042, 2021.

[106] P. Virtanen, R. Gommers, and et al. SciPy 1.0: Fundamental Algorithms for Scientific Computing in Python. *Nature Methods*, 17:261–272, 2020.

[107] J.R. Dormand and P.J. Prince. A family of embedded runge-kutta formulae. *Journal of Computational and Applied Mathematics*, 6(1):19–26, 1980.

[108] F. S. Lawrence. Some practical Runge-Kutta formulas. *Mathematics of Computation*, 46:135–150, 1986.

[109] Miguel Alcubierre, Juan Barranco, Argelia Bernal, Juan Carlos Degollado, Alberto Diez-Tejedor, Miguel Megevand, Dario Nunez, and Olivier Sarbach. ℓ-Boson stars. *Class. Quant. Grav.*, 35(19):19LT01, 2018.

[110] R. Harrison, I. M. Moroz, and P. Tod. A numerical study of the Schrödinger Newton equations. *Nonlinearity*, 16(1):101–122, 2002.

[111] W. Heisenberg and H. Euler. Consequences of dirac theory of the positron, 2006.

[112] Fritz Sauter. On the behavior of an electron in a homogeneous electric field in dirac's relativistic theory. *Z. Phys*, 69:742, 1931.

[113] Julian Schwinger. On gauge invariance and vacuum polarization. *Physical Review*, 82(5):664, 1951.

[114] Sean M. Carroll. *Spacetime and geometry*. Cambridge University Press, 2019.

[115] Jun John Sakurai and Jim Napolitano. *Modern quantum mechanics*. Cambridge University Press, 2020.

[116] Bryce S. DeWitt. Quantum theory of gravity. i. the canonical theory. *Physical Review*, 160(5):1113, 1967.

[117] Bryce S. DeWitt. Quantum theory of gravity. ii. the manifestly covariant theory. *Physical Review*, 162(5):1195, 1967.

[118] Daniel Baumann. *Cosmology*. Cambridge University Press, 2022.

[119] P.J.E. Peebles and A. Vilenkin. Noninteracting dark matter. *Physical Review D*, 60(10):103506, 1999.

[120] Cristian Armendariz-Picon and Alberto Diez-Tejedor. Cosmic energy density: particles, fields and the vacuum. *Journal of Cosmology and Astroparticle Physics*, 2023(11):030, 2023.

[121] Schrödinger, Erwin. The proper vibrations of the expanding universe. *PHYSICA*, 6(7-12):899–912, 1939.

[122] Leonard Emanuel Parker. *The Creation of Particles in AN Expanding Universe.* PhD thesis, Harvard University, Massachusetts, January 1967.

[123] L. Parker. Particle creation in expanding universes. *Phys. Rev. Lett.*, 21:562–564, Aug 1968.

[124] Leonard Parker. Quantized fields and particle creation in expanding universes. i. *Phys. Rev.*, 183:1057–1068, Jul 1969.

[125] Leonard Parker and S. A. Fulling. Adiabatic regularization of the energy-momentum tensor of a quantized field in homogeneous spaces. *Phys. Rev. D*, 9:341–354, Jan 1974.

[126] S.A. Fulling and Leonard Parker. Renormalization in the theory of a quantized scalar field interacting with a robertson-walker spacetime. *Annals of Physics*, 87(1):176–204, 1974.

[127] S.A. Fulling, Leonard Parker, and B.L. Hu. Conformal energy-momentum tensor in curved spacetime: Adiabatic regularization and renormalization. *Physical Review D*, 10(12):3905, 1974.

[128] L.H. Ford and Leonard Parker. Creation of particles by singularities in asymptotically flat spacetimes. *Physical Review D*, 17(6):1485, 1978.

[129] Stephen W. Hawking. Black hole explosions? *Nature*, 248(5443):30–31, 1974.

[130] Viatcheslav F. Mukhanov, Hume A. Feldman, and Robert Hans Brandenberger. Theory of cosmological perturbations. *Physics reports*, 215(5-6):203–333, 1992.

[131] L.H. Ford. Gravitational particle creation and inflation. *Physical Review D*, 35(10):2955, 1987.

[132] Michael S. Turner and Lawrence M. Widrow. Gravitational production of scalar particles in inflationary-universe models. *Physical Review D*, 37(12):3428, 1988.

[133] Daniel J.H. Chung. Classical inflaton field induced creation of superheavy dark matter. *Physical Review D*, 67(8):083514, 2003.

[134] V.A. Kuzmin and Igor I. Tkachev. Ultrahigh-energy cosmic rays, superheavy long-lived particles, and matter creation after inflation. *Journal of Experimental and Theoretical Physics Letters*, 68:271–275, 1998.

[135] N. D. Birrell and P. C. Davies. *Quantum Fields in Curved Sapce*. Cambridge University Press.

[136] Leonard E. Parker and David J. Toms. *Quantum Field Theory in Curved Spacetime*. Cambridge University Press.

[137] Viatcheslav Mukhanov and Sergei Winitzki. *Introduction to quantum effects in gravity*. Cambridge university press, 2007.

[138] Stephen A. Fulling. *Aspects of quantum field theory in curved spacetime*. Number 17. Cambridge university press, 1989.

[139] L.H. Ford. Cosmological particle production: a review. *Reports on Progress in Physics*, 84(11):116901, 2021.

[140] Edward W. Kolb and Andrew J. Long. Cosmological gravitational particle production and its implications for cosmological relics. *Reviews of Modern Physics*, 96(4):045005, 2024.

[141] Ted Jacobson. Introduction to quantum fields in curved spacetime and the hawking effect. In *Lectures on quantum gravity*, pages 39–89. Springer, 2005.

[142] Daniel J.H. Chung, Patrick Crotty, Edward W. Kolb, and Antonio Riotto. Gravitational production of superheavy dark matter. *Physical Review D*, 64(4):043503, 2001.

[143] Daniel J.H. Chung, Edward W. Kolb, and Andrew J. Long. Gravitational production of super-hubble-mass particles: an analytic approach. *Journal of High Energy Physics*, 2019(1):1–23, 2019.

[144] Vadim Kuzmin and Igor Tkachev. Matter creation via vacuum fluctuations in the early universe and observed ultrahigh energy cosmic ray events. *Physical Review D*, 59(12):123006, 1999.

[145] Soichiro Hashiba and Jun'ichi Yokoyama. Gravitational particle creation for dark matter and reheating. *Physical Review D*, 99(4):043008, 2019.

[146] Juho Lankinen, Oskari Kerppo, and Iiro Vilja. Reheating via gravitational particle production in the kination epoch. *Physical Review D*, 101(6):063529, 2020.

[147] Juho Lankinen and Iiro Vilja. Gravitational particle creation in a stiff matter dominated universe. *Journal of Cosmology and Astroparticle Physics*, 2017(08):025, 2017.

[148] Nathan Herring, Daniel Boyanovsky, and Andrew R Zentner. Nonadiabatic cosmological production of ultralight dark matter. *Physical Review D*, 101(8):083516, 2020.

[149] V.M. Frolov, S.G. Mamayev, and V.M. Mostepanenko. On the difference in creation of particles with spin 0 and 1/2 in isotropic cosmologies. *Physics Letters A*, 55(7):389–390, 1976.

[150] J. Audretsch and G. Schafer. Thermal particle production in a radiation dominated robertson-walker universe. *Journal of Physics A: Mathematical and General*, 11(8):1583, 1978.

[151] S.G. Mamaev and V.M. Mostepanenko. Particle creation by the gravitational field, and the problem of the cosmological singularity. *Soviet Astronomy Letters, vol. 4, May-June 1978, p. 111-113. Translation Pisma v Astronomicheskii Zhurnal, vol. 4, May 1978, p. 203-206.*, 4:111–113, 1978.

[152] David H. Lyth, David Roberts, and Michael Smith. Cosmological consequences of particle creation during inflation. *Physical Review D*, 57(12):7120, 1998.

[153] Peter Adshead and Evangelos I Sfakianakis. Fermion production during and after axion inflation. *Journal of Cosmology and Astroparticle Physics*, 2015(11):021, 2015.

[154] Yohei Ema, Kazunori Nakayama, and Yong Tang. Production of purely gravitational dark matter: the case of fermion and vector boson. *Journal of high energy physics*, 2019(7), 2019.

[155] Vadim A. Kuzmin and Igor I. Tkachev. Ultra-high-energy cosmic rays and inflation relics. *Physics Reports*, 320(1-6):199–221, 1999.

[156] Clément Stahl and Eckhard Strobel. Semiclassical fermion pair creation in de sitter spacetime. *arXiv preprint arXiv:1507.01401*, 2015.

[157] Aitor Landete, José Navarro-Salas, and Francisco Torrenti. Adiabatic regularization for spin-1/2 fields. *Physical Review D—Particles, Fields, Gravitation, and Cosmology*, 88(6):061501, 2013.

[158] Aitor Landete, José Navarro-Salas, and Francisco Torrenti. Adiabatic regularization and particle creation for spin one-half fields. *Physical Review D*, 89(4):044030, 2014.

[159] Adrian del Rio, Jose Navarro-Salas, and Francisco Torrenti. Renormalized stress-energy tensor for spin-1/2 fields in expanding universes. *Physical Review D*, 90(8):084017, 2014.

[160] Aitor Landete. Extension of the adiabatic regularization method to spin-1/2 fields. In *Journal of Physics: Conference Series*, volume 600, page 012021. IOP Publishing, 2015.

[161] Suman Ghosh. Creation of spin 1/2 particles and renormalization in flrw spacetime. *Physical Review D*, 91(12):124075, 2015.

[162] Suman Ghosh. Spin 1/2 field and regularization in a de sitter and radiation dominated universe. *Physical Review D*, 93(4):044032, 2016.

[163] Adrian del Rio, Antonio Ferreiro, Jose Navarro-Salas, and Francisco Torrenti. Adiabatic regularization with a yukawa interaction. *Physical Review D*, 95(10):105003, 2017.

[164] J. Fernando Barbero G., Antonio Ferreiro, Jose Navarro-Salas, and Eduardo J.S. Villaseñor. Adiabatic expansions for dirac fields, renormalization, and anomalies. *Physical Review D*, 98(2):025016, 2018.

[165] Aitor Landete, Jose Navarro-Salas, and Francisco Torrenti. Adiabatic regularization for spin-1/2 fields. 5 2013.

[166] S.M. Christensen. Regularization, renormalization, and covariant geodesic point separation. *Physical Review D*, 17(4):946, 1978.

[167] Leonard Parker and SA Fulling. Adiabatic regularization of the energy-momentum tensor of a quantized field in homogeneous spaces. *Physical Review D*, 9(2):341, 1974.

[168] Steven Weinberg. Ultraviolet divergences in cosmological correlations. *Physical Review D—Particles, Fields, Gravitation, and Cosmology*, 83(6):063508, 2011.

[169] Christian Koke, Changsuk Noh, and Dimitris G Angelakis. Dirac equation in 2-dimensional curved spacetime, particle creation, and coupled waveguide arrays. *Annals of Physics*, 374:162–178, 2016.

[170] Felix Finster and Moritz Reintjes. The dirac equation and the normalization of its solutions in a closed friedmann–robertson–walker universe. *Classical and Quantum Gravity*, 26(10):105021, 2009.

[171] Peter Collas and David Klein. *The Dirac Equation in Curved Spacetime: A Guide for Calculations*. Springer, 2019.

[172] Xin-Bing Huang. Exact solutions of the dirac equation in robertson-walker space-time. *arXiv preprint gr-qc/0501077*, 2005.

[173] Nathan Herring and Daniel Boyanovsky. Gravitational production of nearly thermal fermionic dark matter. 5 2020.

[174] Suman Ghosh. Creation of spin 1 /2 particles and renormalization in flrw spacetime. *Physical Review D - Particles, Fields, Gravitation and Cosmology*, 91, 6 2015.

[175] J. Fernando Barberog, Antonio Ferreiro, Jose Navarro-Salas, and Eduardo J.S. Villaseñor. Adiabatic expansions for dirac fields, renormalization, and anomalies. *Physical Review D*, 98, 7 2018.

[176] Daniel J. H. Chung, Lisa L. Everett, Hojin Yoo, and Peng Zhou. Gravitational fermion production in inflationary cosmology. 9 2011.

[177] L. H. Ford. Cosmological particle production: A review, 11 2021.

[178] Yohei Ema, Kazunori Nakayama, and Yong Tang. Production of purely gravitational dark matter: the case of fermion and vector boson. *Journal of High Energy Physics*, 2019(7), jul 2019.

[179] Michael Victor Berry. Quantum phase corrections from adiabatic iteration. *Proceedings of the Royal Society of London. A. Mathematical and Physical Sciences*, 414(1846):31–46, 1987.

[180] VMMSG Mamaev and AA Starobinsky. Particle production and vacuum polarization in an anisotropic gravitational field. *JETP*, 43(5):823, 1976.

[181] Aitor Landete, Jose Navarro-Salas, and Francisco Torrenti. Adiabatic regularization and particle creation for spin one-half fields. 11 2013.

[182] Adrian del Rio, Jose Navarro-Salas, and Francisco Torrenti. Renormalized stress-energy tensor for spin-1/2 fields in expanding universes. 7 2014.

[183] Adrian Del Rio, Antonio Ferreiro, Jose Navarro-Salas, and Francisco Torrenti. Adiabatic regularization with a yukawa interaction. *Physical Review D*, 95, 2017.

[184] Bei-Lok B. Hu and Enric Verdaguer. *Semiclassical and Stochastic Gravity Quantum Field Effects on Curved Spacetime*.

[185] Bruce A. Bassett, Shinji Tsujikawa, and David Wands. Inflation dynamics and reheating, 2006.

[186] Rouzbeh Allahverdi, Robert Brandenberger, Francis-Yan Cyr-Racine, and Anupam Mazumdar. Reheating in inflationary cosmology: Theory and applications. 1 2010.

[187] Peter Collas and David Klein. The dirac equation in general relativity, a guide for calculations. 9 2018.

[188] C. Koke, C. Noh, and D. G. Angelakis. Dirac equation in 2-dimensional curved spacetime, particle creation, and coupled waveguide arrays. 7 2016.

[189] Dag-Morten Sjøstrøm. Bosons and fermions in curved spacetime.

[190] Leonard Parker. Particle creation and particle number in an expanding universe. *Journal of Physics A: Mathematical and Theoretical*, 45, 9 2012.

[191] Clément Stahl and Eckhard Strobel. Semiclassical fermion pair creation in de sitter spacetime. 7 2015.

[192] Miguel Alcubierre, Juan Barranco, Argelia Bernal, Juan Carlos Degollado, Alberto Diez-Tejedor, Miguel Megevand, Darío Núñez, and Olivier Sarbach. Boson stars and their relatives in semiclassical gravity. *Phys. Rev. D*, 107(4):045017, 2023.

[193] I. M. Moroz, R. Penrose, and P. Tod. Spherically symmetric solutions of the Schrodinger-Newton equations. *Class. Quant. Grav.*, 15:2733–2742, 1998.

[194] L. Arturo Urena-Lopez and Argelia Bernal. Bosonic gas as a Galactic Dark Matter Halo. *Phys. Rev. D*, 82:123535, 2010.

[195] J. Yang. *Nonlinear Waves in Integrable and Non-Integrable Systems*. Society for Industrial and Applied Mathematics, USA, 2010.

[196] L. N. Trefethen. *Spectral Methods in MATLAB*. EngineeringPro collection. Society for Industrial and Applied Mathematics, 2000.

[197] Repository. Github.com/Mandy8808/Implementation.git, 2023.

[198] G. H. Derrick. Comments on Nonlinear Wave Equations as Models for Elementary Particles. *Journal of Mathematical Physics*, 5(9):1252–1254, September 1964.

[199] V. K. Khersonskii, A. N. Moskalev, and D. A. Varshalovich. *Quantum Theory Of Angular Momentum*. World Scientific Publishing Company, 1988.

[200] Jitender Singh. Shooting method for solving two-point boundary value problems in ODEs numerically. *arXiv e-prints*, August 2022.

[201] Ricardo A. Flores and Joel R. Primack. Observational and theoretical constraints on singular dark matter halos. *The Astrophysical Journal*, 427:L1, May 1994.

UNIVERSIDAD DE GUANAJUATO

León, Gto., 03 de septiembre del 2025

DR. MODESTO ANTONIO SOSA AQUINO
DIVISIÓN DE CIENCIAS E INGENIERÍAS, CAMPUS LEÓN
DIRECTOR

P R E S E N T E

Por medio de la presente, como miembro del jurado calificador designado para revisar el trabajo de grado con título ***"Higher-Order Dark Matter: From nonrelativistic Proca Stars to Cosmological Spinor Production"*** que sustenta el ***M. Edgar Iván Preciado Govea*** con el fin de obtener el grado de ***Doctor en Física***, hago constar que he leído el trabajo y que avalo el contenido y calidad del mismo como un trabajo de Tesis de Doctorado.

Sin más por el momento le envío saludos cordiales, quedando de usted para cualquier aclaración.

Atentamente,

Lorena Velázquez I.

Dra. Lorena B. Velázquez Ibarra
Departamento de Física
DCI-UG

División de Ciencias e Ingenierías
Loma del Bosque # 103, Col. Loma del Campestre. León, Guanajuato, México. C. P. 37150
Tel: +52 (477) 7885100 Exts. 8420 y 8421, Fax. Ext. 8410. www.dci.ugto.mx

UNIVERSIDAD DE GUANAJUATO

León, Guanajuato, 9 de octubre de 2025

Dr. Modesto Antonio Sosa Aquino
Director
División de Ciencias e Ingenierías
PRESENTE

Por medio de la presente me permito informar que he leído la tesis titulada **"Higher-Order Dark Matter: From non-relativistic Proca Stars to Cosmological Spinor Production"**, que para obtener el grado de Doctor en Física ha sido elaborada por el **Mtr. Edgar Iván Preciado Govea**. En mi opinión, la tesis cumple con los requisitos de calidad correspondientes al grado académico al que se aspira. Las correcciones sugeridas por mi parte han sido atendidas, por lo cual recomiendo se proceda a la defensa de la tesis.

Sin más por el momento quedo a sus órdenes para cualquier aclaración.

Atentamente

Dr. Carlos Alberto Vaquera Araujo
Investigador por México, Secihti
Departamento de Física
DCI, Campus León
vaquera@fisica.ugto.mx

División de Ciencias e Ingenierías, Campus León
Loma del Bosque 103, Fracc. Lomas del Campestre
C.P. 37520, León, Gto., México
www.dci.ugto.mx

UNIVERSIDAD DE GUANAJUATO

Asunto: Revisión de Tesis
León, Guanajuato, octubre de 2025

Dr. Modesto Antonio Sosa Aquino
Director
División de Ciencias e Ingenierías, Campus León
Universidad de Guanajuato
PRESENTE

Estimado Dr. Modesto Sosa:

Por medio de la presente le informo que he revisado la tesis "Higher-Order Dark Matter: From nonrelativistic Proca Stars to Cosmologuical Spinor Production" escrita por el estiudiante de Doctorado en Física de la DCI, Edgar Ivan PreciadoGovea. En mi opinión la tesis esta lista para ser presentada y estoy de acuerdo que se proceda al examen recepcional, una vez que se cumplan los procedimientos administrativos correspondientes.

Sin más por el momento, le envío saludos cordiales.

ATENTAMENTE
"LA VERDAD OS HARÁ LIBRES"

DRA. ARGELIA BERNAL BAUTISTA

División de Ciencias e Ingenierías
Loma del Bosque # 103, Col. Loma del Campestre. León, Guanajuato, México. C. P. 37150
Tel: +52 (477) 7885100 Exts. 8420 y 8421, Fax. Ext. 8410. www.dci.ugto.mx

UNIVERSIDAD DE GUANAJUATO

8 de octubre de 2025

Asunto: Carta de revisión de tesis de Edgar Iván Preciado Govea

Dr. Modesto Antonio Sosa Aquino
Director de la División de Ciencias e Ingenierías, Campus León
Universidad de Guanajuato
Presente

Estimado Dr. Modesto,

En mi calidad de integrante del comité sinodal del estudiante de Doctorado en Física Edgar Iván Preciado Govea, por este medio informo a usted que he revisado su tesis titulada "Higher-Order Dark Matter: From Nonrelativistic Proca Stars to Cosmological Spinor Production" que realizó Edgar con el fin de obtener el grado de Doctor en Física.

El trabajo de Edgar está muy bien estructurado y además posee el contenido y la relevancia necesaria como trabajo de investigación para obtener el grado de Doctor. Edgar ya ha considerado e implementado las correcciones sugeridas por un servidor. Considero que su trabajo de tesis está listo para ser defendido públicamente.

Sin más por el momento, me despido de usted con un cordial saludo.

Dr. José Luis López-Picón
Departamento de Física
División de Ciencias e Ingenierías, Campus León
Universidad de Guanajuato
email: jl_lopez@fisica.ugto.mx

Gustavo Niz Quevedo
Departamento de Física
División de Ciencias e Ingenierías

León, Gto., 7 de Octubre de 2025.

Dr. Modesto Antonio Sosa Aquino
Director de la División de Ciencias e Ingenierías
Universidad de Guanajuato

Estimado Dr. Modesto Antonio Sosa Aquino

Por medio de la presente le informo que he recibido, leído y revisado la tesis de Doctorado titulada "Higher-Order Dark Matter: From nonrelativistic Proca Stars to Cosmological Spinor Production" del alumno Edgar Iván Preciado Govea, bajo la supervisión del Dr. Alberto Diez Tejedor.

Después de la atención a ciertas correcciones menores, creo que el trabajo cumple con los estándares requeridos para la obtención del grado, y apoyo la defensa del mismo en la fecha convenida.

Me pongo a su disposición para cualquier duda sobre la revisión de dicho trabajo de tesis.

Atentamente,

Gustavo Niz

DEPARTAMENTO DE FISICA, DIVISION DE CIENCIAS E INGENIERÍAS, CAMPUS LEÓN
Loma del Bosque 103, Fracc. Lomas del Campestre C.P. 37150 León, Gto., Ap. Postal E-143 C.P. 37000 Tel. (477) 788-5100, http://www.fisica.ugto.mx

Asunto: Revisión de tesis para obtención del grado de Doctor en Física.

October 15, 2025

Estimado: **Dr. Modesto Antonio Sosa Aquino.**
Director División de Ciencias e Ingenierías
Universidad de Guanajuato, Campus León.

PRESENTE.

Por este conducto y en mi carácter de sinodal le comunico que he revisado la tesis: **"Higher-Order Dark Matter: From nonrelativistic Proca Stars to Cosmological Spinor Production"**, escrita por el Maestro en Física **Edgar Iván Preciado Govea**, con efecto de presentarla para la obtención del grado de **Doctor en Física**. El texto de la Tesis se encuentra completo, presentándose resultados novedosos y explicándose en detalle las diferentes metodología desarrolladas y utilizadas. Igualmente, he podido ver que el texto fue modificado por el autor para reflejar las sugerencias y comentarios que le fueron expresados durante la revisión. En mi opinión, la tesis **cumple con los elementos necesarios y suficientes para ser defendida** ante el comité sinodal asignado en fecha próxima.

Agradeciendo su amable atención, y esperando que la presente sirva para generar los trámites administrativos conducentes, me despido de usted enviándole un cordial saludo.

ATENTAMENTE,

Dr. Armando A. Roque Estrada
Investigador Posdoctoral CONAHCYT
Unidad Académica de Física, UAZ.
Cédula: 12847768

UNIVERSIDAD DE GUANAJUATO

www.ugto.mx/campusleon

Asunto: Revisión de Tesis
León, Gto., a 31 de octubre del 2025

DR. MODESTO ANTONIO SOSA AQUINO
DIRECTOR
DIVISIÓN DE CIENCIAS E INGENIERIAS
CL -UNIVERSIDAD DE GUANAJUATO

A través de la presente constato que he revisado la tesis del Mtro. Fis. **Edgar Iván Preciado Govea** con el fin de obtener el grado de Doctor en Física. El trabajo de tesis se titula **"Higher-Order Dark Matter: From nonrelativistic Proca Stars to Cosmological Spinor Production"**. En este proyecto de investigación realizado por Iván se estudian configuraciones de equilibrio no relativistas llamadas estrellas de bosones y estrellas de Proca, que son objetos compactos, autogravitantes y de energía finita que no se dispersan con el tiempo, dónde se exploran distintos regímenes de interacción (atractiva o repulsiva) y tipos de polarización (lineal, circular, radial), determinando cuáles configuran el estado de mínima energía. Además, en otro tema analiza la producción de partículas por transiciones cósmicas en un universo Friedmann–Lemaître–Robertson–Walker, para campos cuánticos escalares y fermiónicos no interactuantes, encontrando para bosones, se puede despreciar la energía del vacío si hay muchas partículas por modo; para fermiones, esto depende de la comparación entre la energía del vacío y la de las partículas. El trabajo de titulación satisface con la completez y solidez de un proyecto de titulación a nivel doctorado. También Iván ha realizado las correcciones pertinentes al documento de la tesis. Además, he cuestionado a Iván sobre los temas relacionados a su trabajo de tesis, demostrando su dominio en los temas abordados en su trabajo de tesis. Por lo que considero que ya se puede proceder con la disertación de tesis.

Sin más por el momento le envío saludos cordiales.

Atentamente

Dr. Carlos Herman Wiechers Medina
Profesor Titular A
Departamento de Física
División de Ciencias e Ingenierías
Campus León
Universidad de Guanajuato
Tel. +52 (477) 7885100 Ext. 3867
Cel. +52 (477) 1080605
e-mail 1: carherwm@fisica.ugto.mx; ch.wiechers@ugto.mx